

# Molecular and Cellular Mechanisms for Microbial Discrimination in Sponges



Angela M. Marulanda G.

---

# Molecular and Cellular Mechanisms for Microbial Discrimination in Sponges

---

Dissertation

in fulfillment of the requirements for the degree  
of Doctor in Natural Sciences  
of the Faculty of Mathematics and Natural Sciences  
at Kiel University

submitted by

**Angela Maria Marulanda Gómez**

Kiel, 2023



*“(...) This above all: to thine own self be true,  
And it must follow, as the night the day,  
Thou canst not then be false to any man (...)”  
- W. Shakespeare*

First examiner: Prof. Dr. Ute Hentschel Humeida

Second examiner: Prof. Dr. Sebastian Fraune

Date of the oral examination: 26.01.2024

---

# Table of Contents

---

Summary .....	5
Zusammenfassung.....	9
General Introduction.....	13
We live in a symbiotic world.....	14
Host-microbe interplay.....	16
The first encounter - Transmission of symbionts .....	16
The force driving sensing and recognition - Immunity .....	16
Phagocytosis as cellular mechanism to facilitate host-microbe interactions .....	17
Host-microbe crosstalk in the marine realm .....	19
Decoding host-microbe dialogue in sponges.....	21
The sponge as an animal host .....	21
The sponge mesohyl and its microbial residents.....	24
Symbiont persistence in the sponge mesohyl .....	26
Research gap .....	27
Thesis Aims and Outline .....	29
Main Chapters .....	30
Chapter 1 The Sponge Immune System .....	33
Chapter 2 Transcriptomic Response of Mediterranean Sponges upon Encounter with Seawater or Symbiont Microbial Consortia.....	45
Chapter 3 A Novel <i>in-vivo</i> Phagocytosis Assay to Gain Cellular Insights on Sponge-Microbe Interactions.....	67
Chapter 4 Characterization of Sponge Phagocytosis upon Native and Foreign <i>Vibrio</i> Encounter in the Breadcrumb Sponge <i>Halichondria panicea</i> .....	97
General Discussion .....	127
The enduring enigma of sponge microbial discrimination.....	128
The physiological perspective - Sponge filtration .....	129
The cellular perspective – Deciphering microbial uptake by sponge cells.....	129
Initial cellular internalization may be indiscriminative .....	129
Possible scenarios after cellular internalization .....	131

Phagocytic plasticity in sponges .....	134
The molecular perspective –Sponge transcriptomic responses to microbes.....	135
Differential Gene Expression as a tool for assessing the sponge reaction to bacteria ..	135
Microbial recognition by sponge immune receptors.....	136
Host-specific traits drive the immune response upon microbial encounter.....	136
Assembling the different perspectives on sponge microbial discrimination .....	139
Conclusion and Final Outlook.....	143
References.....	149
Acknowledgements .....	165
Supplementary Information .....	169
Eidesstattliche Erklärung / Declaration Statement .....	207

---

## Summary

---

Fine-tune crosstalk between animal hosts and associated microbes is the cornerstone in animal-microbe symbioses. Fundamental mechanisms mediating the specificity of these symbiotic interactions have started to be unveiled over the last decades. Increasing evidence poses the immune system as an essential force for microbial recognition, tolerance, and homeostasis within animal holobionts. Early branching metazoans provide an opportunity to investigate the onset and evolution of conserved mechanisms in host-microbe interactions along the animal kingdom. Sponges (phylum Porifera) are diverse basal metazoans present in all aquatic realms and essential components of benthic communities. These filter feeders forage microbes from the surrounding water and at the same time establish tight associations with symbionts that thrive within their bodies. Early observations on differential uptake between seawater and symbiotic bacteria served as the main evidence that sponges can discriminate between different microbes. Yet, the molecular and cellular mechanisms employed by sponges to recognize and differentiate between food to digest, symbionts to incorporate, and pathogens to eliminate remain a conundrum. Immune mechanisms likely to be the essential force in modulating the sponge-microbe crosstalk are introduced sponge-microbe interactions (Busch et al, 2023; Chapter 1). On the molecular side, the diverse repertoire of sponge immune receptors suggests their participation in specific microbial discrimination. On the cellular side, phagocytosis is conceivable to play a role in microbe selectivity. However, in both cases, experimental data is still scarce to validate these assumptions. Therefore, this thesis aimed to elucidate the molecular and cellular immune mechanisms that allow sponges to discriminate between different microbes by adopting an experimental approach. Sponge incubation experiments were used to expose the host to different microbes and characterize its molecular and cellular responses. This experimental setup resembled as much as possible the filter-feeding lifestyle of sponges and thus provided evidence of how the host likely responds to microbial encounters under natural conditions.

The sponge molecular mechanisms were studied in the Mediterranean sponges *Aplysina aerophoba* and *Dysidea avara* by characterizing the host transcriptomic response upon encounter with seawater and symbiont microbial consortia by means of RNA-Seq differential gene expression analysis (Marulanda-Gómez et al., under revision; Chapter 2). *A. aerophoba* and *D. avara* are representative members of sponges harboring high (HMA) and low (LMA) microbial abundances, respectively, and consequently can help test if the HMA-LMA status affects the host immune response to microbial cues. Both sponge species mounted a

moderately low (less than 70 DEGs) but different transcriptomic response upon encounter with natural microbial consortia. The HMA sponge *A. aerophoba* showed little differential gene expression and no participation of receptors upon microbial exposure. In contrast, the LMA sponge *D. avara* responded by regulating Nucleotide Oligomerization Domain (NOD)-Like Receptors (NLRs) genes. These observations suggest that microbial discrimination in sponges is driven by the repertoire of immune genes harbored by the host and the degree to which these are induced. Moreover, it is plausible that the differential response to microbial exposure between sponge species is due to the HMA-LMA status or to species-specific traits.

From the cellular perspective, phagocytosis was investigated as a mechanism for microbial discrimination. The Baltic sponge *Halichondria panicea* (LMA) was used to establish an *in-vivo* phagocytosis assay which consisted of incubating whole sponge individuals with fluorescent particles (i.e., microalgae, bacteria, and latex beads) and coupling this with sponge (host) cell dissociation and fluorescence-activated cell sorting (FACS) to quantify the incorporation of the different particles into sponge cells (from now on termed phagocytosis) (Marulanda-Gómez et al., 2023). Sponge phagocytosis was found to be a fast process within minutes after exposure to the particles. Fluorescent and transmission electron microscopy confirmed particle internalization and provided insights into the size and morphologies of sponge phagocytic cells. The majority of the particles were incorporated into presumably choanocyte-like cells after the 30 min incubations, and after 60 min particles seemed to be translocated to archaeocyte-like cells probably for them to be digested. The assay was further used to compare *H. panicea* phagocytic response upon exposure to a sponge-associated (“native”) and a non-sponge-associated (“foreign”) *Vibrio* isolate (Marulanda-Gómez et al., in preparation). Sponge phagocytosis was analyzed by FACS, fluorescent microscopy, and proteomic analysis after 30 min and 60 min of initial bacterial exposure. Initial *Vibrio* incorporation into the sponge cells was indiscriminately between the isolates, but the distribution of vibrios in the different phagocytic cell types was different between the native and foreign *Vibrio* and seemed to vary over time. Moreover, the exposure to the *Vibrio* isolates caused a differential proteomic response in *H. panicea*, characterized by higher abundances of phagocytic-related proteins in the foreign vs. the native bacterial treatment. These results may indicate that bacterial discrimination in *H. panicea* occurs after cellular internalization and that the difference may rely on how each *Vibrio* isolate is processed by sponge cells.



Overall, the different experimental approaches used in this thesis provided evidence of how sponges respond to microbial encounters on the molecular and cellular levels. It is recommended to combine these two perspectives in future studies by adopting an integrative experimental approach. Simultaneous characterization of cellular and molecular responses would aid in building a framework to unveil the underlying mechanisms involved in the sponge-microbe crosstalk.

---

# Zusammenfassung

---

Eine fein abgestimmte Kommunikation zwischen Wirtsorganismus und assoziierten Mikroben ist die Grundlage einer jeden Symbiose. In den letzten Jahrzehnten wurden die ersten elementaren Mechanismen dieser Kommunikation, die das symbiotische Zusammenspiel von Wirtstieren und assoziierten Mikroben vermitteln, aufgedeckt. Dem Immunsystem wird dabei zunehmend eine wichtige Rolle in der Erkennung, Tolerierung, und der Aufrechterhaltung eines ausgeklügelten Gleichgewichts in Holobionten (Gemeinschaft aus Tier und assoziierten Mikroben) beigemessen. Forschung an basalen, vielzelligen Tieren ermöglicht es, die Entstehung, sowie die Evolution von evolutionär konservierten Mechanismen von Tier-Mikroben Interaktionen zu untersuchen. Schwämme (Phylum Porifera) sind eine diverse Gruppe von basalen, mehrzelligen Tieren, die in allen aquatischen Lebensräumen vorkommt und dort häufig eine wichtige Komponente von benthischen Lebensgemeinschaften darstellt. Diese Filtrierer pumpen große Mengen an Wasser durch ihre Körper und entfernen dabei sehr effizient Mikroben und andere organische Partikel, die sie als Nahrung nutzen. Gleichzeitig gehen sie enge Symbiosen mit Mikroben ein, die in ihren Körpern leben. Bisherige Beobachtungen zeigen, dass Schwämme symbiotische und nicht-symbiotische Bakterien mit unterschiedlicher Effizienz filtrieren und legen daher nahe, dass sie zwischen verschiedenen Bakterien unterscheiden können. Die molekularen und zellulären Mechanismen, die es Schwämmen ermöglichen Bakterien zu erkennen und zwischen Nahrung, Symbionten, und Krankheitserregern zu unterscheiden, bleiben ein Rätsel. Zu Beginn der Dissertation war daher der erste Schritt die bis dato bekannten Immunmechanismen, die für eine Kommunikation zwischen Schwämmen und Mikroben essentiell sind, zusammenzufassen (Busch et al 2023; Kapitel 1). Auf der molekularen Ebene spielt wahrscheinlich ein diverses Repertoire an Schwammimmunrezeptoren eine Rolle bei der Erkennung und Unterscheidung von Mikroben. Auf der zellulären Ebene scheint es, dass Phagozytose ein wichtiger Mechanismus ist. Allerdings gibt es in beiden Fällen nur wenige experimentelle Daten, die diese Annahmen bestätigen. Daher war es das Ziel dieser Dissertation experimentell die molekularen und zellulären Mechanismen, die es Schwämmen erlaubt zwischen verschiedenen Mikroben zu unterscheiden, aufzuklären. Hierzu wurden Schwämme in Inkubationskammern verschiedenen Mikroben ausgesetzt, um ihre molekularen sowie zellulären Antworten zu charakterisieren. Dieser Versuchsaufbau wurde gewählt, da er das natürliche Filtrierverhalten der Schwämme berücksichtigt und somit ihre Reaktionen denen von wilden Individuen weitmöglichst ähneln.

An den zwei Mittelmeerschwämmen *Aplysina aerophoba* und *Dysidea avara* wurden molekulare Mechanismen der Reaktion auf symbiotische und nichtsymbiotische Seewasserbakterien durch Transkriptionsequenzierung und differentielle Genexpressionsanalyse untersucht (Marulanda-Gomez et al., under revision; Kapitel 2). *A. aerophoba* beherbergt eine große Dichte an assoziierten Mikroben (high microbial abundance = HMA), wohingegen *D. avara* eine geringe Anzahl an Mikroben (low microbial abundance = LMA) aufweist. Die Kombination dieser beiden Arten erlaubt es daher zu ergründen, ob der HMA-LMA Status Auswirkungen auf die Immunantwort des Schwammes hat. Beide Arten zeigten eine gering ausgeprägte transkriptionelle Antwort (weniger als 70 differentiell exprimierte Gene) auf die getesteten Bakterien, die sich jedoch zwischen den Arten unterschied. Der HMA Schwamm *A. aerophoba* zeigte nur eine sehr geringe Anzahl an differentiell exprimierten Genen und keine Aktivierung von Immunrezeptoren. Im Gegensatz dazu wurden im LMA Schwamm *D. avara* mehrere Genedifferentiell exprimiert, insbesondere solche des Nucleotide Oligomerization Domain (NOD)-Like-Receptors (NLRs). Diese Beobachtungen legen nahe, dass in Schwämmen die Unterscheidung zwischen Bakterien von dem Repertoire an Immungenen des Wirtstiers, sowie deren Aktivierung gesteuert wird. Außerdem ist es plausibel, dass die unterschiedliche Antwort der zwei getesteten Schwämme auf Bakterien von einer Kombination aus artspezifischen Eigenschaften, sowie des HMA-LMA Status beeinflusst wird.

Auf zellulärer Ebene wurde Phagozytose als Mechanismus zur Unterscheidung von Bakterien untersucht. Ein in-vivo Phagozytoseassay wurde mit dem Ostseeschwamm *Halichondria panicea* (LMA) etabliert. Hierzu wurden (1) Schwämme mit fluoreszierenden Partikeln (natürlichfluoreszierende Mikroalgen, gefärbte Bakterien, oder fluoreszierende Latexpartikel) inkubiert, (2) die Schwammzellen anschließend dissoziiert, und (3) mit Hilfe von fluorescence-activated cell sorting (FACS) die Aufnahme der verschiedenen fluoreszierenden Partikel in Schwammzellen (wird von jetzt an als Phagozytose bezeichnet) quantifiziert (Marulanda-Gómez et al., 2023, Kapitel 3). Die Ergebnisse zeigten, dass Phagozytose in Schwämmen ein schneller Prozess ist, der innerhalb weniger Minuten nach dem Kontakt mit fluoreszierenden Partikeln nachgewiesen werden kann. Mit Hilfe von Fluoreszenz- und Transmissionselektronenmikroskopie konnte außerdem die Aufnahme von Partikeln in die Schwammzellen bestätigt werden, sowie Informationen bezüglich der Zellgröße und des Zelltyps der phagozytierenden Schwammzellen gesammelt werden. Die meisten Partikel

wurden innerhalb von 30 min von Choanozyten-ähnlichen Zellen aufgenommen, und schienen nach 60 min an Archaeozyten-ähnliche Zellen weitergegeben worden zu sein (möglicherweise zur Verdauung). Der etablierte Assay wurde darüber hinaus verwendet um die phagozytäre Antwort von *H. panicea* auf einen assoziierten („eigenen“) und einen nicht assoziierten („fremden“) *Vibrio* zu vergleichen (Marulanda-Gómez et al., in preparation, Kapitel 4). Phagozytose wurde wie zuvor mit FACS und Fluoreszenzmikroskopie, sowie einer zusätzlichen proteomischen Analyse untersucht. Die Aufnahme von *Vibrio* in die Schwammzellen unterschied sich nicht zwischen den beiden *Vibrio*-Isolaten. Allerdings gab es klare Unterschiede welche Zellen (Zellgrößen und -typen) an der Aufnahme der eigenen und fremden *Vibrios* beteiligt waren, was sich auch über die Zeit änderte. Außerdem wurde eine differentielle proteomische Antwort von *H. panicea* detektiert. Nach Phagozytose des fremden *Vibrio*-Isolates, wurde eine höhere Abundanz an Phagozytose-assoziierten Proteinen detektiert im Vergleich zum eigenen *Vibrio*-Isolat. Diese Ergebnisse deuten an, dass die Unterscheidung zwischen Bakterien in *H. panicea* nach der Aufnahme in eine phagozytierende Zelle stattfindet, und dass sich daraufhin die Weiterverarbeitung unterscheidet (z.B. Verdauung versus Ausscheidung ins Mesohyl durch Vomozytose).

Zusammenfassend bestätigen die verschiedenen experimentellen Herangehensweisen in dieser Dissertation, dass (1) Schwämme zwischen verschiedenen Mikroben unterscheiden können, und dass (2) diese Unterscheidung wahrscheinlich von der Art und/oder dem HMA-LMA Status des Schwammes beeinflusst wird. Des Weiteren scheint es, dass (3) Phagozytose zunächst ein willkürlicher Prozess ist, und dass (4) die Unterscheidung nach der Internalisierung stattfindet, was dann über die Weiterverarbeitung (Verdauung versus Abgabe) entscheidet. Um das Zusammenspiel zwischen Schwämmen und Mikroben weiter zu entschlüsseln, schlage ich vor, den hier vorgestellten holistischen Ansatz aus molekularen, zellulären, und proteomischen Analysen weiter zu verfolgen, und bestenfalls mit direkten physiologischen Messungen des Schwammholobints zu ergänzen.

---

## General Introduction

---

## We live in a symbiotic world

Multicellular life originated billions of years ago in an intermediate oxidized ocean. Single-celled organisms dominated the anoxic deep-sea and the variable oxygenated surface waters. It was not until some 1.8 to 0.5 billion years ago that the evolution of eukaryotic stem-lineages (i.e., eukaryogenesis) commenced (Embley & Martin, 2006; Mills et al., 2022). A series of endosymbiotic associations between the cyanobacterial ancestors of chloroplasts and the  $\alpha$ -proteobacterial ancestors of mitochondria allowed the diversification of eukaryotes (Margulis, 1967; Zaremba-Niedzwiedzka et al., 2017). This first symbiotic acquisition has been one of the major evolutionary innovations of life on earth. But it was not until the 19th century that the term “symbiosis” was used for the first time in a biological context. The German botanist Heinrich Anton de Bary defined symbiosis as “a phenomenon in which dissimilar organisms live together” (Oulhen et al., 2016). From then onwards, our comprehension of symbiotic interactions has greatly expanded, and we continue to unravel how animals and plants establish close associations with microbial communities.

In the symbiotic system, the large partner is usually termed the “host” and the smaller partners are called “symbionts”. These synergistic partnerships between eukaryote (host) and microbes (symbionts) are known as “metaorganisms” or “holobionts” (Bosch & McFall-Ngai, 2011; Rosenberg & Zilber-Rosenberg, 2018). The host-symbiont genetic information is further considered as a unit of selection in evolution (i.e., the hologenome theory) which confers adaptive advantages to the holobiont (Zilber-Rosenberg & Rosenberg, 2008). This theory has been debated since observations of host-symbiont coevolution and symbionts evolution for the benefit of the host are not always the rule but rather depend on each particular case (Moran & Sloan, 2015). The main misconceptions of the hologenome theory that have been discussed include assumptions of (1) coevolution, based on parallel phylogenies (phylosymbiosis e.g., (Brucker & Bordenstein, 2013)) of host and symbionts, (2) codiversification, based on similarities of symbiotic communities between related hosts, and (3) selection favoring mutualistic traits, based on the highly intimate host-symbiont associations (Moran & Sloan, 2015). Hence, the parsimonious alternative to this theory is to assume that symbiotic interactions have not evolved from hologenome-selected traits, and instead to test in each case how selection acts on each of the entities (Moran & Sloan, 2015).

The symbiont assemblage is composed of a core microbiota of host-adapted microbes and of a flexible pool of microbes that varies with environmental conditions, and which differentially contributes to the host's fitness. The core symbionts may provide essential or house-keeping functions, while flexible symbionts may offer expanded genetic variation and greater potential for adaptation (Shapira, 2016). In general, the associated microbes provide essential nutrients, protection against pathogens, and signals that trigger developmental steps in the host (Bosch & McFall-Ngai, 2021; Rosenberg & Zilber-Rosenberg, 2016). For example, in the freshwater hydroid *Hydra* sp. the microbiome can modify several developmental processes such as head and bud formation, and differentiation of stem cells (Puntin et al., 2022; Taubenheim et al., 2020). Bacteria interactions also confer *Hydra* protection against fungal infections and are involved in the regulation of the host's body contractions (Fraune et al., 2015; Murillo-Rincon et al., 2017). Likewise, in mammals the symbiotic bacteria stimulate the development, growth, and maturation of immune and neuronal cells which promotes the health of the holobiont (Belkaid & Hand, 2014; Sharon et al., 2016). The health of the holobiont is however not determined merely by the functions of the individual members, but also their interactions with other microbial partners as well as with environmental factors. To illustrate, the microbial populations in coral holobionts are balanced by antagonistic interactions that result in population extinction (top-down control) and by resource limitation (bottom-up control). Competition for resources like nutrients, light and space can limit the growth of beneficial bacteria and promote the proliferation of opportunistic or pathogenic microbes which disrupts homeostasis of the holobiont leading to disease outbreaks (Thompson et al., 2014). The interactions of the symbiotic members within the holobiont environment can be considered as a complex individual ecosystem that in turn interacts with and affects other holobionts in a larger community context. Consequently, host-microbe interactions have cascading effects in the surrounding community and can further impact ecosystem integrity (termed "nested ecosystem" e.g., Pita et al. 2018a). Overall, homeostasis of the holobiont is ensured through the successful transmission, maintenance, and balanced regulation of symbionts along host generations.



## Host-microbe interplay

### The first encounter - Transmission of symbionts

The first interaction between the host and their associated microbes is during symbiont transmission. Transmission of symbionts can occur from parent to offspring (i.e., vertical), from the environment (i.e., horizontal), or through both (i.e., mixed-mode) (Ebert, 2013). Our understanding of the mechanisms behind microbiota transmission are based on systems involving primarily bacteria and some archaea. Such host systems include for example insects, annelids and nematodes for vertical transmission, and the bobtail squid (*Euprymna scolopes*) and the hydrothermal tubeworm (*Riftia pachyptila*) for horizontal transmission (Bright & Bulgheresi, 2010; Moran et al., 2008). Regardless of the transmission strategy, establishment of an intimate association between both partners requires physical contact of the host and the microbes at the right time and in the right place. Entry, acquisition and/or colonization, and maintenance of symbionts is often restricted to a specific host life stage, spatially limited, and involves sophisticated molecular and cellular machineries to sense and recognize each other (Bright & Bulgheresi, 2010). While microbes exhibit a combination of factors to manipulate their host and persist within it (Finlay & McFadden, 2006; McCutcheon, 2021), from here on, I focus on the host side of the interaction.

### The force driving sensing and recognition - Immunity

The first step in selection and maintenance of symbionts is the sensing and recognition of the microbe by the host. Immunity is now regarded as the driving force behind this selection process and not only as a defense system against invasive pathogens (e.g., (Bosch, 2014; Eberl, 2010; Gerardo et al., 2020)). The modern view of the immune system to be tolerant to “self” is still accepted, but the notion of what is considered “self” is modified. Symbionts are now proposed to be part of the “self”, which induce the activation of pattern recognition receptors (PRRs) in the host, but the inflammatory outcome differs from those trigger by injury or pathogens (Eberl, 2010). Microbe-associated molecules derived from symbionts elicit a physiological level inflammation that promotes symbiont colonization and homeostasis within the host, whereas exposure to infections agents induced pathological inflammation (Chu & Mazmanian, 2013; Eberl, 2010). Different immune recognition systems traditionally viewed as defensive army, interestingly also promote host-microbial symbiosis. For example, in the bobtail squid (*E. scolopes*) peptidoglycan recognition proteins aid in the establishment of the

symbiont *Vibrio fischeri* in the squid light organ and attenuate inflammatory responses (Troll et al., 2009). It is now accepted that the commonly perceived duality of “self” and “non-self”, beneficial and pathogenic microbes, and regulatory or inflammatory immunity are not but extremes of a continuous reality (Eberl, 2010), and thus host-microbe interactions are dynamic in space and time.

The interplay between host and symbionts also requires a high degree of specificity for distinguishing between the different microbial players. Contrary to the highly specific antibody-based adaptive immune system of vertebrates, invertebrates rely on a broad and non-specific immune system (i.e., innate immunity; Litman et al. 2005; Buchmann 2014). Yet, pattern recognition receptors (PRRs) of the innate immune system (e.g., Toll-like receptors (TLRs), NOD-like receptors (NLRs), and C-type lectin receptors (CTLRs)) orchestrate the invertebrate-microbe crosstalk (Dierking & Pita, 2020; Rosenstiel et al., 2009). Invertebrates also use other components of innate immunity, such as cellular mechanisms (e.g., phagocytosis) and humoral defenses (e.g. production of antimicrobial peptides or reactive oxygen species), to respond to microbial encounter (reviewed by Nyholm & Graf, 2012). Phagocytic cells are specialized in ingesting and eliminating particles larger than 0.5  $\mu\text{m}$  in diameter (Uribe-Querol & Rosales, 2020) and are known to be involved in symbiont recognition. Symbionts can escape phagocytosis, and thus ensure establishment and maintenance within the host (e.g., Jahn et al., 2019; Nguyen et al., 2014; Nyholm et al., 2009). Evasion of the host immune system by microbes may also include other mechanisms like toxin secretion, apoptosis modulation, signaling interference, among others (Reviewed by Finlay and McFadden 2006). Even though host immunity and symbionts seemed to be intertwined and might have influenced each other’s evolutionary trajectories (Gerardo et al., 2020), only recently the role of immunity in invertebrate-microbe interactions has started to be revealed.

### Phagocytosis as cellular mechanism to facilitate host-microbe interactions

Cell-autonomous defense mechanisms like phagocytosis initially originated as a means for nutrient acquisition and reallocation in unicellular amoeba and was later adapted in specialized immune cells, like macrophages, to fight pathogens (Dunn et al., 2018; Hartenstein & Martinez, 2019). Phagocytosis is a regulated cellular process for ingesting and eliminating large particles (> 0.5  $\mu\text{m}$  in diameter), including microbes, foreign substances, and apoptotic cells, into cytosolic, membrane-bound vacuoles called phagosomes (Fig 1).

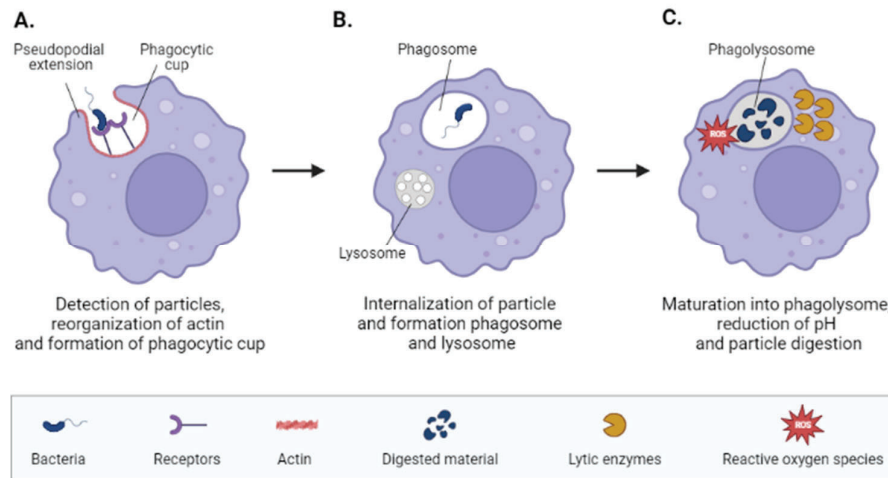


**Fig. 1.** Simplified steps of the phagocytic process. **A.** Detection and ingestion of particles. The phagocytic cell recognizes the target via receptors and remodels its actin filaments for encapsulating the bacteria. **B.** The bacteria reside inside the phagosome, which starts to mature producing ROS. **C.** The fusion of the phagosome with the lysosome results in the phagolysosome. In this acidic and oxidative organelle, bacterial degradation occurs via lytic enzymes. (Figure created in BioRender.com agreement number ZB250VAJ17).

The phagocytic process involves several orchestrated steps (reviewed by Levin et al., 2016; Uribe-Querol & Rosales, 2020). (1) Target particles to be ingested are detected by receptors on phagocytic cells. Once the particles are recognized, various signaling pathways are activated and the internalization process initiates. This involves reorganization of the actin cytoskeleton and depression of the cell membrane, which results in the formation of a phagocytic cup and pseudopodial extensions (Fig. 1 A). (2) These membrane protrusions fuse creating a new vesicle (i.e., the phagosome) containing the engulfed particle (Fig. 1 B). (3) The newly formed phagosome gradually matures into a phagolysosome by transforming its membrane composition and producing reactive oxygen species (ROS) that causes a decrease in pH (Fig. 1 C) Finally, the degradation of the ingested material takes place in the highly acidic and oxidative environment of the phagolysosome through the activity of lytic enzymes. The ultimate goal of this conserved cellular process is to ensure clearance of unwanted material and to maintain homeostasis within the host (Levin et al. 2016).

In host-microbe interactions, phagocytosis has been regarded as a key target for microbial manipulation. Strategies to evade phagocytosis, such as avoiding ingestion, interfering with phagosome maturation, resisting degradation, and even escaping from the phagosome, are well known for intracellular bacterial pathogens like e.g., *Legionella pneumophila* and

*Mycobacterium tuberculosis* (Flanagan et al., 2009; Uribe-Quero & Rosales, 2017). However, the mechanisms mediating host-microbe interactions concerning pathogens and symbionts are quite similar (Hentschel et al. 2000). Symbionts also interact with host phagocytosis, but rather than being eliminated, they are acquired and retained by the host (McCutcheon, 2021). This poses a challenge for the host: how to discriminate between pathogens to eliminate vs. symbionts to acquire? The validation of phagocytosis as a main mechanism for microbe discrimination has recently started to be deciphered in basal animals like amoeba and cnidarians (Bucher et al., 2016; Jacobovitz et al., 2021; Jauslin et al., 2021; Rosental et al., 2017; Sattler et al., 2013; Snyder et al., 2021), as well as other invertebrates such as mollusks and insects (Lamprou et al., 2005; Nyholm & McFall-Ngai, 2021; Roth & Kurtz, 2009; Tame et al., 2022), for which genetic manipulation, isolation of symbiont strains and/or utilization of cellular markers are possible. Studies in these organisms show that regulation of phagocytic activity varies based on the bacteria presented to the animal, but still relatively little is known about the mechanisms allowing symbiont persistence within the host.

### Host-microbe crosstalk in the marine realm

Marine holobiont research involves multiple levels of investigation, from understanding the complex mechanisms of communication between the host and its microbial partners and the implications of these interactions in the biogeochemical cycles, to predicting their effects on the holobiont health (i.e., homeostasis) and its repercussion at the ecosystem level (Pita et al., 2018a; Stévenne et al., 2021). Thus, an increasing number of key marine holobionts, such as cnidarians (Puntin, Craggs, et al., 2022; Wolfowicz et al., 2016), sponges (Hall et al., 2021; Pita et al., 2016), deep-sea tubeworms (Bright & Lallier, 2010; Dubilier et al., 2008; Hinzke et al., 2019), mollusks (McAnulty & Nyholm, 2017; Nyholm & McFall-Ngai, 2021), fish (Douglas, 2019; Kanther & Rawls, 2010), macroalgae (Wichard et al., 2015) and seagrasses (Tarquinio et al., 2019) have been studied over the past decades (Fig.2 A). Nevertheless, the number of model organisms for which reproducible methodologies can be applied to further characterize the functioning of holobionts, and who's associated microbes can be cultivated and manipulated in control environments is still rather limited (Jaspers et al. 2019). Certain marine invertebrates, particularly from the basal phyla Cnidaria and Porifera, have recently emerged as novel experimental systems for host-microbe studies (Fig. 2 B). The cnidarians candidates comprise for example the upside-down jellyfish *Cassiopea xamachana*. (Medina et al., 2021), the sea anemones *Nematostella vectensis*, *Exaiptasia* sp. and *Aiptasia* sp. (Rädecker et al.,

2018; Wolfowicz et al., 2016), and the coral *Galaxea fascicularis* (Puntin, Craggs, et al., 2022), whereas suitable experimental models in porifera include the sponge species *Amphimedon queenslandica*, *Petrosia ficiformes*, *Aplysina aerophoba*, *Dysidea avara*, *Halichondria panicea* (Cerrano et al., 2022; Degnan et al., 2008 Pita et al., 2016; Schmittmann et al., 2022). The research on these emerging model organisms is essential to better understand the role of marine holobionts in natural systems and their impact in ecological processes.

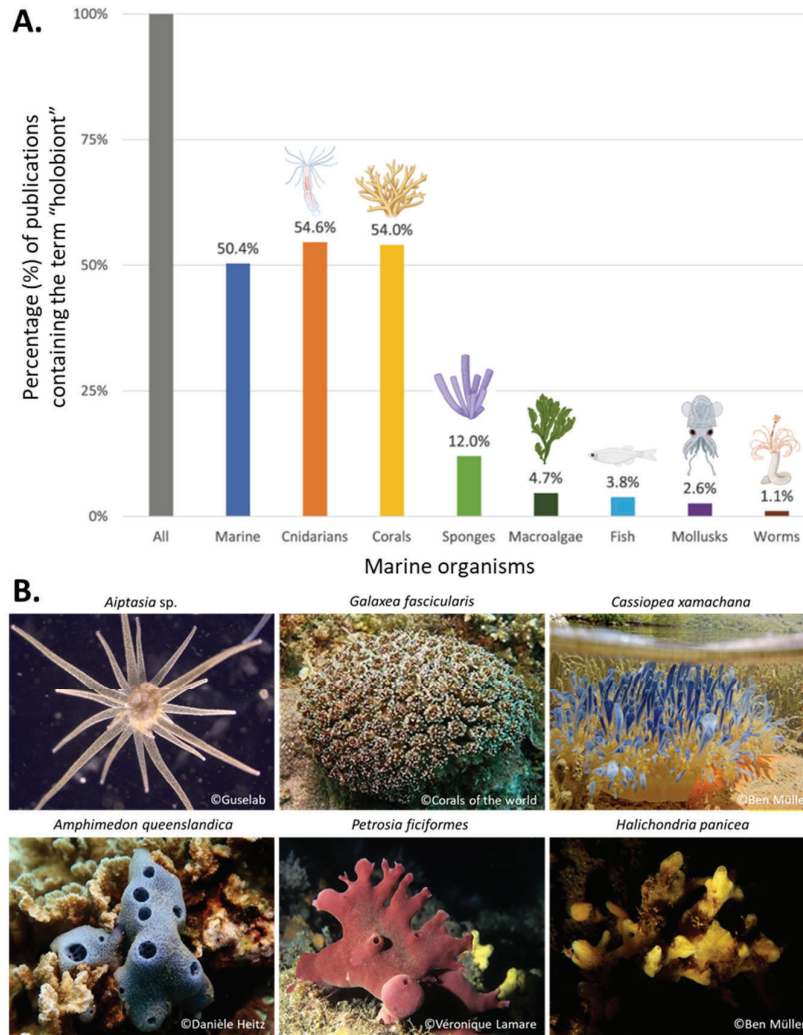


**Fig. 2.** Holobiont models in the marine environment. **A.** Marine publications with the term holobiont in the title, abstract, and/or keywords from 1990 to February 2021 (N = 1269). “All”: entirety of publications containing the term “holobiont” (100%). Other bars: percentage of publications within this list that contained terms related to a certain marine organism. Modified from Stévenne et al. 2021. **B.** Emerging marine model organisms for studying host-symbiosis interactions.

## Decoding host-microbe dialogue in sponges

### The sponge as an animal host

Sponges (phylum Porifera) emerged more than 600 million years ago, early in the Neoproterozoic era (Jackson et al., 2007; Turner, 2021). As sister group of all other metazoan lineages (Juravel et al., 2023; Redmond & McLysaght, 2021), sponges are ancient holobionts that might contain the keys to study the early evolution of animal-microbe symbiosis. This ancient phylum has diversified into more than 8500 species, currently classified into four classes: Demospongiae, Hexactinellida, Calcarea and Homoschleromorpha (van Soest et al., 2012, de Voogd et al. 2023). Demospongiae contains the largest number of described species and includes sponges with skeleton structures made of silica, organic fibers or fibrillar collagen (van Soest et al., 2012, and Systema Porifera). This class has successfully diversified and adapted to all aquatic realms, and thus can be found from freshwater ecosystems, to shallow tropical coral reefs, until the abysmal deep-sea (Maldonado et al., 2017). Demosponges grow in a variety of shapes, sizes, and colors. They can exhibit morphologies resembling thin leather-like encrusting layers (mm) to massive barrel forms (>1 meter). Sponges are abundant and integral components in many benthic communities. For example, in coral reefs 20 to 35% of the reef biomass is represented by sponges (Kornder et al., 2021), and in some deep-sea grounds sponges can constitute about 90% of the benthic biomass (Klitgaard & Tendal, 2004; Murillo et al., 2012). They provide habitat to other organisms and due to their ability to filter large quantities of water (up to 24000 L per sponge kg per day; Taylor et al., 2007; Vogel, 1977), sponges influence nutrient cycling both on the benthos as well as in the water column through benthic-pelagic coupling (Bell, 2008; Bell et al., 2020; Maldonado et al., 2017). Despite the rich biodiversity, global distribution, and multiple functional roles that sponges fulfill, they are often mistakenly consider “simple organisms”.

The misleading view of sponges as “simple animals” derives from the fact that they lack a strict tissue-level organization. Yet, a variety of cell types and skeletal structures (i.e., spicules) assembled the poriferan body plan into an efficient filtering system (Fig 3). Flat epithelial cells (i.e., pinacocytes) configure the outer sponge layer (i.e., the pinacoderm), whereas flagellated cells (i.e., choanocytes) make up their inner layer (i.e., the choanoderm). Enclosed between these two layers rests the mesohyl, a collagenous matrix in which various motile cell types are found (Boury-Esnault & Rutzler, 1997; Simpson, 1984, Funayama 2013) (Fig 3 B). Sponge cells

exhibit different morphologies and carry out specific functions. For example, sclerocytes and spongocytes secrete spicules and sponging fibers for maintaining the skeletal structure. Other fundamental sponge cells include: the archaeocytes, large totipotent amoeboid cells, with a well-defined nucleus, fulfilling digestive functions, and the choanocytes, which flagellum is surrounded by microvilli and are the basic pumping units in demosponges responsible for filtering food particles (Larsen & Riisgard, 1994; Leys & Eerkes-Medrano, 2006) (Fig 3 C). The filter feeding apparatus of sponges consist of a water-conducting system in which water flows into the animal through small pores (i.e., ostia) scattered along the pinacoderm, and is conducted into cavities lined by choanocytes (i.e., choanocyte chambers. Fig 3). Choanocytes create the water flow through the beating of their flagella and act as sieves for capturing bacterio- and phytoplankton, and other particulate organic material, most efficiently < 5  $\mu\text{m}$  in size (e.g., Hanson et al., 2009; Ribes et al., 1999). The filtered water runs along the aquiferous canals and exits through bigger openings (i.e., oscula) on the surface of the sponge (Riisgård & Larsen, 2010). The particles trapped by the choanocytes are transfer to the archaeocytes, which move around the mesohyl translocating the nutritive food to all other cells (Godefroy et al., 2019; Imsiecke, 1993). Apart from capturing food particles from the water column, choanocytes also take up dissolve organic matter (DOM) via macropinocytosis, or “cellular drinking”. The internalization of DOM is a large-scale and unspecific process (Achlati et al., 2019; Rix et al., 2020, Hudspith 2022), and can in some cases account for over approx. 50-90% of the sponge diet (Bart et al., 2021; De Goeij et al., 2008; Yahel et al., 2003).

The endocytic uptake of food particles is facilitated through phagocytosis. The main phagocytic cells driving particle incorporation and digestion in sponges are pinacocytes, choanocytes and archaeocytes (Simpson, 1984; Steinmetz, 2019) (Fig 3C.). Pinacocytes can capture large particles (> ostia) by filopodial extensions and intracellularly digest them to presumably prevent clogging of the filtering system (Frost, 1976; Harrison, 1972; Willenz & Van de Vyver, 1984). Choanocytes share several ultrastructural commonalities with choanoflagellate protists, such as the organization of the flagellum and microvilli, and the presence of heavily amoeboid protrusions. The former structures have evolved to influence the local hydrodynamics, and the latter to capture and phagocytized bacteria (Laundon et al., 2019). Archaeocytes, sometimes also referred as amoebocytes, are mainly recognized to function as stem cells in sponges (Funayama, 2013), but they are also involved in intracellular

digestion and transfer of food or particles to the rest of the cells (Imsiecke, 1993; Maldonado et al., 2010; Turon et al., 1997).

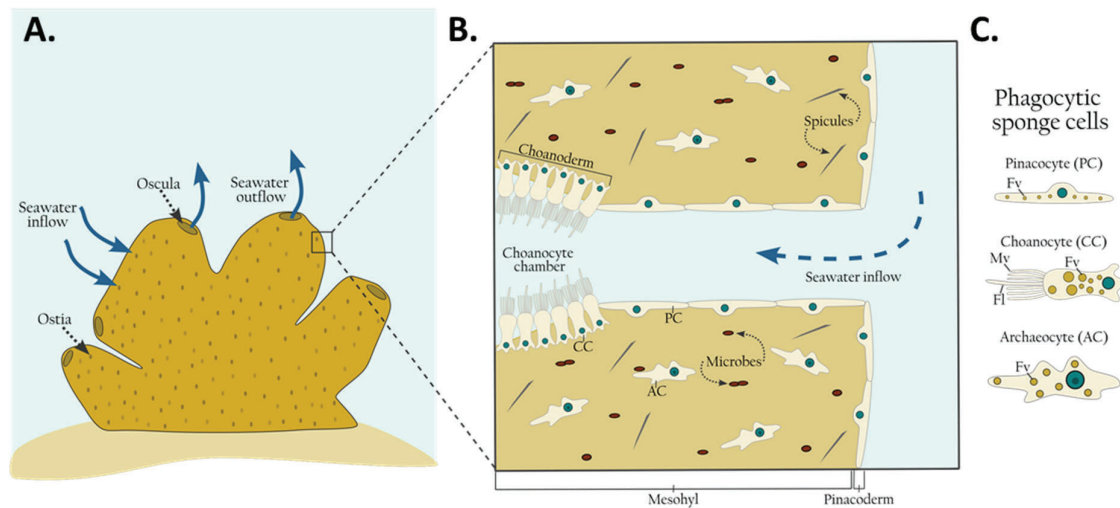


**Fig. 3.** Simplified scheme of sponge body organization of a low microbial abundance (LMA) species. **A.** Seawater entering and exiting the sponge body and **B.** close-up view of the internal structure of a demosponge (based on Hentschel et al. 2012.). The water enters the sponge through the ostia, reaches the choanocyte chambers where food particles are captured choanocytes (CC), and then transferred to the mesohyl where they are processed by archaeocytes (AC). **C.** Typical phagocytic sponge cells involved in particle uptake and digestion. fl: flagella; fv: food vesicle; mv: microvilli (based on Steinmetz 2019).

Due to the absence of a gut, digestion of particles occurs intracellularly in sponges and may imply that digestion and immune functions are closely related in this phylum. The connection between intracellular digestion and immune defense was already noticed over a century ago by Metchnikoff, who proposed that phagocytic immune cells evolved from digestive cells (Tauber, 2003). Even though it is thought that the immune system evolved parallel to the gut to protect the digestive tract, there is an alternative view which proposed that immunity and digestion were indistinguishable in the primitive gut (Broderick, 2015). Although both choanocytes and archaeocytes play a role in sponge phagocytosis, it has been proposed that the context in which they operate may differ. From a phylogenetic point of view, choanocytes are regarded as “enteric phagocytes” (i.e., intestinal-like cells) whose main purpose is food digestion and nutrition. Archaeocytes on the other hand are considered macrophage-like cells specialized in digestion of foreign material that might represent a threat for the animal (Hartenstein & Martinez, 2019). Single-cell RNA analysis in two sponge species, of which one



was the methodologically advanced freshwater sponge species, *Spongilla lacustris*, confirmed that choanocytes and archaeocytes form separate cell clusters and exhibit distinctive expression of gene markers (Musseret et al. 2021; Sebé-Pedrós et al. 2018). Choanocytes were classified in the cluster of digestive cells, which reflected the expression of genes related to phagocytic vesicle and lytic vacuoles. In contrast, archaeocytes fall under the amoeboid-neuroid cluster and expressed genes associated to innate immunity (Musser et al., 2021). Despite the phagocytic activity of all these cell types, sponges still harbor a diverse community of microbes in their mesohyl that seem to circumvent cellular digestion.

### The sponge mesohyl and its microbial residents

Based on the abundance of microbes present extracellularly in their mesohyl, sponges can be categorized as either “high” or “low” microbial abundance (HMA/LMA) species (Hentschel et al., 2003; Vacelet & Donadey, 1977). HMA sponges contain symbiont densities reaching  $10^8 - 10^{10}$  bacteria per gram of sponge wet weight (Fig. 4 A), which surpasses seawater concentrations by 2 – 4 orders of magnitude (Hentschel et al., 2006). In contrast, microbial densities in LMA sponges are close to those of seawater ( $10^5 - 10^6$  bacteria per gram of sponge wet weight) (Hentschel et al., 2006) (Fig. 4 B). This so-called HMA-LMA dichotomy has a phylogenetic basis on the sponge species and genera level, but blurs on higher taxonomic levels. Yet this dichotomy is rather considered as two basic life strategies with further physiological, morphological, and metabolic differences (Gloeckner et al., 2014; Maldonado et al., 2012; T. Morganti et al., 2017; Rix et al., 2020; Weisz et al., 2008). For example, HMA sponges are frequently characterized by a denser mesohyl, a longer and narrower aquiferous system, and smaller and less abundant choanocyte chambers resulting in on average lower pumping rates compared to LMA sponges (Boury-esnault et al., 1990; Poppell et al., 2014; Vacelet & Donadey, 1977; Weisz et al., 2008). Additionally, HMA sponges harbor more diverse, stable, and different microbial communities than their LMA counterparts (Moitinho-Silva et al., 2017). Certain microbial phyla, such as *Chloroflexi*, *Poribacteria*, *Actinobacteria*, *Acidobacteria*, and *Gemmatimonadetes*, are overrepresented in HMA compared to their LMA counterparts. On the other hand, taxa overproportionally abundant in LMA sponges include *Proteobacteria*, *Bacteroidetes*, *Planctomycetes*, and *Flavobacteria* (Bayer et al., 2014; Moitinho-Silva et al., 2017; Pankey et al., 2022).

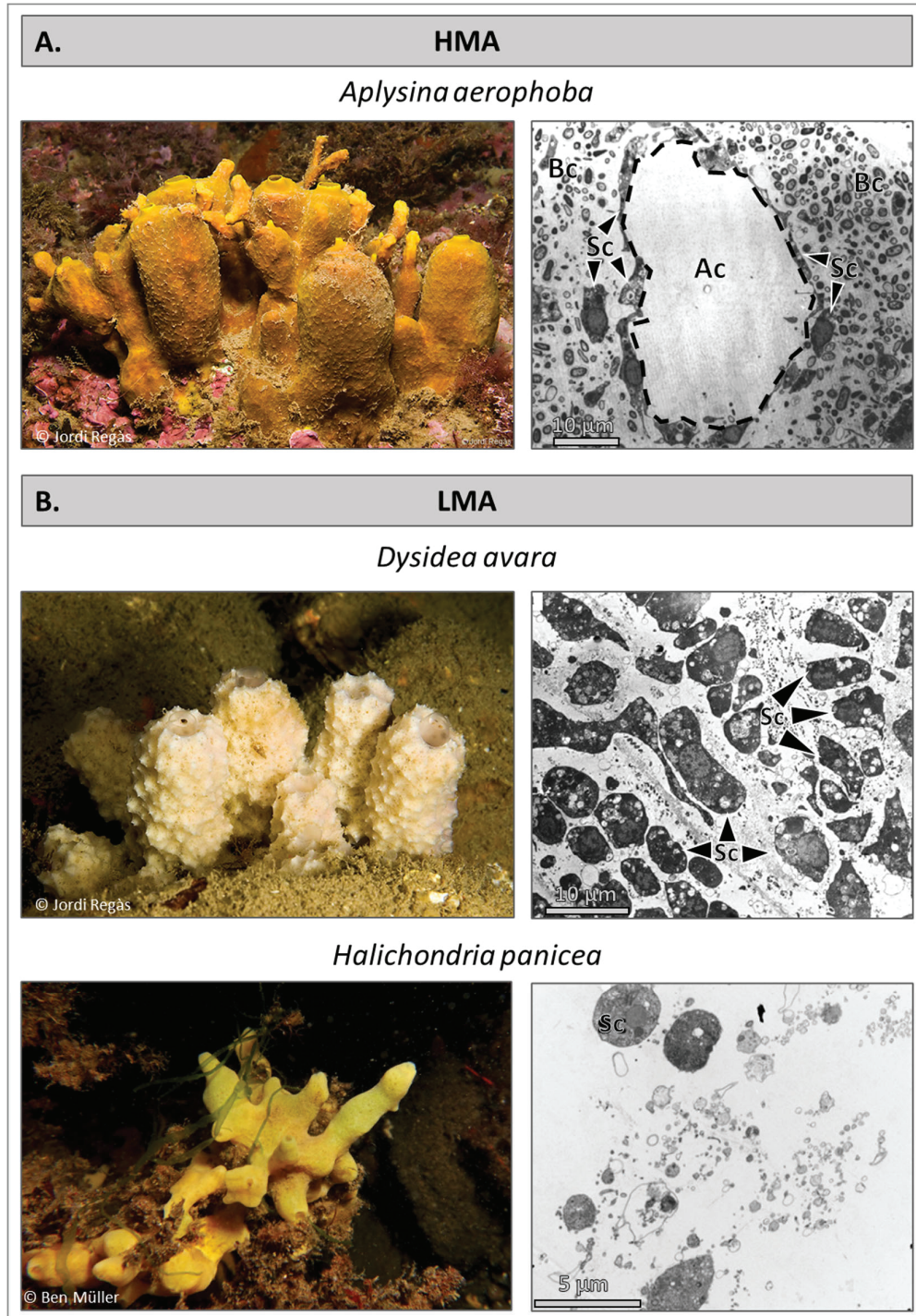


**Fig. 4.** Examples of **A.** HMA and **B.** LMA sponge species used in this thesis. Left: underwater photographs of the sponge individuals in the field. Right: transmission electron microscopy (TEM) pictures showing an overview of the sponges mesohyl and sponge cells. The sponge microbial community is only shown for the HMA sponge. Aq: aquiferous canal; Sc: sponge cell; Bc: bacteria cell. TEM pictures modified from Wehr 2007 and Moitinho-Silva et al. 2017.

Functional characterization of the sponge microbiome was initially challenging due to the inability to cultivate most symbiont taxa and to the lack of an established experimental sponge model. However, the combination of experimental approaches, 16S rRNA, and metagenomics analysis (reviewed by Freeman et al., 2021; Thacker & Freeman, 2012; Webster & Thomas, 2016) has generated first insights into the benefits that symbionts provide to their sponge hosts. Sponge symbionts are involved in metabolic process including carbon and nitrogen fixation, methane oxidation, sulfate reduction, synthesis of vitamins, and production of secondary metabolites for chemical defense (Engelberts et al. 2020; Hudspith et al. 2021; Jensen et al. 2017; Lackner et al. 2017; Moreno-Pino et al. 2021; Ramírez et al. 2023; Rubin-Blum et al. 2019; Song 2021). Overall, the genetic repertoire of sponge microbial communities not only expands the host metabolic capacity (e.g., nutritional specialization of carnitine, sulfate polysaccharides and taurine (Moeller et al., 2022; Slaby et al., 2017)), but also displays distinctive features necessary to colonize and persist within the sponge (Pita et al., 2018b).

### Symbiont persistence in the sponge mesohyl

Most sponge symbionts reside extracellularly within the sponge mesohyl with the host cells, albeit some symbionts also occur intracellularly in specialized cells named bacteriocytes (Cerrano et al., 2022; Maldonado et al., 2012; Vacelet & Donadey, 1977). The acquisition of the microbial associates can be by either horizontal transmission, vertical transmission, or a mixture or both, and these strategies can shift depending on the sponge species and on its developmental stage (reviewed by Carrier et al., 2022; Cristina Díez-Vives et al., 2022). In order to persist within the sponge, symbionts must avoid phagocytosis by the host. Compared to free-living microbes, sponge-associated bacteria have been observed to be enriched for example in eukaryotic-like proteins (ELPs) (Burgsdorf et al., 2015; C. Díez-Vives et al., 2017; M. Liu et al., 2012), or depleted in flagellin (Siegl et al., 2011) and lipopolysaccharide (LPS) antigens (i.e., O-antigen; Burgsdorf et al., 2015). These genetic features could represent a way for the symbionts to evade recognition by host cells (Schmittmann et al. 2020). For instance, the expression of ELPs (i.e., ankyrin repeat proteins) have been shown to modulate bacterial internalization and intracellular survival in freshwater amoeba and in murine macrophages (Jahn et al., 2019; Nguyen et al., 2014). Validation of the aforementioned genetic features is still missing for sponges, mainly due to the lack of well-established in-vivo experimental sponge models. Yet, in-vitro experimentation has greatly advanced, for example with the development of protocols for sponge cell cultures (Conkling et al., 2019; Munroe et al., 2019),

which ultimately led to the establishment of the first continuous marine sponge cell line (Hesp et al., 2023). Despite these advances in sponge cell biology, our understanding on the role of phagocytosis in sponge-microbe interactions is still in its infancy. Exploring this research frontier could provide insights into how symbionts are acquired by the sponge and are able to persist within the host.

## Research gap

Particle selection in sponges has been investigated for at least forty-five years, and was initially considered to be a non-selective process (Bergquist 1978). However, only a few years later first observation of bacteria discrimination by sponges came to light, which showed that sponges positively select for seawater bacteria and negatively select for symbionts (Wilkinson et al., 1984). Approximately a decade later, a second observation supported the differential uptake of microbial seawater consortia compared to symbiont consortia (Wehrl et al., 2007). Despite these promising foundations in the field of sponge-microbe interactions, research on the symbiont side of the interaction has surpassed our understanding of the role of the host. Our knowledge on the unique interactions with diverse microbial communities, including archaea, bacteria, fungi and viruses (Laffy et al., 2018; Naim et al., 2017; Steinert et al., 2020; Thomas et al., 2016), the means how they are transmitted (Carrier et al., 2022; Cristina Díez-Vives et al., 2022), the relation between this diversity and the host metabolism and physiology (Hudspith et al., 2021; Morganti et al., 2017; Rix et al., 2020), and the repercussions of these interactions at the ecosystem level has greatly expanded (Campana et al., 2021; J. de Goeij et al., 2017; Feng & Li, 2019; Maldonado et al., 2021). Yet, the main focus was on the symbiont perspective whereas the role played by the sponge host in this crosstalk has only recently started to be deciphered. A main challenge for studying the sponge side of the interaction has been the establishment of experimental sponge models (Pita et al., 2016). Efforts to improve experimental methods for better understanding sponge-microbe interactions include the manipulation of sponge microbiomes via recolonization and infection experiments (e.g., (Geraghty et al., 2021; Schmittmann et al., 2022)). Furthermore, experimental approaches together with high-throughput sequencing data have revealed that sponges also rely on components of the immune system to sense its surrounding and microbial cues (Geraghty et al., 2021; Koutsouveli, Manousaki, et al., 2020; Pita et al., 2018b; Schmittmann et al., 2021;

Yuen, 2016). However, the underlying molecular and cellular mechanisms of microbial recognition by sponges remain understudied.

On the molecular side, genomic and transcriptomic data in sponges has disclosed high diversity of immune receptors, which resembled great similarity to vertebrate receptors (Dierking & Pita, 2020; Posadas et al., 2021; Riesgo et al., 2014; Ryu et al., 2016; Wu et al., 2022; Yuen, 2016). The conserved domain structure and diversification of some of these receptors indicate that they could be relevant components in the sponge-microbe crosstalk (Degnan, 2015). Currently, there are limited experimental studies characterizing the immune genes involved in the sponge response to microbial cues (e.g., (Geraghty et al., 2021; Pita et al., 2018b; Schmittmann et al., 2021)) and the functional validation of these genes is still lacking.

On the cellular side, early observations of sponge microbial discrimination (Wehrl et al. 2007; Wilkinson et al 1984) pointed to phagocytosis as a key cellular process in sponge-microbe interactions. In recent years, experiments using experimental models closely related to sponges (such as *Acanthamoeba castellanii* (Nguyen et al., 2014) and murine cell lines (Jahn et al., 2019)) revealed that bacteria encoding ankyrin-repeat proteins are capable to evade phagocytosis. Although phagocytosis appears to be an important cellular mechanism involved in the establishment and maintenance of symbioses, knowledge on the control of this mechanism by sponge cells (host) or its manipulation by the bacteria (symbionts) is still missing.

## Thesis Aims and Outline

The **overarching aim** of my thesis was to **elucidate molecular and cellular immune mechanisms that enable sponges to discriminate between microbes and maintain a stable and species-specific microbiota.**

I begin my thesis with a compilation of the current knowledge on sponge immunity (**Chapter 1**). Then, I present experimental approaches for studying the sponge response upon microbial encounters. The Mediterranean sponges *Aplysina aerophoba* (HMA) and *Dysidea avara* (LMA) (Fig. 4 A-B) served as models to investigate the molecular mechanisms involved in bacteria recognition (**Chapter 2**). The Baltic sponge *Halichondria panicea* (Fig. 4 B) was used to establish a quantitative phagocytic assay (**Chapter 3**) that could be apply to explore the role of this cellular mechanism on the response to different types of microbes (**Chapter 4**). The following research aims were identified for each chapter:

**Chapter 1:** Review the current knowledge on the sponge immune system.

**Chapter 2:** Characterize the sponge transcriptomic response of two Mediterranean sponges upon encounter with seawater and symbiont microbial consortia by means of RNA-Seq differential gene expression analysis.

**Chapter 3:** Develop a quantitative *in-vivo* phagocytosis assay in the emerging model sponge *H. panicea* by combining live animal incubations using natural (microalgae and bacteria) and inert particles (latex beads) with fluorescence-activated cell sorting (FACS) and microscopy observations.

**Chapter 4:** Apply the phagocytic assay, microscopy inspections and a proteomic approach to investigate the sponge's phagocytic response upon a native sponge-associated and a foreign non-sponge associated bacteria isolate.

## Main Chapters

This thesis is composed of the following chapters which have already been published or are manuscripts in preparation.

### Chapter 1: The sponge immune system

Section of the book chapter: Busch K\*, **Marulanda-Gómez A.\***, Morganti T., Bayer K., Pita L. Chapter 3. Sponge symbiosis: microbes make an essential part of what it means to be a sponge. (In press). In: *Invertebrate Physiology*, CRC press (Hard ISBN: 9781774914007; E-Book ISBN: 9781003403319). \*Equal contribution.

Preprint available at Figshare: <https://doi.org/10.6084/m9.figshare.23566275.v1>

Participation in	Author initials, responsibility decreasing
Study design	LP/KB, <b>AM</b>
Manuscript writing	<b>AM</b> /LP/KB/TM/KrB
Manuscript reviewing	LP/KB/ <b>AM</b> , TM/KrB

### Chapter 2: Molecular response of Mediterranean sponges upon bacterial encounter

**Marulanda-Gómez A.**, Ribes M., Franzenburg S., Hentschel U., Pita L. Transcriptomic response of Mediterranean sponges upon encounter with seawater or symbiont microbial consortia. Submitted to Genome Biology Evolution (GBE).

Pre-print available at bioRxiv.com doi: 10.1101/2023.11.02.563995v1

Participation in	Author last names, responsibility decreasing
Study design	LP/UH
Method development	LP
Experimental work	LP
Data analysis & interpretation	<b>AM</b> /LP
Manuscript writing	<b>AM</b> /LP, UH
Manuscript reviewing & editing	<b>AM</b> /LP/UH, MR/SF

**Chapter 3:** A novel in-vivo phagocytosis assay to gain cellular insights on sponge-microbe interactions

**Marulanda-Gómez A.**, Bayer K., Pita L., Hentschel U. 2023 A novel in-vivo phagocytosis assay to gain cellular insights on sponge-microbe interactions. *Frontiers in Marine Science, Section Microbial Symbioses*, 10. doi: 10.3389/fmars.2023.1176145

Participation in	Author last names, responsibility decreasing
Study design	AM/LP/UH
Method development	AM/KrB
Experimental work	AM
Data analysis & interpretation	AM, LP/UH, KrB
Manuscript writing	AM, LP/UH
Manuscript reviewing & editing	AM, LP/UH, KrB

**Chapter 4:** Characterization of sponge phagocytosis upon native and foreign *Vibrio* encounter in the breadcrumb sponge *Halichondria panicea*

**Marulanda-Gómez A.**, Mueller B., Bayer K., Abukhalaf M., Tholey A., Pita L., Hentschel U. (in preparation).

Participation in	Author last names, responsibility decreasing
Study design	AM/BM/KrB/LP/UH
Method development	AM/KrB, MA
Experimental work	AM/BM
Data analysis & interpretation	AM/BM, MA/AT, LP/UH/KrB
Chapter writing	AM, BM/LP, UH/KrB
Chapter reviewing & editing	AM, BM/LP/UH, MA/KrB





---

# Chapter 1

## The Sponge Immune System

---

This thesis chapter is a section of the book chapter: Busch K<sup>1§</sup>, **Marulanda-Gómez A<sup>1§</sup>**, Morganti T.M<sup>2</sup>, Bayer K<sup>1</sup>, and Pita L<sup>1,3\*</sup>. Chapter 3. Sponge symbiosis: microbes make an essential part of what it means to be a sponge. (In press). In: *Invertebrate Physiology*, CRC press. Edited by Saleuddin S., Leys S.P., Roer R.D., Wilkie I.C. Copyright 2024 (Hard ISBN: 9781774914007; E-Book ISBN: 9781003403319). <sup>§</sup>Equal contribution. Preprint available at Figshare: <https://doi.org/10.6084/m9.figshare.23566275.v1>

## Differentiating friend from foe

Immunity is the capability of all multicellular organisms to defend themselves against foreign bodies (or “non-self”), including pathogens, while tolerating what belongs to the “self”. The ability of sponges to eliminate non-self particles was described for the first time more than 100 years ago by Elias Metchnikoff while investigating inflammation processes. Metchnikoff observed that sponge motile phagocytotic cells encapsulate foreign material within cell aggregates and then eliminate it (Metchnikoff 1893). Later on, transplantation experiments using sponge cell suspension and tissue fragments showed that sponges fuse with **autografts** and reject **allografts** (see **glossary**), (e.g., Hildemann et al., 1979; Moscona, 1968; Smith & Hildemann, 1986). Different **alloimmune responses** (see **glossary**) can bring allograft rejection. For example, when sponge cells from two different species were mixed, cells from the same species reaggregated only among them and formed **primmorphs** (see **glossary**), (e.g., Custodio et al., 1998). In tissue explants, some species responded to allografts by building physical barriers, while others mounted inflammatory responses to destroy the non-self tissue (e.g., Hildemann et al., 1979; Smith & Hildemann, 1986). These studies highlight the high precision of sponges for recognizing “self” from “non-self”.

In recent years, the holobiont concept and the ubiquity of animal-microbe interactions have challenged the traditional perspective of the immune system as a defense mechanism. Instead, immunity is now regarded as the guardian of **homeostasis** within the holobiont (see **glossary**). But how do animals conceal fighting pathogens while nurturing their microbiota? Immune receptors, signaling pathways, and antimicrobial peptides (AMPs) mediate the immune response to pathogen-derived as well as to symbiont-derived molecules; the former context produces inflammation, and the latter promotes tolerance (Chu & Mazmanian, 2013). To illustrate, in *Hydra* spp. polyps overexpressing the AMP periculin-1a were significantly less colonized by bacteria compared to controls (Fraune et al., 2010). This antimicrobial peptide-based protection strategy in *Hydra* was suggested to control and shape the microbial community during polyps development (Fraune et al., 2010). Another example comes from the symbiosis between the Hawaiian squid *Euprymna scolopes* and the bioluminescent bacterium *Vibrio fischeri*, in which symbiont-derived molecules induce a sequence of events to promote colonization and direct the development of the host light organ (reviewed in Nyholm and McFall-Ngai, 2021). Although the exact underlying control mechanisms for specificity remain largely unknown, increasing evidence shows that the immune system is essential for

establishing and maintaining host-microbe interactions within the holobiont (Bosch, 2014; Gerardo et al., 2020; Kitano & Oda, 2006; McFall-Ngai, 2007; Nyholm & Graf, 2012).

In sponges, the filter-feeding lifestyle might pose the need for them to distinguish between food, pathogens, and symbionts. The early evidence of specific microbial recognition by sponges came from the pioneering immunological compatibility experiments of Wilkinson in the early 1980's (Wilkinson, 1984). He demonstrated different agglutination reactions of bacteria in sponge antisera, depending on the isolation source and phylogeny of the bacteria (Wilkinson, 1984). Wilkinson et al. were also the first to provide evidence that sponges discriminate between seawater bacteria and sponge-associated bacteria (1984). By incubating sponges *in situ* with tritium-labelled bacteria and tracking the bacteria in the sponge tissue using high-resolution radioautography, the authors showed that seawater bacteria were retained by the sponge and frequently found in vacuoles of choanocyte and pinacocyte cells, whereas sponge-associated bacteria were expelled in the exhalant current and rarely incorporated into any sponge phagocytic cell (Wilkinson et al., 1984b). Decades later, Wehrl et al. (2007) built on this work and performed further feeding experiments using culturable marine bacteria (i.e., defined as food bacteria), microbial seawater consortia, and sponge symbiont consortia. The estimated uptake rates of seawater microbes were nearly two orders of magnitude higher compared to symbionts, whereas there was no obvious discrimination among the different types of food bacteria or the different strains of symbionts (Markus Wehrl et al., 2007). These studies demonstrated the capacity of sponges to differentiate between their own bacterial symbionts and food bacteria.

Despite this promising start, the field of sponge symbiosis has focused on the microbial side of the interaction and for long time the role of the sponge host in the symbiosis remained overlooked. How immunity regulates sponge-microbe crosstalk is an emerging frontier of research. In the following section, we will present the current knowledge on the cellular and molecular mechanisms involved in sponge-microbe interactions.

## Immunity in sponge-microbe interactions - Cellular mechanisms

Phagocytosis is a universal and conserved mean of both nutrition and internal defense in the animal kingdom (reviewed by Hartenstein & Martinez, 2019); but it also plays a role in symbiosis (McFall-Ngai, 2007; Nyholm & Graf, 2012). The observations of sponge microbial discrimination point to phagocytosis as a key process to understand the relationship of sponges with microbes. Most of our current knowledge on sponge phagocytosis comes from feeding experiments, which measured clearance rates, examined the fate (i.e., ingestion and digestion process) of different bacteria and particles, and used microscopy observations to identify the cells involved in phagocytosis (e.g., Imsiecke, 1993; Leys & Eerkes-medrano, 2006; Maldonado et al., 2010; Weissenfels, 1976). In the deep-sea sponge *Geodia barretti* (Bowerbank, 1858), electron micrographs revealed that around 4% of the sponge's symbionts were phagocytized by amoeboid cells, likely supplementing sponge's nutrition (Leys et al., 2018). Yet, it remains unclear if there is a real differentiation between immune and feeding phagocytosis in sponges, and to what extent these processes are involved in the discrimination of bacteria by the sponge. With amoeboid cells patrolling the sponge mesohyl, the ability to evade phagocytosis seems an evident prerequisite for symbionts to persist within the sponge holobiont.

In recent years, the first mechanisms for evasion of phagocytosis by sponge symbionts were revealed (Jahn et al., 2019; Nguyen et al., 2014) (Fig. 1). The genomes of sponge-associated bacteria are enriched in ARPs, when compared to free-living bacteria (e.g., Thomas et al., 2010). In human intracellular symbionts and intracellular pathogens, ARPs modulate host phagocytosis, facilitating infection and bacterial intracellular survival (e.g., Al-Khodor et al., 2008; Habyarimana et al., 2008; Pan et al., 2008). Based on the role of ARPs in other systems, Thomas et al. (2010) hypothesized that these proteins could represent a mechanism that mediates the discrimination of associated and non-associated bacteria in sponges. To test this hypothesis, Nguyen et al. (2014) used the free-living amoeba *Acanthamoeba castellanii* as a model organism to approximate sponge cell phagocytosis as it has physiological and structural similarities to amoebocytes. Genetically-modified *Escherichia coli* expressing sponge symbiont-derived ankyrin-repeat proteins, were phagocytized by *A. castellanii* but not digested. The bacteria accumulated in large vacuoles of the amoeba cells (Nguyen et al., 2014).

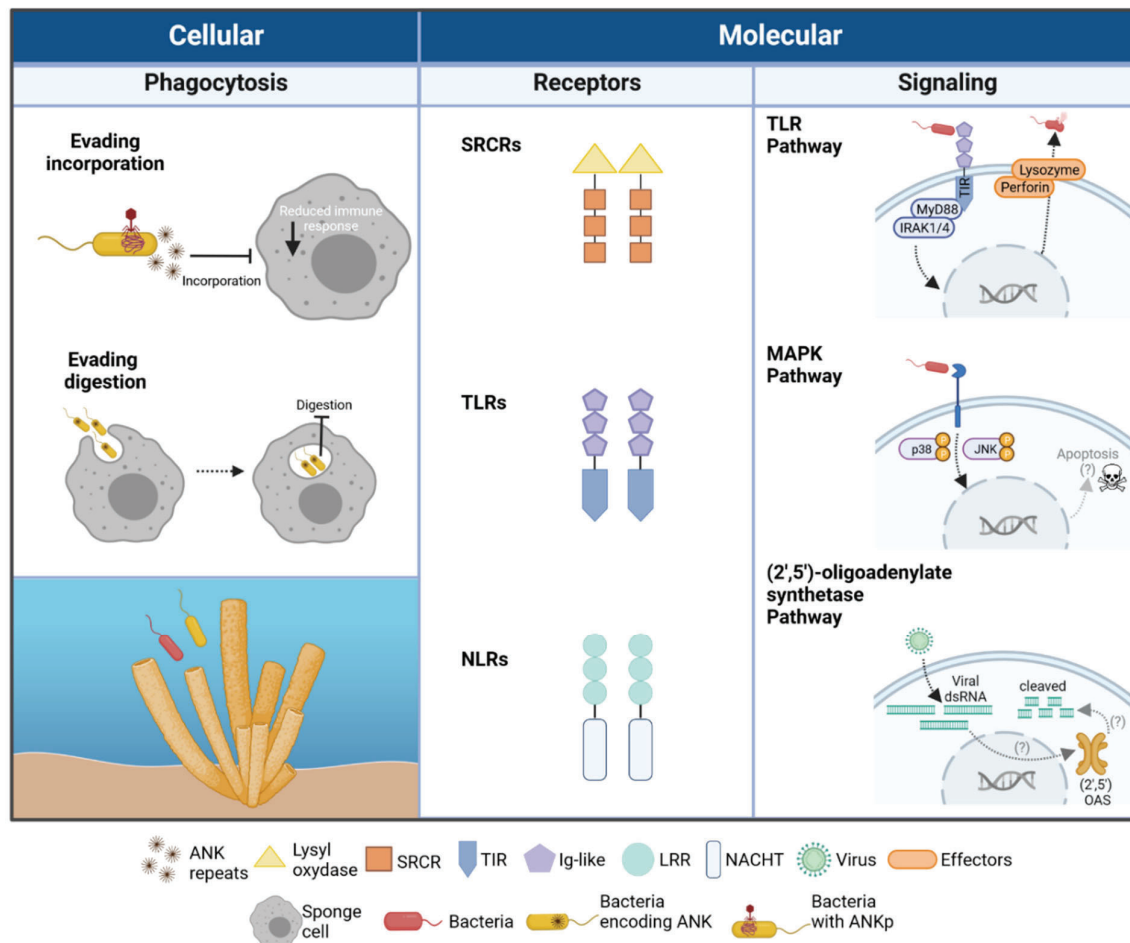


**Fig. 1.** Left panel: symbiont control on sponge phagocytosis, based on findings in Jahn et al., 2019 and Nguyen et al., 2014. Middle panel: main pattern recognition receptors in sponges, according to Hentschel et al., 2012. Right panel: exemplary signaling pathways involved in microbial recognition in sponges, reconstructed based on different studies (see text for references). Question marks represent the potential output of the pathway, inferred from gene annotation. (Figure created in BioRender.com agreement number II260V4H5F).

Further experimental evidence supporting the key role of ankyrin repeats in phagocytosis comes from a surprising finding. Sponge viromes comprised bacteriophages encoding proteins with auxiliary ankyrin repeats (termed “Ankyphages”) (Jahn et al., 2019). Bacteria decorated with the phage-encoded ankyrin repeat protein (i.e., ANKp) downregulated their proinflammatory signaling in human murine macrophages and escaped phagocytosis (Jahn et al., 2019). This study marks a milestone in the research of inter-kingdom interactions within the sponge holobiont (Jahn et al., 2019). Although phagocytosis seems to be an important cellular mechanism for the establishment and maintenance of symbioses, we are still missing the characterization on how bacteria manipulate this process in sponge cells.

## Immunity in sponge-microbe interactions - Molecular mechanisms

The molecular mechanisms of innate immunity rely on the recognition of microbe-associated molecular patterns (MAMPs) by pattern recognition receptors (PRRs), which activate signaling pathways that produce antimicrobial peptides and other effectors. PRRs sense a variety of MAMPs, such as lipopolysaccharide (LPS), peptidoglycan (PNG), or flagellin, which are absent in eukaryotic organisms; and they also detect damage signals coming from the animal cell (Janeway & Medzhitov, 2002). The next step after the receptors recognize and signal the occurrence of microbes or damaged cells is to eliminate the potential threats, repair tissue damage, or promote the tolerance of symbionts. Common effector pathways for eliminating infected or stressed target cells include cytokines and chemokines (Magor & Magor, 2001).

### Pattern recognition receptors

In sponges, genomic and transcriptomic data has revealed high diversity and complexity of Pattern Recognition Receptors (PRRs) remarkably similar in structure to vertebrate genes (Fig. 1). Among these, nucleotide-binding and oligomerization domain (NOD)-like receptors (NLRs), scavenger receptor cysteine-rich (SRCRs) domains, and a receptor type similar to toll-like receptors (TLRs) (Hentschel et al., 2012; Riesgo et al., 2014; Srivastava et al., 2010; Yuen et al., 2014). NLRs and SRCRs are highly diversified in sponges compared to other animal groups (Buckley & Rast, 2015). Another additional expanded receptor family in sponges are G-protein coupled receptors (GPCRs), which are not traditionally considered PRRs but appear to mediate sponge response to different stimuli (e.g., Guzman and Conaco, 2016; Pita et al., 2018b). Yet, the function of all these receptors in sponges is still poorly understood due to lack of experimental evidence. Despite this limitation, the conserved domain structure and diversification of some of the PRRs suggest that these receptors are good candidates for mediating the sponge-microbe crosstalk (Degnan, 2015).

The NLR genes are a family of PRRs characterized by the presence of a nucleotide-binding domain (NACHT) and a C-terminal leucine-rich repeat (LRR) domain. In sponges, NLRs are strikingly diverse. At least 135 NLR genes were identified in the Great Barrier Reef sponge *Amphimedon queenslandica* (Hooper & van Soest, 2006) (based on Yuen et al., 2014), in contrast to the 20 NLR genes in the human genome (which is almost 20 times larger than *A. queenslandica* genome) (Buckley & Rast, 2015). The reference transcriptome of the sponge *Dysidea avara* (Schmidt, 1862) also included a high abundance of NLRs (i.e., 80 *bona fide*

NLRs), of which two were activated in response to LPS and PNG (Lucía Pita et al., 2018). However, in the transcriptomes of other sponges, the repertoire of NLRs is less diverse (e.g., in *A. aerophoba* (Pita et al., 2018b) and in *Vaceletia sp.* (Germer et al., 2017)). Overall, the complex NLR repertoire in sponges and its similarity in structure with the vertebrate counterparts suggests their potential to recognize a broad spectrum of microbial ligands (Degnan, 2015).

The SRCR genes are a family of extracellular PRRs characterized by the presence of Scavenger Receptor Cysteine Rich domains, but their function is not necessarily conserved. In vertebrates, these cell surface or secreted proteins enhance the phagocytic clearance of microbes, environmental particles, and DNA (reviewed by Sarrias et al. 2004). The first report of a SRCR molecule in sponges was a macrophage class A scavenger receptor (SR-A) in the species *Geodia cydonium* (Linnaeus 1767), (based on Pancer et al., 1997) and its function was related to adhesion and cell recognition (Pahler et al., 1998). However, sponges host hundreds of genes within the SRCR family, that appear in combination with many different domains (Ryu et al., 2016). In *A. queenslandica* SRCR domains were enriched in the choanocytes (Sebé-Pedrós et al., 2018). Experimental work revealed that SRCRs take part in the sponge-microbe interactions. For example, *A. queenslandica* juveniles exposed to enriched bacterial suspensions showed differential gene expression of 60 SRC domains (Yuen 2016), and a SRCR domain-containing gene was also differentially expressed in *A. aerophoba* in response to MAMPs (Pita et al., 2018b). Gene screening on individuals of the Mediterranean sponge *Petrosia ficiformis* (Poiret, 1789) showed upregulation of one SRCR-domain containing gene in sponge harboring cyanobacterial symbionts, compared to aposymbiotic (i.e., cyanobacteria-free) specimens (Steindler et al., 2007). Like in vertebrates, most likely the SRCR genes in sponges play complex roles in immunity.

The TLR genes are transmembrane PRRs comprising an extracellular domain (i.e., LRRs: leucine-rich repeats), responsible for the recognition of MAMPs, and an intracellular domain (i.e., TIR: Toll/interleukin-1 receptor), in charge of inducing a signaling cascade. No conventional TLRs are found in sponges (reviewed in Hentschel et al., 2012). Sponges harbor genes containing a TIR domain, homologous to that in vertebrate TLRs (Riesgo et al., 2014), but it is associated with immunoglobulin (Ig) domains instead of the typical LRR motifs (reviewed in Hentschel et al., 2012). It remains unclear whether these type of receptors are



involved in the recognition of MAMPs, but all components of the TLR signaling cascade are present in the sponge (Riesgo et al., 2014).

### Signaling in response to microbial cues

The TLR pathway is one of the most important and well-characterized pathways contributing to innate immunity (Rosenstiel et al., 2009). TLRs recruit cytoplasmic TIR domain-containing adaptor proteins (e.g., MyD88: myeloid differentiation primary response 88 and TRIF: TIR-domain-containing adapter-inducing interferon- $\beta$ ), which trigger a downstream signal that leads to the activation of nuclear factor kappa B (NF- $\kappa$ B), interferon regulatory factors (IRFs), or mitogen-activated protein (MAP) kinases (Kawasaki & Kawai, 2014; Takeda, 2005).

Despite the different structure of poriferan TLRs, the major elements of the TLR pathway have been repeatedly reported in the genomes and transcriptomes of different sponge species (e.g., Germer et al., 2017; Pita et al., 2018b; Riesgo et al., 2014; Schmittmann et al., 2021). Experimental work supports the involvement of the TLR cascade in the sponges' response to MAMPs (Fig. 1). For instance, incubation of *Suberites domuncula* (Olivi, 1792) with LPS showed a strong up-regulation of the TLR adapter molecule MyD88 (Wiens et al., 2005). This adapter binds to a receptor on the sponge cell surface (i.e., LPS-interacting protein), which results in an elevated expression of a perforin-like executing molecule with antibacterial properties (i.e., a macro-phage protein) (Wiens et al., 2005). Moreover, exposing *S. domuncula* to a microbial lipoprotein (LP) revealed that a TLR-like receptor and an IRAK-4I protein are potential mediators of the LP-stimulated signal pathway in this sponge (Wiens et al., 2007). The expression of these two proteins leads to the expression of a caspase-like molecule and to the initiation of the apoptotic machinery (Wiens et al., 2007). Interestingly, TLR transcripts were more abundant in cells on the sponge surface and lining the aquiferous canals (Wiens et al., 2007). These studies demonstrated that sponges are equipped with a TLR-mediated defense mechanism against MAMPs, which ultimately might trigger apoptosis.

A second signaling pathway known to be involved in the response to LPS is the mitogen-activated protein kinase (MAPK) pathway (Fig. 1). *S. domuncula* possesses two MAPKs with high homology to the mammalian p38 and JNK protein kinases (82% and 75% similarity with humans, respectively) which showed to react upon ligation to LPS (Böhm et al., 2001; Böhm et al., 2000). A lectin was deduced to be the potential receptor responsible for activating this signaling cascade in sponge primmorphs (Schröder et al., 2003). Furthermore, differential

gene expression analysis also demonstrated that sponges respond to microbial elicitors by the transduction of signals mediated by serine-threonine protein kinases, which probably yield apoptosis and regulate metabolic processes (Pita et al., 2018b).

A third pathway also implicated in the immune system of sponges is the (2'-5') oligoadenylate synthetase [(2-5)A synthetase] pathway (Fig. 1). This is an efficient defense mechanism against invading microorganisms that is activated in the presence of certain classes of RNA, mainly double-stranded RNA (Kuuskalu et al., 1995). (2-5)A synthetases cloned from *S. domuncula*, *G. cydonium* and *Halichondria panicea* (Pallas 1766) exhibit high similarity with vertebrate enzymes, and the level and activity of these enzymes increase after bacterial infection of the sponge (Grebenjuk et al., 2002). Based on the knowledge in the vertebrate system, the activation of the (2-5)A synthetase system in response to foreign bacteria was proposed to be initiated by the JAK-STAT pathway (Müller & Müller, 2003).

### Effectors of the response to microbial encounters

Elimination of foreign bacteria in sponges is likely to be driven by the activation of endocytosis and the subsequent production of lysosomal enzymes (e.g., cathepsin) (Krasko et al. 1997; Thakur et al. 2005). In *S. domuncula* the *lysozyme* gene is strongly expressed in gray cells that are embedded in the sponge's mesohyl. The enzymes produced by these cells were shown to only digest extracellular bacteria but not the ones occurring in bacteriocytes (Thakur et al., 2005).

An additional effector molecule involved in sponge immunity is the perforin-like protein. In mammals, perforin is a specific cytotoxic mechanism found in T-cells, which operates based on the secretion of lytic proteins, causing cell membrane damage and thus inducing apoptosis (Lowin et al., 1994). In the marine sponge *Tethya lyncurium* (Pallas 1766) a pore-forming protein (i.e., *Tethya* hemolysin) was detected and cloned. Tests conducted in erythrocytes of different animals revealed that this perforin rapidly lysed red blood cell membranes (Mangel et al., 1995). Primmorphs of *S. domuncula* also have the capacity to produce a perforin-like antibacterial protein, whose sequence is highly similar to human perforin I protein (Thakur et al., 2003). The expression of this perforin-like molecule is stimulated after exposure to LPS (Wiens et al., 2005). Interestingly, the expression of the perforin-like molecule in *S. domuncula* was observed to occur when the sponge was exposed to *E. coli* LPS but not when presented with Gram-negative sponge-associated bacteria. This finding indicates that the stimulation of

the perforin-like molecule is not initiated by LPS itself, and provides further evidence on the potential of sponges to differentiate between associated and non-associated bacteria (Gardères et al., 2015).

### Link between cellular and molecular mechanisms - Open questions

Over the last years, molecular data has revealed that sponges possess the essential genes commonly associated with innate immunity. However, the validation of these gene functions and its connection to cellular and physiological responses is still lacking. The signaling cascades and effectors mediating the response to microbes in symbiotic and non-symbiotic contexts are likely wider than the ones investigated so far and presented here. Sponge cellular mechanisms have been mainly studied in the context of developing a sponge cell culture and examining sponge regeneration (e.g., Alexander et al., 2014; Ereskovsky et al., 2019; Schippers et al., 2011); yet the cellular mechanisms involved in the immune response that occurs in intact and functional sponge specimens still needs to be decoded.

Experimental evidence integrating both the molecular and the cellular level will give insights into the genetic repertoire, the potential molecular pathways, and the type of cells that are driving the immune response in sponges. This is relevant since it is still difficult to assign specific functions to sponge cells. For example, it is not clear if the phagocytic activity of archaeocytes is different from the one of choanocytes (i.e., “immune phagocytosis” from “feeding phagocytosis”, respectively; Hartenstein & Martinez, 2019). It is hypothesized that archaeocytes are responsible for providing immunity in sponges (Funayama et al., 2005), but this remains to be tested. Therefore, it is essential to characterizing relevant immune cellular responses (e.g., phagocytosis, apoptosis, or cell proliferation) using different microbial challenges (e.g., sponge-associated vs. non-associated, potential pathogens, bacteria with different structures) and under controlled conditions. This experimental evidence would help to unravel the gene functions and the molecular mechanisms responsible for triggering specific cellular responses. Linking the cellular and molecular level would broaden our understanding on immunity and its role to guard stable and specific interactions between sponges and their microbes.

---

## GLOSSARY

---

**Allografts:** tissue fragment transplanted from one individual to a different one of the same species.

**Alloimmune** responses: immune responses produced against tissue or cells from the same species as they are not recognized as "self".

**Autografts:** tissue fragment transplanted from one part/section of the same individual's body of the same species.

**Homeostasis:** the capacity of the organism to main stable internal conditions via feedback loops (here implying at the level of the holobiont, to ensure its proper functioning).

**Primmorphs:** multicellular aggregates formed from dissociated single cells with proliferative activity reorganized in a spherical body with a continuous pinacoderm, which separates the internal mass of cells from the external environment.

---

### Acknowledgements

We thank the Marine Symbioses Unit at GEOMAR Helmholtz Centre for Ocean Research Kiel for fruitful discussions on the lifestyle of sponge-associated microbes and the implications for the sponge holobiont. AMG was funded by the International Max Planck Research School for Evolutionary Biology and the CRC1182 "Origin and Function of Metaorganisms" (TPB1, PI: Ute Hentschel Humeida).

### Author's affiliations

<sup>1</sup>Marine Symbioses Unit, Department of Marine Ecology, GEOMAR Helmholtz Centre for Ocean Research Kiel, Düsternbrooker Weg 20, 24105 Kiel, Germany

<sup>2</sup> Max Planck Institute for Marine Microbiology; HGF MPG Joint Research Group for Deep-Sea Ecology and Technology, Celsiusstr. 1, 28359 Bremen, Germany

<sup>3</sup>Department of Marine Biology and Oceanography, Institut de Ciències del Mar, ICM-CSIC, Passeig de la Barceloneta 37-49, 08003 Barcelona, Spain



---

## Chapter 2

# Transcriptomic Response of Mediterranean Sponges upon Encounter with Seawater or Symbiont Microbial Consortia

---

**Marulanda-Gómez A<sup>1</sup>**, Ribes M<sup>2</sup>., Franzenburg S<sup>3</sup>., Hentschel U<sup>1,4</sup>., Pita L<sup>2</sup>. Transcriptomic response of Mediterranean sponges upon encounter with seawater or symbiont microbial consortia. Submitted to *Genome Biology Evolution* (GBE). Pre-print available at bioRxiv.com doi: 10.1101/2023.11.02.563995v1

## Abstract

Sponges (phylum Porifera) constantly interact with microbes from the water column while filter-feeding and with the symbiotic partners they harbor within their mesohyl. Despite early observations on differential uptake between symbiont and seawater bacteria, it is still poorly understood how sponges discriminate between different microbial consortia. Initial evidence of the diverse repertoire of sponge immune receptors suggests their involvement in specific microbial recognition, yet experimental data is still scarce. We characterized the transcriptomic response of two sponge species, *Aplysina aerophoba* and *Dysidea avara*, upon incubation with two different microbial consortia, which were either enriched from ambient seawater or extracted from *A. aerophoba*. The sponges were sampled after 1 h, 3 h, and 5 h for RNA-Seq differential gene expression analysis. *D. avara* showed higher expression levels of genes related to immunity, ubiquitination, and signaling when incubated with *A. aerophoba* symbionts, than in incubations with seawater microbial consortia. Interestingly, the different bacteria consortia triggered changes in Nucleotide Oligomerization Domain (NOD)-Like Receptors (NLRs) gene expression in *D. avara*. We here provide the first experimental evidence for NLRs playing a role in distinguishing between different microbes in a sponge. In contrast, the response of *A. aerophoba* involved comparatively few genes and lacked genes encoding for immune receptors. This indicates that *A. aerophoba* is less responsive to microbial encounters than *D. avara*. Our study further reveals different transcriptomic responses between the two sponge species to microbes. The study of sponge responses to microbes aids in understanding the evolution of immune specificity and animal-microbe interactions.

**Keywords:** animal-microbe interactions; microbial consortia, HMA-LMA sponges; immune receptors; RNA-Seq; differential gene expression; symbiosis.

## Significant statement

Animals rely on components of the immune system to recognize specific microbes, whether they are pathogens, food, or beneficial symbionts. However, in marine invertebrates, the mechanisms of microbial discrimination and specificity are not well understood. Our work suggests that: (i) the transcriptomic response by the sponge can be scaled according to the type of exposure, (ii) the response to microbial encounters is species-specific and (iii) NLRs seem to have a prominent role in the differential response to microorganisms, whether symbionts or food bacteria.

## Introduction

Over the last decades, animals were recognized as “metaorganisms” or “holobionts” which encompass the multicellular host and its microbial symbionts, such as bacteria, archaea, viruses, fungi, and algae, (Bosch & McFall-Ngai, 2021; González-Pech et al., 2023; Rosenberg & Zilber-Rosenberg, 2018; Stévenne et al., 2021). Symbionts participate in the general fitness of the host by contributing to developmental cues, nutrient provision, potential metabolic expansion, and defensive traits (Carrier & Bosch, 2022; Gilbert et al., 2015; McFall-Ngai et al., 2013; Wein et al., 2019). Microbes thus provide adaptive advantages and shape animal evolution (Rosenberg & Zilber-Rosenberg, 2016; Roughgarden et al., 2018). These close and complex host-microbe interactions required fine-tuned communication between partners which is now known to be orchestrated by the host immune system (Berg et al., 2019; Dierking & Pita, 2020; Ganesan et al., 2022; Horak et al., 2020).

The immune system has a dual function of defending the animal against potentially harmful intruders and at the same time, establishing and maintaining interactions between the host and its symbiotic microbes (Eberl, 2010; Gerardo et al., 2020). How does immunity differentiate pathogens to be eliminated from symbionts to be acquired/maintained, and how does it safeguard guard homeostasis and equilibrium within the host? In both contexts, animals sense microbe-associated molecular patterns (MAMPs), such as lipopolysaccharide, peptidoglycan, or flagellin, via pattern recognition receptors (PRRs) (Janeway & Medzhitov, 2002). However, the encounter to a pathogenic microbe elicits inflammatory responses to eliminate the intruder, whereas the interaction with symbionts results in tolerance and colonization (Chu & Mazmanian, 2013; Gerardo et al., 2020). Thus, the immune system is able to specifically distinguish between symbiotic, non-symbiotic and pathogenic signals.



Many invertebrate groups such as hydrozoans, cnidarians, mollusks, and echinoderms present large and strikingly complex repertoires of PRRs (Buckley & Rast, 2015; Hamada et al., 2013; Lange et al., 2011; Neubauer et al., 2016; Zhang et al., 2011). The diversity of these receptors contributes to microbial detection by the host, and potentially plays a role in microbial discrimination (Jacobovitz et al., 2021; Neubauer et al., 2016; Saco et al., 2020; Seneca et al., 2020). For example, the coral *Montipora aequituberculata* responds to potentially pathogenic and commensal bacteria *Vibrio coralliilyticus* and *Oceanospirillales* sp., respectively by regulating the expression of Toll-like receptors and via differential upregulation of G protein-coupled receptors (van de Water et al., 2018). On the other hand, the freshwater snail *Biomphalaria glabrata* recognizes different pathogens by different sets of PRRs belonging to the calcium-dependent lectin family and via enzymes and non-canonical immune components, like extracellular actin (Tetreau et al., 2017).

As arguably the earliest branching metazoans (Redmond & McLysaght, 2021; Turner, 2021), sponges (phylum Porifera) offer the opportunity to study the evolution of immune specificity and animal-microbe interactions. As active filter-feeders pumping thousands of liters of seawater per day through their aquiferous system, sponges constantly encounter microbes from the seawater, but, at the same time, harbor specific and complex microbial communities within their mesohyl matrix (Thomas et al., 2016; Webster & Thomas, 2016). Based on the density and diversity of their symbionts, sponges are classified as high microbial or low microbial abundance (HMA and LMA) species. HMA sponges contain three to four order of magnitude more microbes than LMA sponges (Bayer et al., 2014; Hentschel et al., 2006; Moitinho-Silva et al., 2017; Pankey et al., 2022). This long-recognized dichotomy in sponge-microbe symbiosis reflects particular signatures in the structure and persistence of the symbiosis as well as physiological differences such as density of the mesohyl and pumping rates (Gloeckner et al., 2014; Maldonado et al., 2012; Morganti et al., 2021; Weisz et al., 2008). Additionally, LMA sponges are enriched in genes involved in microbial sensing and in host defense, such as SRCRs, NLRs, nucleosome-binding proteins, and bactericidal permeability-increasing proteins compared to HMA sponges (Germer et al., 2017; Ryu et al., 2016). The expression of immune-related genes upon different stimuli thus depends on the microbial abundance and diversity associated with the sponge, but can also be species-specific (Campana et al., 2022; Pita et al., 2018b; Posadas et al., 2021). These observations suggest

that the HMA-LMA status, as well as specific species traits, may affect how the sponge immune system responds to microbial cues.

Early experimental evidence showed that sponges preferentially take up seawater microbial consortia (i.e., bacterioplankton) over sponge symbiont consortia (Wehrl, 2006; Wehrl et al., 2007; Wilkinson et al., 1984). This was taken as evidence that the animal can differentiate between different microorganisms. This differentiation may derive from both host and microbial features. Recently, sponge symbionts were shown to evade phagocytosis by the expression of eukaryotic-like proteins containing ankyrin repeats which silence conserved components of phagocytosis and immune signaling (Jahn et al., 2019). On the host side, the high diversification of PRRs in sponges (Hentschel et al., 2012; Riesgo et al., 2014; Srivastava et al., 2010; Yuen et al., 2014) suggest their potential to recognize different and specific microbial ligands (S. M. Degnan, 2015). Experimental evidence supports the activation of PRR gene expression upon encounter with microbial elicitors (e.g., Wiens et al. 2005; Yuen 2016; Pita et al. 2018b; Schmittmann et al. 2021), but it remains to be shown if (and how) the expression patterns of PRRs may be involved in specific immune responses to different microbes.

Our study aims to better understand the underlying molecular mechanisms of bacterial discrimination in sponges. We characterized the host response upon encounter to seawater- and sponge-derived microbial consortia by RNA-Seq differential gene expression analysis. Specimens of *Aplysina aerophoba* (HMA) and *Dysidea avara* (LMA) were incubated with either microbial consortia enriched from natural seawater or with a sponge-associated symbiotic consortia. Sponge symbiont consortium was obtained from *A. aerophoba* by differential centrifugation, a physical separation used for enrich sponge symbiotic fractions because sponge symbionts remain unculturable (Schmittmann et al., 2022; Markus Wehrl et al., 2007). We collected samples at 1h, 3h, and 5h from the start of the incubation. We hypothesized that (i) both sponges will rely on differential expression of PRRs for microbial discrimination, (ii) differentially-expressed genes will show lower expression levels upon symbiotic (“self”) than seawater microbial consortia (“non-self”) treatment and (iii) that the HMA-LMA status of the host sponge will influence the different transcriptomic response between microbial encounters.

## Material and Methods

### Sponge collection

Specimens of the Mediterranean sponge species *Aplysina aerophoba* (Nardo, 1833) and *Dysidea avara* (Schmidt, 1862) were collected via SCUBA diving at the coast of Girona (Spain) in March 2015 (42.29408 N, 3.28944 E and 42.1145863 N, 3.168486 E; respectively). Sponges were then transported to the Experimental Aquaria Zone (ZAE) located at the Institute of Marine Science (ICM-CSIC) in Barcelona (Spain) and were placed in separated 6 L aquaria in a flow-through system with direct intake of seawater. Temperature and light conditions were set up mimicking natural conditions. Sponges were maintained under these conditions during 10-12 days for acclimation.

### Experimental setup

The experiment was conducted consecutively for each sponge species (end of March for *A. aerophoba*, beginning of April for *D. avara*). Before the microbial exposure experiments, sponges were kept overnight in 1 µm-filtered seawater and an additional 0.1 µm-filter was applied for 3 h before the experiments with the aim to reduce microbial load in seawater to a minimum. The flow-through was stopped during the experiment, but small aquarium pumps (Eheim GmbH & Co.) ensured the mixing of the water in the aquarium. Sponges were incubated with either microbial seawater consortia or symbiont consortia that had been prepared following the protocols below. The concentration of these stock microbial consortia was estimated via flow cytometry (see details in supplementary information, Text S1 and Fig. S1) and adjusted to reach  $10^{5-6}$  bacteria mL<sup>-1</sup> final concentration in the experimental tanks. Sponge specimens that were actively pumping, as visually assessed by the presence of an open oscula, were randomly assigned to each treatment (n = 5 individuals per treatment). For each individual, tissue samples were collected at 1 h, 3 h, and 5 h after adding the microbial consortia to the experimental tanks, then placed in RNAlater at 4°C overnight, and stored at -80°C until processing.

### Symbiont consortia preparation

The *A. aerophoba*-symbiont fraction was obtained as described in Wehrl et al. (2006). Briefly, 20 g of sponge tissue from living individuals that had been cleaned off debris was rinsed in sterile, ice-cold Ca- and Mg-free artificial seawater (CMFASW) with EDTA (as in (Rottmann et al., 1987)), incubated for 30 min at 4°C, and then homogenized with a mortar and pestle. After

filtration through 100  $\mu\text{m}$ -Nitex, the suspension was centrifuged twice at 4°C, 400 g for 20 min to remove sponge cells, which remained in the pellet. The supernatants were combined and centrifuged at 4°C, 4000 g for 20 min to obtain a bacterial pellet. This pellet was washed twice in ice-cold CMFASW and recovered again by centrifugation. Finally, the bacterial pellet was resuspended in sterile ice-cold CMFASW. Symbiont extraction from *D. avara* was not possible because this species represents an LMA sponge and we could not obtain enough microbial extracts for the incubations.

### Seawater microbial consortia preparation

Seawater microbial consortia were enriched from seawater from the aquaria setup (a flow-through system with direct intake of natural seawater), following the protocol by Wehrl et al. (2006). In short, Marine Broth 2216 media was added to 10 L of seawater to a final concentration of 15 mg L<sup>-1</sup>. The enriched seawater was incubated in the dark overnight at ambient temperature and gentle shaking. Aliquots of the enriched seawater were then sampled, and bacteria were recovered by differential centrifugation (4°C, 4000 g for 20 min), then washed twice, and re-suspended in sterile, ice-cold CMFASW.

### Sponge RNA extraction, sequencing, and de novo transcriptome assembly

Total RNA from 30 samples were extracted for each species following the methods in Pita et al. (2018b), but only 22 samples of *D. avara* passed the quality checks (i.e., RIN > 8 in Experion, Bio-Rad, USA). In short, 500 ng of total RNA were used for library construction with the TruSeq stranded mRNA library prep kit (Illumina, Inc., USA), including a poly-A enrichment step. Paired-end sequencing (150 bp) was performed on a NovaSeq S2 system (Illumina, Inc., USA) at the Competence Centre for Genomic Analysis (CCGA; Kiel, Germany). Raw paired-end reads were trimmed and filtered to remove adapters and low-quality reads in Trimmomatic-v0.39 (Bolger et al. 2014). Prokaryotic and microbial eukaryotic reads were filtered in the classifier kaiju-v1.6.2 (Menzel & Krogh, 2015). All samples were used to construct a *de novo* assembly per each sponge species in Trinity-v2.10.0 (Haas et al., 2013). Quality check and completeness of the assemblies were assessed by statistics performed in TransRate-v1.0.2 (Smith-Unna et al., 2016), and by comparing the assemblies against the metazoan-reference data in BUSCO-v3 (Simão et al., 2015).

### Annotation, gene quantification, and differential gene expression analysis

Functional transcriptome annotation was performed following Trinotate-v3.2.0 (Haas et al., 2013). Contigs with blastx or blastp matches to Bacteria, Archaea, or Virus, as well as those annotated as ribosomal RNA were removed from the *de novo* assembly. Gene (i.e., trinity components) abundance was estimated based on RSEM bowtie2 quantification-v1.3.3 (Langmead et al., 2009; Li & Dewey, 2014). Differential gene expression analysis was performed separately for each time point (i.e., 1 h, 3 h, and 5 h) in edgeR (Robinson et al., 2009) as implemented in Trinity-v2.10.0 (Haas et al., 2013) with default parameters. Differentially expressed genes (DEGs) in pairwise- treatment comparisons were defined by False Discovery Rate-corrected (FDR) p-value < 0.005 and  $\log_2|\text{change}| \geq 2$  (i.e., four-fold change) as in (Pita et al., 2018b; Wu et al., 2022).

### Results

We characterized the transcriptomic response of the Mediterranean sponges *A. aerophoba* and *D. avara* to either seawater microbial consortia or to symbiont consortia extracted from *A. aerophoba* tissue. We followed upon the initial work by Wehrl et al. (2007), who observed lower uptake rates of symbionts than seawater bacteria in *A. aerophoba*.

#### Reference transcriptome assembly

We sequenced 29 samples of *A. aerophoba* and 22 samples of *D. avara* corresponding to 3-5 biological replicates per treatment within 1h, 3h, and 5h (Table 1). The number of paired-end Illumina reads generated in this study is summarized in Supplementary Table S1. BUSCO assessments revealed that the *de novo* reference transcriptomic assembly of *A. aerophoba* generated in this study contained 71.4 % of the 902 BUSCO Metazoan core genes, with 76.6 % of the genes found as complete. The reference transcriptome assembly for *D. avara* consisted of 78.2% of the BUSCO Metazoan core genes, with 82.9% of these genes found as complete, suggesting this reference transcriptome is more complete than the reference in Pita et al. (2018b). All statistics of the reference assemblies generated in this study are summarized in Supplementary Table S2. Overall,  $68.89 \pm 0.21\%$  and  $84.37 \pm 17\%$  (average  $\pm$  standard error) of the reads in each sample aligned to the *de novo*-assembled reference transcriptome of *A. aerophoba* and *D. avara*, respectively.

**Table 1.** Biological replicates per condition and time point

Species	Treatment	Time	Replicates
<i>A. aerophoba</i>	Seawater microbial consortia	1h	4
		3h	5
		5h	5
	<i>A.aerophoba</i> symbiont consortia	1h	5
		3h	5
		5h	5
<i>D. avara</i>	Seawater microbial consortia	1h	4
		3h	4
		5h	3
	<i>A.aerophoba</i> symbiont consortia	1h	4
		3h	3
		5h	3

### Transcriptomic response upon seawater microbial and symbiont consortia

Significant differentially expressed genes (DEGs) were defined by edgeR, using a threshold of  $\log_2|FC| \geq 2$  (i.e., 4-fold change) and FDR p-value  $< 0.005$ , as in previous studies (Pita et al., 2018b; Wu et al., 2022). The DEGs were classified as up-regulated and down-regulated in the symbiont treatment when compared to the expression levels in the seawater microbial treatment. The results from the differential expression analysis in edgeR and the full Trinotate annotation reports for the DEGs can be found in Tables S3 to S6.

### *D. avara* differential response to microbial consortia involves immune- and ubiquitin-related genes

We detected a total of 28 DEGs between *D. avara* sponges exposed to seawater and *A. aerophoba*-symbiont consortia and most genes showed higher expression levels in the symbiont treatment (Fig. 1). The highest proportion of DEGs was detected at 5h (Fig. 1A). Blastp provided annotation for 39 % of the total 64 DEGs (Fig. 1B) and searched in the SigP database classified all of them as non-transmembrane signaling peptides (Table S4). Expression profiles of *D. avara* individuals treated with each type of microbial consortia were consistent and biological replicates clustered together at all time points (Fig. 1C).

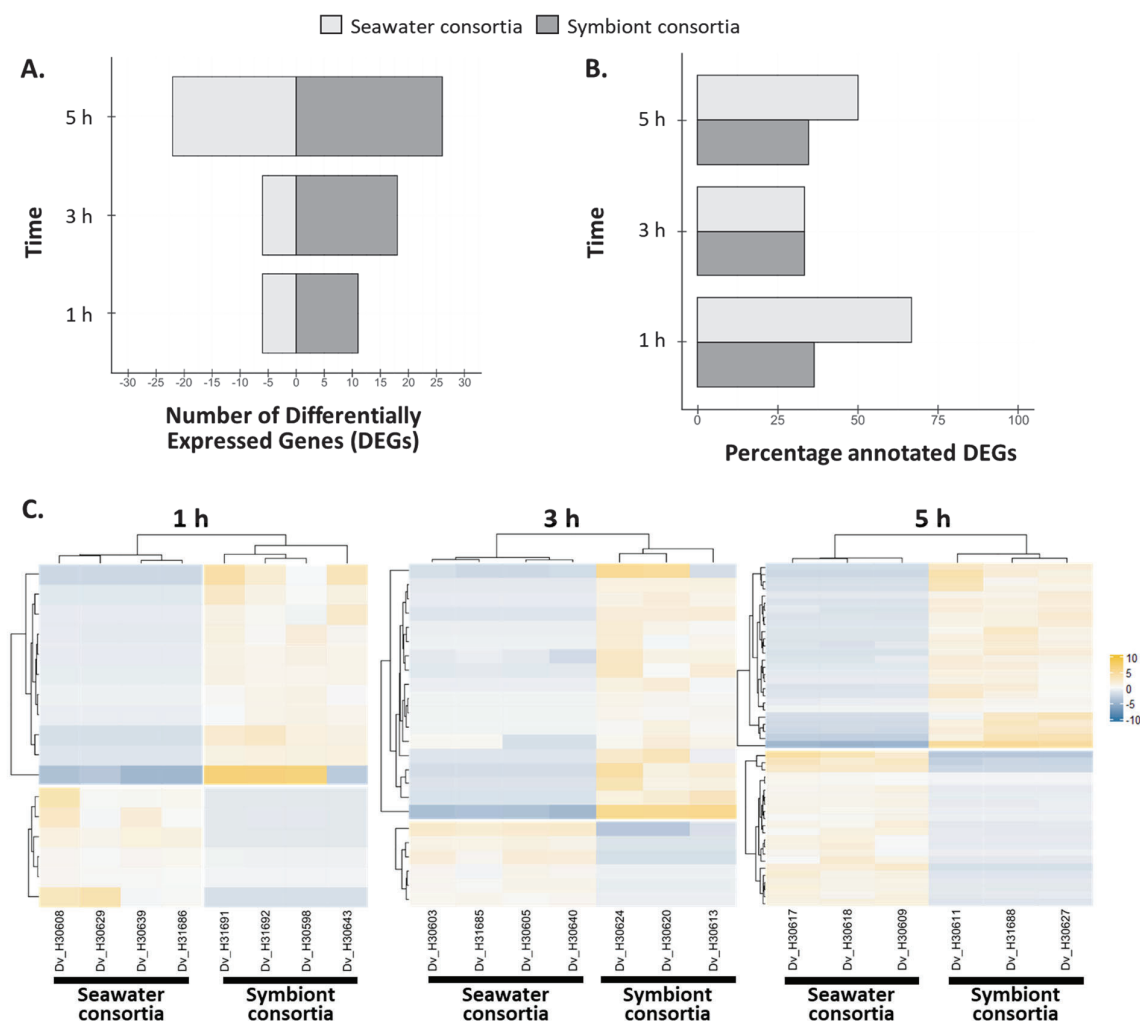


**Fig. 1.** Differential gene expression of *D. avara* individuals treated with seawater microbial vs. *A. aerophoba*-symbiont consortia. **(A)** Number of differentially expressed genes (DEGs). Genes with increased expression upon symbiont encounter compared to seawater microbial consortia have positive values. **(B)** Percentage of DEGs with annotation for each microbial treatment and time point. **(C)** Heatmaps show the TMM-normalized relative expression level per DEG (rows) for each sample (columns) at 1 h, 3 h, and 5 h after microbial treatment. Genes were defined as differentially expressed with edgeR, FDR p-value < 0.005 and  $\log_2|FC| \geq 2$ .

Based on Pfam and blast annotations, we identified five differentially expressed genes encoding for NOD-like receptors (NLRs) (Fig. 2, within “immunity” category). Four out of five differentially expressed NLRs showed higher expression levels upon seawater microbes than upon *A. aerophoba*-symbiont exposure. Three of these (*TRINITY\_DN18609\_c0\_g1*, *TRINITY\_DN65570\_c0\_g1*, *TRINITY\_DN18609\_c0\_g2*) were expressed at all time points and corresponded to incomplete NLRs (only the LRR-domain was detected; PF13516), and annotated as NLRC3 based on Blastp, whereas the fourth gene (*TRINITY\_DN6063\_c1\_g1*),

found only at 5 h (Fig. 2), contained the characteristic NACHT domain of NLRs (PF05729) and a peptidase domain (PF00656), and was assigned to the NLRC4 family based on Blastp annotation (Table S4). In contrast, there was one NLR that showed elevated gene expression in sponges incubated with symbionts in all time points (*TRINITY\_DN42758\_c1\_g2*); it contained a NACHT domain and was assigned to the NLRP3 family based on Blastp annotation (Fig. 2; and Table S4).

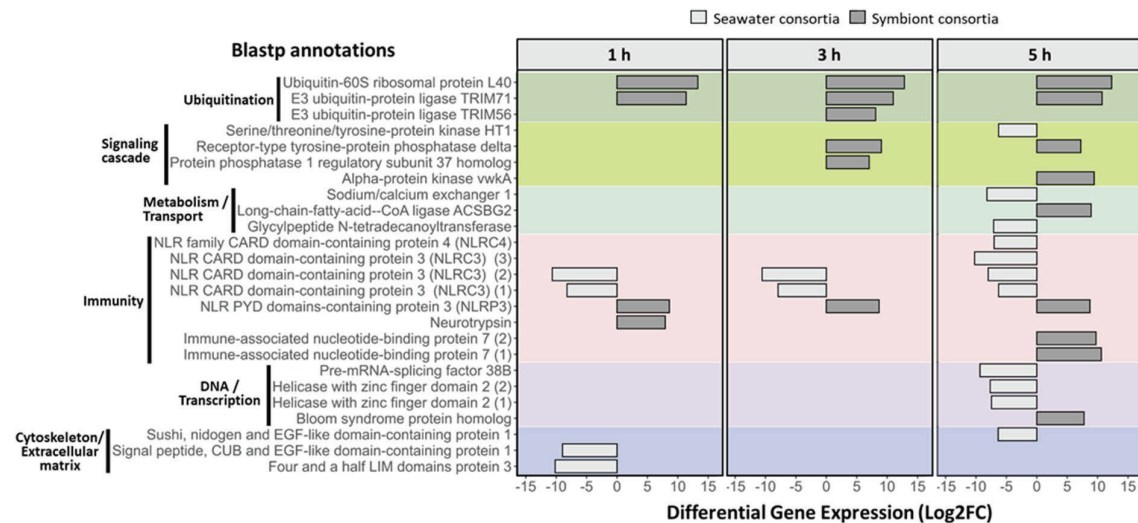


**Fig. 2.** Functions and expression levels of differentially expressed genes in *D. avara* at 1 h, 3 h, and 5 h after seawater microbial and *A. aerophoba*-symbiont consortia treatment. Genes with increased expression upon symbiont encounter compared to seawater microbial consortia have positive Log2FC values. Genes were defined as differentially expressed with edgeR, FDR p-value < 0.005 and  $\log_2|FC| \geq 2$ . Only genes with Blast annotations are included. Numbers in brackets indicate different genes with the same annotation.

In addition to NLRs, we detected other DEGs potentially involved in innate immunity and ubiquitination that showed higher expression levels upon encounter to *A. aerophoba* symbionts than to seawater microbes (Fig. 2). Among the immune genes, we detected a SRCR-containing gene associated to neurotrypsin (*TRINITY\_DN137847\_c3\_g1*; PF00530), and two genes related to an immune-associated GTP-binding protein (PF04548) (*TRINITY\_DN1745\_c0\_g1* and *TRINITY\_DN5077\_c0\_g1*) (Fig. 2; and Table S4). The regulation of ubiquitination was evident by the differential expression of three genes: one ubiquitin-60S ribosomal protein L40-like (*TRINITY\_DN322946\_c0\_g1*) and two E3 ubiquitin ligases (*TRINITY\_DN739\_c0\_g4* and *TRINITY\_DN37530\_c0\_g1*, Fig. 2; and Table S4). The *A. aerophoba*-symbiont consortium also stimulated genes annotated as protein phosphatases



(*TRINITY\_DN4437\_c1\_g1* and *TRINITY\_DN33881\_c0\_g1*) with fibronectin (PF00041) or LRR (PF13516) domains, an alpha-protein kinase (*TRINITY\_DN61539\_c1\_g1*), a CoA ligase (*TRINITY\_DN2791\_c1\_g1*), and a DEAD box-containing protein (*TRINITY\_DN9624\_c0\_g1*; PF00270) (Fig. 2; and Table S4).

The seawater microbial treatment showed higher expression levels of genes involved in cell surface and cytoskeleton organization than compared to the symbiont consortia treatment, including a calmodulin-ubiquitin and epidermal growth factor-like containing gene (*TRINITY\_DN5241\_c0\_g1*), and a LIM domain-containing gene (*TRINITY\_DN182729\_c0\_g1*) (Fig. 2 and Table S4). At 5h, genes related to functions such as DNA regulation and transcription, metabolism and transport, and signaling cascades showed elevated gene expression levels in seawater microbial treatment. For example, two genes (*TRINITY\_DN9504\_c0\_g1* and *TRINITY\_DN41910\_c0\_g1*) for helicases with a zinc finger domain (HELZ2) belonging to the superfamily of P-loop NTPases (PF13087 and PF04851) which are predicted to be nuclear co-activators of the peroxisome proliferator-activated receptors (Fig. 2 and Table S4) were identified. We also detected two genes (*TRINITY\_DN9504\_c0\_g1* and *TRINITY\_DN41910\_c0\_g1*) involved in the molecular function of calcium and calmodulin binding. One of these genes contained a nidogen-like domain (PF06119), which is predicted to enable Notch binding activity and to be involved in cell-matrix adhesion, whereas the other gene with a Calx-beta motif (PF03160) regulates the transport of calcium and sodium across the cell membrane. In addition, a serine/threonine tyrosine-protein kinase (*TRINITY\_DN63\_c1\_g1*), a glycolipid N-tetradecanoyltransferase (*TRINITY\_DN16852\_c2\_g2*) involved in lipid modification, and an mRNA-splicing factor (*TRINITY\_DN150336\_c1\_g1*) showed also higher gene expression levels 5 h after seawater consortia treatment than in symbiont treatment (Fig. 2 and Table S4).

### *A. aerophoba* differential response to microbial consortia involves signaling genes, ubiquitination-related genes and kinases

Differential gene expression between *A. aerophoba* sponges incubated with seawater microbial and symbiont consortia was only observed at 5 h, ( $\log_2|FC| \geq 2$  (i.e., 4-fold change) and FDR p-value < 0.005), (Fig. 3A) and showed consistently elevated expression profiles in seawater microbial treatment than symbiont treatment (Fig. 3B). Within the total 11 DEGs detected, 9 genes were signaling peptides, as reported by signalP (and two contained a

transmembrane domain Table S6). We identified three genes with additional blast annotation. A leucine-rich repeat receptor like protein kinase (*TRINITY\_DN146410\_c5\_g2*) with similarity to a *Dictyostelium discoideum* gene (YTYK2; DDB\_G0283397), an ubiquitin ligase (*TRINITY\_DN163315\_c3\_g2*; LIN41), and a transposase-derived protein antagonist of heterochromatin (*TRINITY\_DN169091\_c1\_g1*; ALP1) (Fig. 3B). If relaxing the significance threshold ( $\log_2|FC| \geq 1$  (2-fold change) and FDR p-value < 0.05), the number of DEGs increased but the pattern of elevated expression levels of DEGs in the seawater microbial consortia than symbiont treatment was consistent (Fig. S2).

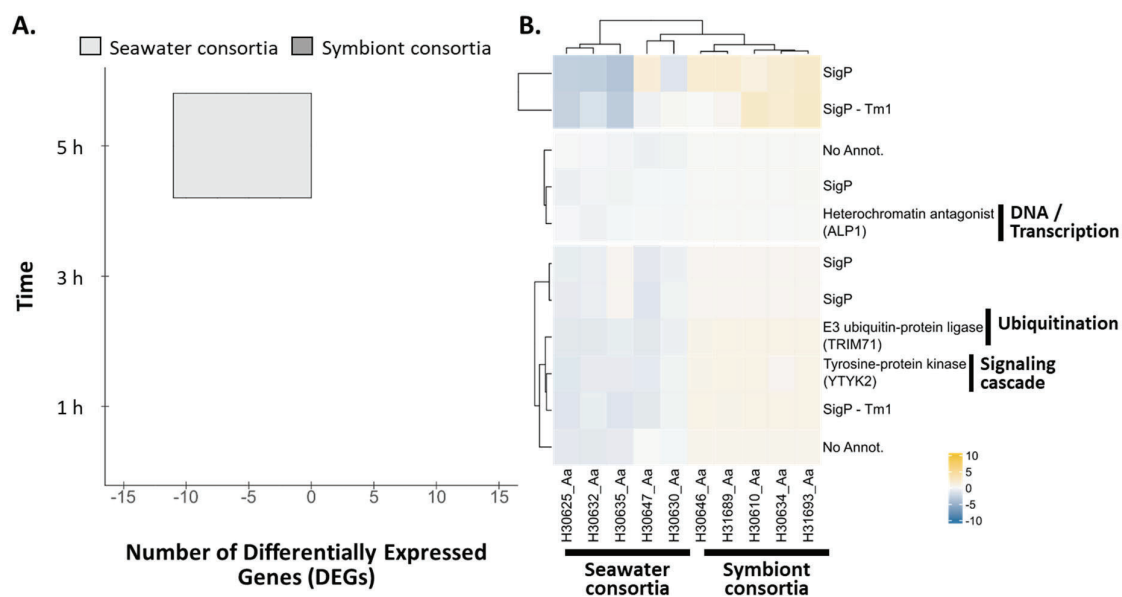


**Fig. 3.** Differential gene expression of *A. aerophoba* individuals treated with seawater microbial consortia vs. sponge own symbionts. **(A)** Number of differentially expressed genes (DEGs). Genes with increased expression upon symbiont encounter compared to seawater microbial consortia have positive values. **(B)** Heatmap show the TMM-normalized relative expression level per DEG (rows) for each sample (columns) at 5 h after microbial treatment. Functions of DEGs are included only for genes with Blast annotations (right bold legend). Genes were defined as differentially expressed with edgeR, FDR p-value < 0.005 and  $\log_2|FC| \geq 2$ .

## Discussion

In this study, we characterized the transcriptomic responses of the Mediterranean sponges *A. aerophoba* and *D. avara* upon incubation with either microbial seawater or *A. aerophoba*-symbiont consortia. Previous studies comparing filtration rates showed that sponges take up seawater bacteria at higher rates than symbiotic bacteria (Wehrl et al., 2007; Wilkinson et al.,

1984). Among transcriptomic studies in which sponges were subject to different stimuli (Koutsouveli et al., 2020; Pita et al., 2018b; Posadas et al., 2021; Schmittmann et al., 2021; Wu et al., 2022), this one is among the first to simulate natural conditions and consequently, the overall host responses involved moderately fewer DEGs. The sponge species investigated responded differently to the experiment. The LMA sponge *D. avara* discriminated between treatments via NLR receptors, whereas no PRRs were differentially regulated in the HMA sponge *A. aerophoba*. This is the first time that the differential regulation of various NLR families is linked to microbial discrimination in sponges. While differentially-expressed genes in *D. avara* showed higher levels of expression upon symbiont consortia encounter than to seawater microbial consortia, little differential expression between both treatments was observed in *A. aerophoba*. We propose that the way sponges distinguish between microbes may depend on the HMA-LMA status as well as on species-specific traits.

### Moderate transcriptional response of sponges to microbial exposure

The exposure of *A. aerophoba* and *D. avara* to seawater microbial consortia and *A. aerophoba*-symbionts showed differential gene expression of few genes (i.e., < 70 genes) for both sponge species investigated (Fig. 1A and Fig. 3A), even when significance threshold was relaxed (Fig. S2). In the current study, we detected a relatively lower transcriptional response (i.e., number of DEGs) than in previous studies, particularly for *A. aerophoba*. A previous experiment assessing the response of both sponge species studied here to commercial microbial elicitors (i.e., lipopolysaccharide and peptidoglycan), compared to a sham injection with filtered artificial seawater, detected > 400 DEGs and ca. 49 DEGs in *A. aerophoba* and *D. avara*, respectively (Pita et al., 2018b). In another study, the transcriptional response of *A. aerophoba* to wounding included thousands of DEGs (Wu et al., 2022). Furthermore, *A. queenslandica* juveniles in response against its native bacteria compared to foreign bacteria involved the differential gene expression of >1000 genes (Yuen, 2016). Besides potential differences due to bioinformatics analysis, we propose that, to some extent, the different magnitude of differential gene expression observed in previous, and this study are linked to the microbial stimuli applied (commercial vs. “natural”), the way they were presented to the sponge (injection vs. incubation), and the life stage (juveniles vs. adults) of the sponges. It thus appears that the magnitude of the host response is scalable depending upon the treatment, ranging from low (natural bacterial consortia), to medium (commercial elicitors), to high (mechanical damage). Figuratively speaking, in this study we are listening to the sponge

“whispering”, as opposed to “talking” upon injection with elicitors (Pita et al., 2018b), and even to “screaming” upon mechanical damage and snail predation (Wu et al., 2022). Furthermore, the higher number of immune related genes between in *A. queenslandica* juveniles compared to adult *D. avara* and *A. aerophoba* individuals could also be related to the maturation of the sponge immune system. The development and acquisition of immunity remains to be studied in sponges, but in other organisms (e.g., zebrafish, honey bees, mice and humans) a series of maturation steps are required for achieving immunocompetence, and this competence is adapted to the different life stages and previous encounters of the host with microbial cues (Gätschenberger et al., 2013; Lam et al., 2004; Park et al., 2020; Yang et al., 2015).

The present study presented the microbes in a way that is closer to natural conditions, in which sponge filter-feeding lifestyle translates into constant encounter with microbes in the surrounding water. The maintenance and implementation of immune mechanisms is energetically demanding, and the physiological costs may represent trade-offs between other metabolic activities (Ardia et al., 2012; Palmer, 2018). Thus, we speculate that the immune activity is constitutive in adult sponges due to their constant interactions with microbes. In fact, constitutive expression of a great variety of PRRs has been observed in the sponge *Halichondria panicea* (Schmittmann et al., 2021). Induced responses will be activated upon other type of stimuli, like “damage signals”, as in the response of *A. aerophoba* to wounding (Wu et al., 2022). In contrast, the response to microbes is based on “fine-tuning” of immune components that are already in place. The constant interactions of sponges with their microbiome and seawater bacteria including potential pathogens may favor constitutive expression over induced activation of immune components. This strategy challenges traditional views on induced immunity from terrestrial animals, but it may indeed be widespread among marine invertebrates (Schmittmann et al., 2021; Williams & Gilmore, 2022).

### Sponges recognize microbial consortia differently

*D. avara* individuals incubated with *A. aerophoba*-symbiont consortia showed an overall approx. 50 % higher number of DEGs compared to *A. aerophoba* sponges (Fig. 1A and 3A). We observed a differential expression of immune receptors in *D. avara* such as NLRs (Fig 2 and Fig. 4A), whereas no PRRs were differentially expressed in *A. aerophoba* (Fig. 3B and Fig. 4B).

Moreover, *A. aerophoba* showed a lower transcriptomic response to symbiont (“self”) than to seawater microbial consortia (“non-self”). The few genes differentially regulated in *A. aerophoba*, showing mainly reduced expression levels upon its own symbiont treatment (Fig. 3B), could indicate that the sponge detects microbes in a different way than *D. avara*. The low transcriptomic response in *A. aerophoba* could be the result of the sponge recognizing its own symbionts as “self” or of its HMA status. Since we did not detect high differential gene expression between the microbial treatments in *A. aerophoba*, we argue this to be related to the sponge HMA status rather than with “self”/“non-self” recognition. Ideally, we would have included a fourth treatment consisting of *D. avara*-symbiont consortia exposure to clarify these hypotheses, but we were not able to extract symbionts from *D. avara* in sufficient quantity for our incubations, due to its LMA status. Moreover, we cannot exclude the possibility that *A. aerophoba* sponge cells were remaining in the microbial symbiont fraction and, thus, affected the transcriptional responses. However, we would expect that those sponge cells will activate a transcriptional response in both *D. avara* and *A. aerophoba*, if any, because studies on sponge self- and non-self-transplants suggest active rejection of cells from other sponges, even if derived from other individuals of the same species (Hildemann et al., 1979; Hirose et al., 2021; Saito, 2013). Overall, our results show a lack of a differential transcriptomic response in a HMA sponge against microbes that we interpret as an adaptation to the permanent presence of symbionts within the sponge mesohyl system. More sponge species representative of the HMA-LMA categories will however be needed to validate and elaborate this hypothesis.

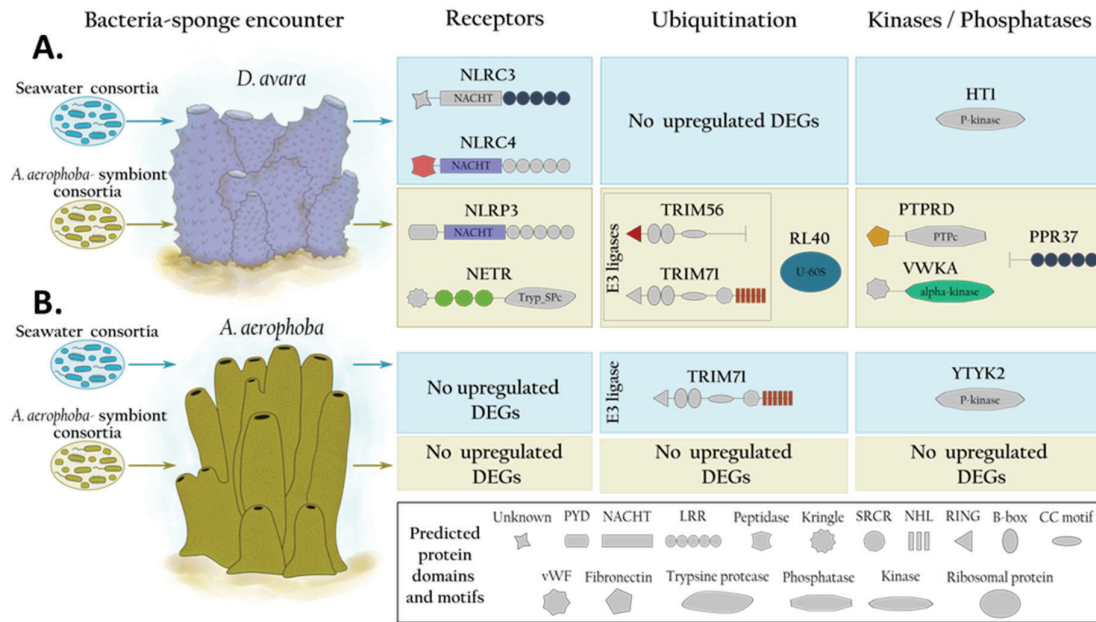


**Fig. 4.** Overview of the transcriptomic response in **(A)** *D. avara* and **(B)** *A. aerophoba* upon microbial consortia encounter, derived either from seawater or symbiont preparations. DEGs detected after each treatment and annotated as receptors or related to ubiquitination and signaling are shown along with UniProt ID of best blastp hits. Colored domains had a Pfam annotation, whereas gray-shaded ones were not detected, and the potential structure of each gene was drawn based on smart.embl.de.

### *D. avara* and *A. aerophoba* employ different sets of genes

The differential transcriptomic response of *D. avara* individuals to symbionts and seawater microbial consortia involved several immune genes including one SRCR-containing receptor and two GTP-binding proteins. The genes encoding for the immune-associated GTP-binding protein (IAN) in *D. avara* are part of the GIMAP family. IAN genes were not detected in any other early divergent metazoans including the genome of the sponge *A. queenslandica*, but are broadly and patchy distributed among eukaryotes, and orthologs have been reported in plants, corals, and molluscs as means of microbial defense (Coelho et al., 2022; C. Liu et al., 2008; McDowell et al., 2016; Weiss et al., 2013). GIMAP family is conserved among vertebrates, where it is implicated in the development and maintenance of immune cells (e.g., lymphocytes (Limoges et al., 2021)). SRCRs are involved in the recognition of a broad range of ligands and are highly diversified in invertebrates (Buckley & Rast, 2015; Neubauer et al., 2016; Smith et al. 2018). These receptors are also expanded in sponges (Pita et al., 2018b; Ryu et al., 2016; Schmittmann et al., 2021) and potentially play a role in sponge symbiosis. For instance, a SRCR-domain containing gene was up-regulated in symbiotic individuals of the sponge

*Petrosia ficiformis* compared to aposymbiotic individuals (i.e., photosymbiont-free), suggesting the involvement of this immune receptor in sponge symbiosis (Steindler et al., 2007). Moreover, in juveniles of *A. queenslandica*, different SRCRs were upregulated in response to native and foreign bacteria (Yuen, 2016). Altogether, SRCRs arise as putative mediators of sponge-microbe interactions in different sponge species and the GIMAP family may as well deserve more attention in future studies.

In comparison to *D. avara*, the lower differential transcriptomic response of *A. aerophoba* was limited to reduced expression of a kinase-like receptor, an E3 ligase and an antagonist of heterochromatin in symbiont vs. seawater microbial consortia treatment (Fig 3B and Fig. 4B). The antagonist of like-heterochromatin protein (ALP1) in plants acts as a transposase mediating various cellular pathways and capable of silencing gene expression involving E3 ubiquitin ligases (Golbabapour et al., 2013; Ohtsubo et al., 2008). The role of this transposase in inhibiting transcriptional responses is proposed to have evolved as a means for evading surveillance by the hosts (Liang et al., 2015). In fact, pathogens cause a variety of transcriptional changes (e.g., alteration of chromatin structure, proteolytic degradation, deactivation of transcription factors, etc.) to exploit a wide range of pathways which enhances their survival within the host (De Monerri & Kim, 2014; Villares et al., 2020). We therefore hypothesize that the late (i.e., at 5h) down-regulation of both ALP1 and E3 ubiquitin ligase in symbiont compared to seawater microbial exposure (Fig. 3B) could indicate active host gene silencing by symbionts, to prevent becoming target material for degradation. Functional studies are imperative to validate the processes in which the detected DEGs are involved, yet this remains a challenge in sponges as models for genetic manipulation are currently limited to explants or cells of two sponge species (Hesp et al., 2020; Revilla-I-Domingo et al., 2018).

#### *D. avara* distinguishes between seawater microbial and symbiont consortia via NLRs

*D. avara* sponges differentiated between seawater microbes and symbionts via differential expression of NLRs. Moreover, the differentially-expressed NLRs with higher expression levels in sponges incubated with seawater microbial consortia were similar to the NLRC3 and NLRC4 families (based on Blastp results; Fig 2 and Fig. 4A), whereas the NLR that exhibited higher expression levels in response to *A. aerophoba* symbionts showed similarity to the NLRP3 family (Fig 2 and Fig. 4A). A phylogenetic analysis of these NLRs was not possible because our

transcripts for these NLR-like genes were incomplete (i.e., lacking NACHT or LRR domains, Fig 4A). To confirm if these NLRs belonged to different subfamilies, we performed an additional blast search (at protein level, e-value < 1e-5; Table S7) of the differentially expressed NLRs in *D. avara* against the freshwater sponge *Ephydatia muelleri*, for which a chromosome-level genome is available (Kenny et al., 2020). The best hits of differentially-expressed *D. avara* NLRs in *E. muelleri* support that the NLRs activated in response to seawater bacteria belong to a different NLR subfamily than the one responding to *A. aerophoba* symbiont consortia (Table S7).

Differential gene expression of NLRs in *D. avara* was accompanied by differential expression of ubiquitination, kinases and phosphatases (Fig 2 and Fig. 4A). We speculate that the different types of NLRs (i.e., NLRC3, NLRC4 and NLRP3) activate different downstream signaling pathways in *D. avara* whose ultimate goal is to regulate microbial recognition by the sponge. In humans and mice these NLR families regulate inflammatory pathways (Pan et al., 2022; Schneider et al., 2013; Sun et al., 2022; Uchimura et al., 2018; Walle & Lamkanfi, 2016). Inflammation requires various post-translational modifications comprising ubiquitin ligases, kinases and phosphatases (Akther et al., 2021; Song & Li, 2018; Yang et al., 2017), and the ubiquitin system, which is crucial in many biological process, is proposed as an essential innate immunity regulator and as a modulator of host-microbe interactions (Li et al., 2016; Zhang et al., 2021). Overall, our results show experimentally for the first time the role of NLRs in microbial discrimination by sponges and suggest their role in sponge-symbiont interactions. Importantly, LMA sponges are known to contain an expanded and diverse set of NLRs compared to HMAs (e.g., (Germer et al., 2017; Ryu et al., 2016; Schmittmann et al., 2021; Yuen et al., 2014)). The regulation of NLRs in the LMA sponge *D. avara*, compared to the non-regulation of these receptors in the HMA sponge *A. aerophoba*, may further support the previous hypothesis that the HMA-LMA status may influence how the sponge immune system responds to microbial encounters. The first experimental evidence of enhanced NLRs expression in sponges was reported in *D. avara* as a response to commercial microbial elicitors (Pita et al., 2018b). Our results build on these observations and support the participation of poriferan NLRs in specific microbial recognition. Future studies should focus on identifying the ligand of this different NLRs to finally provide functional evidence of the role of sponge NLRs in immune specificity.



## Conclusion

The molecular mechanisms employed in early divergent metazoans for microbial discrimination are still only poorly understood. In the present study, we characterized the transcriptomic response of two sponge species upon incubations with seawater microbes and sponge-derived symbionts by RNA-Seq differential gene expression analysis. Our observations showed that sponges mount a moderately low (less than 70 DEGs) but different transcriptomic response to natural microbial encounters. Microbial discrimination in sponges seems to be driven by the repertoire of immune genes harbored by the host and the degree in which these are induced. The HMA sponge *A. aerophoba* showed little differential gene expression and no participation of PRRs upon microbial exposure. Contrastingly, our results support the involvement of NLRs in specific microbial discrimination in the studied LMA sponge. We hypothesize that the different NLR families under regulation might trigger various signaling pathways in *D. avara* which are tuned to recognize among different microbial cues. Furthermore, we suggest that the differential response to microbial exposure between sponge species could be the result of species-specific traits or HMA-LMA features that influence the regulation of immune components in the host. To unveil more potential sponge molecular adaptations to microbial encounters it is crucial to investigate different sponge species along the LMA-HMA spectrum, under experimental setups that resemble as much as possible natural conditions, and to test different microbial structures that may induce or silence the transcriptomic response of the host. Finally, conducting comparative studies between the relevant genes mediating microbial discrimination in sponges and other early divergent invertebrates would further expand our understanding on the role of PRRs on microbial recognition and place sponges with their unique life-styles in an evolutionary context.

## Supplementary Material

Supplementary data are available at end of this thesis and at bioRxiv: <https://doi.org/10.1101/2023.11.02.563995>.

## Acknowledgments

We are grateful to Rafel Coma and Manel Bolívar (CEAB-CSIC) for assistance during the sponge collection. We thank Marc Catllà and the personal from the ZAE at ICM-CSIC for assistance during the experimental work in Barcelona. We acknowledge the staff from IKMB sequencing facilities for cDNA library preparation and sequencing. We also thank Dr. Lara Schmittmann

and Dr. Vasiliki Koutsouveli for helpful discussions and feedback in the data analysis. LP received supported by “la Caixa” Foundation (ID 10010434), co-financed by the European Union’s Horizon 2020 research and innovation program under the Marie Skłodowska-Curie grant agreement No 847648), fellowship code is 104855. LP and MR received additional institutional support by the “Severo-Ochoa Centre of Excellence” accreditation (CEX2019-000928-S). This is a contribution from the Marine Biogeochemistry and Global Change research group (Grant 2021SGR00430, Generalitat de Catalunya). UH was supported by the DFG (“Origin and Function of Metaorganisms”, CRC1182-TP B01) and the Gordon and Betty Moore Foundation (“Symbiosis in Aquatic Systems Initiative”, GBMF9352).

### Data availability

The raw reads, metadata, transcriptome assembly and full annotation for this study have been deposited in the European Nucleotide Archive (ENA) at EMBL-EBI under the accession number PRJEB61959 (ERP147040).

### Author’s affiliations

<sup>1</sup>RU Marine Symbioses, RD3 Marine Ecology, GEOMAR Helmholtz Centre for Ocean Research Kiel, Germany

<sup>2</sup>Institut de Ciències del Mar, ICM – CSIC, Spain

<sup>3</sup>Research Group Genetics and Bioinformatics/Systems Immunology, Institute of Clinical Molecular Biology, Christian-Albrechts-Universität Kiel, Germany

<sup>4</sup>Christian-Albrechts-Universität Kiel, Germany



---

## Chapter 3

# A Novel *in-vivo* Phagocytosis Assay to Gain Cellular Insights on Sponge-Microbe Interactions

---

Original publication by *Frontiers in Marine Science*. Copy right under the terms of the Creative Commons Attribution License (CC BY).

**Marulanda-Gómez A.**, Bayer K., Pita L., Hentschel U. 2023 A novel in-vivo phagocytosis assay to gain cellular insights on sponge-microbe interactions. *Frontiers in Marine Science*, Section Microbial Symbioses, 10. doi: 10.3389/fmars.2023.1176145.

## Abstract

Sponges harbor diverse, specific, and stable microbial communities, but at the same time, they efficiently feed on microbes from the surrounding water column. This filter-feeding lifestyle poses the need to distinguish between three categories of bacteria: food to digest, symbionts to incorporate, and pathogens to eliminate. How sponges discriminate between these categories is still largely unknown. Phagocytosis is conceivable as the cellular mechanism taking part in such discrimination, but experimental evidence is missing. We developed a quantitative in-vivo phagocytosis assay using an emerging experimental model, the sponge *Halichondria panicea*. We incubated whole sponge individuals with different particles, recovered the sponge (host) cells, and tracked the incorporation of these particles into the sponge cells. Fluorescence-activated cell sorting (FACS) and fluorescent microscopy were used to quantify and verify phagocytic activity, defined here as the population of sponge cells with incorporated particles. Sponges were incubated with a green microalgae to test if particle concentration in the seawater affects the percentage of phagocytic activity, and to determine the timing where the maximum of phagocytic cells are captured in a pulse-chase experiment. Lastly, we investigated the application of our phagocytic assay with other particle types (i.e., fluorescently-labeled bacteria and fluorescent beads). The percentage of sponge cells that had incorporated algae, bacteria, and beads ranged between 5 to 24 %. These phagocytic sponge cells exhibited different morphologies and sizes depending on the type of particle presented to the sponge. Particle incorporation into sponge cells was positively related to algal concentration in the seawater, suggesting that sponge cells adjust their phagocytic activity depending on the number of particles they encounter. Our results further revealed that sponge phagocytosis initiates within minutes after exposure to the particles. Fluorescent and TEM microscopy rectified algal internalization and potential digestion in sponge cells. To our knowledge, this is the first quantitative in-vivo phagocytosis assay established in sponges that could be used to further explore phagocytosis as a cellular mechanism for sponges to differentiate between different microorganisms.

**Keywords:** sponge-microbe symbiosis, phagocytosis, fluorescence-activated cell sorting (FACS), particle uptake, sponge cells

## Introduction

Early branching metazoans provide an opportunity to investigate the evolution of host-microbe interactions. Sponges (phylum Porifera) are benthic suspension feeders that actively filter large volumes of water. Due to this filter-feeding lifestyle, they are constantly exposed to high numbers of particles, which poses the question of how sponges distinguish and process between the different types of microbes they encounter. Sponges exhibit three well-defined cell layers: the external pinacoderm composed of T-shaped or flattened cells (i.e., pinacocytes) which covers the outside of the animal; the internal choanoderm containing the flagellated cells (i.e., choanocytes); and the mesohyl, a matrix within which other sponge cells, skeletal components, and most symbiotic microbes reside (Simpson, 1984; Leys and Hill, 2012). These filter feeders evolved a complex branched water canal system (i.e., the aquiferous system) comprised of several choanocytes arranged into hollow chambers which generate water flow by the beating of their flagella. Water enters the sponge through small pores, or ostia, which spread along the animals' outer surface, circulates through the incurrent canals into the choanocyte chambers, and exits through excurrent canals to larger outflow openings, or oscula. The particles (e.g., bacterio- and phytoplankton) that are filtered by the choanocytes are translocated to amoebocyte-like cells (i.e., archaeocytes) which are regarded as potential nutrient transporters within the sponge (Imsiecke, 1993; Leys and Eerkes-Medrano, 2006; Steinmetz, 2019). The participation of both choanocytes and archaeocytes in intracellular digestion is supported by single-cell transcriptomic data which shows enrichment in genes related to e.g., engulfment and motility, lysosomal enzymes, and phagocytic vesicles (Seb Pedr s et al., 2018; Musser et al., 2021). Despite this filter-feeding lifestyle, sponges harbor a highly diverse community of associated microbes in their mesohyl that is remarkably different from the bacterioplankton in the surrounding seawater (Hentschel et al., 2006; Thomas et al., 2016; Moitinho-Silva et al., 2017). It remains enigmatic if, and how, sponges distinguish between food to digest, symbionts to acquire, and pathogens to eliminate.

Selectivity in particle uptake continues to be a controversial topic in sponge physiology. Some studies regard particle size as the main parameter driving the selection of microbes during the filtering process (Reiswig, 1971; Turon et al., 1997; Ribes et al., 1999; Pile and Young, 2006), whereas others propose a size-independent discrimination between particles involving individual particle recognition, sorting, and transport through the sponge tissue during the

digestion process (Reiswig, 1971; Leys and Eerkes-Medrano, 2006; Yahel et al., 2006; Maldonado et al., 2010; McMurray et al., 2016). Furthermore, two feeding experiments with culturable bacteria provide first evidence that sponges take up seawater bacteria but not sponge-associated bacteria (Wilkinson et al., 1984; Wehrl et al., 2007). The latter studies hypothesized that the lower uptake rates of sponge-associated bacteria isolates result from slime capsules or secondary metabolites that protected symbionts from being recognized and ingested by the sponge. How the sponge host exactly discriminates microbes at the cellular level is still unclear, yet we posit that this cellular host-microbe recognition mechanism must be essential for establishing and maintaining symbiotic interactions and a stable microbiome in sponges.

We thus hypothesize that phagocytosis will play a major role in sponge-microbe interactions. Hijacking of phagocytosis promotes the colonization and maintenance of microbes during symbiotic interactions (Nyholm and Graf, 2012). Phagocytosis includes the recognition and ingestion of particles larger than 0.5  $\mu\text{m}$  within a plasma-membrane envelope (i.e., phagosome) (Rosales and Uribe-Querol, 2017). It is a highly conserved cellular process from unicellular to multicellular organisms, involved in nutrition, defense, homeostasis and symbiosis (Nyholm and Graf, 2012; Lim et al., 2017; Hartenstein and Martinez, 2019). Symbionts from diverse hosts such as amoeba, leech and squid are capable of escaping different stages of the phagocytic process, avoiding either incorporation or digestion by host cells (e.g., Silver et al., 2007; Nyholm et al., 2009; Nguyen et al., 2014), in their way to colonize and persist in the animal host.

In sponges, transcriptomic studies have revealed that upon exposure to microbes or microbial elicitors the host activates phagocytic-related genes (Yuen, 2016; Pita et al., 2018b; Geraghty et al., 2021; Schmittmann et al., 2021). Furthermore, sponge-associated bacteria are enriched in ankyrin proteins compared to non-associated sponge bacteria (Silver et al., 2007; Thomas et al., 2010; Siegl et al., 2011; Díez-Vives et al., 2017). These proteins modulate host phagocytosis in humans assisting the infection and intracellular survival of symbionts and pathogens (Al-Khodori et al., 2008; Habyarimana et al., 2008; Pan et al., 2008). Functional evidence on how ankyrins from sponge symbionts modulate host phagocytosis is only probed in non-sponge systems, in particular in free-living amoeba and murine macrophages (Nguyen et al., 2014; Jahn et al., 2019), due to the lack of experimental assays in sponges. Interestingly, bacteria expressing ankyrin-repeat proteins were phagocytized, but not digested by the

amoeba *Acanthamoeba castellanii* (Nguyen et al., 2014), whereas bacteria decorated with phage encoded ankyrins evaded phagocytosis in murine macrophages (Jahn et al., 2019). These pioneering studies serve as evidence that the host phagocytic machinery is targeted by sponge-associated microbes and highlights the importance to develop an assay that allows to test these functions testing these functions in the sponge host.

Feeding experiments shed some light on the filtration and particle internalization by sponges, a process usually referred to in a generic way as “phagocytosis” in sponge literature (Imsiecke, 1993; Leys and Eerkes-Medrano, 2006; Maldonado et al., 2010). However, the laborious and time-consuming microscopic observations in combination with the lack of well-established methodologies to study cellular processes in sponges hampers our current understanding of the implications of phagocytosis on sponge-microbe interactions. In other eukaryote phyla such as Amoebozoa and Cnidaria, advances in genetic manipulation, isolation of symbiont strains and identification of cellular markers have started to pave the way to study phagocytosis as the underlying mechanism for microbe discrimination (e.g., *Dictyostelium* sp., *Aiptasia* sp., *Pocillopora damicornis*, and *Nematostella vectensis*) (Sattler et al., 2013; Bucher et al., 2016; Rosental et al., 2017; Jacobovitz et al., 2021; Jauslin et al., 2021; Snyder et al., 2021). In hexacorallians, fluorescence-activated cell sorting (FACS) and microscopy allowed further identification and mechanistic characterization of specialized phagocytic cells capable of lysosomal degradation and production of reactive oxygen species (ROS) upon microbe engulfment (Snyder et al., 2021). The development of methods and establishment of model systems are thus fundamental for studying the function of host phagocytosis in microbe selectivity.

In the present study, we describe the development of an *in-vivo* phagocytosis assay based on combining live sponge incubation experiments with fluorescent particles followed by sponge cell dissociation and flow cytometry to quantify the incorporation of different particles into sponge cells (from now on termed phagocytosis). We used the Baltic Sea sponge *Halichondria panicea*. This shallow water sponge is widely distributed along the North Atlantic and its ecology and physiology have been studied both in natural and aquaria conditions (e.g., feeding experiments with microalgae and bacteria (Barthel, 1988; Riisgård et al., 2016; Luskow et al., 2019)). *H. panicea* is a low microbial abundance (LMA) sponge with a dominant and stable bacterial symbiont (i.e., *Candidatus Halichondribacter symbioticus*, relative abundance approx. 25%–80% based on 16S rRNA gene amplicon data) (Knobloch et al., 2019), and



presumably also harbors intracellular green algae (Vethaak et al., 1982; Goldstein and Funch, 2022). The sponge microbiome can be experimentally manipulated (Schmittmann et al., 2022) and the host transcriptomic response has been characterized using microbial elicitors (Schmittmann et al., 2021). These features make *H. panicea* a promising model for studying sponge symbiosis (Pita et al., 2016). We quantified the incorporation of inert (beads) and natural particles (microalgae and bacteria) into *H. panicea* cells. We chose these particles because of their size (1-3  $\mu\text{m}$  in diameter), clear fluorescence signal, and ecological relevance [i.e., *H. panicea* naturally feeds on phytoplankton and bacteria (Riisgård et al., 2016; Lüsrow et al., 2019)]. Fluorescence-activated cell sorting (FACS) served to quantify, in a high-throughput way, particle incorporation into sponge cells, which was also confirmed by fluorescence and transmission electron microscopy. To our knowledge, this is the first quantitative *in-vivo* phagocytosis assay established in sponges which could be used to further explore the mechanistic underpinnings of recognition and differentiation between sponges and diverse microorganisms (food, friend, or foe).

## Material and methods

### Sponge collection

Individuals of the breadcrumb sponge *Halichondria panicea* (Pallas, 1766) were collected for establishing the assay between Jun 2020 to Jun 2022. The sponge individuals for which data is presented were collected in Aug 2022 at the coast of Schilksee (54.424278 N, 10.175794 E; Kiel, Germany). Sponges were collected at water depths of between 1-3 m and were carefully removed from the crevices of a breakwater structure using a metal spatula. The individuals were directly transferred to the KIMMOCC climate chamber facilities at GEOMAR Helmholtz Centre for Ocean Research (Kiel, Germany), and maintained in 10 L tanks in a semi-flow through aquaria system supplied with sand-filtered seawater pumped from the Kiel fjord at 6 m depth. The sponges ( $n = 10$  individuals) were cut with a scalpel into approximately equal-sized fragments ( $3.9 \pm 1.0$  g wet weight [average  $\pm$  S.D.]), cleared of epibionts, and randomly placed back in the 10 L tanks supplied with the natural seawater from the flow-through system at KIMMOCC facilities (3-4 sponge fragments per tank). The water flow in the tanks was  $0.5 \text{ L min}^{-1}$  and a mini-pump with a maximum flow rate of  $300 \text{ L h}^{-1}$  (Dupla TurboMini) enhanced further water movement in each tank. Sponges were left on top of clay tiles ( $6.3 \times 1 \text{ cm} - \varnothing \times$

H) to heal and attach for 8 days at 10°C room temperature, 17°C water temperature, and a salinity of 16 PSU.

### Tracer preparation for the in-vivo phagocytosis assay

The particles included the microalgae *Nannochloropsis* sp., the *Vibrio* sp. isolate PP-XX7 (16S rRNA gene sequence similarity of 98.6% with *Vibrio* sp. NBRC 101805 as the next related strain in the NCBI database based on blastn), and 1 µm polystyrene-based latex beads. The *Nannochloropsis* sp. live culture was purchased from BlueBio Tech (Germany). The stock algal culture concentration was  $12 \times 10^9$  algae cells mL<sup>-1</sup>, and was kept at 4°C, protected from light until the experiments were performed, as recommended by the manufacturer. The *Vibrio* strain was initially isolated from the top 1 cm sediment sampled in our sponge collection site. The bacteria culture was prepared by inoculating 100 mL of liquid marine broth (Zobell 2216) with a culture that grew for 24h on an agar plate. The liquid culture was incubated on a shaker at 120 rpm, at 25°C, for 48 hours until the culture reached the mid to late exponential phase. After this incubation time, the culture OD<sub>600</sub> was measured (OD<sub>600</sub> = 1.45) to estimate the aimed bacteria concentration of approx.  $10^5$ - $10^6$  bacteria mL<sup>-1</sup>. The culture was centrifuged at 5000 x g for 5 min to recover the bacteria pellet, resuspended in 0.22 µm-filtered artificial seawater (FASW), and stained the same day of the experiment with the fluorescent dye 5 - TAMRA/SE™ (Thermo Fisher Scientific, C1171) at a final concentration of 1 µM (as in (Wehrl et al., 2007)). The bacteria suspension was incubated with the dye for 90 min in the dark at room temperature, the excess dye was washed off by centrifuging at 5000 x g for 5 min, and the bacteria pellet was resuspended in FASW. The bacteria suspension was kept at 4°C in the dark until the experiment was performed. The bead stock solution (Fluoresbrite YG microsphere, Cat. 17154-10, Polyscience) with a concentration of  $4.55 \times 10^{10}$  particles mL<sup>-1</sup>, was sonicated for 5 min and vortexed immediately before the experiment.

### In-vivo sponge phagocytosis assay

The phagocytosis assay consisted of incubating individual fragments of *H. panicea* with a specific particle for 30 min and tracking its incorporation into the sponge (host) cells. The sponges attached to the ceramic tiles were placed in individual 1 L straight-sided polypropylene wide-mouth Nalgene bottles (ThermoFisher; cat. no. 2118-0032) filled with unfiltered natural seawater from the aquaria system inlet. The tiles were laid on a PVC support under which a magnetic stirring bar was positioned, and the bottles were placed on top of a

stirring plate to ensure constant water flow and uniform mixing of the particles during the incubation. Incubations were performed in a climate chamber in which temperature was kept at 10°C. In all cases, sponges incubated in the absence of tracer particles and natural seawater incubations served as controls (n = 4 biological replicates per control and sponges).

First, we tested whether initial particle concentration in seawater had an effect on the percentage of sponges incorporating particles. We incubated the sponge with three different *Nannochloropsis* sp. concentrations, as this was the natural particle given the clearest readout. We added 10 µL, 100 µL, or 1000 µL of the live algal stock culture to each incubation chamber to get a final concentration of approx.  $10^5$ ,  $10^6$  and  $10^7$  algae mL<sup>-1</sup>, respectively. Secondly, we performed a pulse-chase experiment using *Nannochloropsis* sp. to identify the time when we could capture the highest percentage of cells with incorporated particles. Sponges were incubated separately with algae ( $10^6$  algae cells mL<sup>-1</sup> final concentration) over a 30 min pulse phase, and then transferred to the flow-through aquaria with clean natural seawater for a 30 min and 150 min chase phase. Sponges were sampled at t = 0 min (immediately after the 30 min pulse phase was over), at t = 30 min, and at t = 150 during the chase phase (n = 4 biological replicates per time point). Lastly, we aimed to extend the application of our phagocytic assay to other particles. We incubated for 30 min *H. panicea* individuals with TAMRA-stained bacteria and fluorescent bead solution, separately (n = 4 biological replicates per tracer). We aimed at a particle concentration similar to the bacteria concentration naturally encountered by the sponge (Lüskow et al., 2019) (i.e., final start concentration of approx.  $10^5$  bacteria cells mL<sup>-1</sup> and  $10^6$  beads mL<sup>-1</sup>). The sponge cell dissociation was performed immediately after the incubation time (i.e., no pulse-chase design was applied in this case).

### Particle uptake estimation

Water samples (1.8 mL) were taken along the incubation period at 0 min, 2 min, 5 min, 7 min, 14 min, 22 min and 30 min to assess whether sponges were filtering the particles from the water column (i.e., particle uptake) during each in-vivo assay. The sampled water was immediately fixed with a mixture of paraformaldehyde (PFA) and glutaraldehyde in 1x PBS (final concentration 1% and 0.05%, respectively), kept in the dark for 30 min, and stored at -80°C until flow cytometry analysis was performed (following (Gasol and Del Giorgio, 2000)). Algal, bacterial, and bead concentrations from the water samples were estimated using the

Accuri C6 Plus flow cytometer (BD Biosciences). Each sample was run for 1 min at a flow rate of  $14 \mu\text{L min}^{-1}$ . The cell populations of interest were identified based on the fluorescence of each tracer particle and the side scatter (SSC) using the BD Accuri C6 Plus Software. Differences in particle uptake between sponge and control incubations were analyzed using an exponential regression approach (as in (Scheffers et al., 2004; De Goeij and Van Duyl, 2007; Yahel et al., 2007)). In each case, the concentrations were corrected based on the average initial concentration of all incubations. The standardized data was fitted to an exponential model (as proposed by (De Goeij et al., 2008)) and this was used to estimate the concentration of particles in the seawater at the start ( $C_0$ ) and end ( $C_{30}$ ) of the incubation. The total number of particles that were taken up by the sponge was calculated as  $(C_0 - C_{30}) \times$  volume of incubation (i.e., 1000 mL), and with this the percentage of particles reduced by the end of the incubation was estimated. The regression fits and values used for estimating particle uptake can be found in <https://doi.org/10.1594/PANGAEA.956281>.

### Sponge cell dissociation, preparation, and staining

Immediately after each *in-vivo* assay, *H. panicea* fragments were used to extract the sponge cell fraction by tissue dissociation and centrifugation methods [adapted from (Fieseler et al., 2004; Wehrl et al., 2007)]. All buffers and solutions used during the dissociation were adjusted to the salinity (16 PSU) and pH (8.1) of the aquaria at the moment of running the experiment to prevent the cells from undergoing an osmotic or pH shock. Calcium- and magnesium-free artificial seawater (CMFASW; as in (Rottmann et al., 1987)) was used through the whole dissociation process as it prevents sponge cells from reaggregating and minimize unspecific cell-cell interactions. The entire sponge fragments were rinsed in sterile, ice-cold CMFASW, and subsequently cut with a disposable scalpel into small pieces while removing any leftover epibionts or dirt. The tissue fragments were transferred into 50 mL sterile Falcon tubes prefilled with 25 mL of sterile fresh ice-cold CMFASW containing EDTA (25mM) and incubated on ice while gently shaking the tubes horizontally for 15 min. Samples were filtered through  $40 \mu\text{m}$  cell strainers (Corning Inc.) into 50 mL sterile Falcon tubes by gently squeezing the tissue against the walls of the sieve with sterile forceps to remove dissociated tissue fragments and spicules. Ice-cold CMFASW was added to the resulting cell suspension until reaching a total volume of 25 mL and the samples were centrifuged for 5 minutes at  $500 \times g$  at  $4^\circ\text{C}$  in a swinging rotor. The supernatant was discarded, and the sponge cell pellet was resuspended in 4 mL of fresh sterile ice-cold CMFASW resulting in a total sponge cell suspension of approx. 5 mL,

which was divided into 1 mL aliquots in sterile Eppendorf tubes. The aliquots were fixed by adding PFA to the cell suspension (final concentration 4% in CMFASW) and stored at 4°C in the dark overnight. The fixative was washed off the cells by centrifugation for 5 minutes at 500 x g at 4°C. Finally, the pellet was resuspended in 1 mL of ice-cold CMFASW. The concentration of sponge cells for each sample was estimated by an automated cell counter (Fluidlab R-300, Anvajo) and adjusted to approx.  $5 \times 10^7$  cells mL<sup>-1</sup> by diluting the cells with ice-cold CMFASW. The fixed cell suspensions were stored at 4°C in the dark for later FACS quantification. For each sample, 200 µL of cell suspension was diluted into 4 mL of ice-cold CMFASW and filtered through a 40 µm-cell strainer into a 5 mL round-bottom Falcon tube. From the filtered cell suspension, an 2 mL aliquot was used for staining sponge cell nuclei with 14 µL of 100 ng mL<sup>-1</sup> DAPI in a 2 mL cell suspension (final concentration 0.7 ng µL<sup>-1</sup>). The cells were gently mixed by pipetting and incubated for 30 min at 4°C in the dark. The remaining cell suspension aliquot served as control for the DAPI staining (i.e., non-stained aliquot).

### FACS quantification of phagocytic active cells

We define phagocytic active cells as those that had incorporated the tracer particle presented to the sponge during the incubation. Sponge cells were analyzed on a MoFlo Astrios EQ<sup>®</sup> cell sorter (Beckman Coulter) fitted with a 70 µm nozzle and 355nm, 488nm, 561nm and 640 nm wavelength lasers to identify and quantify phagocytic cells. Each sample was analyzed three times (i.e., technical replicates) with FACS for 1 min, and the voltage and pressure were adjusted to ensure to record a similar number of events (i.e., approx. 5k) per second for all samples. The gating was performed with the Summit software (V6.3.1) based on the emission of DAPI and the fluorescence of the respective particle used during the incubation. The strategy we developed for detecting and quantifying the phagocytic active sponge cells of interest followed the subsequent steps. First, to differentiate debris from the “bulk” sponge cells we compared the DAPI emission of non-stained cell aliquots with the DAPI stained aliquots by using the 355 nm UV laser and a filter with a band pass of 448/59 nm (Figure 1A). A scatter plot was created by selecting the DAPI filter channel on the x-axis and the forward scatter (FCS) on the y-axis, and the DAPI positive cell population was gated. Second, to identify the relative percent of “bulk” sponge cells that had incorporated *Nannochloropsis* sp. cells, the DAPI gate was used to create a new scatter using the laser (561 nm) and filter settings (692/75 nm) in the y-axis to detected algae fluorescence (Figure 1B). This approach allowed us to distinguish between sponge cells that had incorporated algae from the rest of the sponge

cells (i.e., phagocytic from non-phagocytic sponge cells, respectively). We confirmed this gating by comparing the fluorescence of the control sponges (i.e., without algae) with the sponges provided with algae (Figure 1B). To identify sponge cells that had incorporated TAMRA-labelled *Vibrio* sp. bacteria from the other sponge cells a scatter plot was created using the side scatter (SSC) on the x-axis and the bacteria fluorescence (laser 561 nm and filter 692/75 nm) in the y-axis (Figure 1C). On the other hand, sponge cells phagocytizing beads were detected by plotting the particle size [forward scatter (FCS): x-axis] against the bead fluorescence (laser 488 nm and filter 526/52 nm: y-axis) (Figure 1D). In all cases, the phagocytic and non-phagocytic sponge cell populations were gated and sorted directly onto microscopy slides (2k-3k cells) for fluorescent microscopy inspection of each tracer (Figure 4). After this verification, the number of events of each gate was used to estimate the relative (%) phagocytic and non-phagocytic cell fraction in relation to the total number of events from these two gates (the complete data set can be found in <https://doi.org/10.1594/PANGAEA.956281>).

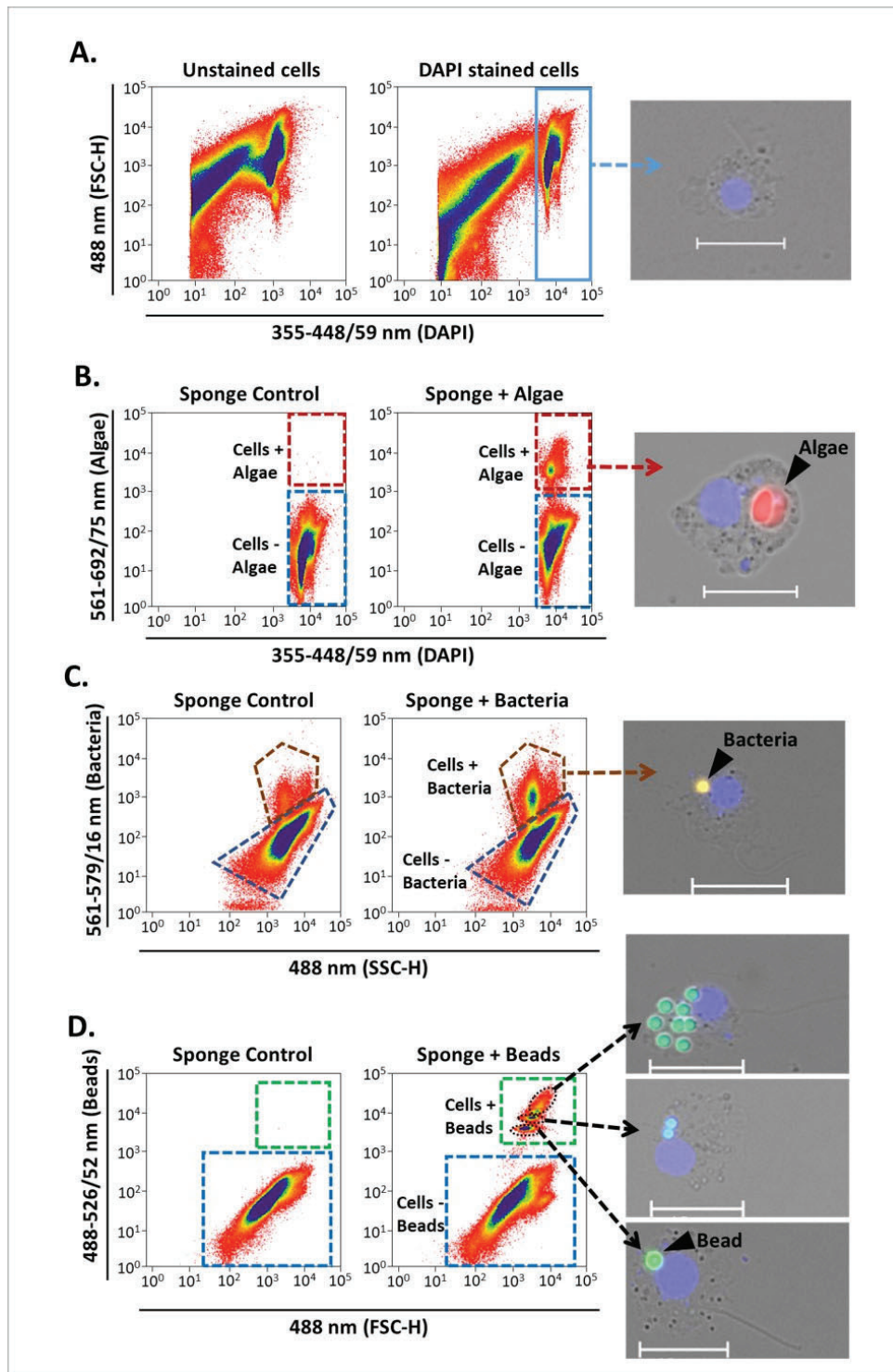


**Fig. 1.** Sponge cell gating strategy for identification and quantification of phagocytic active sponge cells using FACS. Representative cytograms show **A.** identification of the “bulk sponge cells” population after DAPI staining (blue rectangle). Gates of phagocytic cells with (+) incorporation of **B.** algae, **C.** bacteria, and **(D)** beads (red, brown, and green dashed outlines, respectively). Fluorescent microscopy pictures of sorted cells to verify the different gates. Sponge cell nuclei (blue) stained with DAPI. Scale bars: 10  $\mu\text{m}$ . Gates for cells without (-) particle incorporation are shown in each case (blue dashed outlines). Sponges incubated without particles served as controls.

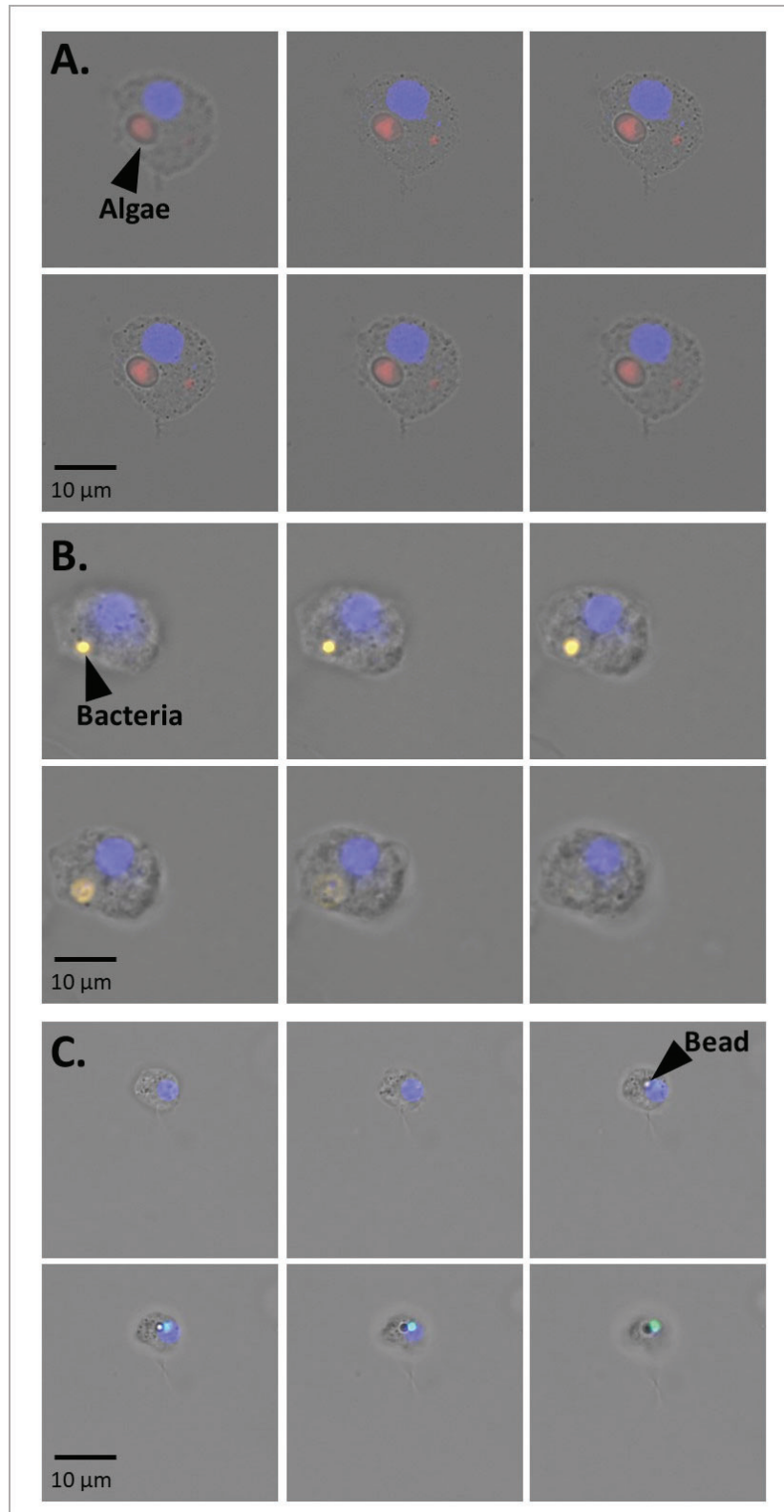


**Fig. 2.** Representative fluorescent microscopy pictures of z-stacks series showing the internalization of **A.** algae **B.** bacteria and **C.** beads into *H. panicea* cells. The series consists of photos taken every 4 to 5 μm. Sponge cell nuclei (blue).



## Results

We estimated the sponge's phagocytic activity as the percentage of sponge cells with incorporated fluorescent particles over the total of sponge cells recovered by coupling incubation experiments with whole *H. panicea* individuals with sponge cell dissociation and FACS. Sponges were incubated with three types of fluorescent particles: *Nannochloropsis* sp., TAMRA-stained *Vibrio* sp., and fluorescent latex beads. Our optimized cell dissociation protocol for *H. panicea* host cells yielded an average recovery of  $1.4 \times 10^7 \pm 5.5 \times 10^6$  cells g<sup>-1</sup> (sponge wet weight) (Fig. S1). The recovered cell suspension was analyzed by FACS (Fig 1) to quantify the relative number (%) of phagocytic active (+fluorescent signal) to the total of +DAPI cells. Fluorescent microscopy z-stack images of the sorted phagocytic active cells supported the incorporation of the particles into the sponge cells (Fig. 2).

### Testing tracer concentration for the phagocytic assay

We tested the effect of different tracer concentration on phagocytosis and particle uptake. The total amount of *Nannochloropsis* sp. cells (mean  $\pm$  SD throughout the text, unless stated otherwise) taken up by *H. panicea* was  $4.9 \times 10^4 \pm 2.5 \times 10^4$  cells and  $2.4 \times 10^5 \pm 3.5 \times 10^5$  cells (Fig. 3A) during the incubation with low ( $\times 10^5$  cells mL<sup>-1</sup>) and medium ( $\times 10^6$  cells mL<sup>-1</sup>) algae concentration, respectively. This uptake corresponds to a reduction in algal concentration in seawater of  $19.6 \pm 9.4$  % and  $12.2 \pm 14.6$  %, respectively. The algal uptake for the highest ( $\times 10^7$  cells mL<sup>-1</sup>) *Nannochloropsis* sp. concentration used during the phagocytic assay was inconclusive (Fig. 3A) presumably because algal cells might have clumped together and the sponge became oversaturated during the incubation.

The percentage of phagocytic cells was  $0.6 \pm 0.4$  % for the low concentration ( $\times 10^5$  cells mL<sup>-1</sup>),  $4.9 \pm 2.1$  % for the medium concentration ( $\times 10^6$  cells mL<sup>-1</sup>), and  $8.8 \pm 3.9$  for the high-concentration ( $\times 10^7$  cells mL<sup>-1</sup>) (Fig. 3B). There was a significant effect of algal concentration in seawater on the percentage of phagocytic cells in *H. panicea* (ANCOVA,  $F = 11.03$ ,  $p < 0.01$ ;  $df = 2$ ). The high algal concentration yielded on average an approx. 15-fold increase in the percentage of phagocytic cells compared to the lowest concentration. At the medium concentration, the percentage of phagocytic cells appeared to yield on average an approx. 8-fold and 2-fold increase compared to the low and high concentration, respectively. However, the medium treatment was neither statistically different from the low ( $p = 0.09$ ) nor the high ( $p = 0.10$ ) algal treatment (Fig. 3B). For the high concentration treatment, it is worth noting

that even though the algal uptake estimates based on flow cytometry measurements of seawater samples were inconclusive (Fig. 3A), we did detect an increase in phagocytic activity, and observed incorporation of algae into the sponge cells (Fig. 3B).

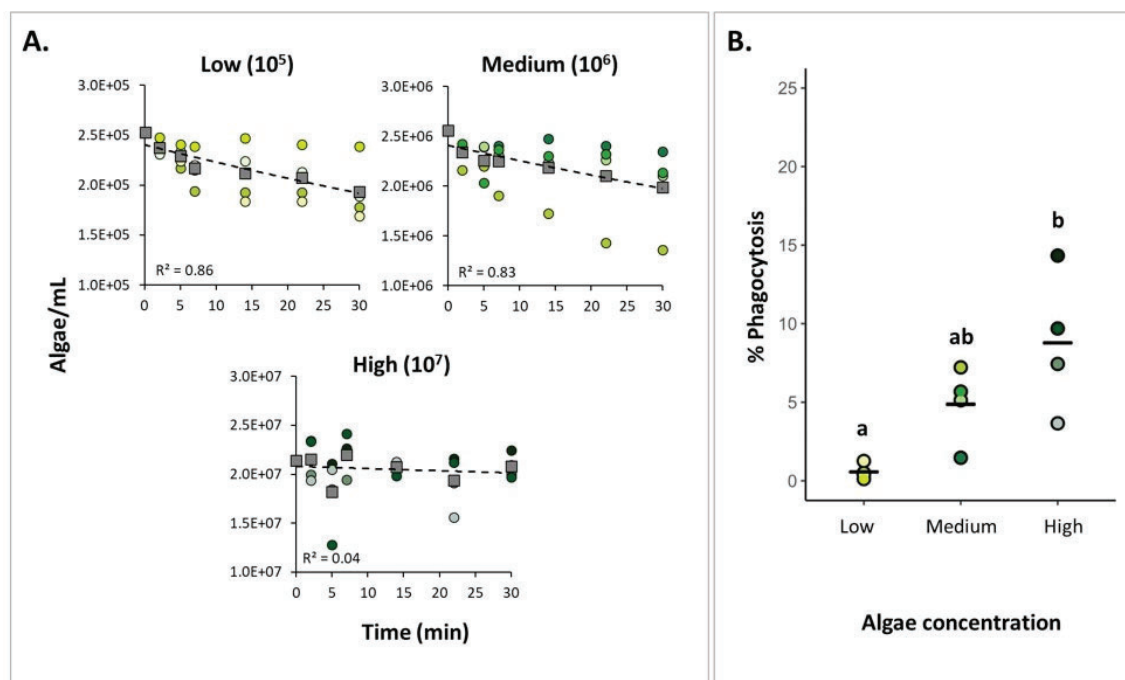


**Fig. 3.** Testing tracer concentration for the phagocytic assay. **A.** Algal uptake by *H. panicea* individuals incubated at three algal concentrations (Low:  $\times 10^5$ ; Medium:  $\times 10^6$ ; and High:  $\times 10^7$  algae mL<sup>-1</sup>) based on seawater sample analyses. Dots of the same color: biological replicates (n = 4 per treatment). Squares and dash lines: averaged data fitted to an exponential model. **B.** Estimates of phagocytic active sponge cells based on FACS analyses. Bold line: average for the 4 biological replicates. Treatments marked with different letters are significantly different at  $\alpha=0.05$ .

### Assessing timing of algal phagocytosis

We performed a pulse-chase experiment using *Nannochloropsis* sp. to assess at what time point after presenting the algae to *H. panicea* yielded the highest percentage of phagocytic sponge cells. The total number of algal cells taken up by the sponges after the 30 min pulse period was  $3.3 \pm 2.5 \times 10^5$  cells, which translates to a  $13.7 \pm 10.6$  % algal reduction (Fig. 4A). The percentage of phagocytic cells was  $4.9 \pm 2.1$  % after 0 min,  $2.2 \pm 0.78$  % after 30 min, and  $2.0 \pm 0.4$  % after 150 min chase-period (Fig. 4B). The percentage of phagocytic cells was positively related with algal uptake (ANCOVA,  $F = 6.53$ ,  $p = 0.03$ ;  $df = 1$ ). After removing the effect of particle uptake on the response variable, phagocytic activity significantly decreased during the chase period (i.e., phagocytosis decreased with time after initial particle exposure) (ANCOVA,  $F = 9.80$ ,  $p < 0.01$ ;  $df = 2$ ). The phagocytic activity peaked at 0 min chase, then

significantly decreased by approx. 50 % at 30 min chase, but there was no further significant decline in the percentage of phagocytic cells after 150 min chase.

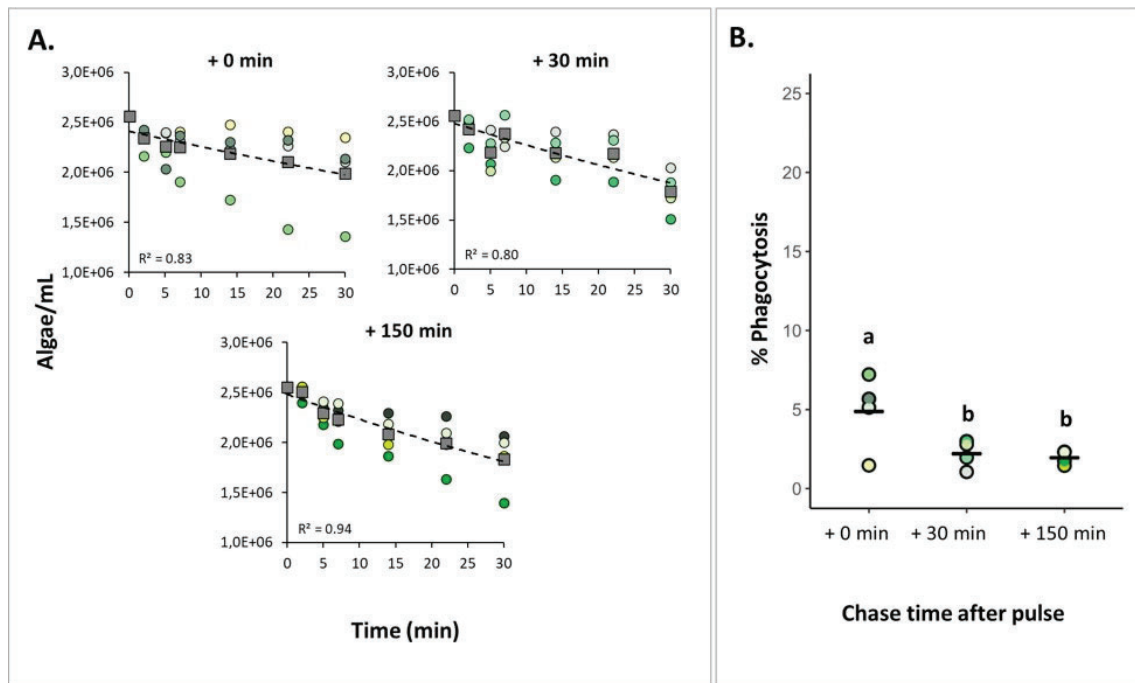


**Fig. 4.** Assessing the starting time of algal phagocytosis. *H. panicea* individuals were incubated for 30 min (pulse period) with an initial algal concentration of  $\times 10^6$  algae  $\text{mL}^{-1}$  and sampled after three chase periods (+ 0 min, + 30 min, and + 150 min). **A.** Algal uptake by sponges during the pulse period based on flow cytometry analysis of seawater samples taken at time intervals. Dots of the same color: biological replicates ( $n = 4$  per treatment). Squares and dash lines: averaged data fitted to an exponential model. **B.** Estimates of phagocytic active sponge cells based on FACS analyses. Bold line: average for the 4 biological replicates. Treatments marked with different letters are significantly different at  $\alpha=0.05$ .

### Bacteria and latex beads as tracers of phagocytosis

When bacteria and beads were provided as tracers, the total number of particles taken up by the sponge was  $2.7 \times 10^4 \pm 7.9 \times 10^3$  bacteria and  $2.4 \times 10^5 \pm 2.3 \times 10^5$  beads, corresponding to a  $31.0 \pm 8.6 \%$  and  $14.3 \pm 16.0 \%$  reduction of particle concentration in seawater after each assay, respectively (Fig. 5A). Particle uptake varied among *H. panicea* individuals. Some sponge individuals only reduced the particle concentration by 1 to 4 %, while other individuals decreased the concentration by 22 to 37 %. The differences in particle uptake between individuals could be derived from variations in the filtration activity of the sponges. It is known that filtration rates of *H. panicea* can considerably change over time due to osculum contractions (e.g., (Goldstein et al., 2020; Riisgård et al., 2016)), and we cannot discard this to

be the cause of the observed variations. Despite this, there was overall no significant difference in particle uptake between bacteria, beads, and algae (ANOVA,  $F = 0.57$ ,  $p = 0.59$ ;  $df = 2$ ). In the bacteria experiment, sponge control samples (i.e., individuals incubated without bacteria) showed some events in the gate used for quantifying cells with incorporated fluorescent signals (Fig. 1C).

Based on our microscopy observations using the filter set 43 HE DsRed (538-562 nm), the signal may correspond to natural auto-fluorescent granules present in the *H. panicea* cells. After subtracting the events estimated in the control samples, the percentage of cells phagocytizing bacteria in the treated sponges was  $8.0 \pm 2.3$  % (Fig. 5B). In the assay with the beads, we identified a distinct population of phagocytic sponge cells consisting of at least three subpopulations (Fig. 1D). Fluorescent microscopy of the sorted cells within these three subpopulations revealed differences in the number of beads phagocytized per sponge cell. Most cells from the lower subpopulation in the  $\gamma$ -axis (i.e., green fluorescence) showed incorporation of one bead, while cells from the medium and highest subpopulation contained 2-3 and  $> 3$  beads per cell, respectively (Fig. 1D). Overall, the percentage of sponge cells phagocytizing beads was  $11.6 \pm 7.6$  % (Fig. 5B). When comparing the phagocytic activity of *H. panicea* individuals exposed to bacteria, beads, and algae, we detected no significant difference between tracers after controlling for particle uptake (ANCOVA,  $F = 1.52$ ,  $p = 0.28$ ;  $df = 2$ ).

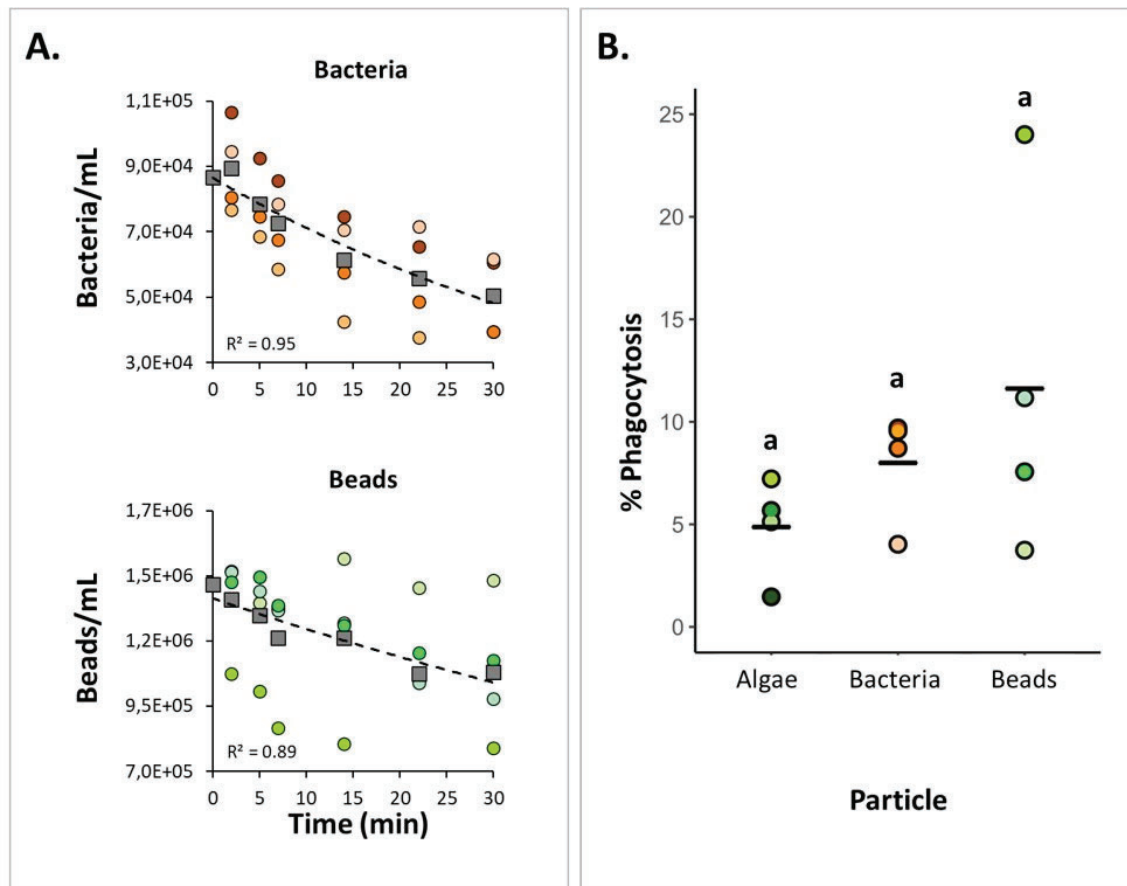


**Fig. 5.** Testing bacteria and beads as tracers for the phagocytic assay. *H. panicea* individuals were incubated for 30 min with TAMRA-stained bacteria (*Vibrio* sp.) and fluorescent latex beads (1  $\mu\text{m}$ ) at an initial concentration of around  $\times 10^5$  to  $\times 10^6$  particles  $\text{mL}^{-1}$ . **A.** Bacterial and bead uptake by sponges during the incubation period based on flow cytometry analysis of seawater samples taken at time intervals. Dots of the same color: biological replicates ( $n = 4$  per treatment). Squares and dash lines correspond to the averaged data fitted to an exponential model. **B.** Estimates of phagocytically active sponge cells in comparison to the algal assay. Bold line: average for the 4 biological replicates. There was no significant difference between samples.

### Cellular insights into the phagocytic process

Fluorescent microscopy of *H. panicea* dissociated cells revealed diversity in terms of morphology and size of the sponge cells engaged in phagocytosis (Fig. 6A-C). In general, we observed relatively small cells (approx. 5  $\mu\text{m}$ ) with a clear nucleus of around 2  $\mu\text{m}$  and a flagellum of various length, which we presume are choanocytes. Medium to big cells (approx. 6 to 10  $\mu\text{m}$ , and 10 to 12  $\mu\text{m}$ , respectively) with a nucleus of around 5  $\mu\text{m}$ , and no flagella that resemble archaeocyte-like cells were also visible. For all particle types (i.e., algae, bacteria, and beads), 39 to 50 % of the cells performing phagocytosis were choanocyte-like cells (Table S1). However, medium to big phagocytic cells (10 to 12  $\mu\text{m}$ ) engaged more often in algal

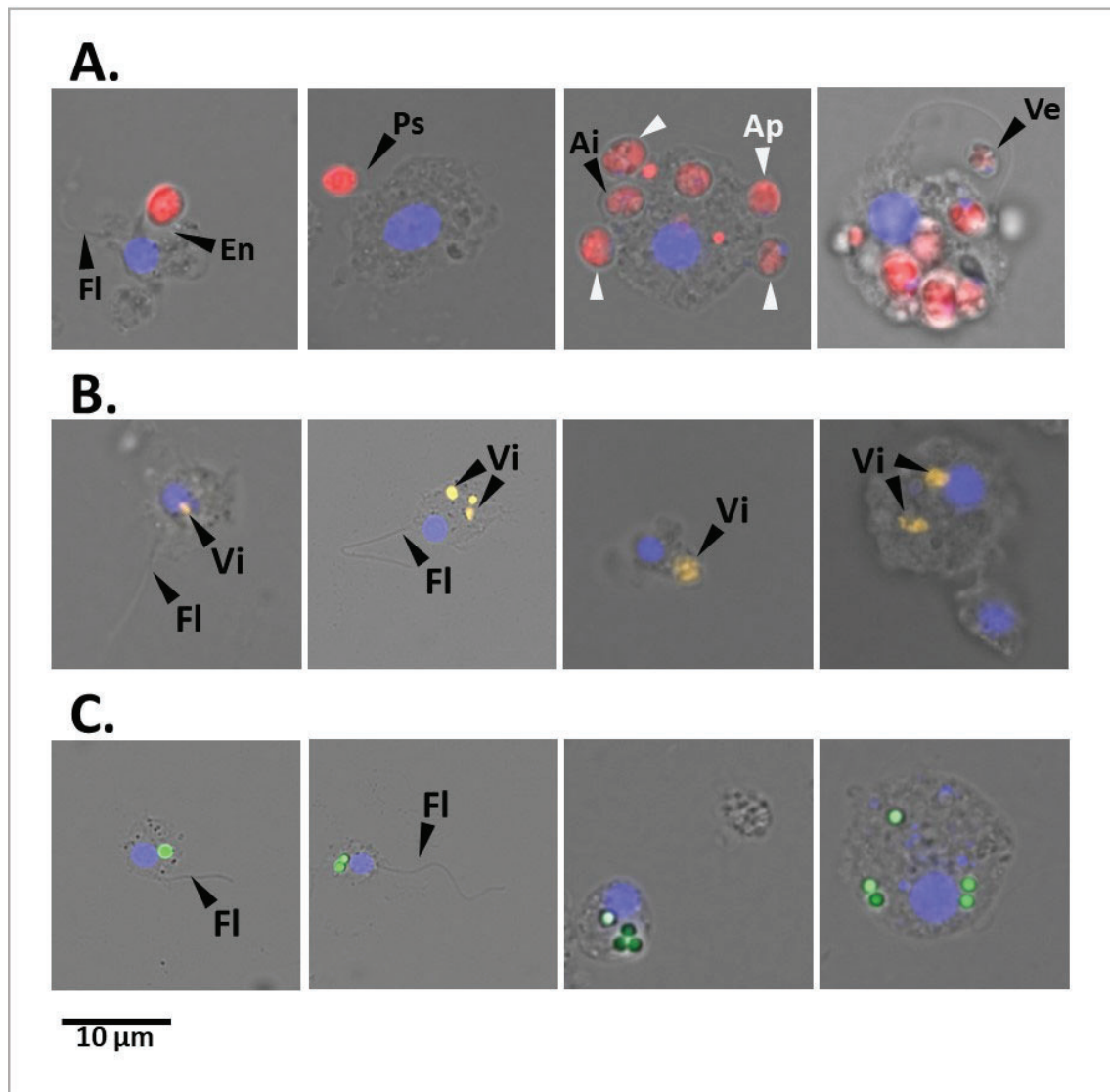


**Fig. 6.** Representative fluorescent microscopy pictures of cells dissociated from *H. panicea* tissue after phagocytic assays using different tracers. Sponge cells phagocytizing **A.** microalgae (*Nannochloropsis* sp.; red). Flagellum (Fl); evagination (Ev) and pseudopodium (Ps) of sponge cell membrane for incorporating algae; algal cells in the periphery (Ap) and internalized (Ai) in the sponge cell; and vesicle (Ve) with algal cell. **B.** TAMRA-stained *Vibrio* sp. (Vi; yellow) and **C.** fluorescent latex beads (1 µm; green) internalized in different cell types. Sponge cell nuclei (blue) stained with DAPI. Scale bar: 10 µm in all cases.

phagocytosis (29 and 18 % of total phagocytic cells, respectively) compared to bacteria (13 and 4 %, respectively) and beads (10 and 3 %, respectively) (Table S1). In the pulse-chase experiment with alga incubations, we identified potential early stages of algal phagocytosis at + 0 min chase, in which the sponge cell membrane evaginates, protrudes into pseudopodia-like structures, or extends vesicles to incorporate *Nannochloropsis* sp. cells (Fig. 6A).

Furthermore, the percentage of phagocytic choanocyte-like cells showed a 3 to 7-fold significant reduction (Table S1) one and three hours after the assay started (i.e., + 30 min and + 150 min time point, respectively). In contrast, the proportion of archaeocyte-like cells continued to increase significantly by up to 30 % at + 150 min (Table S1).

TEM observations on *H. panicea* tissue samples from the algal assays provided additional evidence of *Nannochloropsis* sp. incorporation and processing into the sponge cells. Intact algal cells were observed in the extracellular matrix of the sponge (i.e., the mesohyl), exhibiting characteristic structures like the cell wall, thylakoids, and vacuole (Fig. 7A). Whole *Nannochloropsis* sp. cells internalized in sponge cells were detected in the inspected samples (Fig. 7B-C). We also observed phagosome-like structures with potential remnants of cell wall and thylakoids, which we presume, is the result of algal digestion (Fig. 7D-F).

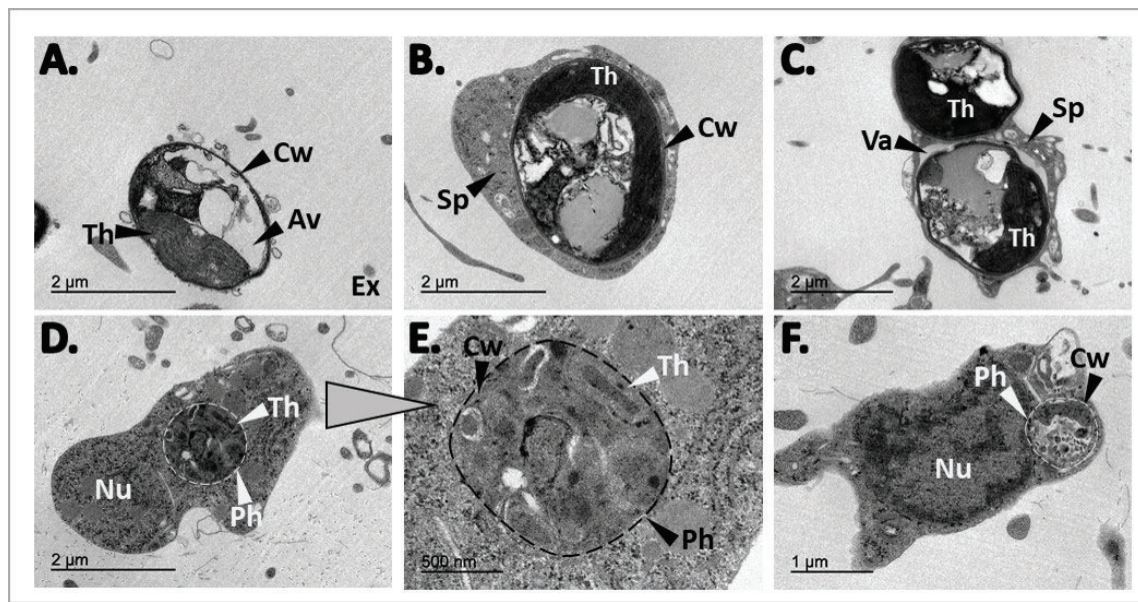


**Fig. 7.** TEM observations from *H. panicea* tissue after algal phagocytosis. **A.** Free, intact *Nannochloropsis* sp. cell in the sponge extracellular (Ex) matrix. The cell wall (Cw), thylakoids (Th), and the algae vacuole is visible. **B.** and **C.** sponge cells (Sp) with one and two internalized algal cells, respectively. One of the algae is inside a vacuole (Va). **D.** to **F.** Potential algal digestion in which possible remnants of algal cells are observed in phagosome-like structures (Ph). Nucleus (Nu).

## Discussion

The aim of this study was to establish a high-throughput method for quantifying particle incorporation into the cells of whole sponge individuals by coupling live sponge incubations using fluorescent tracers, with sponge cell (host) dissociation, FACS analysis, and microscopy inspections. We adopted an *in-vivo* rather than an *in-vitro* cellular assay approach to replicate and accurately predict, as much as possible, the natural behavior of cells in *H. panicea*. *In-vitro* work in sponges is challenging mainly because their cells reaggregate fast, and the use of chemicals to induce disaggregation can reduce cell viability and inhibit essential cellular processes (Pomponi, 2006). With the established *in-vivo* phagocytic assay, we were able to successfully quantify the incorporation of algae, bacteria, and beads into *H. panicea* cells, and identify different sponge cell types involved in the process of particle incorporation.

Even though the incorporation of the different tracers into the sponge cells was evident via z-stack images (Figure 2), we cannot discard that some of the particles were not internalized but rather attached to the cell's surface. Yet, our cell dissociation protocol applies CMFASW which, besides preventing sponge cells from aggregating, should also minimize unspecific cell-cell interactions. Thus, we speculate that the cells identified as phagocytic were indeed in the process of internalizing particles (e.g., Figure 6A). Besides phagocytosis, there are other endocytic pathways (e.g., micropinocytosis and macropinocytosis) by which particles can be internalized into cells. Based on the size of the particles we used during our assays (1 $\mu$ m to 3 $\mu$ m in diameter), internalization must happen either via phagocytosis or macropinocytosis. We acknowledge that evidence regarding the involvement of ligand-receptors, which is the main difference between these two endocytic processes, is not provided in the manuscript. In the sponge research field, particle internalization into the cells has been, to our knowledge, extensively termed and described as phagocytosis (e.g., Imsiecke, 1993; Leys and Eerkes-Medrano, 2006; Maldonado et al., 2010; Leys et al., 2018) based on microscopy observations. Transcriptomic data in *H. panicea* and in other sponge species have already pointed to the activation of phagocytic-related genes upon sponge encounter with microbes or microbial elicitors (Yuen, 2016; Pita et al., 2018b; Geraghty et al., 2021; Schmittmann et al., 2021). Indeed, it is very plausible that phagocytosis is the mechanism by which particles enter the sponge cells. Unlike other invertebrates (e.g., amoeba, corals, mussels, insects, etc.), detailed studies on the phagocytic process have not been conducted in sponges yet. We are convinced that the developed assay in *H. panicea* has enormous potential to be used as a tool to



investigate how sponge phagocytosis works by combining, for example, dyes for lysosomal activity, actin filaments, and oxidative stress, among others, which could even be coupled with FACS analysis to resolve subpopulations of phagocytic sponge cells [as done e.g., in cnidarians (Snyder et al., 2021)].

### Tracer concentration and phagocytic activity

In each experiment, we quantified clearance of particles as indicator for sponge filtering activity (as in (Leys et al., 2011; Mueller et al., 2014; Riisgård et al., 2016; Luskow et al., 2019)). We observed that an increase in tracer concentration resulted in a linear increase in algal removal by *H. panicea*. This is consistent with previous findings of concentration-dependent particle removal rates in sponges (e.g (Yahel et al., 2006; Mueller et al., 2014)). In our algal assays, most of the sponge individuals were actively filtering the tracer during the 30 min incubations with low and medium *Nannochloropsis* sp. concentrations ( $10^5$  and  $10^6$  cells mL<sup>-1</sup>, respectively), as the algal abundance declined exponentially over time. The algal uptake for the highest ( $10^7$  cells mL<sup>-1</sup>) *Nannochloropsis* sp. concentration used during the phagocytic assay was inconclusive. Algal cells might have clumped hindering the detection of changes in algal concentration during the assay and thus, we recommend working with particle concentrations below  $10^7$  cells mL<sup>-1</sup>. The overall (mean  $\pm$  SD) algal clearance rate of our sponges ( $1.5 \pm 0.2$  mL water mL sponge<sup>-1</sup> min<sup>-1</sup>) is also in line with previous reports for *H. panicea* ( $1.5$  to  $1.9 \pm 0.8$  to  $1.1$  mL water mL sponge<sup>-1</sup> min<sup>-1</sup> (Scheffers et al., 2004)). Filtration rates of *H. panicea* can considerably vary in laboratory conditions (Riisgård et al., 2016), and even though we observed variation in the filtration activity of certain individuals, our incubation setup for the phagocytic assay proved overall to ensure the sponge filtration activity, which is an important factor to control.

We further hypothesized initial tracer concentration to positively affect the percentage of phagocytic active cells since this relation has been observed in other phagocytic assays (e.g (Lindner et al., 2020)). Indeed, we found a positive relation between algal concentration in the seawater and the percentage of sponge cells that incorporated particles. Studies in cnidaria (Bucher et al., 2016), fish (Li et al., 2006), and mice (Tartaro et al., 2015) also reported phagocytosis to increase with particle concentration (i.e., when using fluorescent beads, bacteria and algae). In our assay, increasing the algal concentration from  $10^5$  to  $10^7$  algae mL<sup>-1</sup> (i.e., low to high concentration treatment) resulted in a significant 15-fold increase in the

sponge phagocytic activity. While the phagocytic activity seemed to also increase when increasing the concentration from low to medium (8-fold), and from medium to low (2-fold), this trend was not significant. This indicates that sponge cells can adjust their phagocytic activity depending on the number of algal cells they encounter. These results suggest that an algal concentration of approx.  $10^6$  cells  $\text{mL}^{-1}$  is optimal for performing algal phagocytosis assays in *H. panicea*.

### Onset of phagocytosis

The observations from our pulse-chase experiment revealed incorporation of algae into the sponge cells at + 0 min chase, then after 30 min chase phagocytic activity significantly decreased 2-fold, but then remained constant (i.e., + 150 min chase) (Figure 7B). After 30 min exposure to the algae, during the chase phase, sponges were transferred to particle-free water, yet our FACS results showed that approx. 75% of the algae that were taken up by the sponge were found as “intact algae” (i.e., present in the sponge fraction but not incorporated in sponge cells) at + 0 min and + 30 min chase (Figures 7A, S2). Our dissociation protocol was designed to be gentle enough to keep sponge cells intact and this was evident since we observed delicate structures like flagella (Figure 6). We suggest that intact algae are either algae that were loosely attached to sponge cells (e.g., Figure 6A) and got detached during the sponge cell dissociation process or during the FACS. Interestingly, at + 150 min chase the percentage of intact algae decreased to 56% (Figure S2), supporting that intact *Nannochloropsis* sp. cells were taken up by the sponge during the pulse chase and were in the process of incorporation during the chase phase.

We propose that the decrease in phagocytic activity between + 0 min chase and + 30 min chase is the consequence of algal digestion (e.g., Figures 7D–F), and during this process, internalization of intact algae might decrease. Once digestion is completed the process of internalization could be resumed and hence, the maintenance of phagocytic activity between + 30 min and + 150 min chase. In freshwater sponges, algae internalization and translocation between sponge cells occurs within minutes after feeding, whereas digestion takes a couple of hours. For example, in young individuals of *Spongilla lacustris* hatched from gemmules, extensive digestion of algal cells by phagocytes was evident 5 h after feeding (Imsiecke, 1993). Likewise, in algal-free (i.e., “aposymbiotic”) *Ephydatia muelleri* intracellular algal symbionts were observed to be internalized in archaeocytes 4 h post-infection (Geraghty et al., 2021).

Our findings together with the above observations reveal that algal phagocytosis in sponges initiates within minutes after particle exposure and takes a couple of hours to be completed. We further suggest that the fact that some *Nannochloropsis* sp. cells were taken up by *H. panicea* but not internalized, due to potential digestion events of other algal cells, indicates a decoupling in time between algal uptake, internalization, and digestion by sponge cells.

### Algae, bacteria, and beads as tracers for the phagocytic assay

The percentage of phagocytic cells estimated with our assay for *H. panicea* using algae, bacteria, and beads as tracer particles ranged overall between 5 to 24%. It is difficult to compare our estimates to other studies since, to our knowledge, similar quantifications of phagocytic sponge cells have not been done yet. Thus, we have compared our results to well-established models for phagocytosis. For example, amoebal phagocytic activity of *Dictyostelium discoideum* upon exposure to GFP-tagged *Legionella pneumophila* was estimated to be < 2% based on FACS counts (Hägele et al., 2000), whereas in *Acanthamoeba castellanii* microscopy counts showed 15-35% of amoeba cells phagocytizing *E. coli* (Nguyen et al., 2014). *In-vitro* phagocytosis experiments in cnidarians estimated with FACS percentages of coral and sea anemone phagocytic cells between 2.2 to 7.8% and 9 to 18% after feeding cells with 1  $\mu\text{m}$  latex beads and fluorescently labeled *Escherichia coli*, respectively (Rosental et al., 2017; Snyder et al., 2021). Although the aforementioned assays diverge from ours in the sense that they were performed in cell suspensions, under different conditions, and not in whole sponge individuals, the reported phagocytic activity in those studies is comparable to our estimates in *H. panicea*.

Our data suggest that phagocytosis differs depending on the sponge filtration activity (i.e., particle uptake) and on the type of particle used during the assay. The percentage of phagocytic cells tends to increase with increased particle uptake in all tracer types, but this relationship seems to be tracer-specific (Figure S3). The increase in phagocytic cells appeared to be faster for beads, followed by bacteria, and at a lower degree for algae (Figure S3). The beads tend to accumulate in the cells (Figures 1D, 6C) as they cannot be digested by the sponge. For *H. panicea*, we speculate that once the sponge cells are saturated with beads ( $\geq 5$  beads per cell) new cells need to engage in the phagocytic process, which could explain the steeper increase in bead incorporation (Figure S3). In *E. muelleri* high accumulation of beads in the choanocytes occurs within 13 min of exposure to the particle, and after 15 min bead

incorporation extends to the archaeocytes (Funayama et al., 2005). Thus, the fast uptake and high number of sponge cells with incorporated beads may be the result of the participation of more choanocytes within the first 30 min of exposure to the particles.

In the case of bacteria, the number of *Vibrio* cells incorporated per sponge cell was difficult to resolve because the resolution acquired with the fluorescent microscope was not high enough, and it was difficult to accurately distinguish our fluorescent bacteria from natural fluorescence occurring in the sponge cells. However, FACS allowed us to subtract the natural fluorescence based on the signal in control samples and we estimate that an approx. 50% increase in bacterial uptake would yield a 50% increase in the percentage of phagocytic cells (Figure S3). NanoSIMS experiments in the marine encrusting sponge *Halisarca caerulea* using isotopically labeled bacteria indicate that bacteria are rapidly phagocytized by choanocytes (Hudspeth et al., 2021). Within 15 min after feeding the sponge with labeled bacteria, 90 to 100% of the choanocyte cells incorporated bacteria and individual bacteria cells were visible in intracellular vesicles. Moreover, bacterial digestion and assimilation processes can vary depending on the bacteria encountered by the sponge. For example, *Hymeniacidon perlevis* can rapidly process *E. coli*, whereas assimilation of *Vibrio anguillarum* is more laborious. *Vibrio* cells are semi-digested by choanocytes 4 h after feeding and digestion is further completed by amoeba-like cells (Maldonado et al., 2010).

In the case of the algae, the percentage of sponge cells engaged in phagocytosis tended to be lower compared to the other tracers, however this trend was not significant. Algal phagocytosis only increased by 1.5% despite an approx. 30% increase in algal uptake (Figure S3). It is plausible to suggest that the bigger size and cell wall structure of the *Nannochloropsis* cells requires more time for the sponge to digest the algae (see previous section for details). Overall, our results indicate that the phagocytic response of *H. panicea* depends on the nature of the particle the sponge encounters. Indigestible particles (i.e., latex beads) trigger a faster incorporation into the sponge cells (Figure S3) and likely involved different cell types (Figure 6C). Whereas for microorganisms that can be digested (i.e., bacteria and algae), phagocytosis seems to vary with particle size. Big algal cells are incorporated at a slower rate than smaller bacterial cells (Figure S3), and a higher rate of translocation between sponge cell types is evident (Table S1).

## Prospects of the phagocytosis assay to investigate microbial discrimination by sponges

The established phagocytosis assay is a high-throughput method for quantifying particle incorporation in cells of whole sponge individuals, which can be applied to a variety of sponge species, and even other marine invertebrates. Other established methodologies like NanoSIMS can provide microscopic details into cellular mechanisms, but only a small portion of the organisms can be analyzed, and the methodology is expensive and not easily accessible. Although our assay may require the FACS for initial validations and certain applications, estimates of phagocytic cells could be done in a normal flow cytometer, an instrument that is common in most marine institutes and which can even be used in research vessels.

Furthermore, our assay could be used to investigate the mechanistic bases of phagocytosis on microbe recognition and differentiation by sponges. For example, the *in-vivo* assay can be used to compare sponge phagocytosis of symbiont vs. non-symbiont bacteria and would aid to unveil if sponges discriminate “friend” from “foe” through this conserved cellular mechanism. It is known that sponge-associated bacteria express ankyrin-repeat proteins which can interfere with phagocytosis (e.g., (Nguyen et al., 2014; Jahn et al., 2019)). Utilizing the established assay to query whether bacteria expressing ankyrins evade phagocytosis would provide further evidence on the role of ankyrin proteins as mediators of symbiont recognition by sponges. Moreover, combining the developed *in-vivo* assay with cell markers would aid to resolve which types of sponge cells activate a phagocytic response upon bacterial encounter, and whether the population of phagocytic cells change when the sponge is presented with different types of microbes.

## Conclusion and perspectives

Here we present a novel, *in-vivo* assay to quantify phagocytic active sponge cells in whole *H. panicea* individuals. Coupling sponge incubations with sponge cell (host) dissociation and FACS analysis proved to be a suitable approach to track fluorescent tracers (i.e., algae, bacteria, and beads) from the surrounding seawater into the sponge cells, and to quantify the relative proportion of *H. panicea* cells incorporating those tracers. The percentage of cells incorporating particles ranged between 5 to 24% and was not significantly different between algae, bacteria and beads. The number of particles filtered by *H. panicea* and the degree of digestion by the sponge cells seemed to be tracer-dependent. Furthermore, our method gave

us hints on the process of particle incorporation itself. Particle incorporation by sponges is fast, initiating within minutes and concluding within < 60 min of exposure to the tracers, and involves different cell types (presumably choanocyte- and archaeocyte-like cells) and possible translocation between cells based on our microscopy observations.

Sponges as ecologically relevant basal metazoans are ideal models to investigate the evolution of host-microbe interactions. We envision our high-throughput assay as a tool to query whether sponges process different microbes (e.g., food, symbiont, and pathogens) distinctively through the conserved cellular mechanism of phagocytosis. Based on our observations, we speculate that particle discrimination might occur upon internalization and the difference might rely on how each particle type is processed (e.g., digested or expelled). Hence, we hypothesize that symbionts are incorporated and/or digested to a lesser extent by sponge cells compared to non-symbionts, and that certain microbial structures (e.g., ankyrins) mediate phagocytosis evasion. Using the developed assay to compare phagocytosis of symbiont vs. non-symbiont (e.g., bacterioplankton) bacteria, as well as bacteria encoding ankyrin proteins, would expand on previous works to better understand the role of phagocytosis in sponge-microbe interactions. Furthermore, to fully characterize the diversity of sponge cells capable of engaging in the phagocytic process developing of cellular marker for marine sponges is needed (e.g., for detecting lysosomal activity and reactive oxygen species (ROS) production (Snyder et al., 2021)). Fluorescent *in-situ* hybridization probes (e.g (Musser et al., 2021)) together with our experimental approach and FACS analysis could aid to identify sponge cell types responsible for different steps of the phagocytosis process, and to investigate if their activity changes after encountering different microbes or environmental stressors (e.g., elevated temperatures, ocean acidification, sedimentation) impair this process. As phagocytosis is an essential component of the innate immune system responsible to recognize and protect against foreign particles and damage cells (Uribe-Querol and Rosales, 2020), we expect sponge phagocytic activity to increase upon exposure to foreign bacteria and under environmental conditions inducing cellular damage. Lastly, coupling single-cell RNA sequencing of populations of phagocytic cells could shed light on the molecular machinery behind sponge phagocytosis. Adapting our assay to other early evolutionary metazoans (e.g., the freshwater sponge *E. muelleri*, the sea anomes *Nematostella sp.* and *Aiptasia sp.*, and the Mytilid mussel *Bathymodiolus sp.*) and adopting comparative analyses could further help to

better understand this conserved cellular mechanism and may therefore have the potential to unravel the role of phagocytosis in basal animal-microbe interactions.

### Data availability statement

Data is publicly available in Pangea at <https://doi.org/10.1594/PANGAEA.956281>.

### Author contributions

AM-G, LP and UH conceived the idea. AM-G planned and conducted the experiments. KB and AM-G performed the FACS analysis and fluorescent microscopy. LP performed the TEM inspections. The initial draft of the manuscript was written by AM-G and UH. All authors contributed to improving the article and approved the submitted version.

### Funding

UH was supported by the DFG (“Origin and Function of Metaorganisms”, CRC1182-TP B01) and the Gordon and Betty Moore Foundation (“Symbiosis in Aquatic Systems Initiative”, GBMF9352). LP received supported by “la Caixa” Foundation (ID 10010434), co-financed by the European Union’s Horizon 2020 research and innovation program under the Marie Skłodowska-Curie grant agreement No 847648), fellowship code is 104855. Additional funding support to LP was provided by the “Severo-Ochoa Centre of Excellence” accreditation (CEX2019-000928-S). This is a contribution from the Marine Biogeochemistry and Global Change research group (Grant 2021SGR00430, Generalitat de Catalunya).

### Acknowledgments

We are grateful to Dr. Lara Schmittmann for the field collection support, and Dr. Ben Mueller for helpful discussions. We further acknowledge Sabrina Jung for technical assistance in the lab, Andrea Hethke for support with the cell dissociations, Fabian Wendt for technical support with the algae culture and experimental setup logistics, Janis Müller for his experimental support. We thank the TEM-SEM Electron Microscopy Unit from Scientific and Technological Centers (CCiTUB), Universitat de Barcelona, for their support and advice on TEM technique, and the International Max Planck Research School for Evolutionary Biology for supervision effort of AM-G.

---

## Conflict of interest

The authors declare that the research was conducted in the absence of any commercial or financial relationships that could be construed as a potential conflict of interest.

## Publisher's note

All claims expressed in this article are solely those of the authors and do not necessarily represent those of their affiliated organizations, or those of the publisher, the editors and the reviewers. Any product that may be evaluated in this article, or claim that may be made by its manufacturer, is not guaranteed or endorsed by the publisher.

## Supplementary material

The Supplementary Material for this article can be found online at: <https://www.frontiersin.org/articles/10.3389/fmars.2023.1176145/full#supplementary-material>

*COPYRIGHT © 2023 Marulanda-Gómez, Bayer, Pita and Hentschel. This is an open-access article distributed under the terms of the Creative Commons Attribution License (CC BY). The use, distribution or reproduction in other forums is permitted, provided the original author(s) and the copyright owner(s) are credited and that the original publication in this journal is cited, in accordance with accepted academic practice. No use, distribution or reproduction is permitted which does not comply with these terms*





---

Chapter 4  
Characterization of Sponge Phagocytosis  
upon Native and Foreign *Vibrio* Encounter  
in the Breadcrumb Sponge  
*Halichondria panicea*

---

**Marulanda-Gómez A<sup>1</sup>**, Mueller B<sup>2,3</sup>, Bayer K<sup>1</sup>, Abukhalaf M<sup>4</sup>, Tholey A<sup>4</sup>, Pita L<sup>5</sup>, Hentschel U<sup>1,6</sup>. (manuscript in preparation).

## Abstract

Phagocytosis is a conserved cellular mechanism for digestion and defense in the animal kingdom but is also one of the main gates for microbes to enter and colonize their hosts. Symbiont acquisition and persistence within the host are likely to occur through the manipulation of certain steps of the phagocytic process. Yet, how the host differentiates between symbionts to retain vs. pathogens to eradicate is just starting to be decoded in marine invertebrates. Early branching metazoans such as sponges (Porifera) represent an evolutionary and ecologically important phylum for gaining insights into the role of phagocytosis in animal-microbe interactions. We used a recently developed phagocytic assay to compare the phagocytic activity of the breadcrumb sponge *Halichondria panicea* upon incubation with a native sponge-associated (Hal 281) vs. a foreign non-sponge-associated isolate (NJ 1) *Vibrio* isolate. The sponge (host) cell fraction was recovered after 30 min and 60 min exposure to the isolates and the relative abundance of phagocytic cells was estimated by fluorescence-activated cell sorting (FACS). Moreover, we implemented, for the first time, proteomic analysis to quantify the total number of differentially abundant proteins putatively involved in phagocytosis. The phagocytic assay revealed no difference in the percentage of phagocytic sponge cells between the *Vibrio* isolates and an increase in phagocytosis over time in both bacterial treatments. Furthermore, the number of *Vibrio* cells distributed in the different phagocytic cells was different between Hal 281 and NJ 1. Fluorescence microscopy observations showed that the majority (53-55%) of *Vibrio* cells were phagocytized by choanocyte-like cells, accumulating up to five bacteria per cell. We also detected differences in the sponges' proteomic response, which was characterized by a higher percentage of differentially abundant proteins related to phagocytosis in sponges exposed to NJ 1 compared to Hal 281. Overall, our results suggest that the sponge *H. panicea* may discriminate the isolates upon cellular internalization and the differences may rely on the phagocytic components that are activated for processing each type of *Vibrio*. The integration of approaches targeting the cellular (FACS and microscopy) and molecular (proteomics) levels is essential to gain a holistic understanding of the role of phagocytosis in animal-microbe interactions.

**Keywords:** sponge-microbe symbiosis, phagocytosis, fluorescence-activated cell sorting (FACS), proteomics, sponge cells, *Vibrio* isolates

## Introduction

Multicellular life originated and evolved in a microbial world. Metazoans descended approximately 700-800 Mya (Carr et al., 2008), and from then onwards, the foundations (i.e., nutrition, recognition, cell adhesion, and signaling) of animal-bacterial interactions started to forge (McFall-Ngai et al., 2013). Furthermore, the evolutionary animal-microbe arms race has driven the acquisition of cell-autonomous defense mechanisms, which provide rapid antimicrobial responses as a defense against potential pathogens (Randow et al. 2013). These intrinsic cellular defense mechanisms are often assumed to be unique to immune cells of higher metazoans, yet in fact, have been inherited from eukaryotic ancestors. For example, cell-defense mechanisms like phagocytosis initially emerged as a means for nutrient acquisition and reallocation in unicellular amoeba and was subsequently adapted in specialized immune cells, like macrophages, to eliminate pathogens (Dunn et al., 2018; Hartenstein & Martinez, 2019). Phagocytosis is a cellular process for ingesting and digesting large particles (> 0.5  $\mu\text{m}$  in diameter), including microbes, foreign substances, and apoptotic cells, into cytosolic, membrane-bound vacuoles (i.e., phagosomes). The phagocytic process comprises a number of regulated steps (reviewed by Levin et al., 2016; Uribe-Querol & Rosales, 2020): particle recognition via receptors, reorganization of the actin cytoskeleton for particle internalization, and intracellular digestion of the target particle (see General Introduction for details). The ultimate aim of the phagocytic process is to safeguard the host from potential hazard particles and to ensure its homeostasis (Levin et al. 2016).

Due to its pivotal role in the internal defense system, phagocytosis is often targeted by pathogens and subjected to manipulations. For example, intracellular bacterial pathogens like *Legionella pneumophila* and *Mycobacterium tuberculosis* can circumvent host phagocytosis by evading ingestion, interfering with phagosome maturation, resisting degradation, and even escaping from the phagosome (Flannagan et al., 2009; Uribe-Quero & Rosales, 2017). Apart from defending against external pathogens and to eliminate those who managed to enter the organism, all metazoans form close relationships with unicellular organisms, including bacteria, fungi, and (animal host including associate microbes; Bosch & McFall-Ngai, 2011; Rosenberg & Zilber-Rosenberg, 2018). These symbiotic relationships are often essential for the host organism for example by providing nutrients, stimulating development and growth and protecting against pathogens (Bosch & McFall-Ngai, 2021; Murillo-Rincon et al., 2017;

Shapira, 2016; Taubenheim et al., 2020). Symbionts use analogous mechanisms to pathogens that aid in their colonization, acquisition and maintenance within the host (McCutcheon, 2021). This raises the question on how the animal host differentiates between pathogens to eradicate vs. symbionts to retain? The acceptance of phagocytosis as a target mechanism for microbe discrimination has started to be decoded in certain metazoan taxa (e.g., amoeba, cnidarians, mollusks, and insects) for which cultivation of symbionts, genetic manipulation and/or implementation of cellular markers is established (Jacobovitz et al., 2021; Jauslin et al., 2021; Nyholm & McFall-Ngai, 2021; Schmitz et al., 2012; Silver et al., 2007; Snyder et al., 2021; Tame et al., 2022). From these observations, it is evident that the interplay between microbe and phagocytosis is a pivotal step for allowing symbiont persistence within the host.

An evolutionary and ecological relevant group to study the role of phagocytosis in animal-microbe interactions are the members of the early branching phylum Porifera. Sponges are benthic filter feeders constantly encountering bacteria from the water column and interacting with the distinctive microbial communities they harbor. The poriferan cells are organized in defined layers (i.e., pinacoderm, choanoderm and mesohyl), and at least three cell types are regarded as the main phagocytic cells: pinacocytes, choanocytes and archeocytes (see General Introduction for details). As the symbiont communities of sponges are distinct from the seawater microbial consortia (Hentschel et al., 2006; Moitinho-Silva et al., 2017; Thomas et al., 2010), it is plausible to hypothesize that sponges recognize and select between food, symbiotic and/or pathogenic microbes. There are limited indications of bacterial discrimination by sponges (Wehrl et al., 2007; Wilkinson et al., 1984), and in these cases it was suggested that the reduced uptake of symbionts compared to seawater bacteria was a result of symbionts avoiding sponge phagocytosis. From the host side, recent transcriptomic experiments have shown the stimulation of genes related to signaling, cytoskeleton rearrangement, and oxidative stress, which hints to the activation of a phagocytic response upon microbial encounter (e.g., (Pita et al. 2018; Geraghty et al. 2021; Schmittmann et al. 2021)). Yet, cellular insights into how the sponge phagocytic machinery responds during the interaction with different microbes remains poorly understood.

Here, we aimed to implement a recent established *in-vivo* phagocytic assay (Marulanda-Gomez et al. 2022; Chapter 3) for decoding sponge phagocytosis as a mechanism for bacterial discrimination. Previous phagocytosis assays in the marine sponge *Halichondria panicea* using different particles (i.e., fluorescent latex beads, microalgae, and bacteria) revealed that this

cellular process initiates within minutes and concludes within 1 h after particle exposure, and that the morphology and size of the phagocytic sponge cells varies with the type of particle presented to the sponge (Marulanda-Gomez et al. 2022). To further compare the sponge phagocytic activity upon encounter with different bacteria, we incubated individuals of *H. panicea* with a sponge-associated (hereafter termed “native”) and a non-sponge-associated *Vibrio* (hereafter termed “foreign”) isolate and quantified the relative abundance of sponge phagocytic cells (i.e., with incorporated fluorescently labeled *Vibrio*) by fluorescence-activated cell sorting (FACS). Sponge phagocytic active cells were additionally inspected using fluorescence microscopy to determine their size and morphological type. Furthermore, the total number of differentially abundant proteins putatively involved in phagocytosis after 30 min and 60 min of initial bacterial exposure were analyzed using a proteomic approach. *Vibrios* are diverse  $\gamma$ -proteobacteria ubiquitous in marine environments, possessing plastic genomes, metabolic versatility, and high colonization potential (Ceccarelli & Colwell, 2014; Le Roux & Blokesch, 2018). These bacteria can establish both beneficial and pathogenic associations with marine organisms (Destoumieux-Garzón et al., 2020; Takemura et al., 2014). I hypothesized that sponge phagocytic activity and proteomic response will be reduced upon exposure to the native sponge-associated *Vibrio* isolate than to the foreign isolate. My hypothesis is based on the assumption that symbionts might possess elements to avoid incorporation by sponge cells (e.g., ankyrin repeats (Burgsdorf et al., 2015; Díez-Vives et al., 2017; Jahn et al., 2019)). I secondly predict that more differentially abundant proteins are present upon exposure to the foreign *Vibrio* isolate which is expected to induce a stronger immune response.

## Materials and methods

### Sponge collection

Specimens of the sponge *H. panicea* (Pallas, 1766) were collected at the Kiel fjord (54.329659 N, 10.149104 E; Kiel, Germany) at 1 m water depth in Aug 2023, cleaned from epibionts, trimmed to size, and left to heal and recover from collection on an *in-situ* nursery at the collection site (Fig. S1) for 10 days (Alexander et al. 2015). The volume and wet weight of the collect individuals was on average ( $\pm$  S.D.)  $32.3 \pm 1.8$  mL and  $5.9 \pm 1.7$  g. On the same day of the experiment, individuals were brought to the climate-controlled aquaria facilities of GEOMAR Helmholtz Centre for Ocean Research (Kiel, Germany), placed in a semi-flow through aquaria system supplied with natural seawater pumped from the collection site, and left to

acclimatize for 2 h at 18°C room temperature, 17°C water temperature, and a salinity of 16-17 PSU.

### Bacteria preparation for the in-vivo phagocytosis assay

The *Vibrio* isolates for the assay included the native sponge-associated isolate Hal 281 (extracted from *H. panicea*) and the foreign non-sponge-associated isolate NJ 1 (extracted from the sea anemone *Nematostella vectensis*). The similarity of 16S rRNA gene sequences between the two isolates was 95.62% (Table 1) and neighbor joining phylogenetic analysis showed they belong to different clusters (Fig.S2). *Vibrio* cultures were freshly grown in 100 mL of liquid marine broth, at 120 rpm, 25°C, for 48 hours before the day of the experiment. The concentrations of the cultures were estimated by OD<sub>600</sub> and flow cytometry measurements. The bacteria pellet was recovered by centrifugation (4000 x g for 10 min), resuspended in filtered artificial seawater (FASW), and fluorescently stained with TAMRA™ (Thermo Fisher Scientific, C1171) the same day of the experiment (5 μM final concentration, for 90 min in the dark, at room temperature). The excess dye was washed off by centrifugation (4000 x g for 10 min) and the bacteria were resuspended in FASW and kept at 4°C until the experiment took place.

**Table 1.** Molecular and morphological comparison between the native and foreign *Vibrio* sp. Hal 281 and NJ 1, respectively. Average ± SD

Isolate	Origin	16S rRNA gene Sequence length (bp)	Related type strains based on 16S rRNA gene sequence	Accession numbers of 16S rRNA from the related strains	Similarity (%)	Average ± SD cell length (μm)	Average ± SD cell width (μm)
Hal 281	<i>Halichondria panicea</i>	1517	<i>Vibrio atlanticus</i> VB 11.11, CECT 7223, LMG 24300 (Atlantic Ocean) / <i>Vibrio cyclitrophicus</i> P-2P44, ATCC 700982, CIP 106644	EF599163/ AB682659	99.47/ 99.80	1.98 ± 0.25	0.90 ± 0.08
NJ 1	<i>Nematostella vectensis</i> (anemone)	1455	<i>Vibrio diazotrophicus</i> NBRC 103148 / <i>Vibrio plantisponsor</i> MSSRF60	BBJY01000042/ GQ352641	99.40/ 99.37	2.39 ± 0.86	0.31 ± 0.14

## Phagocytosis assay

We followed a similar methodology and experimental approach as described in Marulanda-Gomez et al. 2023 (Chapter 3), a brief description of the methodology follows. Individual specimens of *H. panicea* were randomly assigned to one of the three treatments and incubated for 30 min and 60 min with the native and foreign TAMRA-stained *Vibrio* isolates ( $n = 5$  biological replicates per isolate and per time point). The target concentration was  $10^5$ - $10^6$  Vibrios  $\text{mL}^{-1}$ . Sponges incubated in natural seawater without *Vibrio* addition ( $n = 4$ ) served as controls for FACS estimates. Water samples for flow cytometry were taken through the incubation period to assess bacterial uptake (Text S1 and Fig. S3). The entire sponge individuals were recovered at the end of each incubation and used to extract the host cells following an established sponge cell dissociation protocol (adjusted after Fieseler et al., 2004; Wehrl et al., 2007).

## Sponge cell dissociation

The *H. panicea* cell fraction was extracted immediately after each assay as described in Marulanda-Gomez et al. (2023). Briefly, the entire sponge fragments were rinsed with sterile, ice-cold Ca- and Mg-free artificial seawater (CMFASW; Rottmann et al., 1997), cut in small fragments, and incubated for 15 min in ice-cold CMFASW with EDTA (25 mM) on a shaker. Samples were filtered through a cell strainer (40  $\mu\text{m}$ ) and the homogenate was centrifuged at 500 x g, for 5 min at 4°C. The supernatant was discarded and the sponge cell pellet was resuspended in 4 mL of ice-cold CMFASW. Aliquots (1 mL) of the cell suspension were either sampled for proteomics analysis (see below) or fixed with PFA (final concentration 4%) overnight for estimating phagocytosis using FACS. The fixative was washed off the cells by centrifugation (500 x g, for 5 min at 4°C) and the pellet was resuspended in 1 mL of ice-cold CMFASW.

## Estimation of *Vibrio* phagocytosis by sponge cells

Phagocytosis of the *Vibrio* isolates by sponge cells was estimated using fluorescence-activated cell sorting (FACS) following the protocol by Marulanda-Gomez et al. (2023). Shortly, the concentration of the dissociated sponge cells was adjusted to approx.  $3 \times 10^7$  cells  $\text{mL}^{-1}$ . Prior to the analysis, sponge cells were filtered again through a cell strained (40  $\mu\text{m}$ ) and their nuclei was stained with DAPI (final concentration 0.7 ng  $\mu\text{L}^{-1}$ ) in order to detect the “bulk” sponge



cells population based on the dye fluorescence (355 nm UV laser and filter 448/59 nm). FACS analysis was performed on a MoFlo Astrios EQ<sup>®</sup> cell sorter (Beckman Coulter) using the Summit software (v6.3.1). Each sample was run five times and a total of 500k events were recorded for each technical replicate. The side scatter (SSC), DAPI, and the TAMRA-stained bacteria fluorescence (laser 561 nm and filter 692/75 nm) were used to identify and quantify the sponge cells that had incorporated the *Vibrio* isolates. The control sponges (i.e., individuals incubated without isolates) were used to correct for events corresponding to natural auto-fluorescence in the cells (as in Marulanda-Gomez et al. 2023). We define sponge phagocytic cells as those that had incorporated the fluorescent Vibrios during the assay, whereas non-phagocytic cells as those without incorporated Vibrios (i.e., according to the presence or lack of fluorescence signal in the TAMRA channel, respectively). The relative (%) phagocytic and non-phagocytic cell fraction in relation to the total number of events from these two gates was estimated after microscopy verification of the gates (for details see Marulanda-Gómez et al. 2023). To test the effect of the *Vibrio* type (i.e., native vs. foreign) and of incubation time (i.e., 30 vs. 60 min), a two-way ANOVA analysis was performed (significance was determined at the  $\alpha = 0.05$  level). Statistical analysis was performed in R-studio (V4.2.1; Rstudio Team 2022) by fitting an analysis of variance model (aov () function).

### Determination of phagocytic sponge cells using fluorescence microscopy

Dissociated sponge cell suspensions of three random individuals per treatment were subsampled and inspected by fluorescence microscopy to determine the cell types involved in phagocytosis of native and foreign Vibrios. A total of 30 phagocytic cells per individual were counted, and the size of the cells as well as the number of TAMRA-stained *Vibrio* cells incorporated per cell was recorded. Cells were mounted on microscopy slides using ROTI mount FlourCare DAPI and examined under an inverted fluorescence microscope equipped with a camera (Axio Observer Z1 with AxioCam 506 and HXP-120 light; Zeiss), at a total magnification of 100x, using the filters 49 DAPI (335-383 nm for sponge nuclei) and 43 HE DsRed (538-562 nm for TAMRA-stained *Vibrio sp.*). ZEN Blue Edition software (Zeiss) was used for acquiring and editing pictures. Sponge cells were classified in four categories (Fig 1A): (1) small-sized flagellated cells (3-6  $\mu\text{m}$ ), (2) small-sized cells with no visible flagella (3-6  $\mu\text{m}$ ), (3) medium-sized cells (7-10  $\mu\text{m}$ ), and (4) big cells (> 10  $\mu\text{m}$ ). We further estimated the number of TAMRA-stained *Vibrio* cells that were incorporated per observed sponge phagocytic cell. The number of Vibrios per sponge cell was divided into four categories (Fig. 1B): 1 *Vibrio*, 2

Vibriosis, 3-5 Vibriosis, > 5 Vibriosis. One-way ANOVAs were run per treatment condition (i.e., per *Vibrio* type and per incubation time separately) to test if the cell types involved in the bacteria incorporation, as well as the number of *Vibrio* cells incorporated per phagocytic cell differ between the *Vibrio* isolates presented to *H. panicea*. Additionally, a PERMANOVA ((adonis2 () function), package vegan in R-studio) was performed in the combined data set to test if the distribution of phagocytic cell types as well as the number of Vibriosis incorporated per cell changed between *Vibrio* isolates and over time.

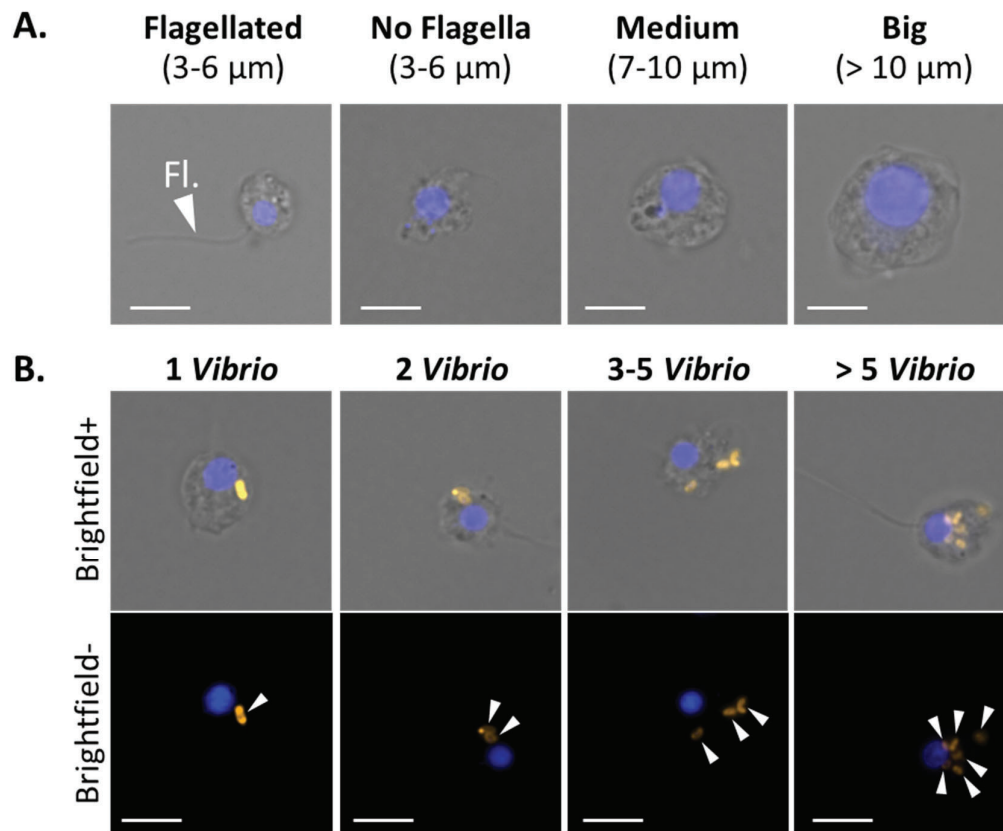


**Fig. 1.** Phagocytic cell types of *H. panicea* individuals exposed to *Vibrio* isolates based on fluorescence microscopy. Representative fluorescent microscopy pictures showing (A) different phagocytic cell categories and (B) different amounts of *Vibrio* cells incorporated into sponge cells. Scale bars: 5  $\mu\text{m}$ . Sponge cell nuclei (blue) stained with DAPI. Fl: flagella. Arrowheads: TAMRA-stained *Vibrio*.

### Identification of differentially abundant proteins using proteomic analysis

Sponge cell aliquots (1 mL) from the dissociated sponge cell suspensions were washed by centrifugation (500 x g, for 5 min at 4°C), the supernatant was discarded, and the cell pellet was resuspended in 1 mL of lysis buffer (5 M urea, 1% Triton x-100, 5 mmol L<sup>-1</sup> Dithiothreitol,

1x cComplete™ mini EDTA-free, and 50 mM Tris; pH 7.5-8). Samples were thoroughly vortexed for 30 s and incubated in a shaker (1500 rpm) for 40 min at 37°C. Through this step, samples were vortexed every 10 min for 30 s. Subsequently, they were placed in an ultrasonic bath for 5 min. Debris was pelleted by centrifugation (20,000 x g, for 30 min at 10°C) and the supernatant was transferred into a new tube and stored at -80°C until further processing. Protein concentrations were determined using the Pierce™ BCA Protein assay kit (Thermo) according to manufacturer's instructions. 50 µg protein of each sample were processed further according to the SP3 protocol (Hughes et. al, 2019) as follows. Proteins were reduced by addition of Dithiothreitol (DTT; 10 mM final concentration) and mixing at 1000 rpm, 56°C for 30 min. Alkylation was performed by addition of chloroacetamide (50 mM final concentration) and mixing at 1000 rpm, 25°C for 20 min. 50 µL of mixture of hydrophobic and hydrophilic SP3 beads (20 µg µl<sup>-1</sup>) were added reaching a 20:1 (beads:protein) ratio. Binding to beads was induced by adding ethanol to 54% and then mixing at 1500 rpm, 25°C for 15 min. Beads were washed 3 times, each washing step consisted of: centrifugation (21,000 g, 25°C for 2 min), binding beads to a magnet and discarding the supernatant, adding 400 µL of 80% Ethanol and ultrasonically until beads disperse, and finally vortexing for 10 s. The remaining supernatant was discarded after the last washing step and beads were reconstituted in 100 µL of Triethyl ammonium bicarbonate (100 mM). Proteins were digested at 37°C overnight with 0.7 µg Trypsin/Lys-C. Afterwards, supernatant containing peptides were vacuum dried then reconstituted in 100 µL 3% Acetonitrile (ACN) and 0.1% Trifluoroacetic acid (TFA). An additional cleaning step was performed using Pierce™ C18 100 µL pipette tips as follows. Tips were washed twice with 100 µL (50% ACN) and equilibrated twice with 100 µL (3% ACN, 0.1% TFA). Peptides were loaded by pipetting up and down 10x and then washed 2x with 100 µL (3% ACN, 0.1% TFA). A first peptides elution was done with 100 µL 50% ACN and 0.1% TFA and a final elution with 50 µL 70% ACN, 0.1% TFA. Eluted peptides were vacuum dried, reconstituted in 3% ACN, 0.1% TFA and analyzed by liquid chromatography–mass spectrometry (LC-MS). Chromatographic separation was performed on a Dionex U3000 nanoHPLC system equipped with an Acclaim pepmap100 C18 column (2 µm particle size, 75 µm × 500 mm) coupled online to a mass spectrometer. The eluents used were; eluent A: 0.05% Formic acid (FA), eluent B: 80% ACN + 0.04% FA. The separation was performed over a programmed 132 min run. Initial chromatographic conditions were 4% B for 2 min followed by linear gradients from 4% to 50% B over 100 min, then 50 to 90% B over 5 min, and 10 min

at 90% B. Following this, an inter-run equilibration of the column was achieved by 15 min at 4% B. A constant flow rate of 300 nL min<sup>-1</sup> was employed. Two technical replicates of each sample were analyzed and wash runs were performed between samples. Data acquisition following separation was performed on a QExactive Plus (Thermo). Full scan MS spectra were acquired (300-1300 m z<sup>-1</sup>, resolution 70,000) and subsequent data-dependent MS/MS scans were collected for the 15 most intense ions (Top15) via HCD activation at NCE 27.5 (resolution 17,500, isolation window 3.0 m z<sup>-1</sup>). Dynamic exclusion (20 s duration) and a lock mass (445.120025) was enabled.

MS raw data were analyzed against a *H. panicea* predicted proteome (268,992 sequences; from Schmittmann et al., 2021) and known contaminants (cRAP) using CHIMERYS identification search engine linked to Proteome Discoverer™ 3.0 (Thermo). Enzyme was set to Trypsin with 2 missed cleavages tolerance. 20 ppm fragment ion mass errors were tolerated. Carbamidomethylation of cysteine was set as a fixed modification and oxidation of methionine (M) was tolerated as a variable modification. Strict parsimony criteria were applied, filtering peptides and proteins at 1% false discovery rate (FDR). Label-free quantification method based on the intensities of the precursor ions was used. Proteins were filtered to have “High” FDR combined confidence and at least 2 identified peptides. Data was further analyzed by Excel and Perseus v 1.6.15.0 (Tyanova et. al 2016). Protein intensities were averaged for technical replicates and then normalized by median based normalization. Log2 transformed intensities were grouped in six groups depending on the *Vibrio* treatment and incubation time (each with four biological replicates), and filtered to contain four values in at least one group. Missing values were imputed from a normal distribution separately for each replicate (Width 0.3, Downshift 1.8). Statistical analysis was done using ANOVA, permutation-based FDR of 0.05 or 0.01, as indicated. Identified protein sequences were annotated to Uniprot identifiers of *Amphimedon queenslandica* proteome (Uniprot UP000007879\_444682) by BlastP or to KEGG identifiers by BLASTKOALA using Eukaryotes KEGG gene database (Kanehisa et al. 2016). Based on the blast and Uniprot annotation description, as well as KEGG terms, proteins were manually classified as phagocytic-related proteins or as proteins related to other processes. KEGG terms used for the broad protein classification included cytoskeletal (ko04812), membrane trafficking (ko04131), endocytic (ko04144), exosomal (ko04147), lysosomal (ko04142) and phagosomal (ko04145) proteins.

## Results

We compared the phagocytic activity of *H. panicea* individuals exposed to a sponge-associated (Hal 281) vs. a non-sponge associated (NJ 1) *Vibrio* isolate (Table 1). Sponges were incubated with each isolate for 30 min and 60 min, and the sponge cell fraction was immediately recovered to estimate the percentage of cells with incorporated fluorescently-labelled *Vibrio* using FACS. Microscopy inspection of the phagocytic cells gave information regarding the size and types of cells involved in the incorporation of the isolates and on the number of *Vibrio* cells internalized per sponge cell. We further characterized the proteomic response of *H. panicea* to *Vibrio* encounter by characterizing and comparing differentially abundant proteins involve in phagocytosis between the three treatments (i.e., Hal 281, NJ 1 and control)

### Phagocytosis of native and foreign *Vibrio* isolates

The averaged ( $\pm$  SD) number of sponge cells recovered after dissociation was approx.  $4.89 \times 10^7 \pm 3.00 \times 10^7$  cells mL<sup>-1</sup>. These cells were used to compare the percentage of sponge cells that had phagocytized (i.e., incorporated) the isolates Hal 281 and NJ 1 after 30 min and 60 min. The relative number (%) of cells phagocytizing the bacterial cells (+ fluorescent signal) to the total DAPI-stained cells was estimated via FACS analysis (the complete data set can be found in Table S2). The population of phagocytic cells of the *H. panicea* individuals incubated with the *Vibrio* isolates (Fig. 2B and 2C) was clearly distinct from the corresponding gate in the control sponges (i.e., individuals incubated without isolates. Fig. 2A). For NJ 1, it is worth noting that despite a decline in bacterial concentration in seawater was not evident based on flow cytometry estimates (Fig. S3 E and G), we did detect sponge cells phagocytizing this isolate with the phagocytosis assay by FACS analysis (Fig. 2C) and by visual inspection of the phagocytic cells.

In the 30 min assays, the percentage of phagocytic cells were on average  $28.9 \pm 2.6$  % for the native and  $28.2 \pm 3.9$  % for the foreign *Vibrio* (Fig. 3A) with no significant difference between the isolates (one-way ANOVA,  $F = 6.1$ ,  $p = 0.99$ ;  $df = 3$ ). In the 60 min assays, the average percentage of phagocytic sponge cells was  $38.3 \pm 3.8$  % for Hal 281 and  $33.6 \pm 6.0$  % for NJ 1. These percentages represent on average, a 9.3% and 5.4% increase for Hal 281 and NJ 1, respectively, compared to the estimates for the 30 min assays (Fig. 3A). Our observations showed that there was no effect of the *Vibrio* isolate on the phagocytic activity of *H. panicea* cells (two-way ANOVA,  $F = 1.9$ ,  $p = 0.19$ ;  $df = 1$ ; Fig. 3A), whereas bacterial incorporation into

the sponge cells significantly increased with incubation time (i.e., exposure time with the bacteria. Two-way ANOVA,  $F = 15.9$ ,  $p = 0.001$ ;  $df = 1$ ; Fig. 3A).

FACS cytograms also revealed a population of TAMRA positive fluorescent cells, but low DAPI signals. These corresponded to TAMRA-stained *Vibrio* cells that were taken up by *H. panicea*, but were not incorporated into sponge cells (Fig. 3B-C, “free *Vibrio* cells”). In the 30 min assays, this fraction of free *Vibrio* cells included  $16427 \pm 5047$  cells for Hal 281 and  $8906 \pm 2187$  cells for NJ 1, (average  $\pm$  SD) (Fig. 3B). Thus, the number of free Hal 281 cells was on average 1.8 times higher than the free NJ 1 cells after 30 min (two-way ANOVA,  $F = 10.4$ ,  $p = 0.006$ ;  $df = 1$ ; Fig. 3B). In the 60 min assays, the number of free *Vibrio* cells increased by 1.7 to 1.9 times, compared to the 30 min assays, in sponges incubated with Hal 281 and NJ 1, respectively (Fig. 3B). Exposure time had an effect on the number of free bacteria observed in both *Vibrio* treatments (two-way ANOVA,  $F = 11.2$ ,  $p = 0.004$ ;  $df = 1$ ; Fig. 3B).

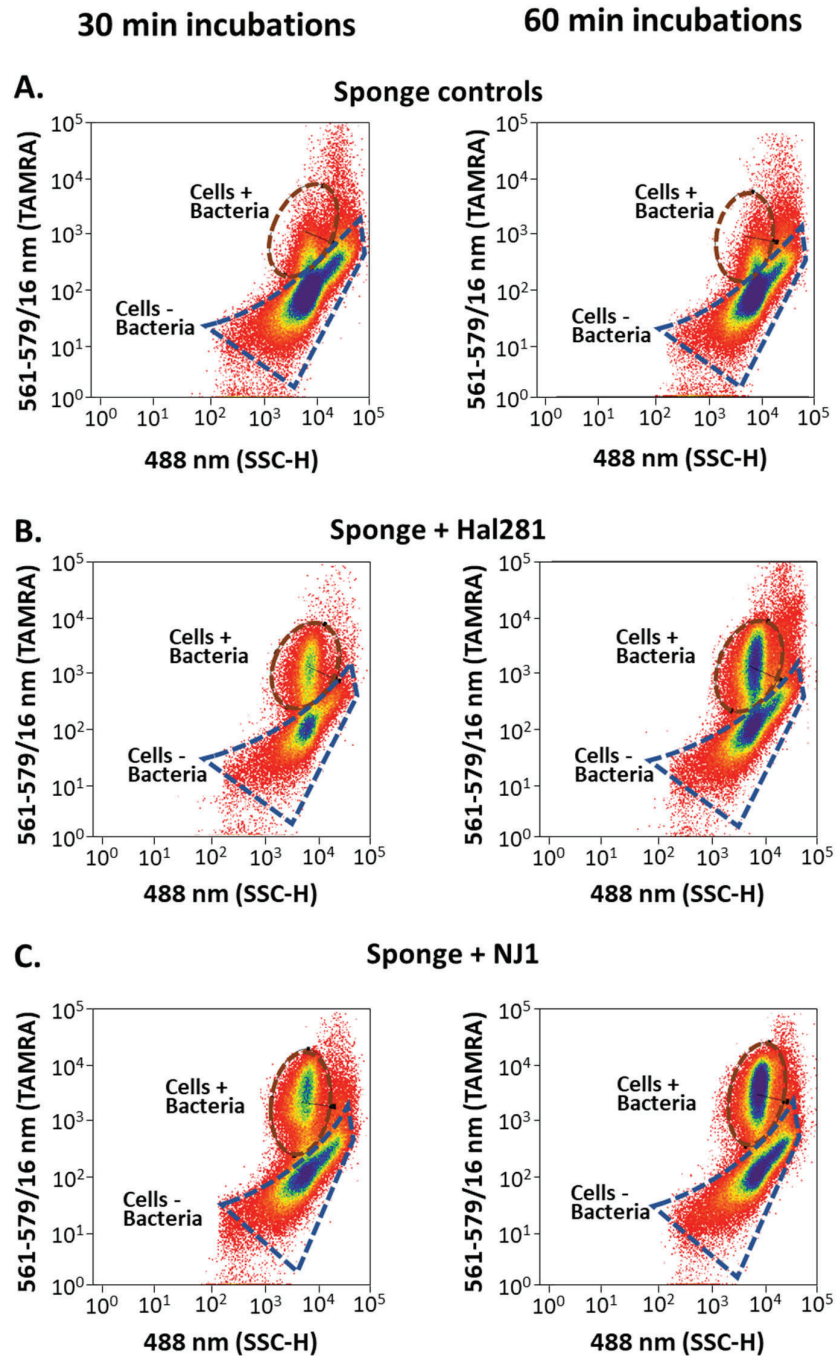


**Fig. 2.** Representative cytograms for (A) sponge controls (incubated without *Vibrio*) and sponges incubated with the (B) native Hal 281 and (C) foreign NJ 1 *Vibrio* isolates, for 30 min (left) and 60 min (right) obtained by fluorescence-activated cell sorting (FACS). Brown and blue dashed outlines: gates of phagocytic cells with (+) or without incorporation of bacteria, respectively. In each case a total of 5k events were recorded.

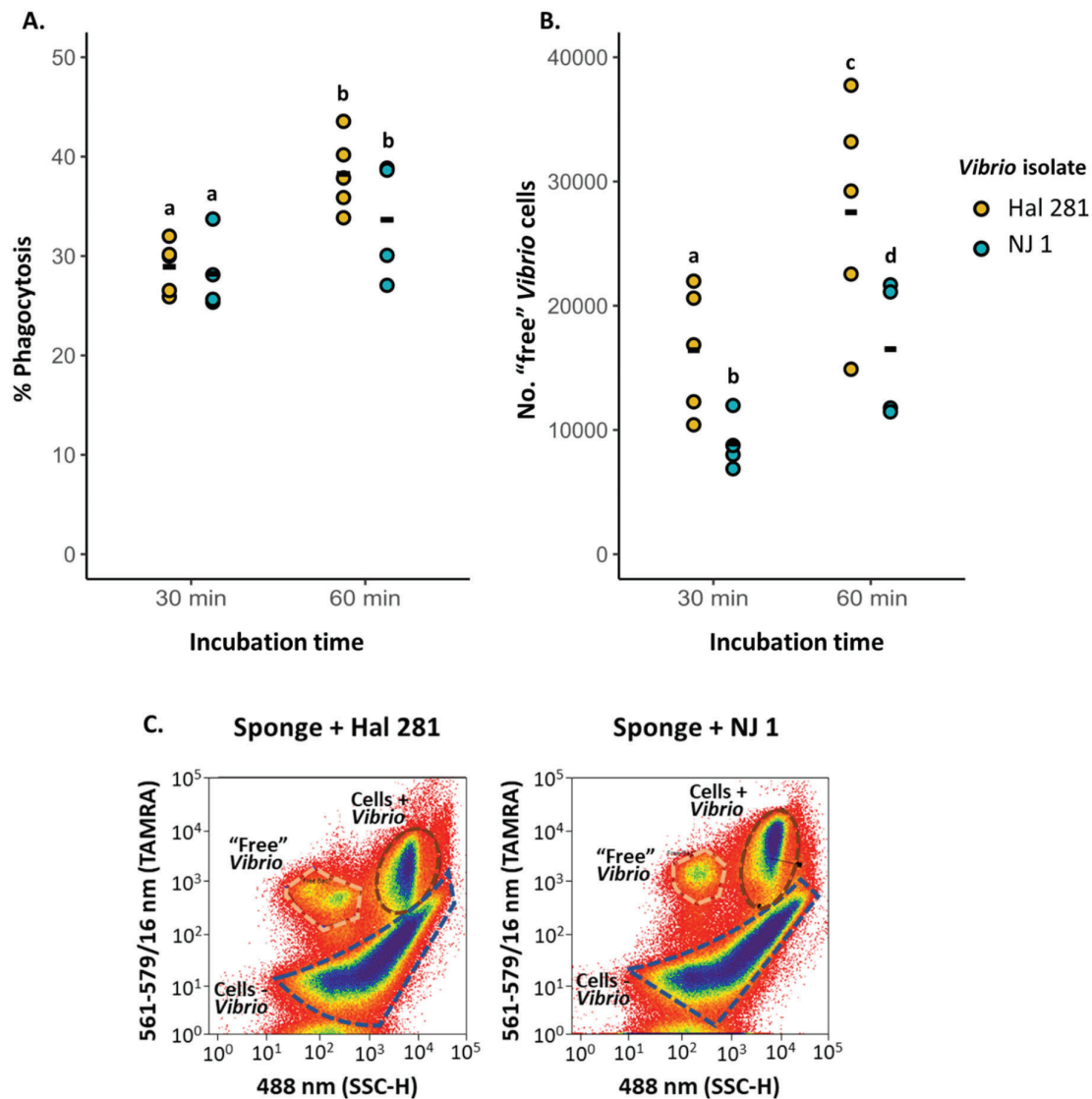


**Fig. 3.** Fluorescence-activated cell sorting (FACS) analyses estimates of (A) phagocytic active sponge cells and (B) *Vibrio* sp. cells found inside the sponge tissue of *H. panicea* incubated with the native and foreign *Vibrio* isolates Hal281 and NJ1, respectively, for 30 min and 60 min. Bold line: average for the 4-5 biological replicates. Treatments marked with different letters are significantly different at  $\alpha=0.05$ . (C) cells Representative FACS cytograms showing the population of intact, "free" Hal281 and NJ1 cells (dashed pale orange). Brown and blue dashed outlines: gates of phagocytic cells with (+) or without incorporation of bacteria, respectively.

### Size range of sponge cells participating in phagocytosis of the *Vibrio* isolates

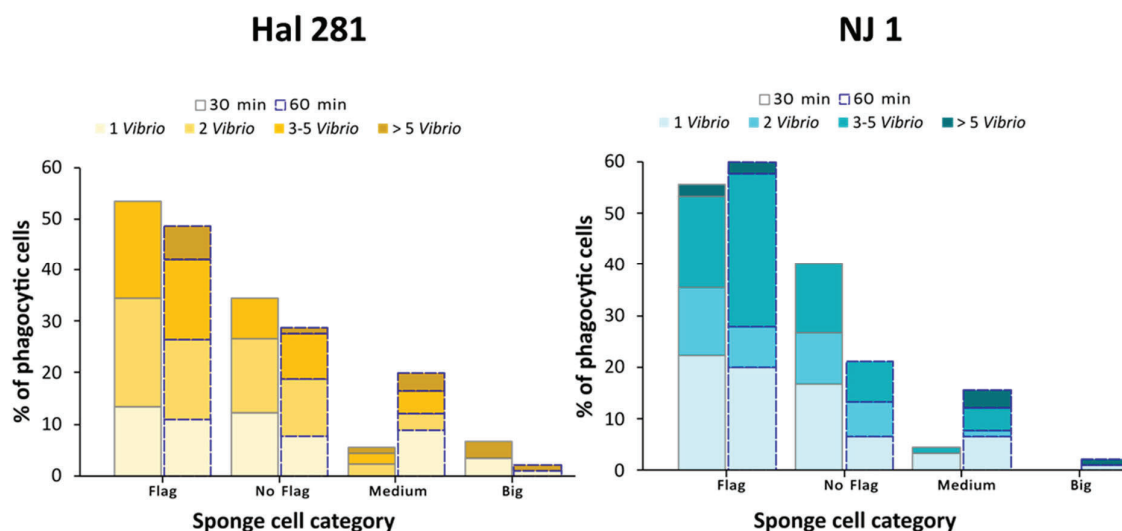
Fluorescence microscopy observations of phagocytic cells showed that *Vibrio* phagocytosis was performed by sponge cells with different sizes and morphologies (Fig. 1). In both *Vibrio* treatments, 87-95% of the total phagocytic cells observed in the 30 min assays comprised small flagellated cells (53-55%) and cells with no visible flagella (34-40%) (Fig. 4, Fig S3 and



Table S3). Medium and big cells only represented approx. 5-7% of the recorded cells (one-way ANOVA,  $F = 18.6$ ,  $p < 0.001$ ;  $df = 7$ ; Fig. S4). After the 60 min assays, the small flagellated cells continued to be significantly higher than the other cell types for sponges exposed to Hal 281 and NJ 1 (one-way ANOVA,  $F = 28.3$ ,  $p < 0.001$ ;  $df = 7$ ; Fig. S4). When combining the two data sets, a significant interaction between time (30 min vs. 60 min) and *Vibrio* isolate (Hal 281 vs. NJ 1) on the distribution of cell types involved in phagocytosis was revealed explaining 24% of the variation in the data (PERMANOVA,  $F = 7.8$ ,  $p = 0.003$ ;  $df = 1$ ; Fig. 4 and table S4). Thus, time had a significant effect on this distribution, yet differed between the two *Vibrio* isolates.

### Number of *Vibrio* cells incorporated per phagocytic cell

The number of TAMRA-stained *Vibrio* cells that were incorporated per observed sponge phagocytic cell was also estimated (Fig. 4 and Table S3). For both *Vibrio* isolates the percentage of phagocytic cells with  $> 5$  *Vibrio* cells was significantly lower (less than 5%) than the other categories in the 30 min incubations (one-way ANOVA,  $F = 17.4$ ,  $p < 0.001$ ;  $df = 7$ ; Fig. S5). After 60 min incubations with Hal 281, the number of *Vibrio* cells found in sponge cells was around 30 % for each of the 1 *Vibrio*, 2 *Vibrio*, and 3-5 *Vibrio* categories, whereas a higher variation (15-42%) in the percentage of cells within these categories was observed in the incubations with NJ 1 (Fig. 4 and Fig. S5). A combined analysis of both data sets showed that the number of Vibrios incorporated per cell was not affected by time, but by *Vibrio* isolate. Overall, the *Vibrio* type (i.e., Hal 281 vs. NJ 1) presented to the sponge influenced the number of *Vibrio* cells incorporated into *H. panicea* cells (PERMANOVA,  $F = 2.9$ ,  $p = 0.03$ ;  $df = 1$ , Fig. 4 and table S5). The higher percentage of sponge cells incorporating 3-5 NJ 1 cells, compared to Hal 281, seemed to be the main difference between the isolates. Additionally, the distribution of *Vibrio* cells over the different types of phagocytic cells was significantly different between Hal 281 and NJ 1, and this effect of the *Vibrio* isolate explains 19% of the variation in the data (PERMANOVA,  $F = 2.5$ ,  $p = 0.02$ ;  $df = 1$ , Fig. 4 and table S6). The difference was especially evident in the flagellated cells, which seemed to be able to incorporate a higher number of NJ 1 cells compared to Hal 281. An effect of exposure time over this distribution of Vibrios among cell types was not detected.



**Fig. 4.** Distribution of *Vibrio* cells in the different phagocytic cell types after 30 min (gray outlined bars) and 60 min (blue dashed bars) incubations with the native isolate Hal 281 (left) and foreign isolate NJ 1 (right) based on microscopy cell counts.

### Differentially abundant phagocytic-related proteins upon sponge-*Vibrio* encounter

Proteomics analysis was performed on sponge cells from the *H. panicea* individuals used for the phagocytic assays (4 biological replicates per treatment within 30 min and 60 min). In total, 4753 and 4893 proteins were quantified after the 30 min and the 60 min incubations, respectively (Fig. S6). The principal component analysis (PCA) revealed that the NJ 1 treated sponges clustered away from control and Hal 281 treated individuals on component 3 (14.1%) (Fig. 5 A). After 60 min incubations, the NJ 1 treated sponges clustered away on component 1 (26%) while Hal 281 clustered away from control individuals on component 2 (14.5%) (Fig. 5 B). This shows that 60 min exposure to the *Vibrio* isolates had a more prominent effect on the proteome, therefore, we decided to focus only on this incubation time.

To identify significant differentially abundant proteins (DAPs), an ANOVA (FDR = 0.05) statistical analysis was performed between all the treatment groups (Hal 281, NJ 1 and control). DAPs were z-score normalized and a hierarchal clustering on rows and columns based on Euclidean distance was performed. A total of 285 DAPs were identified and around 53% of these proteins had annotations (Fig. 5 C and D). Abundance profiles of *H. panicea* individuals treated with each type of *Vibrio* isolate were consistent and biological replicates clustered together (Fig 6). The profile of sponges exposed to the native isolate Hal 281 was more similar

to the control than the individuals exposed to the foreign isolate NJ 1. Moreover, DAPs were separated into six main clusters based on profile similarities (Fig. 6). Proteins putatively involved in phagocytosis were identified based on Blastkoala and Uniprot description, KEGG terms, and literature search. The DAPs were then annotated as phagocytic-related proteins or as proteins related to other processes. From the total number of DAPs, around 15% were classified as phagocytic-related proteins. This corresponded to approx. 28% of all DAPs that had an annotation based on Blastkoala (Table S7).

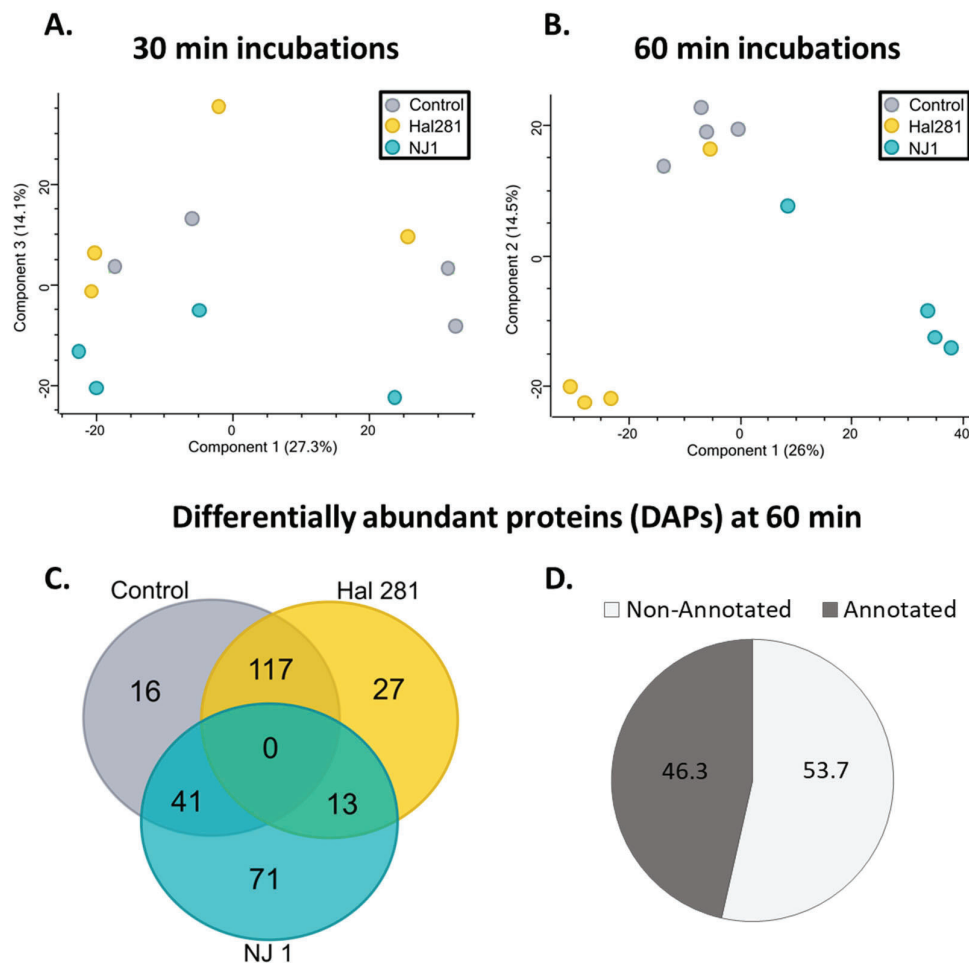


**Fig. 5.** Proteome comparison of *H. panicea* cells after 30 min and 60 min sponge incubations with the native and foreign *Vibrio* isolates Hal 281 and NJ 1, respectively. Sponges incubated without the addition of *Vibrio* isolates served as controls. (A) - (B) Principal component analysis showing the clustering of treatments for each time point. (C) Number of significantly differentially abundant proteins (DAPs) per treatment. Proteins were defined as differentially abundant with ANOVA permutation-based FDR = 0.05. (D) Percentage of DAPs that could be annotated based on Blastkoala.

Sponges treated with the isolate NJ 1 had a relatively high percentage of phagocytic-related proteins (40%, corresponding to 15 DAPs) and the majority of these DAPs were cytoskeletal and membrane trafficking proteins (Fig. 6 and Table S7). The proteins related to cytoskeletal components (ko0481) can regulate the assembly of microtubules (TUBA and TUBB) and the polymerization, binding and organization of actin (ACTR3, AP4E1, PPP1C and WASF3). The membrane trafficking category (ko04131) included five proteins (AP4E1, COPB2, COG6, SEC23, and VAMP7) known to mediate vesicle formation, sort cargo molecules, and transport of vesicles between the endosomes, the Golgi apparatus and the endoplasmic reticulum. The foreign *Vibrio* also increased the abundance of two lysosomal enzymes (ko04142; ARSA and GNS) and one exosomal (ko04147; HSPA1) protein. Finally, we identified an ankyrin-like protein (ANKRD13) differentially abundant in sponge individuals exposed to the foreign *Vibrio*, which supposedly regulates the internalization of ligand-activated epidermal growth factor receptor (EGFR) via ubiquitination (Fig. 6 and Table S7).

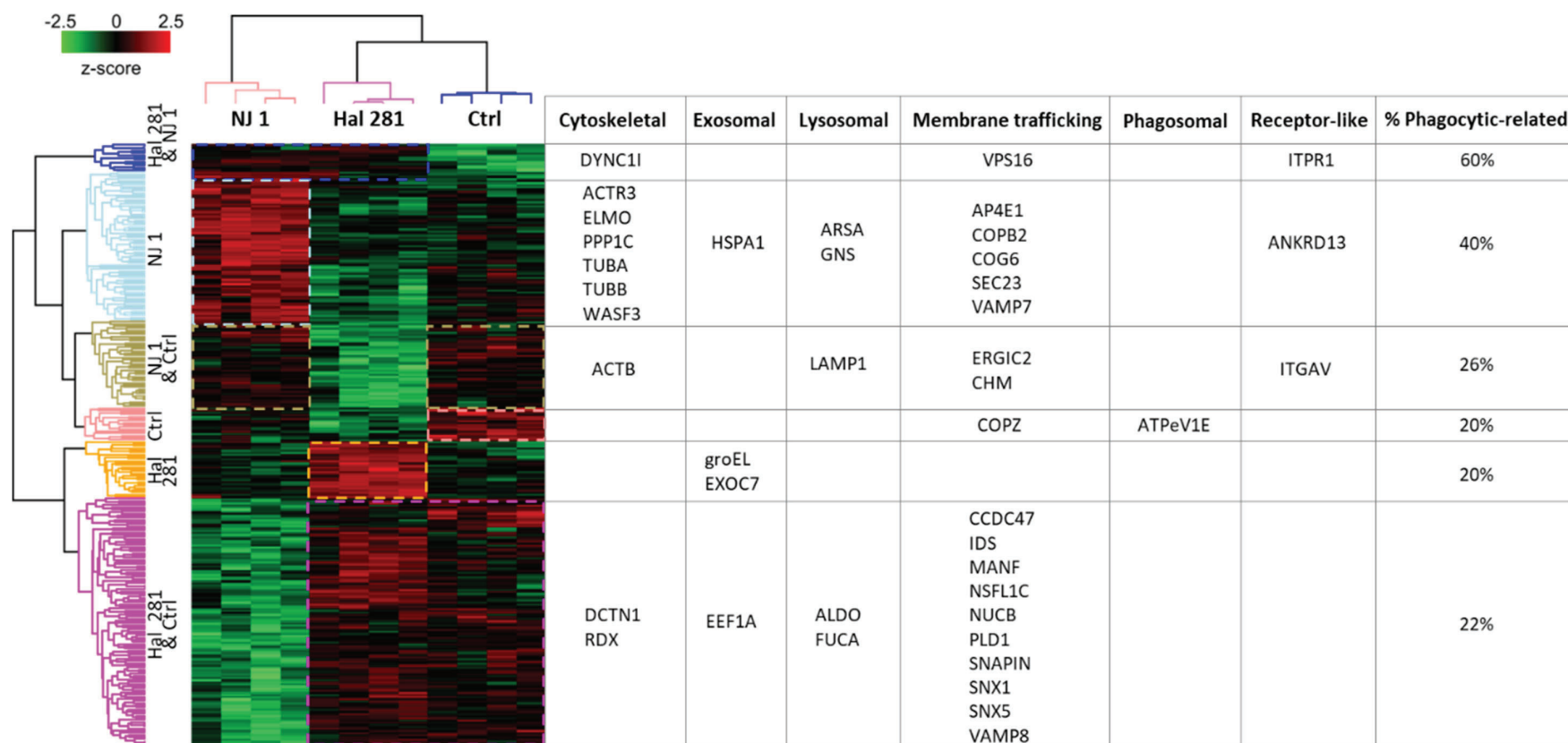


**Fig. 6.** Heatmap of differentially abundant proteins in *H. panicea* cells after 60 min incubations with the native and foreign *Vibrio* isolates Hal 281 and NJ 1, respectively. Sponges incubated without the addition of *Vibrio* isolates served as controls. Proteins were defined as differentially abundant with ANOVA permuted-based FDR p-value < 0.05, n = 4. Table contains the names of the phagocytic-related proteins and are classified in broad functional category based on blastp, Uniprot and KEGG terms and annotations. Percentage of phagocytic-related proteins compared to proteins involved in other process based on the number of annotated DAPs is presented.

In contrast, in *H. panicea* individuals exposed to Hal 281 around 20% of the DAPs (i.e., 2 proteins) were related to phagocytosis (Fig. 6 and Table S7). These two DAPS (EXOC7 and GroEL/HSPA1) are associated with exocytic or exosomal regulation (ko04147) and are known to mediate the fusion of lysosomes, endosomes or exocytic vesicles with the plasma membrane. The sponge proteomic response also showed phagocytic-related DAPs (approx. 60% of the annotated proteins) that were common in both *Vibrio* treatments. These included a cytoskeletal protein (DYNC11), a membrane trafficking protein (VPS16) and a receptor-like protein (ITPR1), which are described to regulate tubulin binding, sort and deliver vacuolar proteins, and mediate the activation of the NOD-like signaling pathway (ko04621), respectively. Furthermore, we identified DAPs putatively involved in phagocytosis that were shared between the *Vibrio* treatments and the control sponges (i.e., individuals not exposed to isolates; Fig. 6 and Table S7).

## Discussion

In the current study, we analyzed the phagocytic response of *H. panicea* upon encounter to a native sponge-associated (Hal 281) and a foreign non-sponge-associated (NJ 1) *Vibrio* isolate after 30 min and 60 min bacterial exposure using a recently established *in-vivo* assay (Marulanda-Gomez et al. 2023). The percentage of sponge cells engaged in phagocytic activity did not differ between isolates. Yet, the phagocytic response differed on a cellular level between Hal 281 and NJ 1, both in the type of sponge cells involved as well as the number of Vibrios incorporated per cell. Moreover, we detected a higher percentage of differentially abundant proteins related to phagocytosis in sponges exposed to the foreign isolate compared to the native isolate. This novel combination of *in-vivo* phagocytosis assay, fluorescence microscopy, and proteomic analysis proved to be a powerful tool to unravel differential processing of a native and foreign bacteria in an early branching metazoan.

### Cellular insights into *Vibrio* phagocytosis by sponge cells

Fluorescence activated cell sorting revealed comparable abundances of phagocytic active cells between the native sponge-associated (Hal 281) and the foreign non-associated (NJ 1) *Vibrio* isolate (Fig. 3). Extending the incubation time and thereby exposure to the *Vibrio* isolates yielded a 5-9% increase in phagocytic activity, yet no significant differences between the isolates. These observations suggest that the initial incorporation of *Vibrio* into *H. panicea* cells is not strain-specific, but that differences may be found in the subsequent processing on a


cellular level. Fluorescence microscopy inspections provided a deeper understanding on the cell types involved in the incorporation of the *Vibrio* isolates. More than 50% of the phagocytic active cells (i.e., with internalized Vibrios) were in the size range of 5-6  $\mu\text{m}$  and therefore resemble choanocyte-like cells (Fig. 1 and Fig. 4). Choanocytes are flagellated cells with a cylindrical collar at their apical end. Their main function is to generate water currents, take up particulate and dissolved food and to transfer these nutrients to other cells via vesicles (Funayama 2013). The size of the choanocytes in *H. panicea* varies between 3  $\mu\text{m}$  to 7  $\mu\text{m}$  (Riisgård et al., 2023; Sokolova et al., 2019) and in some cases the absence of flagella was reported even when using scanning electron microscopy to describe ultrastructures (Riesgo et al., 2022). In the current study we observed also cases of cells in the size range of choanocytes without visible flagellum (Fig. 1 A) and it is plausible that some of these cells are indeed choanocytes that either lost their flagellum during the sponge dissociation process or were not noticeable due to the resolution obtained by fluorescence microscopy. Altogether, these results are in accordance with observations by live-cell imaging and NanoSIMS which showed that bacteria and other small particles ( $\leq 2 \mu\text{m}$ ) were captured by choanocytes (Funch et al. 2023) and incorporated within 15 min (Hudspith et al., 2021) in *H. panicea* and the encrusting tropical sponge *Halisarca caerulea*. The medium (7-10  $\mu\text{m}$ ) and big (>10  $\mu\text{m}$ ) phagocytic active cells (Fig. 1 A) are most likely archaeocyte-like cells, given their bigger size compared to the other observed cells and the presence of a large nucleus, which in some cases contained a distinctive nucleolus. Archaeocytes are amoeboid totipotent stem cells which move throughout the sponge mesohyl and participate in intracellular digestion and transport of food and particles between cells (Funayama, 2013; Imsiecke, 1993; Maldonado et al., 2010). Interestingly, the distribution of different cell types involved in *Vibrio* phagocytosis changed over time for both isolates. Specifically, the percentage of medium and big archaeocyte-like cells increased from 30 min to 60 min incubation times. In combination with an increase in the amount of Vibrios contained per phagocytic cell (Fig. 4), this may suggest that after reaching a maximum saturation capacity (e.g., 5 or more *Vibrio* cells), choanocyte-like cells translocate incorporated Vibrios to archeocyte-like cells for further processing and transport within the mesohyl.




The change in distribution of Vibrios among sponge cell types over time differed between the *Vibrio* isolates (Fig. 4) and further indicates *Vibrio*-specific processing in *H. panicea*. A similar observation was reported by Maldonado et al. (2010) who found that the duration of digestion

and the cell types involved in this process differ between various microbial cells in the sponge *Hymeniacidon perlevis*. Reports from *Amphimedon queenslandica* additionally show that native bacteria were rapidly translocated from choanocytes to archaeocytes, whereas foreign bacteria remain in choanocytes where they are digested (Yuen, 2016). The involvement of multiple cell types as well as microbe-specific processing is not restricted to sponges, but appears to be wide-spread among marine invertebrates (Table 2). For instance, in the larvae of the sea urchin *Strongylocentrotus purpuratus*, the filopodial phagocytic cells elicit a weak response upon *E. coli* encounter, whereas *Vibrio diazotrophicus* and fungal Zymosan induce a robust response involving interaction with amoeboid cells (Ho et al., 2016). In the case of the deep-sea mussel *Bathmodiolus japonicus*, symbiotic and non-symbiotic bacteria were phagocytized indiscriminately across different phagocytic gill cells, but symbionts were retained without digestion while exogenous bacteria were eliminated through intracellular digestion (Tame et al., 2022). Indiscriminately phagocytosis is also known to take place in the larvae of the sea anemone *Aiptasia* sp., in which the host unselectively incorporates different microalgae and only retains the symbiotic strains while the non-symbionts are expelled without lysis via vomocytosis (Jacobovitz et al., 2021). As endocytic and exocytic process, such as phagocytosis and vomocytosis, are conserved cellular mechanisms from amoeba to humans (Bajgar & Krejčová, 2023; Mandujano-Tinoco et al., 2021; Seoane & May, 2020), it is likely that sponges employ similar mechanisms for microbial discrimination.



**Table 2.** Phagocytic response in marine invertebrates upon encounter with different particles.

Organism	Stage	Particle type	Response	Reference
 <i>H. panicea</i>	Adult	Non-symbiotic microalgae ( <i>Nannochloropsis</i> sp.)	Phagocytosis by choanocyte-like cells initiates within 30 min. Algal translocation to archaeocyte-like cells for presumably digestion takes place after 30 min. Phagocytosis and algal concentration were positively related.	Marulanda-Gomez et al. 2023
		Non-symbiotic bacteria ( <i>Vibrio</i> PPXX7)	Phagocytized primarily by choanocyte-like cells already within 30 min.	
		Latex beads (1 $\mu$ m)	Phagocytized primarily by choanocyte-like cells already within 30 min, where they accumulated as they cannot be digested by the sponge cells.	
	Single osculum explants	Non-symbiotic bacteria ( <i>Cyanobium bacillare</i> )	Phagocytized by choanocytes within approx. 40 min.	Funch et al. 2023
		Non-symbiotic microalgae <i>Rhodomonas salina</i>	Initially phagocytized in incurrent canals by exopinacocytes and transferred to the mesohyl by amoeboid cells for further digestion withing approx. 60 min.	
		Plastic beads (2 $\mu$ m)	Captured by choanocytes and phagocytized by exopinacocytes on the outer sponge surface and in endopinacocytes lining the excurrent canals, and subsequently expelled into excurrent canals after approx. 60 min.	
		Plastic beads (10 $\mu$ m)	Phagocytized by exopinacocytes on the outer sponge surface, in endopinacocytes in the mesohyl, and in endopinacocytes lining the excurrent canals, and transferred to the mesohyl by amoeboid cells. Subsequently, they were expelled into excurrent canals after approx. 95 min.	

 <i>Strongylocentrotus purpuratus</i> (sea urchin)	Larvae	Non-symbiotic bacteria ( <i>E. coli</i> )	Weak phagocytosis; bacteria were rarely incorporated by filopodial cells.	Ho et al. 2016
		Zymosan A	Rapid phagocytosis by filopodial and ovoid cells within 30 min.	
		Non-symbiotic bacteria ( <i>V. diazotrophicus</i> )	Robust phagocytosis by filopodial cells. Involves migration of pigment and amoeboid cells. Around 80-90% of the bacteria are phagocytosed after 2 h.	
 <i>Bathmodiolus japonicus</i> (deep-sea mussel)	Adult	Symbiotic bacteria (Methane-oxidizing consortia)	Phagocytized by gill cells and retained in bacteriocytes. No acidification of bacteriocytes was observed within 24 h.	Tame et al. 2022
		Non-symbiotic bacteria ( <i>E. coli</i> and <i>V. tubiashii</i> )	Phagocytized by gill cells and digested. Acidification of phagocytic cells started within 2 h and continued to increase after 24 h.	
 <i>Aiptasia</i> sp. (sea anemone)	Larvae	Symbiotic microalgae ( <i>Breviolum minutum</i> )	Phagocytized by endodermal cells. Involves accumulation of LAMP1 which allows symbiont intracellular persistence.	Jacobovitz et al. 2021
		Non-symbiotic microalgae ( <i>N. oculata</i> )	Phagocytized by endodermal cells and subsequent expulsion via vomocytosis after approx. 6 h	
		Polystyrene beads		

Images downloaded from Biorender or drawn by the author in Inkscape (no copyright).

## Sponge proteomic response to *Vibrio* encounter

The sponge proteomic response differed between the native isolate (Hal 281), the foreign isolate (NJ 1), and the control (i.e., incubated in natural unfiltered seawater without addition of *Vibrio* isolates) treatments, and this response was more pronounced in the 60 min than the 30 min assays (Fig. 5B). To our knowledge, this is among the first experimental studies using proteomics analysis in sponges, and thus provides evidence that in order to capture differentially abundant proteins during sponge incubation experiments at least of 1 hour of exposure to the treatment is required. The proteomic response of *H. panicea* individuals incubated with Hal 281 was more similar to sponge controls (i.e., sponges not exposed to *Vibrio*) than to individuals incubated with NJ 1. This suggests that not the bacterial type (i.e., *Vibrio* vs. seawater bacterial consortium) and associated morphological features such as size, shape, or general surface properties, but the distinction between known/native and foreign (seawater bacterial consortium and Hal 281 vs. NJ 1) primarily drive the response in differentially abundant proteins. Previous amplicon sequencing analysis by Schmittmann 2022 showed that Hal 281 is not exclusively found in *H. panicea* tissue, but also occurs in environmental water samples. Additionally its closest relative strain (i.e., *Vibrio atlanticus*, Table 1) was also isolated from another filter-feeder, the Atlantic clam *Ruditapes* sp. (Diéguez et al., 2011). Hal 281 could be therefore considered an environmental or transient bacteria, that may be utilized regularly as a food item by *H. panicea*. In contrast, the non-sponge *Vibrio* NJ 1 isolated from *N. vectensis* has not been reported to occur in environmental seawater samples and is therefore unlikely to be encountered by *H. panicea*.

In general, more differentially abundant proteins related to phagocytosis were detected in individuals exposed to the foreign isolate NJ 1 than to the native isolate Hal 281 (Fig. 6). Particularly cytoskeletal, membrane trafficking, and lysosomal proteins were present in sponges incubated with NJ 1. In contrast, only exosomal proteins were detected in individuals treated with Hal 281. This may indicate that the native *Vibrio* is not digested after phagocytosis, but expelled in the mesohyl through vomocytosis or a similar process as earlier mentioned in the sea anemone *Aiptasia* sp. following initial phagocytosis (Jacobovitz et al., 2021). Such a process could also explain the high number of free *Vibrio* cells found in the cell suspension of sponges exposed to Hal 281 (Fig. 3B). During the multiple washing steps of the sponge cell-dissociation protocol free *Vibrio* cells should have been removed. Thus, the free

Vibrios detected were most likely bound to the cell membrane of dissociated sponge cells and were detached during the FACS analysis, either at an early stage of phagocytosis (i.e., entering the cell) or in a late stage of vomocytosis (i.e., exiting the cell membrane). The almost two-times higher number of free Vibrios in sponges treated with Hal 281 could be the result of detached bacterial cells both entering and exiting, whereas in specimens exposed to NJ 1 this free fraction may originate predominantly from Vibrios entering the sponge cells.

Apart from pronounced differences in the proteomic responses between the two *Vibrio* strains, at least two differentially abundant signaling proteins were shared between these treatments. The Inositol 1,4,5-trisphosphate receptor type 1 (ITPR1; UniProt: Q14643) which participates in the NOD-like receptor signaling pathway (KEGG: ko04621), and a nucleoside diphosphate kinase (NDK) described as a G-protein coupled receptors family 1 profile domain-containing protein (UniProt: A0A182P2I5; Table S7). In fact, the reference transcriptome of *H. panicea* contains a large variety of NLRs and GPCRs (Schmittmann et al., 2021). This could indicate that *Vibrio* sensing and recognition in *H. panicea* involves NLR- and GPCR-like receptors.

### Reproducibility and improvement of the *in-vivo* phagocytic assay

The FACS analysis on *H. panicea* (host) dissociated cells showed that the identified gates of the “bulk” DAPI stained cells, as well as of the phagocytic cells (i.e., bacteria-containing cells) were highly consistent as previously described (Marulanda-Gomez et al. 2023). The results were successfully reproduced using sponge individuals collected in a different year, but around the same period (Jul-Aug), and exposed to a different *Vibrio* strain than the individuals used for establishing the assay. Importantly, the current assay yielded a 20-30% percentage increase of phagocytic cells compared to the previous study (Marulanda-Gomez et al. 2023). This improvement was achieved by increasing the concentration of TAMRA by 5-fold, resulting in a clearer distinction of the population of phagocytic cells compared to the corresponding gate in the control sponges (i.e., individuals incubated without isolates) during the FACS analysis (Fig. 2). Moreover, the higher estimates of phagocytic cells could be related to the physiological state of the used sponge individuals. In this study, collected *H. panicea* individuals were allowed to recover and heal from handling *in-situ*, and were only placed in the aquaria system 2 hours before each assay was performed. In contrast, sponges from the aforementioned study (Marulanda-Gomez et al. 2023) were kept in the aquaria system for

approx. 8 days at bacterial concentrations up to two orders of magnitude lower than typically found in the sponge's natural environment (Mueller 2022). Food limitation is likely to reduce the *H. panicea* fitness and thus might have had a negative effect on the phagocytic activity of the sponge. Nevertheless, we cannot discard the possibility that the difference we observed in the percentage of phagocytic cells is also a result of natural variation between used sponges. Moreover, microscopy inspections of sponge cells provided evidence on the involvement of phagocytic cells with different sizes and morphologies in *Vibrio* phagocytosis by *H. panicea*. Even though the analysis of phagocytic cell types was performed by microscopy counts, the phagocytic assay has the potential to also detect these cellular differences. For example, using specific cellular stains for tubulin (e.g., Phalloidin) to label flagellated cells (Laundon et al., 2019), or adapting fluorescence *in-situ* hybridization probes already

## Conclusion

In the present study we validated and further improved the application of a recently established *in-vivo* phagocytosis assay (Marulanda-Gomez et al. 2023) for quantifying the incorporation of a native and a foreign *Vibrio* isolate into *H. panicea* cells. Initial *Vibrio* incorporation into phagocytic sponge cells did not differ between isolates, but complementary microscopy inspections revealed that the distribution of Vibrios into different phagocytic cell types differed between the native and the foreign isolate. Similarly, *Vibrio* isolates elicited a differential proteomic response characterized by higher abundances of phagocytic-related proteins associated with cytoskeletal, membrane trafficking, and lysosomal functions in the foreign vs. exosomal functions in the native treatment. These findings support earlier reports from other marine invertebrates that suggest an initial indiscriminate incorporation of microbes via phagocytosis, followed by a subsequent differential processing of foreign and native microbes, resulting in intracellular digestion and/or escape. The different approaches used here to study phagocytosis provided more detailed insights into the cell types and for the first time, proteins involved in bacterial incorporation by sponge cells. Combining FACS, microscopy, and proteomic approaches proved to be a powerful tool to elucidate the cellular and molecular basis of phagocytosis, a conserved cellular mechanism from amoeba, to sponges, and humans.

## Data availability

The authors confirm that the data supporting the results and conclusions of this study are accessible within this thesis and its supplementary information. If further data is required it will be made available by the authors on request.

## Supplementary material

The supplementary material for this chapter can be found at the end of this thesis.

## Authors affiliations

<sup>1</sup>Research Unit Marine Symbioses, GEOMAR Helmholtz Centre for Ocean Research Kiel, Kiel, Germany

<sup>2</sup>Department for Freshwater and Marine Ecology, University of Amsterdam, Amsterdam, The Netherlands. <sup>3</sup>Current address: Department for Marine Ecology, University of Bremen, Bremen, Germany

<sup>4</sup>Systematic Proteomics and Bioanalytics, Institute for Experimental Medicine, <sup>5</sup>Christian-Albrechts-Universität Kiel, Kiel, Germany

<sup>5</sup>Institut de Ciències del Mar–CSIC, Marine Biology and Oceanography, Marine Biogeochemistry, Atmosphere and Climate, Barcelona, Spain

<sup>6</sup>Christian-Albrechts-Universität Kiel, Kiel, Germany

## Authors contributions

AMMG, LP and UH conceived the idea. AMMG and BM planned and conducted the experiments. KB performed the FACS analysis and AMMG the fluorescence microscopy inspections. MA and AT performed the proteomics analysis. The initial draft of the chapter was written by AMMG. All authors contributed to improving the article and approved the submitted version.

## Funding

UH was supported by the DFG (“Origin and Function of Metaorganisms”, CRC1182-TP B01) and the Gordon and Betty Moore Foundation (“Symbiosis in Aquatic Systems Initiative”, GBMF9352). LP received supported by “la Caixa” Foundation (ID 10010434), co-financed by the European Union’s Horizon 2020 research and innovation program under the Marie Skłodowska-Curie grant agreement No 847648), fellowship code is 104855. Additional funding support to LP was provided by the “Severo-Ochoa Centre of Excellence” accreditation

(CEX2019-000928-S). This is a contribution from the Marine Biogeochemistry and Global Change research group (Grant 2021SGR00430, Generalitat de Catalunya).

## Acknowledgements

We are grateful to Prof. Dr. Sebastian Fraune and Nida Kaya for helpful discussions on the experimental design and for providing the isolates from *N. vectensis*. We further acknowledge Andrea Hethke for technical assistance in the lab, and Jutta Wiese and Tanja Rahn for their support with the sequencing and phylogenetic analysis of the bacteria isolates. We thank the International Max Planck Research School for Evolutionary Biology and the Collaborative Research Centre “Origin and Function of Metaorganisms” (CRC1182) for supervision effort of AMMG.

---

## General Discussion

---



The aim of this Ph.D. thesis was to explore the mechanisms that regulate microbial discrimination in sponges. I adopted the host perspective and focused on the emerging research field of sponge immunity. By reviewing the current knowledge on the cellular and molecular mechanisms of sponge immunity (Chapter 1), I could showcase that the immune system is one of the forces driving sponge-microbe recognition. I provided experimental evidence of immune molecular components involved in sponge microbial discrimination, by experimentally demonstrating the role of Poriferan NLR-like receptors in the sensing of microbes and in the recognition between seawater and sponge-derived microbial communities (Chapter 2). Moreover, the discrimination of microbial consortia was observed to be species-specific which suggests that the sponge host is involved in the recognition process and that this process is not exclusively controlled by microbial structures of the symbionts. I expect the HMA-LMA status to play a role on how sponges sense and recognize microbes. Following a holistic approach, I subsequently focused on the most probable cellular mechanism involved in the recognition and incorporation of microbial cells: phagocytosis. Thereto, I developed (Chapter 3) and established (Chapter 4) an in-vivo high-throughput assay to quantify sponge phagocytosis. This novel method provided insights into the process of particle incorporation into sponge cells and has great potential to study the role of phagocytosis in sponge-microbe interactions, as well as in other metazoans. In the following sections, the key outcomes of this PhD thesis are discussed and the outlook for future research is presented.

### **The enduring enigma of sponge microbial discrimination**

Particle selection by sponges is a controversial debated topic. Despite initial observations of sponges positively selecting seawater bacteria and negatively selecting symbiont bacteria (Wehrli et al., 2007; Wilkinson et al., 1984), we are still trying to unveil how microbial discrimination operates in the host. In recent years we have discovered that sponges respond to microbial stimuli via components of the immune system (e.g., (Pita et al., 2018; Schmittmann et al., 2021)), and it is becoming more evident that immunity is a main force behind microbial discrimination by sponges (e.g., Chapter 2, (Geraghty et al., 2021; Yuen, 2016)). In order to continue untangling the part that the host plays in the sponge-microbe crosstalk it is necessary to study this interaction at different levels. Particle selectivity by the sponge can potentially occur at different stages and hence can be studied on the physiological,

cellular, and/or molecular level. For instance, discrimination can occur either during particle filtration from the surrounding water (difference in uptake rates) and/or after the particle has been filtered and is in contact with or has been internalized by sponge cells (difference in phagocytic activity and/or activation of receptors).

### The physiological perspective - Sponge filtration

The filtering process is determined by physical constraints of the sponge and/or particle properties, such as the opening of the animal incurrent canals, pumping rates (i.e., volume of water clear per unit of time), and particle size and concentration (e.g., (Morganti, 2019; Mueller et al., 2014; Pile & Young, 2006; Riisgård & Larsen, 2010; Robertson et al., 2017)). Particle removal rates estimated in this thesis for the sponge *H. panicea* (Chapter 3) did not differ between different particle types (i.e., latex beads, microalgae, and bacteria). Suspension feeders in general are regarded as non-selective within the particle size range that their physiology is adapted to (Hamann & Blanke, 2022). Size-independent discrimination is reported for sponges (Leys & Eerkes-Medrano, 2006; McMurray et al., 2016; Yahel et al., 2006; but see Turon et al., 1997, Ribes et al., 1999, Pile and Young, 2006) and selectivity is shown to vary with particle concentration (Hanson et al., 2009, Mueller et al., 2014). The filtration estimates for *H. panicea* (Chapter 3) support the view of size-independent and concentration-dependent particle selection. Particle size (1-3  $\mu\text{m}$  in diameter) and surface properties (inert vs. natural) did not directly affect particle selection during the filtering process, whereas increase in algal concentration resulted in higher particle removal by *H. panicea* (Chapter 3). The highly filtration efficiency of sponges for particles of different sizes and composition suggest that selection occurs post-filtration during particle internalization (i.e., phagocytosis) into the sponge cells (Leys & Eerkes-Medrano, 2006; Maldonado et al., 2010, Chapter 3).

### The cellular perspective – Deciphering microbial uptake by sponge cells

#### Initial cellular internalization may be indiscriminative

Phagocytosis is a conserved immune mechanism regarded as a key driver for microbial discrimination in invertebrates such as cnidarians, mollusks and insects (e.g., (Nyholm & McFall-Ngai, 2021; Roth & Kurtz, 2009; Tame et al., 2022; Wolfowicz et al., 2016), yet, to my best knowledge, this mechanism has only been studied in the context of sponge symbiosis using experimental models that resemble sponge cells (Nguyen et al., 2014, Jahn et al., 2019)

Investigating cellular mechanisms in sponges is challenging since we still know very little about such processes. The field of sponge cellular biology has mainly advanced in the context of cell culture, regeneration, proliferation, and cellular processing of dissolved and particulate food (e.g., Alexander et al., 2014; Ereskovsky et al., 2019; Schippers et al., 2011, Achlatis et al., 2019; Hudspith et al., 2021). To unravel the role of phagocytosis in sponge-microbe discrimination, an *in-vivo* quantitative assay was developed using the sponge *H. panicea* (Chapter 3). This high-throughput phagocytic assay allowed to compare phagocytosis of food, symbiont, and pathogenic bacteria. In fact, the assay was further used within this thesis (Chapter 4) to assess if sponge-associated bacteria (native) were differentially phagocytized compared to non-sponge-associated bacteria (foreign) This was the first attempt to apply the phagocytic assay as a tool to investigate if sponges discriminate “friend” from “foe” through this conserved cellular.

Initial cellular internalization of different particle types (Chapter 3), as well as of sponge-associated vs. non-sponge-associated bacterial isolates (Chapter 4), was indiscriminative in *H. panicea*. Yet, the difference between particles and isolates appeared to rely on the number of particles incorporated and on their distribution along the different types of phagocytic sponge cells over time, as well as on the proteins putatively involved in the phagocytic process (Chapter 3 and 4). The increase in the percentage of phagocytic cells seemed to be faster for indigestible particles (i.e., latex beads), and at a lower degree for digestible microbes (i.e., bacteria and microalgae). This difference is likely to be the result of the sponge digestion behavior. The beads tend to accumulate in the sponge cells (primarily choanocytes) as they cannot be digested. Once the cells are saturated with beads it is likely that phagocytosis is initiated by other choanocyte-like cells (Chapter 3). The big microalgae cells were incorporated at a slower rate and algal translocation between choanocyte- and archaeocyte-like cells was evident. This suggests that sponge cells may need more time to digest big-size algal particles. Similarly, in other sponge species initial incorporation of particles into sponge cells is also reported to be indiscriminative and the digestion process is likely to vary with size and type of the particle (Leys & Eerkes-Medrano, 2006; Maldonado et al., 2010). Based on these observations, it is plausible to hypothesize that particle internalization into sponge cells may be indiscriminative, but how the sponge processes it may differ from one particle type to another.

Selective and non-selective phagocytosis has been reported as the prevalent mode of symbiont entry into the host in several non-sponge-microbe symbioses. For instance, in the *Aiptasia*-dinoflagellate symbiosis first evidence suggests phagocytosis to be a size-selective process, where large-sized symbiont strains are less prone to colonize the host (Biquand et al., 2017). Furthermore, while exogenous bacteria are non-selectively phagocytized and digested by the deep-sea mussel *Bathamodiolus japonicus*, symbionts are differentially processed and retained after engulfment by the host cell (Tame et al., 2022). While these findings may appear to be contradictory, this wide range of findings could be explained by the nature of the phagocytosis process itself. Phagocytosis comprises several steps: (1) detection, (2) internalization and (3) processing of particles (see introduction for details). If indeed the initial step of particle internalization by sponge cells is indiscriminative, then it is plausible to suggest that microbial discrimination occurs at a later step of the phagocytic process (e.g., particle digestion). A combination of pulse-chase experiments (as applied in Chapter 3) using symbiotic and non-symbiotic isolates, and long-term monitoring of microbial phagocytosis by sponges could provide insightful information in this front.

### Possible scenarios after cellular internalization

Sponge microbial discrimination upon cell internalization could either be a microbe- or a host-dominated process, or likely both. The interaction between host phagocytosis and symbiotic bacteria is poorly understood in comparison with pathogenic bacteria. Yet, cellular mechanisms for entering to, persisting within, and escaping from the host (e.g., interference with phagosome maturation, resistance to degradation, physical escape from the phagosome, among others. Fig. 1) are suggested to be convergent between symbionts and pathogens based on reproducible genomic patterns (McCutcheon, 2021). Intracellular bacterial pathogens secrete different effector proteins to manipulate host cell signaling pathways and disarm immune defense mechanisms (Cornejo et al., 2017; Uribe-Quero & Rosales, 2017). For example, *Mycobacterium tuberculosis* causes the lung infection tuberculosis by the activation of the ESX-1 secretion system which arrests phagosome maturation and promotes the persistence of the bacteria in an early-endosome-like vacuole (Omotade & Roy, 2019). In the case of the pathogen *Brucella abortus*, which causes abortion and sterility in mammals, maturation of the phagosome does occur but the T4SS secretion system (i.e., VirB) prevents the fusion of the bacteria-containing vacuoles with the lysosomes (Celli, 2019). Endosymbiotic bacteria have developed similar strategies for gaining entry into host cells and evading

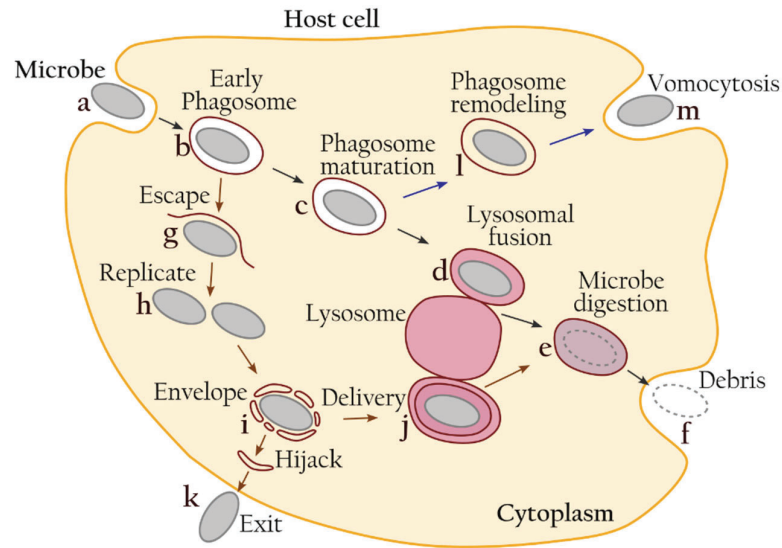


**Fig. 1** Strategies employed by microbes to persist or escape host cells. (a) Microbe is recognized the host cell and (b) incorporated in a nascent phagosome which (c) undergoes maturation. (d) Lysosomal fusion occurs in the late phagosome and the (e) microbe is digested. (f) the unused cell debris is exocytosed. (g) Some microbes escape the phagosome and (h) replicate in the host cytoplasm. (i) Autophagosomal membranes enveloped the microbe and deliver it to lysosomes in for destruction. (k) Some microbes can hijack the autophagy machinery to force their exit from the host cell without been killed, while (m) others can be released intact via vomocytosis. Redrawn base on McCutcheon 2021.

degradation. For instance, the aphid symbiont *Buchnera aphidicola* impedes the normal formation of the phagolysosome with the aim of residing in specialized host cells called bacteriocytes (McCutcheon, 2021). Due to limitation in experimental assays in sponges, modulation of host phagocytosis by sponge symbionts has only been tested in non-sponge systems (i.e., free-living amoeba and murine macrophages (Nguyen et al., 2014; Jahn et al., 2019)). The established phagocytosis assay within this thesis (Chapter 3) now provides the means to test if microbes with different structures are also able to hijack the sponge's phagocytic machinery as observed in intracellular pathogens and other symbiosis systems. For example, the "arrested phagosome hypothesis" in cnidarians (Malcolm & April, 2012) states that *Symbiodinium* species avoid degradation by mimicking a phagosome digested prey by realizing zooxanthella-derived compounds. The arrest of phagosome maturation by dinoflagellates does promote their establishment in the host (Mohamed et al., 2020). The successful reproducibility and improvement of the phagocytic assay to investigate if different types of bacteria trigger a differential phagocytic response (Chapter 4) demonstrates the potential of this experimental approach to test for example if similar mechanisms operate in

sponges harboring symbiotic zooxanthellae, or if sponge bacterial symbionts are capable to avoid cellular digestion by comparable means.

From the sponge host side, no cellular mechanism of how symbionts are selected and differentiate among other microbes after phagocytosis are yet confirmed experimentally. It can be expected that the fate of the bacteria is controlled by the host, for example by facilitating the persistence of symbionts via suppression of its immune response, whereas activating intracellular digestion of non-symbiotic microbes. Indeed, a dampening of immune-related features was observed when the HMA sponge *A. aerophoba* was presented with its own symbionts (Chapter 2). However, how this immune suppression translated into specific cellular mechanisms remains to be tested. An alternative differential cellular response of the sponge (if there is one) to digestion of non-symbiotic microbes could be the extracellular expulsion of these bacteria. This response has been observed in the larvae of the anemone *Aiptasia*. The larvae first phagocytize microalgae indiscriminately, but subsequently expel non-symbiotic algae from the phagocytes (without lysis via vomocytosis) while symbiotic algae are retained within the phagosome and remain within the host tissue (Jacobovitz et al., 2021). Interestingly, symbionts are also prone to vomocytosis in other organisms. In the pea aphids, the host has the ability to control its symbiont population by remodeling the symbiont-containing vacuoles and expelling the bacteria in a vomocytosis-like process (Koga et al. 2008). This process is dependent of the developmental stage of the host as means of symbiont transmission to the next generation and of exploiting its microbes for nutrients (McCutcheon, 2021). As vomocytosis is a conserved process of exocytosis from amoeba to humans (Seoane & May, 2020) it is conceivable that a similar mechanism might be involved in microbial discrimination in sponges.

During the phagocytic assays with microalgae in *H. panicea* (Chapter 3) approx. 75% of the algae that were taken up by the sponge were present in the sponge cell fraction during the FACS analysis as “free algae”. Likewise, in the phagocytic assays with the *Vibrio* isolates (Chapter 4) around 60-80% of the bacteria were also observed as “free” *Vibrio* cells. It was suggested that these “free particles” represented algae and bacteria that were loosely attached to sponge cells. However, they could potentially represent cases of algae and bacteria that were in the process of been expelled from the sponge cells. Capture and subsequent expulsion of inert particles from the sponge cells has been observed in *H. panicea*

(Funch 2023), and thus it is possible that expulsion of certain microbes can also occur. So far, food bacteria seemed to be rapidly digested (Maldonado et al., 2010; Markus Wehrl et al., 2007), while sponge symbionts have been rarely observed to be ingested by sponge cells (Markus Wehrl et al., 2007; Wilkinson et al., 1984a). But note that in some cases symbionts were frequently detected in choanocytes and translocated to archeocytes for further processing (Yuen, 2016). Overall, this line of thoughts raises several questions: (1) are sponge symbionts phagocytized, and then expelled into the mesohyl where they reside and are maintained? or (2) are they phagocytized and further digested? And (3) is there a combination of endocytic and exocytic mechanisms involved in microbe selection that varies with microbe strain as well as with abiotic and biotic factors?

### Phagocytic plasticity in sponges

Future experimental approaches, including the here developed phagocytic assay (Chapter 3 and Chapter 4), are required to unravel how the incorporation and further processing of symbiotic and non-symbiotic microbes change in sponge individuals displaying different physiological states and/or under different environmental conditions. For instance, during the reproductive season, the main phagocytic cells in sponges (i.e., choanocytes and archeocytes) differentiate into sperm cells and oocytes, respectively, and digestion of symbionts is intensified to secure nutrient supply (Díez-Vives et al., 2022; Koutsouveli et al., 2020). Acquisition vs. digestion of symbionts might thus change with the sponge reproductive stage and nutrient availability. Phagocytosis of symbionts is also known to occur under low food conditions in deep-sea sponges and mussels (Leys et al., 2018; Tame et al., 2023), as well as in corals (Wiedenmann et al., 2023) to meet the required nutritional demands of the host.

Lastly, it is not known yet if phagocytic activity in sponges has different layers depending on the context (i.e., feeding, immunity and symbiosis). Some evidence suggests that choanocytes might have a dual role in immunity and digestion (Yuen, 2016), whereas archaeocyte-like cells are enriched in immune features (Musser et al., 2021). While choanocytes may be functionally considered to represent gut phagocytes and archeocytes immune macrophages, there is still not molecular evidence for the homology between these cells (Bajgar & Krejčová, 2023; Hartenstein & Martinez, 2019; Steinmetz, 2019). Combining the phagocytic assay (Chapter 3 and Chapter 4) with cellular markers or fluorescent *in-situ* hybridization probes (as in Musser et al., 2021; Snyder et al., 2021) would allow to investigating which sponge cell types are

involved in the phagocytic process and if there is a different type of phagocytic response when encountering different microbes. Such an approach would further allow to depict specific phagocytic cells, containing symbionts vs. non-symbionts, and conduct single-cell RNA sequencing to identify if there are specific genes involved in phagocytosis related to digestion, defense and/or symbiosis (as recently observed in *E. muelleri* (Geraghty et al., 2021)), or if instead, phagocytosis could be considered as a “general sponge response to microbes” (similar as oxidative stress and cell death in the general “coral environmental stress response” (Dixon et al., 2020)). In general, a better understanding of how phagocytosis operates in early divergent animals such as sponges could shed light into the emergence and evolution of nutrient acquisition, host defense, and cellular mechanisms of symbiosis.

## The molecular perspective –Sponge transcriptomic responses to microbes

### DGE as a tool for assessing the sponge reaction to bacteria

Incubation experiments with sponge symbiont fraction followed by RNA-Seq differential gene expression (DGE) analysis, proved to be a good alternative to characterize the sponge molecular response in the lack of a sponge phenotypic trait to evaluate the host reaction upon microbial encounter (Chapter 2). Recovering the sponge microbial fraction from live sponge tissue by differential centrifugation (Schmittmann et al., 2022; Wehrl, 2006) can aid in circumventing the limitation of uncultivable sponge symbionts, as this microbial fraction comprises the sponge-associated microbial community. Similar approaches of isolating associated microbes from sponge tissue and presenting them to the host with the aim of characterizing the repertoire of immune genes have, to my knowledge, only been applied to the freshwater sponge *E. muelleri* (Geraghty et al., 2021) and to the marine sponge *A. queenslandica* (Yuen, 2016). Conversely, in other transcriptomic studies sponges were injected with commercial microbial elicitors to induce a strong immune response (Pita et al., 2018; Schmittmann et al., 2021). The magnitude of the sponge transcriptomic response appears to be scalable dependent on the type of cue and how the treatment is applied (as discussed in Chapter 2). Thus, implementing experimental setups that mimic natural conditions as close as possible provides a more realistic readout on the molecular mechanisms that are most likely employed by sponges in the interaction with microbes under natural conditions.



### Microbial recognition by sponge immune receptors

Immune receptors belonging to the class NLRs and SRCRs have been suggested to serve as a powerful “tool-kit” for sponges to detect diverse arrays of ligands, and hence to regulate the sponge-microbe crosstalk (Degnan, 2015; Yuen, 2016). Within the context of this thesis, I experimentally showed that different types of NLRs, and a SRCR-containing gene, were involved in the recognition between seawater microbes and sponge-derived microbes in the LMA sponge *D. avara* (Chapter 2) confirming the previous hypothesis derived from transcriptomic characterization (Degnan, 2015; Yuen, 2016). Hence, not only sponge symbionts have the potential to evade recognition by the host via specific structures (e.g., eukaryote-like proteins (Díez-Vives et al., 2017; Jahn et al., 2019)), but also the sponge host is equipped (or not) with immune mechanisms that can likely be used for recognizing different microbial players. A new avenue to be explored is how poriferan NLRs detect microbial cues: do they detect only microbial ligands, or do they also perceive microbial effectors? For mammals and plants NLR-mediated microbial detection can occur both through direct or indirect interactions with effector molecules and these strategies are proposed to function as powerful on-off switches depending on the context of the signal (Duxbury et al., 2021; Jones et al., 2016).

### Host-specific traits drive the immune response upon microbial encounter

The sponge host transcriptomic response to microbial encounters differed between the HMA and the LMA species tested in Chapter 2. The fact that sponge species sense microbial communities differently might be linked to different layers of immunity (i.e., constitutive vs. induced) operating in each species. Constitutive immune mechanisms provide an immediate response to microbial activities, cellular stress and metabolic alterations by inducing antimicrobial effector functions and limiting the activation of PRRs, whereas inducible mechanisms mediated by PRRs are only activated upon stimuli, and require tight control and negative regulatory systems (Paludan et al., 2021). It was previously proposed that HMA sponges require a lower constitutive expression and more fine-tuned regulation of their immune genes compared to LMA species in order to avoid conflicts between external microbial stimuli and the signals from their highly dense microbial community (Pita et al., 2018; Schmittmann et al., 2021). The fact that *A. aerophoba* (HMA) showed a low transcriptomic response, and no activation of PRRs neither upon seawater microbial nor symbiont consortia (Chapter 2), might instead suggest that HMA species rely more

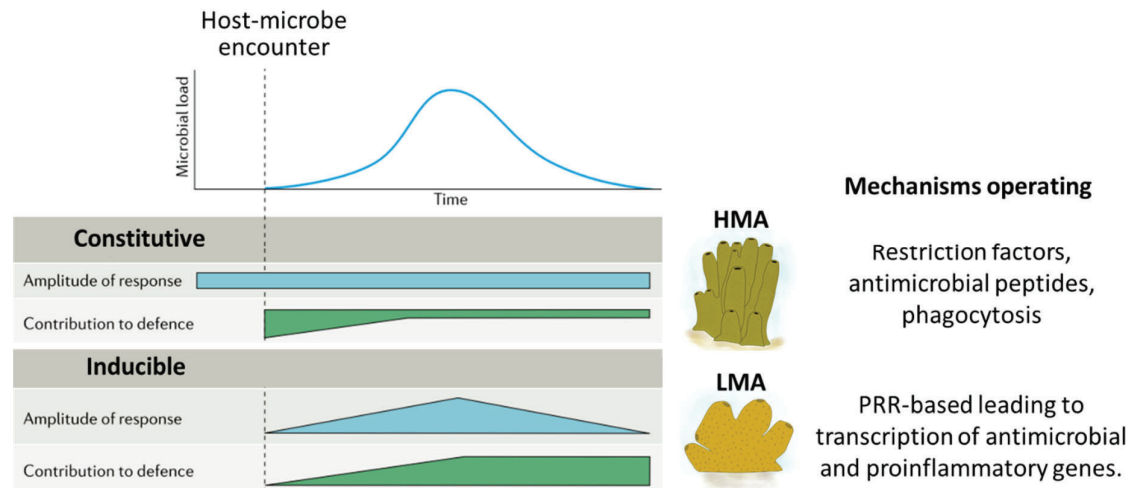


**Fig. 2.** Constitutive vs. inducible immune responses. After microbial encounter the amplitude of each response and their impact on the host defense vary over time (modified from Paludan et al., 2021). In sponges, the type of immune response upon microbial exposure is proposed to be linked to the HMA-LMA status. HMA sponges may rely on constitutive immune mechanisms that limit PRR stimulation, while inducible responses based on PRR activation and downstream signaling may be favored in LMA species.

on constitutive mechanisms to respond to microbial encounters which are expressed at a basal level. Mechanisms of constitutive immunity are activated through pre-existing molecules to directly eliminate danger and cannot be amplified. In contrast, PRR-induced immunity operates primarily via inducible transcription-dependent proinflammatory responses which have the ability to be amplified many times but can also lead to excess inflammation (Paludan et al., 2021). It is plausible that HMA sponges lean on constitutive mechanisms to avoid the constant induction and amplification of immune responses when interacting with its abundant microbiome as well as the surrounding seawater microbial community, and thereby preserving energy and reducing the risk of disrupting homeostasis (Fig 2). Contrary, the lower interactions of LMA sponges with symbionts, compared to HMAs, might favor inducible mechanisms over constitutive ones (Fig 2). In corals, allocation of energy to immunity varies among species with differing life histories. Disease-resistant corals invest more resources into constitutive immunity (Palmer, 2018), show highly plastic gene expression patterns (MacKnight et al., 2022), and exhibit low changes in the expression of immune-related genes even upon bacterial challenge (Wright et al., 2017), compared to more susceptible species. Comparative studies between sponge species with diverse life traits (e.g., juveniles vs. adults, temperate vs. tropical, shallow vs. deep-sea, etc.) and expose to various

microbial elicitors would aid to identify constitutive or inducible species-specific expression of immune genes associated to microbial differentiation in sponges.

Differences in the immune response of HMA and LMA sponges to microbial encounters could also be due to the differences in their microbiota. Symbiotic interactions can shape the host immune system and further regulate the activation of PRRs (Brown & Clarke, 2017; Gerardo et al., 2020). The diverse and abundant microbial communities of HMAs might provide the sponge with a greater reservoir of defense mechanisms than LMAs. The metagenomes of sponge symbionts are enriched in genes related to microbial defense (e.g., restriction-modification systems, toxin-antitoxin systems, clustered regularly interspaced short palindromic repeats (CRISPR) (Horn et al., 2016; Moreno-Pino et al., 2020; Slaby et al., 2017)) and these might compensate for the activation of host immune mechanisms upon interaction with microbes. Moreover, the recognition of microbes in the sponge could also be potentially mediated by its symbionts through sensing mechanisms such as quorum sensing, which could then activate or suppress competition regulating the colonization of other microbial players. To illustrate, in the symbiosis between the Hawaiian bobtail squid and *Vibrio fischeri* the symbiont can regulate the activity of a secretion system (i.e., T6SS) via quorum sensing which promotes strain incompatibility within the host (Guckes et al., 2023). Hence, sensing and competition mechanisms in the microbiome of HMA sponges might help balance the interactions between its highly diverse microbial consortia and the external microbial communities to ensure a stable state, whereas LMA sponges might rather rely on mechanisms from the host. However, the role of the sponge microbiome, as well as on potential molecular tools employed by it for aiding in microbial discrimination requires further investigation.

## Assembling the different perspectives on sponge microbial discrimination

A direct link between physiological, cellular and molecular mechanisms for microbial discrimination was beyond the scope of this thesis. Nevertheless, combining lessons learned within this project and from previous studies concerning the different perspectives, allowed me to formulate new working hypotheses regarding the process of microbial discrimination by sponges. Here, a hypothetical generalization between mechanisms that are operating in HMA and LMAs species is presented.

I propose that in HMA sponges microbial discrimination is facilitated extracellularly as they might need to better regulate the entrance of microbes into their populated mesohyl. The discrimination is likely to take place early, upon first contact of the sponge cells with the microbes, in which extracellular receptors recognize the different bacteria and allow or deny their entrance into the sponge (Fig 3). This is in line with the previously observed negative selection of its own symbionts (Wehrl et al., 2007; Wilkinson et al., 1984). Moreover, the activation of extracellular and transmembrane receptors (SRCRs and GPCRs) upon microbial elicitors in the HMA sponge *A. aerophoba* (Pita et al., 2018) could indicate that microbial structures are recognized during the transition of the microbe along the aquiferous canals. Thus, sponge cells lining the choanoderm may prevent microbe incorporation into the mesohyl and expelling them back into the water (Fig. 3 A). As HMAs already harbor dense symbiont communities, acquiring symbiotic microbes from the water column might not be required by the sponge, and hence their entrance is impeded. In contrast, seawater bacteria are positively selected (Wehrl et al., 2007; Wilkinson et al., 1984), probably because they are recognized as food and their access into the sponge mesohyl is granted as means for nutrient supply (Fig 3 B). The fact that no receptors were detected upon symbiont and seawater microbial encounter in *A. aerophoba* (Chapter 2) does not *per se* indicate that they are not involved in bacterial recognition. Instead, it may indicate that there is no differential response on their activity when the sponge is exposed to different bacteria and can further support the idea of a constitutive over an induced immune expression (as discussed in the previous section).

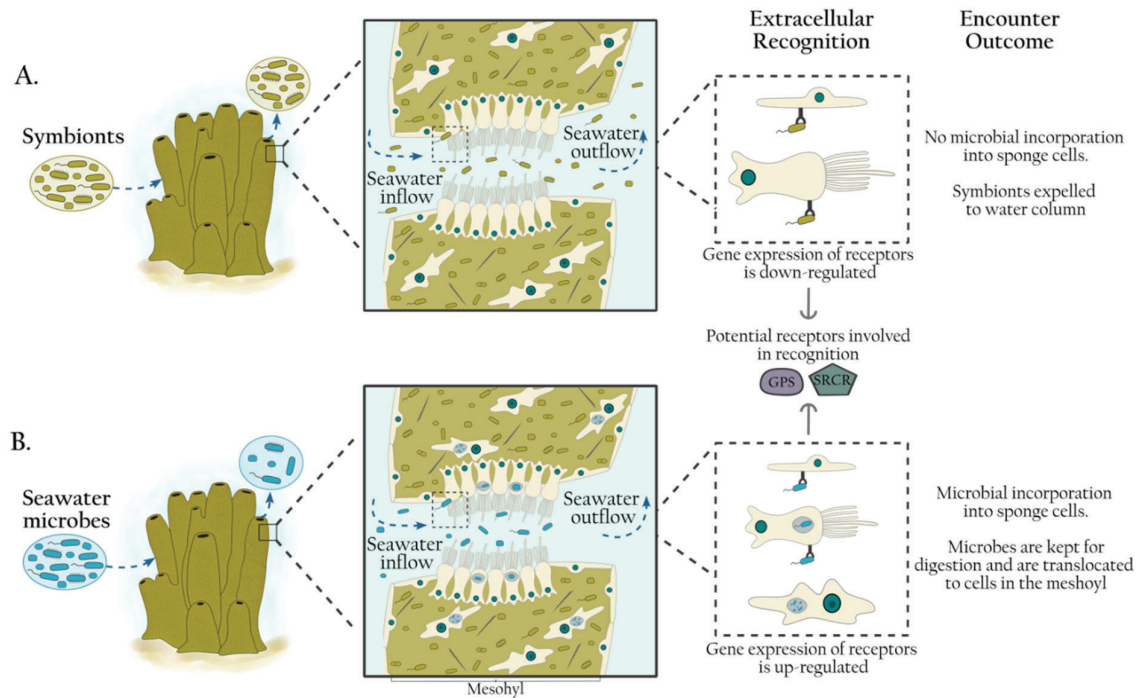


**Fig. 3.** Proposed microbial discrimination by HMA sponges. Recognition of microbes is proposed to occur extracellularly, probably via receptors such as G protein-coupled receptors (GPS) and scavenger receptor cysteine-rich (SRCRs) (based on Pita 2018). **A.** Symbionts are negatively selected by sponge cells and expelled back into the water column. **B.** Seawater microbes are positively selected as food elements, incorporated into the sponge cells and further translocated to other cells in the mesohyl for further digestion.

For LMA sponges, I propose intracellular microbial discrimination. LMA species have a lower microbial abundance compared to HMAs and thus may have a greater need to obtain microbes that could potentially be exploited by the sponge either as symbionts or as food. Bacteria filtered by the sponge can either serve as food or as a seed bank for symbionts (Webster & Thomas, 2016). Preliminary studies in LMA species showed no evidence of bacteria selection during the filtration process between sponge derived symbionts and seawater bacteria (Wehrl et al., 2007; Wilkinson et al., 1984). Likewise, no differential uptake was observed when the LMA sponge *H. panicea* was incubated with different particle types (microalgae, bacteria and latex beads. Chapter 2). Interestingly, internalization into the sponge cells of *H. panicea* was also not different between particles (Chapter 2). I hypothesize that microbes are filtered and internalized indiscriminately in LMAs and that the selection process takes place after entering the sponge cells via intracellular receptors (Fig. 4). The expanded repertoire of intracellular receptors, such as NLRs (Pita et al., 2018; Schmittmann et

al., 2021), and their activation upon microbial exposure in LMA species (Chapter 2), supports the idea of recognition occurring inside the sponge cells. After intracellular recognition, the fate of the microbe would be determined, which could result in either expulsion into the mesohyl for acquisition (Fig. 4 A.I), elimination back into the seawater (Fig. 4 A.II), or digestion for nutrition (Fig. 4 A.II and 4 B).

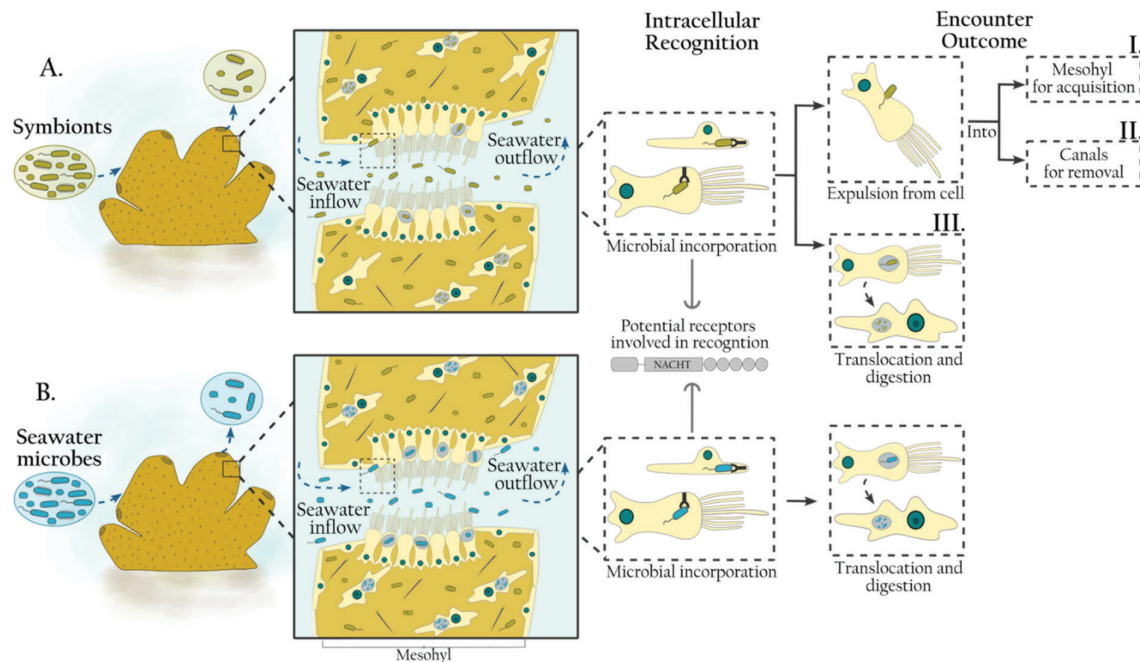


**Fig. 4.** Proposed microbial discrimination by LMA sponges. Recognition of microbes is proposed to occur intracellularly potentially via receptors such as NLRs. Upon internalization into sponge cells **A**. Symbionts are likely to (I) be expelled into the mesohyl where they are kept, (II) expelled into the aquiferous canals to be removed back to the water column, or (III) be translocated to other cells in the mesohyl for further digestion, similar as it is for **B**. Seawater microbes. Overall, the fate of the symbiont would depend on the recruitment and nutrition needs of the sponge.

These working hypotheses remain to be tested. A potential way to validate if extracellular microbial recognition takes place in HMAs would be to implement the phagocytic assay to assess if different types of microbes are internalized or not and into which cells (similar as in Chapter 4). In the case of LMAs, it is still unknown how the sponge responds upon exposure to its own symbionts because the abundance of the sponge-associated microbes is very low and challenging to extract in sufficient quantities for incubation experiments, and sponge symbionts remain mainly unculturable. An alternative for LMA species that harbored dominant and stable bacterial symbionts, as *H. panicea* and the symbiont *Candidatus Halichondribacter symbioticus* (Knobloch et al., 2019; Schmittmann et al., 2022), is to obtain

an enriched fraction of the symbiont via fluorescence-activated cell sorting that could then be used for phagocytosis assays. Following the sponge phagocytic progression over time is essential to reveal differences in the processing of symbiotic and non-symbiotic bacteria. The proposed mechanisms are likely to vary with species, life stage and environmental conditions. Thus, a range of sponge species along the HMA-LMA gradient need to be tested to identify signatures that are either related to this dichotomy or that are species-specific.

---

## Conclusion and Final Outlook

---



An overarching limitation to continue expanding our understanding of sponge immunity are the lack of well-established sponge models and methodologies to experimentally test and study molecular and cellular aspects of sponge-microbe interactions (Pita et al., 2016). Moreover, performing experiments with sponge symbionts is challenging as the majority of these microbes remain recalcitrant to cultivation (Dat et al., 2021). This thesis provides alternative experimental approaches to overcome such limitations and to explore the molecular and cellular mechanisms involve microbial discrimination by sponges. Implementing incubation experiments to expose sponges to microbes, using natural microbial fractions extracted or isolated from sponges, and characterizing the sponge transcriptomic and cellular response via RNA-Seq differential gene expression analysis and phagocytic assays, respectively, contributed to shed light into different immune elements involved in the sponge-microbe crosstalk. On the molecular side, it was learned that (i) the sponge transcriptomic response to natural microbial consortia is relatively low, (ii) this response is species-specific, and (iii) NLRs receptors have a noticeable role in the differential response to symbiotic or seawater microbes (Chapter 2). On the cellular side, observations suggest that (i) particle incorporation into sponge cells is indiscriminative, (ii) the type of phagocytic sponge cells involved in the internalization process varies after exposure to a sponge-associated vs. a non-associated bacteria as well as with microbial exposure time, and (iii) bacteria discrimination may take place after cellular internalization and the difference may rely on how each type of microbe is processed (e.g., digested or expelled) (Chapter 3 and 4). Overall, these results support the importance of adopting experimental approaches for acquiring meaningful evidence on how the poriferan immune system shapes the interactions between the sponge and its microbial partners.

Only a handful of the differentially expressed genes upon microbial encounter could be assigned to immunity, ubiquitination, and signaling function (Chapter 2). However, less than 30% of the differentially expressed genes could be annotated. This highlights the current limitation of available sponge host genome (i.e., < 10). Fortunately, this number is expected to increase in the near future thanks to the sequencing efforts of the Aquatic Symbiosis Genomics Project (<http://portal.aquaticsymbiosisgenomics.org/data>). Likewise, genetic manipulation of sponges is still a constraint, which makes it challenging to link gene expression and function. The ability to silence specific genes to perform loss-of-function experiments would allow testing hypothesis of the genes that have been identified to play a role in sponge-

bacteria interactions. In cnidarian models, such as *Hydra sp.*, *Aiptasia sp.*, and *Cassiopea xamancha* (Jones et al., 2018; Klimovich et al., 2019; Medina et al., 2021), generation of transgenic lines by embryo microinjection makes it possible to characterize gene function to elucidate the molecular mechanisms underlying host-symbiont interactions. Transgenesis in sponges has so far been established for *Suberites domuncula* explants (Revilla-I-Domingo et al., 2018) and for *G. barretti* cells (Hesp et al., 2020) using a transfection plasmid and a CRISPR/Cas12a gene editing system, respectively. These promising advances in the genetic manipulation of sponges have strong potential for targeting the expression (i.e., knockout) of specific genes shown to respond upon microbial exposure (e.g., NLRs, ubiquitin ligases, kinases, etc.) and to validate their function in the context of the sponge-microbe crosstalk.

Finally, it is imperative to follow a holistic approach integrating physiological, cellular and molecular aspects to truly reveal the underlying mechanisms involved in the sponge-microbe cross talk. Integration of these different levels is greatly missing yet crucial since linking gene functions with cellular and physiological traits remains a challenge. Likewise, assigning specific functions to sponge cells is difficult due to their high plasticity and capacity to transdifferentiate from one cell type to another (Funayama, 2018). I therefore propose an integrative experimental approach for future studies to analyze the sponge response upon symbiont vs. non-symbiont bacteria encounter, for example, by measuring uptake rates (i.e., physiology), quantifying the incorporation of bacteria into different sponge cell types (i.e., cellular), and characterizing the transcriptomic response targeting phagocytic-related genes (i.e., molecular) (Fig. 1). However, what should be presented as symbiont when we are limited by uncultivable sponge symbionts? And how to draw a line between what the sponge may consider a symbiotic and non-symbiotic (food and/or pathogenic) microbe? Alternatives to the limitation of symbionts are to use the sponge microbial fraction recovered by differential centrifugation (as in Chapter 2), strains isolated from the sponge (as in Chapter 3), genetically modified microbes enriched in symbiotic features (e.g., eukaryote-like proteins (C. Díez-Vives et al., 2017; Reynolds & Thomas, 2016)), and/or enriched microbes obtained by culture-independent techniques (e.g., “omics” approaches combined with cell sorting; Thompson et al. 2013; Chandarana et al. 2023). Microbes considered as food source could be derived from enriching the seawater microbial community (as in Chapter 2) and/or environmental isolates or cultures (as in Chapter 3), whereas an alternative to pathogens is to use beads coated with specific conjugates that mimic virulence factors of pathogenic bacteria. Experiments

consisting on exposing the sponge to this diversity of microbes and including inhibitors of immune mechanisms known to be essential in symbiotic interactions (e.g., phagocytosis) may aid to validate the cellular processes involved in sponge-microbe interactions. Moreover, techniques such as transcriptomics and proteomics could provide information on the molecular bases of such mechanisms, while microscopy observations could give evidence on where in the host these are operating. Combining the above approaches would help to build a framework to unravel the role of immune mechanisms in microbial discrimination by sponges.

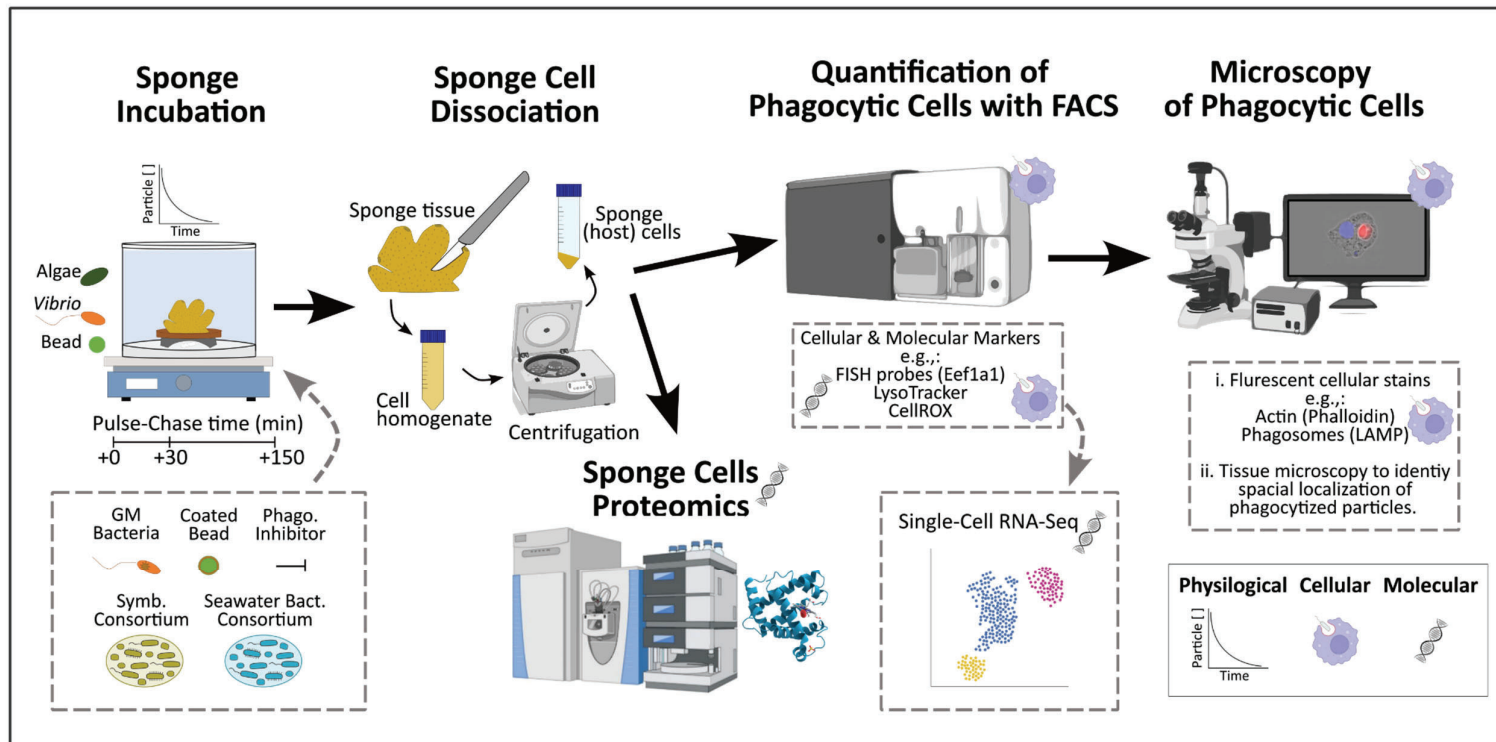


**Fig. 1** Established and proposed integrative experimental approach for studying sponge response upon microbial encounter. Overview of the phagocytic assay developed within this thesis (black arrows): **Sponge Incubations** with different particles, followed by **Sponge (host) Cell Dissociation** and **FACS** analysis to quantify the relative abundance of phagocytic cells. Corroborative flow cytometry of water samples to assess the sponge's filtration throughout the incubation. **Fluorescence microscopy** providing insights into size and morphology of phagocytic cells. **Proteomic analysis** to identify phagocytic-related proteins. The assay established during this thesis has the potential to be further expanded in each of the different steps (gray dashed boxes and arrows) to better understand the cellular and molecular bases of the phagocytic process: **Cellular & Molecular Markers** to specifically collect certain cell types during the FACS sorting process and to apply **Single-Cell RNA-Seq** on these cells. Cell-component-specific **Fluorescent stains** in combination with **Tissue Microscopy** to spatially localize the phagocytic activity.



---

## References

---

- Achlatis M, Pernice M, Green K, de Goeij JM, Guagliardo P, Kilburn MR, Hoegh-Guldberg O, Dove S. (2019) Single-cell visualization indicates direct role of sponge host in uptake of dissolved organic matter. *Proc. R. Soc. B* 286(1916), 20192153. doi:10.1098/rspb.2019.2153
- Akther, M., Haque, M. E., Park, J., Kang, T. B., & Lee, K. H. (2021). NLRP3 ubiquitination—a new approach to target NLRP3 inflammasome activation. *Int. J. Mol. Sci.* 22(16), 8780. doi:10.3390/ijms22168780
- Alexander, B. E., K. Liebrand, R. Osinga, et al. (2014). Cell turnover and detritus production in marine sponges from tropical and temperate benthic ecosystems. *PLoS One* 9: e109486. doi:10.1371/journal.pone.0109486
- Al-Khodor, S., Price, C. T., Habyarimana, F., Kalia, A., and Abu Kwaik, Y. (2008). A Dot/Icm-translocated ankyrin protein of *Legionella pneumophila* is required for intracellular proliferation within human macrophages and protozoa. *Mol. Microbiol.* 70 (4), 908–923. doi:10.1111/j.1365-2958.2008.06453.x
- Ardia, D. R., Gantz, J. E., Schneider, B. C., & Strebler, S. (2012). Costs of immunity in insects: an induced immune response increases metabolic rate and decreases antimicrobial activity. *Funct. Ecol.* 26(3), 732–739. doi:10.1111/j.1365-2435.2012.01989.x
- Bajgar, A., & Krejčová, G. (2023). On the origin of the functional versatility of macrophages. *Front. Physiol.* 14, 1–20. doi:10.3389/fphys.2023.1128984
- Barthel, D. (1988). On the ecophysiology of the sponge *Halichondria panicea* in Kiel Bight. II. Biomass, production, energy budget and integration in environmental processes. *Mar. Ecol. Prog. Ser.* 43, 87–93. doi:10.3354/meps043087
- Bayer, K., Moitinho-Silva, L., Brümmer, F., Cannistraci, C. V., Ravasi, T., & Hentschel, U. (2014). GeoChip-based insights into the microbial functional gene repertoire of marine sponges (high microbial abundance, low microbial abundance) and seawater. *FEMS Microbiol. Ecol.* 90(3), 832–doi:10.1111/1574-6941.12441
- Berg, M., Monnin, D., Cho, J., Nelson, L., Crits-Christoph, A., & Shapira, M. (2019). TGFβ/BMP immune signaling affects abundance and function of *C. elegans* gut commensals. *Nat. Commun.* 10(1). doi:10.1038/s41467-019-08379-8
- Biquand, E., Okubo, N., Aihara, Y., Rolland, V., Hayward, D. C., Hatta, M., Minagawa, J., Maruyama, T., & Takahashi, S. (2017). Acceptable symbiont cell size differs among cnidarian species and may limit symbiont diversity. *ISME J.* 11(7), 1702–1712. doi:10.1038/ismej.2017.17
- Böhm, M., H. C. Schröder, I. M. Müller, W. E. G. Müller, and V. Gamulin. (2000). The mitogen-activated protein kinase p38 pathway is conserved in metazoans: Cloning and activation of p38 of the SAPK2 subfamily from the sponge *Suberites domuncula*. *Biol. Cell* 92: 95–104. doi:10.1016/S0248-4900(00)89017-6
- Böhm, M., U. Hentschel, A. Friedrich, L. Fieseler, R. Steffen, V. Gamulin, I. Müller, and W. Müller. (2001). Molecular response of the sponge *Suberites domuncula* to bacterial infection. *Mar. Biol.* 139: 1037–1045. doi:10.1007/s002270100656
- Bosch, T. C. G. (2014). Rethinking the role of immunity: lessons from *Hydra*. *Trends Immunol.* 35: 495–502. doi:10.1016/j.it.2014.07.008
- Bosch, T. C. G., & McFall-Ngai, M. (2021). Animal development in the microbial world: Re-thinking the conceptual framework. *Curr. Top. Dev. Biol.* 141, 399–427. doi:10.1016/bs.ctdb.2020.11.007
- Brown, R. L., & Clarke, T. B. (2017). The regulation of host defences to infection by the microbiota. *Immunol.* 150(1), 1–6. doi:10.1111/imm.12634
- Bucher, M., Wolfowicz, I., Voss, P. A., Hambleton, E. A., and Guse, A. (2016). Development and symbiosis establishment in the cnidarian endosymbiosis model *Aiptasia* sp. *Sci. Rep.* 6, 1–11. doi:10.1038/srep19867
- Buckley, K. M., and J. P. Rast. (2015). Diversity of animal immune receptors and the origins of recognition complexity in the deuterostomes. *Dev. Comp. Immunol.* 49: 179–189. doi:10.1016/j.dci.2014.10.013

- Busch, K., Wurz, E., Rapp, H. T., Bayer, K., Franke, A., and Hentschel, U. (2020). *Chloroflexi* dominate the deep-sea golf ball sponges *Craniella zetlandica* and *Craniella infrequens* throughout different life stages. *Front. Mar. Sci.* 7, 1–12. doi:10.3389/fmars.2020.00674
- Campana, S., Riesgo, A., Jongepier, E., Fuss, J., Muyzer, G., & de Goeij, J. M. (2022). Meta-transcriptomic comparison of two sponge holobionts feeding on coral- and macroalgal-dissolved organic matter. *BMC Genom.*, 23(1), 1–16. doi:10.1186/s12864-022-08893-y
- Carr, M., Leadbeater, B. S. C., Hassan, R., Nelson, M., & Baldauf, S. L. (2008). Molecular phylogeny of choanoflagellates, the sister group to Metazoa. *PNAS.* 105(43), 16641–16646. doi:10.1073/pnas.0801667105
- Carrier, T. J., & Bosch, T. C. G. (2022). Symbiosis: the other cells in development. *Development (Cambridge)*. 149(13). doi:10.1242/dev.200797
- Ceccarelli, D., & Colwell, R. R. (2014). *Vibrio* ecology, pathogenesis, and evolution. *Front. Microbiol.* 5. doi:10.3389/fmicb.2014.00256
- Celli, J. (2019). The intracellular life cycle of *Brucella* spp. *Microbiol. Spectr.* 7(2). doi:10.1128/microbiolspec.BAI-0006-2019
- Chandarana, K. A., Gohil, K., Dwivedi, M. K., & Amaresan, N. (2023). Culture-independent and culture-dependent approaches in symbiont analysis. *Microbial Symbionts* (Elsevier), 723–742. doi:10.1016/b978-0-323-99334-0.00046-3
- Chu, H., and S. K. Mazmanian. (2013). Innate immune recognition of the microbiota promotes host-microbial symbiosis. *Nat. Immunol.* 14: 668–75. doi:10.1038/ni.2635
- Coelho, J. C., Calhoun, E. D., Calhoun, G. N., & Poole, A. Z. (2022). Patchy distribution of GTPases of immunity-associated Proteins (GIMAP) within cnidarians and dinoflagellates suggests a complex evolutionary history. *GBE.* 14(2), evac002. doi:10.1093/gbe/evac002
- Cornejo, E., Schlaermann, P., & Mukherjee, S. (2017). How to rewire the host cell: a home improvement guide for intracellular bacteria. *J. Cell Biol.* 216(12), 3931–3948. doi:10.1083/jcb.201701095
- Custodio, M.R., Prokic, I., Steffen, R., Koziol, C., Borojevic, R., Brümmer, F., Nickel, M., Müller, W.E.G. (1998). Primmorphs generated from dissociated cells of the sponge *Suberites domuncula*: a model system for studies of cell proliferation and cell death. *Mechanisms of Ageing and Development* 105 (1-2 Elsevier), 45–59. doi:10.1016/s0047-6374(98)00078-5
- Dat, T. T. H., Steinert, G., Cuc, N. T. K., Smidt, H., & Sipkema, D. (2021). Bacteria cultivated from sponges and bacteria not yet cultivated from sponges — A review. *Front. Microbiol.* 12, 1–18. doi:10.3389/fmicb.2021.737925
- De Goeij, J. M., and Van Duyl, F. C. (2007). Coral cavities are sinks of dissolved organic carbon (DOC). *Limnol. Oceanogr.* 52 (6), 2608–2617. doi:10.4319/lo.2007.52.6.2608
- De Goeij, J. M., Van Den Berg, H., Van Oostveen, M. M., Epping, E. H. G., and Van Duyl, F. C. (2008). Major bulk dissolved organic carbon (DOC) removal by encrusting coral reef cavity sponges. *Mar. Ecol. Prog. Ser.* 357, 139–151. doi:10.3354/meps07403
- De Monerri, N. C., & Kim, K. (2014). Pathogens hijack the epigenome: a new twist on host-pathogen interactions. *Am. J. Pathol.* 184(4), 897–911. doi:10.1016/j.ajpath.2013.12.022
- Degnan, S. M. (2015). The surprisingly complex immune gene repertoire of a simple sponge, exemplified by the NLR genes: A capacity for specificity? *Dev. Comp. Immunol.* 48: 269–274. doi:10.1016/j.dci.2014.07.012
- Destoumieux-Garzón, D., Canesi, L., Oyanedel, D., Travers, M. A., Charrière, G. M., Pruzzo, C., & Vezzulli, L. (2020). *Vibrio*–bivalve interactions in health and disease. *Environ. Microbiol.* 22(10), 4323–4341. doi:10.1111/1462-2920.15055
- Diéguez, A. L., Beaz-Hidalgo, R., Cleenwerck, I., Balboa, S., de Vos, P., & Romalde, J. L. (2011). *Vibrio atlanticus* sp. nov. and *Vibrio artabrorum* sp. nov., isolated from the clams *Ruditapes philippinarum* and *Ruditapes decussatus*. *IJSEM.* 61(10), 2406–2411. doi:10.1099/ij.s.0.025320-0
- Dierking, K., & Pita, L. (2020). Receptors mediating host-microbiota communication in the metaorganism: the invertebrate perspective. *Front. Immunol.* 11(June), 1–17. doi:10.3389/fimmu.2020.01251



- Díez-Vives, C., Moitinho-Silva, L., Nielsen, S., Reynolds, D., & Thomas, T. (2017). Expression of eukaryotic-like protein in the microbiome of sponges. *Mol. Ecol.* 26(5), 1432–1451. doi:10.1111/mec.14003
- Díez-Vives, C., Moitinho-Silva, L., Nielsen, S., Reynolds, D., and Thomas, T. (2017). Expression of eukaryotic-like protein in the microbiome of sponges. *Mol. Ecol.* 26 (5), 1432–1451. doi:10.1111/mec.14003
- Díez-Vives, Cristina, Koutsouveli, V., Conejero, M., & Riesgo, A. (2022). Global patterns in symbiont selection and transmission strategies in sponges. *Front. Ecol. Evol.* 10, 1–30. doi:10.3389/fevo.2022.1015592
- Dixon, G., Abbott, E., & Matz, M. (2020). Meta-analysis of the coral environmental stress response: *Acropora* corals show opposing responses depending on stress intensity. *Mol. Ecol.* 29(15), 2855–2870. doi:10.1111/mec.15535
- Dunn, J. D., Bosmani, C., Barisch, C., Raykov, L., Lefrançois, L. H., Cardenal-Muñoz, E., López-Jiménez, A. T., & Soldati, T. (2018). Eat, prey, live: *Dictyostelium discoideum* as a model for cell-autonomous defenses. *Front. Immunol.* 8. doi:10.3389/fimmu.2017.01906
- Duxbury, Z., Wu, C. H., & Ding, P. (2021). A comparative overview of the intracellular guardians of plants and animals: NLRs in innate immunity and beyond. *Annu. Rev. Plant Biol.* 72, 155–184. doi:10.1146/annurev-arplant-080620-104948
- Eberl, G. (2010). A new vision of immunity: homeostasis of the superorganism. *Mucosal Immunol.* 3(5), 450–460. doi:10.1038/mi.2010.20
- Ereskovsky, A. V., D. B. Tokina, D. M. Saidov, S. Baghdiguan, E. Le Goff, and A. I. Lavrov. (2019). Transdifferentiation and mesenchymal-to-epithelial transition during regeneration in Demospongiae (Porifera). *J. Exp. Zool. Part B Mol. Dev. Evol.* 334: 37–58. doi:10.1002/jez.b.22919
- Fieseler, L., Horn, M., Wagner, M., and Hentschel, U. (2004). Discovery of the novel candidate phylum “Poribacteria” in marine sponges. *Appl. Environ. Microbiol.* 70 (6), 3724–3732. doi:10.1128/AEM.70.6.3724-3732.2004
- Flanagan, R. S., Cosío, G., & Grinstein, S. (2009). Antimicrobial mechanisms of phagocytes and bacterial evasion strategies. *Nat. Rev. Microbiol.* 7(5). doi:10.1038/nrmicro2128
- Fraune, S., R. Augustin, F. Anton-Erxleben, J. Wittlieb, C. Gelhaus, V. B. Klimovich, M. P. Samoilovich, and T. C. G. Bosch. (2010). In an early branching metazoan, bacterial colonization of the embryo is controlled by maternal antimicrobial peptides. *Proc. Natl. Acad. Sci. U. S. A.* 107: 18067–18072. doi:10.1073/pnas.1008573107
- Funayama, N. (2018). The cellular and molecular bases of the sponge stem cell systems underlying reproduction, homeostasis and regeneration. *Int. J. Dev. Biol.* 62(6–8), 513–525. doi:10.1387/ijdb.180016nf
- Funayama, N., Nakatsukasa, M., Hayashi, T., and Agata, K. (2005). Isolation of the choanocyte in the fresh water sponge, *Ephydatia fluviatilis* and its lineage marker, Ef annexin. *Dev. Growth Differ.* 47 (4), 243–253. doi: 10.1111/j.1440-169X.2005.00800.x
- Funch, P., Kealy, R. A., Goldstein, J., Brewer, J. R., Solovyeva, V., & Riisgård, H. U. (2023). Fate of microplastic captured in the marine demosponge *Halichondria panicea*. *Mar. Pollut. Bull.* 194(PA), 115403. doi:10.1016/j.marpolbul.2023.115403
- Ganesan, R., Wierz, J. C., Kaltenpoth, M., & Flórez, L. V. (2022). How it all begins: bacterial factors mediating the colonization of invertebrate hosts by beneficial symbionts. *Microbiol. Mol. Biol. Rev.* 86(4). doi:10.1128/mmbr.00126-21
- Gardères, J., G. Bedoux, V. Koutsouveli, S. Crequer, F. Desriac, and G. Le Pennec. (2015). Lipopolysaccharides from commensal and opportunistic bacteria: characterization and response of the immune system of the host sponge *Suberites domuncula*. *Mar. Drugs* 13: 4985–5006. doi:10.3390/md13084985
- Gasol, J. M., and Del Giorgio, P. A. (2000). Using flow cytometry for counting natural planktonic bacteria and understanding the structure of planktonic bacterial communities. *Sci. Mar.* 64 (2), 197–224. doi: 10.3989/scimar.2000.64n2197

- Gätschenberger, H., Azzami, K., Tautz, J., & Beier, H. (2013). Antibacterial immune competence of honey bees (*Apis mellifera*) is adapted to different life stages and environmental risks. *PLoS One*. 8(6). doi:10.1371/journal.pone.0066415
- Geraghty, S., Koutsouveli, V., Hall, C., Chang, L., Sacristan-Soriano, O., Hill, M., et al. (2021). Establishment of host-algal endosymbioses: genetic response to symbiont versus prey in a sponge host. *Genome Biol. Evol.* 13 (11), 1–16. doi: 10.1093/gbe/evab252
- Gerardo, N. M., K. L. Hoang, and K. S. Stoy. (2020). Evolution of animal immunity in the light of beneficial symbioses. *Philos. Trans. R. Soc. Lond. B. Biol. Sci.* 375: 20190601. doi:10.1098/rstb.2019.0601
- Germer, J., N. Cerveau, and D. J. Jackson. (2017). The holo-transcriptome of a calcified early branching metazoan. *Front. Mar. Sci.* 4: 1–19. doi:10.3389/fmars.2017.00081
- Gilbert, S. F., Bosch, T. C. G., & Ledón-Rettig, C. (2015). Eco-Evo-Devo: developmental symbiosis and developmental plasticity as evolutionary agents. *Nat. Rev. Genet.* 16(10), 611–622. doi:10.1038/nrg3982
- Gloeckner, V., Wehrl, M., Moitinho-Silva, L., Gernert, C., Hentschel, U., Schupp, P., Pawlik, J. R., Lindquist, N. L., Erpenbeck, D., Wörheide, G., & Wörheide, G. (2014). The HMA-LMA dichotomy revisited: an electron microscopical survey of 56 sponge species. *Biol. Bull.* 227(1), 78–88. doi:10.1086/BBLv227n1p78
- Golbabapour, S., Majid, N. A., Hassandarvish, P., Hajrezaie, M., Abdulla, M. A., & Hadi, A. H. A. (2013). Gene silencing and polycomb group proteins: an overview of their structure, mechanisms and phylogenetics. *OMICS*. 17(6), 283–296. doi:10.1089/omi.2012.0105
- Goldstein, J., and Funch, P. (2022). A review on the Genus *Halichondria* (Demospongiae, Porifera). *J. Mar. Sci. Eng.* 10 (9), 1312. doi:10.3390/jmse10091312
- Goldstein, J., Bisbo, N., Funch, P., and Riisgård, H. U. (2020). Contraction- expansion and the effects on the aquiferous system in the demosponge *Halichondria panicea*. *Front. Mar. Sci.* 7, 1–12. doi:10.3389/fmars.2020.00113
- González-Pech, R. A., Li, V. Y., Garcia, V., Boville, E., Mammone, M., Kitano, H., Ritchie, K. B., & Medina, M. (2023). The evolution, assembly, and dynamics of marine holobionts. *Ann. Rev. Mar. Sci.* 14(41), 1–24. doi:10.1146/annurev-marine-022123-104345
- Grebenjuk, V. A., A. Kuusksalu, M. Kelve, J. Schütze, H. C. Schröder, and W. E. G. Müller. (2002). Induction of (2'-5')oligoadenylate synthetase in the marine sponges *Suberites domuncula* and *Geodia cydonium* by the bacterial endotoxin lipopolysaccharide. *Eur. J. Biochem.* 269: 1382–1392. doi:10.1046/j.1432-1033.2002.02781.x
- Guckes, K. R., Yount, T. A., Steingard, C. H., & Miyashiro, T. I. (2023). Quorum sensing inhibits interference competition among bacterial symbionts within a host. *Curr. Biol.* 33 (19), 14244–4251. doi:10.1016/j.cub.2023.08.051
- Guzman, C., and C. Conaco. (2016). Gene expression dynamics accompanying the sponge thermal stress response. *PLoS One* 11: e0165368. doi:10.1371/journal.pone.0165368
- Haas, B. J., Papanicolaou, A., Yassour, M., Grabherr, M., Philip, D., Bowden, J., Couger, M. B., Eccles, D., Li, B., et al. (2013). De novo transcript sequence reconstruction from RNA-Seq: reference generation and analysis with Trinity. *Nat. Protoc.* 8 (8). doi:10.1038/nprot.2013.084.
- Habyarimana, F., Al-Khodori, S., Kalia, A., Graham, J. E., Price, C. T., Garcia, M. T., et al. (2008). Role for the Ankyrin eukaryotic-like genes of *Legionella pneumophila* in parasitism of protozoan hosts and human macrophages. *Environ. Microbiol.* 10 (6), 1460–1474. doi:10.1111/j.1462-2920.2007.01560.x
- Hägele, S., Köhler, R., Merkert, H., Schleicher, M., Hacker, J., and Steinert, M. (2000). *Dictyostelium discoideum*: A new host model system for intracellular pathogens of the genus *Legionella*. *Cell Microbiol.* 2 (2), 165–171. doi:10.1046/j.1462-5822.2000.00044.x
- Hamada, M., Shoguchi, E., Shinzato, C., Kawashima, T., & Miller, D. J. (2013). The complex NOD-like receptor repertoire of the coral *Acropora digitifera* includes novel domain combinations. *Mol. Biol. Evol.* 30(1), 167–176. doi:10.1093/molbev/mss213
- Hamann, L., & Blanke, A. (2022). Suspension feeders: diversity, principles of particle separation and

- biomimetic potential. *J.R. Soc. Interface*. 19(186). doi:10.1098/rsif.2021.0741
- Hartenstein, V., and Martinez, P. (2019). Phagocytosis in cellular defense and nutrition: a food-centered approach to the evolution of macrophages. *Cell Tissue Res*. 377 (3), 527–547. doi:10.1007/s00441-019-03096-6
- Hentschel, U., J. Piel, S. M. Degnan, and M. W. Taylor. (2012). Genomic insights into the marine sponge microbiome. *Nat. Rev. Microbiol.* 10: 641–54. doi:10.1038/nrmicro2839
- Hentschel, U., Usher, K. M., and Taylor, M. W. (2006). Marine sponges as microbial fermenters. *FEMS Microbiol. Ecol.* 55 (2), 167–177. doi:10.1111/j.1574-6941.2005.00046.x
- Hesp, K., Flores Alvarez, J. L., Alexandru, A. M., van der Linden, J., Martens, D. E., Wijffels, R. H., & Pomponi, S. A. (2020). CRISPR/Cas12a-Mediated gene editing in *Geodia barretti* sponge cell culture. *Front. Mar. Sci.* 7(December), 1–10. doi:10.3389/fmars.2020.599825
- Hildemann, W.H., I.S. Johnson, P.L. Jokiel. (1979). Immunocompetence in the lowest metazoan phylum: Transplantation immunity in sponges. *Science*. 204, 420–422. doi:10.1126/science.441730
- Hirose, Y., Aini, S. N., & Yamashiro, H. (2021). Contact reactions between individuals of the coral-killing sponge, *Terpios hoshinota*. *Zool. Stud.* 60, 1–9. doi:10.6620/ZS.2021.60-41
- Ho, E. C. H., Buckley, K. M., Schrankel, C. S., Schuh, N. W., Hibino, T., Solek, C. M., Bae, K., Wang, G., & Rast, J. P. (2016). Perturbation of gut bacteria induces a coordinated cellular immune response in the purple sea urchin larva. *Immunol. Cell Biol.* 94(9), 861–874. doi:10.1038/icb.2016.51
- Horak, R. D., Leonard, S. P., & Moran, N. A. (2020). Symbionts shape host innate immunity in honeybees. *Proc. Royal Soc. B.* 287(1933). doi:10.1098/rspb.2020.1184
- Horn, H., Slaby, B. M., Jahn, M. T., Bayer, K., Moitinho-Silva, L., Förster, F., Abdelmohsen, U. R., & Hentschel, U. (2016). An enrichment of CRISPR and other defense-related features in marine sponge-associated microbial metagenomes. *Front. Microbiol.* 7, 1–15. doi:10.3389/fmicb.2016.01751
- Hughes, C.S., Moggridge, S., Müller, T. et al. (2019). Single-pot, solid-phase-enhanced sample preparation for proteomics experiments. *Nat. Protoc.* 14(1), 68–85 doi:10.1038/s41596-018-0082-x
- Hudspith, M., Rix, L., Achlatis, M., Bougoure, J., Guagliardo, P., Clode, P. L., et al. (2021). Subcellular view of host–microbiome nutrient exchange in sponges: insights into the ecological success of an early metazoan–microbe symbiosis. *Microbiome* 9 (1), 1–15. doi:10.1186/s40168-020-00984-w
- Imsiecke, G. (1993). Ingestion, digestion, and egestion in *Spongilla lacustris* (Porifera, Spongillidae) after pulse feeding with *Chlamydomonas reinhardtii* (Volvocales). *Zoomorphology* 113 (4), 233–244. doi:10.1007/BF00403314
- Jacobovitz, M. R., Rupp, S., Voss, P. A., Maegele, I., Gornik, S. G., and Guse, A. (2021). Dinoflagellate symbionts escape vomocytosis by host cell immune suppression. *Nat. Microbiol. [Internet]*. 6 (6), 769–782. doi:10.1038/s41564-021-00897-w
- Jahn, M. T., Arkhipova, K., Markert, S. M., Stigloher, C., Lachnit, T., Pita, L., et al. (2019). A phage protein aids bacterial symbionts in eukaryote immune evasion. *Cell Host Microbe* 26 (4), 542–550.e5. doi:10.1016/j.chom.2019.08.019
- Janeway, C. A., and R. Medzhitov. (2002). Innate immune recognition. *Annu. Rev. Immunol.* 20: 197–216. doi:10.1146/annurev.immunol.20.083001.084359
- Jauslin, T., Lamrabet, O., Crespo-Yañez, X., Marchetti, A., Ayadi, I., Ifrid, E., et al. (2021). How phagocytic cells kill different bacteria: A quantitative analysis using *Dictyostelium discoideum*. *MBio* 12 (1), 1–13. doi:10.1128/mBio.03169-20
- Jones, J. D. G., Vance, R. E., & Dangl, J. L. (2016). Intracellular innate immune surveillance devices in plants and animals. *Science*. 354(6316). doi:10.1126/science.aaf6395
- Jones, V. A. S., Bucher, M., Hambleton, E. A., & Guse, A. (2018). Microinjection to deliver protein, mRNA, and DNA into zygotes of the cnidarian endosymbiosis model *Aiptasia* sp. *Sci. Rep.* 8(1), 1–11. doi:10.1038/s41598-018-34773-1

- Kanehisa, M., Sato, Y., & Morishima, K. (2016). BlastKOALA and GhostKOALA: KEGG tools for functional characterization of genome and metagenome sequences. *J. Mol. Biol.* 428(4), 726–731. doi:10.1016/j.jmb.2015.11.006
- Kawasaki, T., and T. Kawai. (2014). Toll-like receptor signaling pathways. *Front. Immunol.* 5: 1–8. doi:10.3389/fimmu.2014.00461
- Kenny, N. J., Francis, W. R., Rivera-Vicéns, R. E., Juravel, K., de Mendoza, A., Díez-Vives, C., Lister, R., et al. (2020). Tracing animal genomic evolution with the chromosomal-level assembly of the freshwater sponge *Ephydatia muelleri*. *Nat. Commun.* 11(1), 1–11. doi:10.1038/s41467-020-17397-w
- Kitano, H., and K. Oda. (2006). Robustness trade-offs and host-microbial symbiosis in the immune system. *Mol. Syst. Biol.* 2: 1–10. doi:10.1038/msb4100039
- Klimovich, A., Wittlieb, J., & Bosch, T. C. G. (2019). Transgenesis in *Hydra* to characterize gene function and visualize cell behavior. *Nat. Protoc.* 14(7), 2069–2090. doi:10.1038/s41596-019-0173-3
- Knobloch, S., Jóhannsson, R., & Marteinson, V. (2019). Bacterial diversity in the marine sponge *Halichondria panicea* from Icelandic waters and host-specificity of its dominant symbiont “*Candidatus Halichondriabacter symbioticus*.” *FEMS Microbiol. Ecol.* 95(1), 1–13. doi:10.1093/femsec/fiy220
- Knobloch, S., Jóhannsson, R., and Marteinson, V. (2019). Genome analysis of sponge symbiont “*Candidatus Halichondriabacter symbioticus*” shows genomic adaptation to a host-dependent lifestyle. *Environ. Microbiol. [Internet]*. 22, 1462–2920. doi:10.1111/1462-2920.14869
- Koutsouveli, V., Cárdenas, P., Conejero, M., Rapp, H. T., & Riesgo, A. (2020). Reproductive biology of *Geodia* Species (Porifera, Tetractinellida) from Boreo-Arctic North-Atlantic deep-sea sponge grounds. *Front. Mar. Sci.* 7, 1–22. doi:10.3389/fmars.2020.595267
- Koutsouveli, V., Manousaki, T., Riesgo, A., Lagnel, J., Kollias, S., Tsigenopoulos, C. S., Arvanitidis, C., et al. (2020). Gearing up for warmer times: transcriptomic response of *Spongia officinalis* to elevated temperatures reveals recruited mechanisms and potential for resilience. *Front. Mar. Sci.* 6(January), 1–14. doi:10.3389/fmars.2019.00786
- Krasko, A., Gamulin, V., Seack, J., Steffen, R., Schröder, H. C., & Müller, W. E. (1997). Cathepsin, a major protease of the marine sponge *Geodia cydonium*: purification of the enzyme and molecular cloning of cDNA. *Mol Mar Biol Biotechnol*, 6(4), 296-307.
- Kuusksalu, A., A. Pihlak, W. E. G. Müller, and M. Kelve. (1995). The (2'-5')oligoadenylate synthetase is present in the lowest multicellular organisms, the marine sponges: Demonstration of the existence and identification of its reaction products. *Eur. J. Biochem.* 232: 351–357. doi:10.1111/j.1432-1033.1995.351zz.x
- Lam, S. H., Chua, H. L., Gong, Z., Lam, T. J., & Sin, Y. M. (2004). Development and maturation of the immune system in zebrafish, *Danio rerio*: a gene expression profiling, *in situ* hybridization and immunological study. *Dev. Comp. Immunol.* 28(1), 9–28. doi:10.1016/S0145-305X(03)00103-4
- Lange, C., Hemmrich, G., Klostermeier, U. C., López-Quintero, J. A., Miller, D. J., Rahn, T., Weiss, Y., Bosch, T. C. G., & Rosenstiel, P. (2011). Defining the origins of the NOD-like receptor system at the base of animal evolution. *Mol. Biol Evol.* 28(5), 1687–1702. doi:10.1093/molbev/msq349
- Langmead, B., Trapnell, C., Pop, M., & Salzberg, S. L. (2009). Ultrafast and memory-efficient alignment of short DNA sequences to the human genome. *Genome Biol.* 10(3). doi:10.1186/gb-2009-10-3-r25
- Laundon, D., Larson, B. T., McDonald, K., King, N., & Burkhardt, P. (2019). The architecture of cell differentiation in choanoflagellates and sponge choanocytes. *PLoS Biol.* 17(4), e3000226. doi:10.1371/journal.pbio.3000226
- Le Roux, F., & Blokesch, M. (2018). Eco-evolutionary dynamics linked to horizontal gene transfer in *Vibrios*. *Annu. Rev. Microbiol.* 72(1), 89–110. doi:10.1146/annurev-micro-090817-062148
- Levin, R., Grinstein, S., & Canton, J. (2016). The life cycle of phagosomes: formation, maturation, and resolution. *Immunol. Rev.* 273(1), 156–179. doi:10.1111/imr.12439

- Leys, S. P., A. S. Kahn, J. K. H. Fang, T. Kutti, and R. J. Bannister. (2018). Phagocytosis of microbial symbionts balances the carbon and nitrogen budget for the deep-water boreal sponge *Geodia barretti*. *Limnol. Oceanogr.* 63: 187–202. doi:10.1002/lno.10623
- Leys, S. P., and Eerkes-Medrano, D. I. (2006). Feeding in a calcareous sponge: particle uptake by pseudopodia. *Biol. Bull.* 211 (2), 157–171. doi: 10.2307/4134590
- Leys, S. P., and Hill, A. (2012). “The physiology and molecular biology of sponge tissues,” in *Advances in Marine Biology*, 1st ed (Elsevier Ltd), 1–56. doi:10.1016/B978-0-12-394283-8.00001-1
- Leys, S. P., Kahn, A. S., Fang, J. K. H., Kutti, T., and Bannister, R. J. (2018). Phagocytosis of microbial symbionts balances the carbon and nitrogen budget for the deep-water boreal sponge *Geodia barretti*. *Limnol. Oceanogr.* 63 (1), 187–202. doi:10.1002/lno.10623
- Leys, S. P., Yahel, G., Reidenbach, M. A., Tunnicliffe, V., Shavit, U., and Reisswig, H.M. (2011). The sponge pump: The role of current induced flow in the design of the sponge body plan. *PLoS One* 6 (12). doi:10.1371/journal.pone.0027787
- Li, B., & Dewey, C. N. (2014). Assembly of non-unique insertion content using next-generation sequencing. *BMC Bioinformatics.* 12(6), 21–40. doi:10.1201/b16589
- Li, J., Barreda, D. R., Zhang, Y. A., Boshra, H., Gelman, A. E., LaPatra, S., et al. (2006). B lymphocytes from early vertebrates have potent phagocytic and microbicidal abilities. *Nat. Immunol.* 7 (10), 1116–1124. doi:10.1038/ni1389
- Li, J., Chai, Q. Y., & Liu, C. H. (2016). The ubiquitin system: a critical regulator of innate immunity and pathogen-host interactions. *Cell. Mol. Immunol.* 13(5), 560–576. doi:10.1038/cmi.2016.40
- Liang, S. C., Hartwig, B., Perera, P., Mora-García, S., de Leau, E., Thornton, H., de Alves, F. L., Rapsilber, J., et al. (2015). Kicking against the PRCs – a domesticated transposase antagonises silencing mediated by polycomb group proteins and is an accessory component of polycomb repressive complex 2. *PLoS Genet.* 11(12), 1–26. doi:10.1371/journal.pgen.1005660
- Lim, J. J., Grinstein, S., and Roth, Z. (2017). Diversity and versatility of phagocytosis: Roles in innate immunity, tissue remodeling, and homeostasis. *Front. Cell Infect. Microbiol.* 7, 1–12. doi:10.3389/fcimb.2017.00191
- Limoges, M. A., Cloutier, M., Nandi, M., Ilangumaran, S., & Ramanathan, S. (2021). The GIMAP family proteins: an incomplete puzzle. *Front. Immunol.* 12(May), 1–15. doi:10.3389/fimmu.2021.679739
- Lindner, B., Burkard, T., and Schuler, M. (2020). Phagocytosis assays with different pH-sensitive fluorescent particles and various readouts. *Biotechniques* 68 (5), 245–250. doi:10.2144/btn-2020-0003
- Liu, C., Wang, T., Zhang, W., & Li, X. (2008). Computational identification and analysis of immune-associated nucleotide gene family in *Arabidopsis thaliana*. *J. Plant Physiol.* 165(7), 777–787. doi:10.1016/j.jplph.2007.06.002
- Lowin, B., M. Hahne, C. Mattmann, and J. Tschopp. (1994). Cytolytic T-cell cytotoxicity is mediated through perforin and Fas lytic pathways. *Nature* 370: 650–652. doi:10.1038/370650a0
- Lüskow, F., Riisgård, H. U., Solovyeva, V., and Brewer, J. R. (2019). Seasonal changes in bacteria and phytoplankton biomass control the condition index of the demosponge *Halichondria panicea* in temperate Danish waters. *Mar. Ecol. Prog. Ser.* 608, 119–132. doi:10.3354/meps12785
- MacKnight, N. J., Dimos, B. A., Beavers, K. M., Muller, E. M., Brandt, M. E., & Mydlarz, L. D. (2022). Disease resistance in coral is mediated by distinct adaptive and plastic gene expression profiles. *Sci. Adv.* 8(39), 1–15. doi:10.1126/sciadv.abo6153
- Magor, B. G., and K. E. Magor. (2001). Evolution of effectors and receptors of innate immunity. *Dev. Comp. Immunol.* 25: 651–682. doi:10.1016/S0145-305X(01)00029-5
- Malcolm, H., & April, H. (2012). The magnesium inhibition and arrested phagosome hypotheses: new perspectives on the evolution and ecology of *Symbiodinium* symbioses. *Biol. Rev.* 87(4), 804–821. doi:10.1111/j.1469-185X.2012.00223.x
- Maldonado, M., Ribes, M., & van Duyl, F. C. (2012). Nutrient fluxes through sponges. biology, budgets, and ecological implications. *Adv. Mar. Biol.* 62, 113–182. doi:10.1016/B978-0-12-394283-8.00003-5

- Maldonado, M., Zhang, X., Cao, X., Xue, L., Cao, H., and Zhang, W. (2010). Selective feeding by sponges on pathogenic microbes: A reassessment of potential for abatement of microbial pollution. *Mar. Ecol. Prog. Ser.* 403, 75–89. doi:10.3354/meps08411
- Mandujano-Tinoco, E. A., Sultan, E., Ottolenghi, A., Gershoni-Yahalom, O., & Rosental, B. (2021). Evolution of cellular immunity effector cells; perspective on cytotoxic and phagocytic cellular lineages. *Cells.* 10(8). doi:10.3390/cells10081853
- Mangel, A., J. Leitao, R. Batel, H. Zimmermann, W. E. G. Müller, and H. C. Schröder. (1995). Purification and characterization of two exopolyphosphatases from the marine sponge *Tethya lyncurium*. *Eur. J. Biochem.* 1245: 17–28. doi:10.1016/0304-4165(95)00067-L
- Marulanda-Gómez A.M., Bayer K, Pita L and Hentschel U (2023) A novel *in-vivo* phagocytosis assay to gain cellular insights on sponge-microbe interactions. *Front. Mar. Sci.* 10. doi:10.3389/fmars.2023.117614
- McCutcheon, J. P. (2021). The genomics and cell biology of host-beneficial intracellular infections. *Annu. Rev. Cell Dev. Biol.* 37(1), 115–142. doi:10.1146/annurev-cellbio-120219-024122
- McDowell, I. C., Modak, T. H., Lane, C. E., & Gómez-Chiarri, M. (2016). Multi-species protein similarity clustering reveals novel expanded immune gene families in the eastern oyster *Crassostrea virginica*. *Fish Shellfish Immunol.* 53, 13-23. doi:10.1016/j.fsi.2016.03.157
- McFall-Ngai, M. (2007). Adaptive immunity: Care for the community. *Nature* 445: 153. doi:10.1038/445153a
- McFall-Ngai, M., Hadfield, M. G., Bosch, T. C. G., Carey, H. V, Domazet-Lošo, T., Douglas, A. E., Dubilier, N., et al. (2013). Animals in a bacterial world, a new imperative for the life sciences. *PNAS.* 110 (9), 3229–3236. doi:10.1073/pnas.1218525110
- McMurray, S. E., Johnson, Z. I., Hunt, D. E., Pawlik, J. R., and Finelli, C. M. (2016). Selective feeding by the giant barrel sponge enhances foraging efficiency. *Limnol. Oceanogr.* 61 (4), 1271–1286. doi:10.1002/lno.10287
- Medina, M., Sharp, V., Ohdera, A., Bellantuono, A., Dalrymple, J., Gamero-Mora, E., Steinworth, B., Hofmann, et al. (2021). The upside-down jellyfish *Cassiopea xamachana* as an emerging model system to study cnidarian-algal symbiosis. *Handbook of Marine Model Organisms in Experimental Biology: Established and Emerging* (CRC Press), 149–171. doi:10.1201/9781003217503-9
- Menzel, P., & Krogh, A. (2015). Fast and sensitive taxonomic classification for metagenomics with Kaiju. *Nat. Commun.* 7(1), 11257. doi:10.1101/031229
- Metchnikoff, E. (1893). Lectures on the comparative pathology of inflammation.
- Mohamed, A. R., Andrade, N., Moya, A., Chan, C. X., Negri, A. P., Bourne, D. G., Ying, H., Ball, E. E., & Miller, D. J. (2020). Dual RNA-sequencing analyses of a coral and its native symbiont during the establishment of symbiosis. *Mol. Ecol.* 29(20), 3921–3937. doi:10.1111/mec.15612
- Moitinho-Silva, L., Nielsen, S., Amir, A., Gonzalez, A., Ackermann, G. L., Cerrano, C., et al. (2017). The sponge microbiome project. *Gigascience* 6 (10), 1–7. doi:10.1093/gigascience/gix077
- Moitinho-Silva, L., Steinert, G., Nielsen, S., Hardoim, C. C. P., Wu, Y. C., McCormack, G. P., López-Legentil, S., Marchant, R., Webster, N., Thomas, T., & Hentschel, U. (2017). Predicting the HMA-LMA status in marine sponges by machine learning. *Front. Microbiol.* 8(May), 1–14. doi:10.3389/fmicb.2017.00752
- Moreno-Pino, M., Cristi, A., Gillooly, J. F., & Trefault, N. (2020). Characterizing the microbiomes of Antarctic sponges: a functional metagenomic approach. *Sci. Rep.* 10(1), 1–12. doi:10.1038/s41598-020-57464-2
- Morganti, T. M., Ribes, M., Yahel, G., & Coma, R. (2019). Size is the major determinant of pumping rates in marine sponges. *Front. Physiol.* 10. doi:10.3389/fphys.2019.01474
- Moscona, A.A. (1968). Cell aggregation: Properties of specific cell-ligands and their role in the formation of multicellular systems. *Dev. Biol.* 18, 250–277. doi:10.1016/0012-1606(68)90035-3
- Mueller, B., De Goeij, J. M., Vermeij, M. J. A., Mulders, Y., van der Ent, E., Ribes, M., et al. (2014). Natural diet of coral-excavating sponges consists mainly of dissolved organic carbon (DOC). *PLoS One* 9 (2). doi:10.1371/journal.pone.0090152

- Müller, W. E. G., and I. M. Müller. (2003). Origin of the metazoan immune system: Identification of the molecules and their functions in sponges. *Integr. Comp. Biol.* 292: 281–292. doi:10.1093/icb/43.2.281
- Müller, J. (2022). Assessing bacterial carbon uptake and respiration rates of the Baltic Sea sponge *Halichondria panicea* : comparing natural vs. aquaria conditions. Master thesis, University of Rostock. <https://oceanrep.geomar.de/id/eprint/57137>
- Musser, J. M., Schippers, K. J., Nickel, M., Mizzon, G., Kohn, A. B., Pape, C., et al. (2021). Profiling cellular diversity in sponges informs animal cell type and nervous system evolution. *Science* 374 (6568), 717–723. doi:10.1126/science.abj2949
- Neubauer, E. F., Poole, A. Z., Weis, V. M., & Davy, S. K. (2016). The scavenger receptor repertoire in six cnidarian species and its putative role in cnidarian-dinoflagellate symbiosis. *PeerJ.* 4, e2692. doi:10.7717/peerj.2692
- Nguyen, M. T. H. D., Liu, M., and Thomas, T. (2014). Ankyrin-repeat proteins from sponge symbionts modulate amoebal phagocytosis. *Mol. Ecol.* 23 (6), 1635–1645. doi:10.1111/mec.12384
- Nyholm, S. V., and Graf, J. (2012). Knowing your friends: Invertebrate innate immunity fosters beneficial bacterial symbioses. *Nat. Rev. Microbiol.* 10 (12), 815–827. doi:10.1038/nrmicro2894
- Nyholm, S. V., and M. J. McFall-Ngai. (2021). A lasting symbiosis: How the Hawaiian bobtail squid finds and keeps its bioluminescent bacterial partner. *Nat. Rev. Microbiol.* 10. doi:10.1038/s41579-021-00567-y
- Nyholm, S. V., Stewart, J. J., Ruby, E. G., and McFall-Ngai, M. J. (2009). Recognition between symbiotic *Vibrio fischeri* and the haemocytes of *Euprymna scolopes*. *Environ. Microbiol.* 11 (2), 483–493. doi:10.1111/j.1462-2920.2008.01788.x
- Ohtsubo, M., Yasunaga, S., Ohno, Y., Tsumura, M., Okada, S., Ishikawa, N., Shirao, K., Kikuchi, A., et al. (2008). Polycomb-group complex 1 acts as an E3 ubiquitin ligase for Geminin to sustain hematopoietic stem cell activity. *PNAS.* 105(30), 10396–10401. doi:10.1073/pnas.0800672105
- Omotade, T. O., & Roy, C. R. (2019). Manipulation of host cell organelles by intracellular pathogens. *Microbiol. Spectr.* 7(2). doi:10.1128/microbiolspec.BAI-0022-2019
- Pahler, S., B. Blumbach, I. Müller, and W. E. G. Müller. (1998). Putative multi adhesive protein from the marine sponge *Geodia cydonium*: Cloning of the cDNA encoding a fibronectin-, an SRCR-, and a complement control protein module. *J. Exp. Zool.* 282: 332–343. doi:10.1002/(SICI)1097-010X(19981015)282:3<332::AID-JEZ6>3.0.CO;2-N
- Palmer, C. V. (2018). Immunity and the coral crisis. *Commun. Biol.* 1(1), 1–7. doi:10.1038/s42003-018-0097-4
- Paludan, S. R., Pradeu, T., Masters, S. L., & Mogensen, T. H. (2021). Constitutive immune mechanisms: mediators of host defence and immune regulation. *Nat. Rev. Immunol.* 21(3), 137–150. doi:10.1038/s41577-020-0391-5
- Pan, X., Lührmann, A., Satoh, A., Laskowski-Arce, M. A., and Roy, C. R. (2008). Ankyrin repeat proteins comprise a diverse family of bacterial type IV effectors. *Science* 320 (5883), 1651–1654. doi:10.1126/science.1158160
- Pan, Y., Cai, W., Huang, J., Cheng, A., Wang, M., Yin, Z., & Jia, R. (2022). Pyroptosis in development, inflammation and disease. *Front. Immunol.* 13(September), 1–17. doi:10.3389/fimmu.2022.991044
- Pancer, Z., J. Münkner, I. Müller, and W. E. G. Müller. (1997). A novel member of an ancient superfamily: Sponge (*Geodia cydonium*, Porifera) putative protein that features scavenger receptor cysteine-rich repeats. *Gene* 193: 211–218. doi:10.1016/S0378-1119(97)00135-2
- Pankey, M., Plachetzki, D. C., Macartney, K. J., Gastaldi, M., Slattery, M., Gochfeld, D. J., & Lesser, M. P. (2022). Cophylogeny and convergence shape holobiont evolution in sponge–microbe symbioses. *Nat. Ecol. Evo.* 6(6), 750–762. doi:10.1038/s41559-022-01712-3
- Park, J. E., Jardine, L., Gottgens, B., Teichmann, S. A., & Haniffa, M. (2020). Prenatal development of human immunity. *Science.* 368(6491), 600–603. doi:10.1126/science.aaz9330
- Pile, A. J., and Young, C. M. (2006). The natural diet of a hexactinellid sponge: Benthic–pelagic coupling

- in a deep-sea microbial food web. *Deep Res. Part I Oceanogr. Res. Pap.* 53 (7), 1148–1156. doi:10.1016/j.dsr.2006.03.008
- Pita, L., Fraune, S., and Hentschel, U. (2016). Emerging sponge models of animal-microbe symbioses. *Front. Microbiol.* 7, 1–8. doi:10.3389/fmicb.2016.02102
- Pita, L., Rix, L., Slaby, B. M., Franke, A., & Hentschel, U. (2018b). The sponge holobiont in a changing ocean: from microbes to ecosystems. *Microbiome* 6(1). doi:10.1186/s40168-018-0428-1
- Pita, L., Hoepfner, M. P., Ribes, M., and Hentschel, U. (2018b). Differential expression of immune receptors in two marine sponges upon exposure to microbial-associated molecular patterns. *Sci. Rep.* 8 (1), 1–15. doi:10.1038/s41598-018-34330-w
- Pomponi, S. A. (2006). Biology of the porifera: cell culture. *Can. J. Zool.* 84 (2), 167–174. doi:10.1139/z05-188
- Posadas, N., Baquiran, J. I. P., Nada, M. A. L., Kelly, M., & Conaco, C. (2021). Microbiome diversity and host immune functions influence survivorship of sponge holobionts under future ocean conditions. *ISME J.* 16(1), 58–67. doi:10.1038/s41396-021-01050-5
- Redmond, A. K., & McLysaght, A. (2021). Evidence for sponges as sister to all other animals from partitioned phylogenomics with mixture models and recoding. *Nat. Commun.* 12(1). doi:10.1038/s41467-021-22074-7
- Reiswig, H. M. (1971). Particle feeding in natural populations of three marine demosponges. *Biol. Bull.* 141 (3), 568–591. doi:10.2307/1540270
- Revilla-I-Domingo, R., Schmidt, C., Zifko, C., & Raible, F. (2018). Establishment of transgenesis in the demosponge *Suberites domuncula*. *Genetics.* 210(2), 435–443. doi:10.1534/genetics.118.301121
- Ribes, M., Coma, R., and Gili, J. M. (1999). Natural diet and grazing rate of the temperate sponge *Dysidea avara* (Demospongiae, Dendroceratida) throughout an annual cycle. *Mar. Ecol. Prog. Ser.* 176, 179–190. doi:10.3354/meps176179
- Riesgo, A., N. Farrar, P. J. Windsor, G. Giribet, and S. P. Leys. (2014). The analysis of eight transcriptomes from all poriferan classes reveals surprising genetic complexity in sponges. *Mol. Biol. Evol.* 31: 1102–1120. doi:10.1093/molbev/msu057
- Riesgo, A., Santodomingo, N., Koutsouveli, V., Kumala, L., Leger, M. M., Leys, S. P., & Funch, P. (2022). Molecular machineries of ciliogenesis, cell survival, and vasculogenesis are differentially expressed during regeneration in explants of the demosponge *Halichondria panicea*. *BMC Genom.* 23(1). doi: 10.1186/s12864-022-09035-0
- Riisgård, H. U., Kumala, L., Charitonidou, K. (2016). Using the F/R-ratio for an evaluation of the ability of the demosponge *Halichondria panicea* to nourish solely on phytoplankton versus free-living bacteria in the sea. *Mar. Biol. Res.* 12 (9), 907–916. doi:10.1080/17451000.2016.1206941
- Riisgård, H. U., Kealy, R. A., Goldstein, J., Brewer, J. R., Solovyeva, V., & Funch, P. (2023). Choanocyte dimensions and pumping rates in the demosponge *Halichondria panicea*. *J. Exp. Mar. Bio. Ecol.* 569, 151957. doi: 10.1016/j.jembe.2023.151957.
- Robertson, L. M., Hamel, J. F., & Mercier, A. (2017). Feeding in deep-sea demosponges: influence of abiotic and biotic factors. *Deep-Sea Res. Part I: Oceanogr. Res. Pap.* 127, 49–56. doi:10.1016/j.dsr.2017.07.006
- Robinson, M. D., McCarthy, D. J., & Smyth, G. K. (2009). edgeR: a Bioconductor package for differential expression analysis of digital gene expression data. *Bioinform.* 26(1), 139–140. doi:10.1093/bioinformatics/btp616
- Rosales, C., Uribe-Querol, E. (2017). Phagocytosis: A fundamental process in immunity. *BioMed. Res. Int.* 2017, 1–18. doi:10.1155/2017/9042851
- Rosenberg, E., & Zilber-Rosenberg, I. (2016). Microbes drive evolution of animals and plants: the hologenome concept. *MBio*, 7(2). doi:10.1128/mBio.01395-15
- Rosenberg, E., & Zilber-Rosenberg, I. (2018). The hologenome concept of evolution after 10 years. *Microbiome.* 6(1), 78. doi:10.1186/s40168-018-0457-9



- Rosenstiel, P., E. E. R. Philipp, S. Schreiber, and T. C. G. Bosch. (2009). Evolution and function of innate immune receptors - Insights from marine invertebrates. *J. Innate Immun.* 1: 291–300. doi:10.1159/000211193
- Rosental, B., Kozhekbaeva, Z., Fernhoff, N., Tsai, J. M., and Traylor- Knowles, N. (2017). Coral cell separation and isolation by fluorescence-activated cell sorting (FACS). *BMC Cell Biol.* 18 (1), 1–12. doi:10.1186/s12860-017-0146-8
- Roth, O., & Kurtz, J. (2009). Phagocytosis mediates specificity in the immune defence of an invertebrate, the woodlouse *Porcellio scaber* (Crustacea: Isopoda). *Dev. Comp. Immunol.* 33(11), 1151–1155. doi:10.1016/j.dci.2009.04.005
- Rottmann, M., Schröder, H. C., Gramzow, M., Renneisen, K., Kurelec, B., Dorn, A., et al. (1987). Specific phosphorylation of proteins in pore complex-laminae from the sponge *Geodia cydonium* by the homologous aggregation factor and phorbol ester. Role of protein kinase C in the phosphorylation of DNA topoisomerase II. *EMBO J.* 6 (13), 3939–3944. doi:10.1002/j.1460-2075.1987.tb02735.x
- Roughgarden, J., Gilbert, S. F., Rosenberg, E., Lloyd, E. A., Gilbert, S. F., & Lloyd, E. A. (2018). Holobionts as units of selection and a model of their population dynamics and evolution. *Biol. Theory.* 13(1), 44–65. doi:10.1007/s13752-017-0287-1
- Ryu, T., L. Seridi, L. Moitinho-Silva, et al. (2016). Hologenome analysis of two marine sponges with different microbiomes. *BMC Genom.* 17: 158. doi:10.1186/s12864-016-2501-0
- Saco, A., Rey-Campos, M., Novoa, B., & Figueras, A. (2020). Transcriptomic response of mussel gills after a *Vibrio splendidus* infection demonstrates their role in the immune response. *Front. Immunol.* 11(December), 1–18. doi:10.3389/fimmu.2020.615580
- Saito, Y. (2013). Self and nonself recognition in a marine sponge, *Halichondria japonica* (Demospongiae). *Zool. Sci.* 30(8), 651–657. doi:10.2108/zsj.30.651
- Sarrias, M. R., Gronlund, J., Padilla, O., Madsen, J., Holmskov, U., and Lozano, F. (2004). The Scavenger Receptor Cysteine-Rich (SRCR) Domain: an ancient and highly conserved protein module of the innate immune system. *Critical Reviews in Immunology* 24(1, Begell House), 1–38. doi:10.1615/critrevimmunol.v24.i1.10
- Sattler, N., Monroy, R., and Soldati, T. (2013). Quantitative analysis of phagocytosis and phagosome maturation. *Methods Mol. Biol.* 983, 383–402. doi:10.1007/978-1-62703-302-2\_21
- Scheffers, S. R., Nieuwland, G., Bak, R. P. M., and Van Duyl, F. C. (2004). Removal of bacteria and nutrient dynamics within the coral reef framework of Curaçao (Netherlands Antilles). *Coral Reefs.* 23 (3), 413–422. doi:10.1007/s00338-004-0400-3
- Schippers, K. J., D. E. Martens, S. A. Pomponi, and R. H. Wijffels. (2011). Cell cycle analysis of primary sponge cell cultures. *Vitr. Cell. Dev. Biol. Anim.* 47(4), 302–311. doi:10.1007/s11626-011-9391-x
- Schmittmann, L., Jahn, M. T., Pita, L., & Hentschel, U. (2020). Decoding cellular dialogues between sponges, bacteria, and phages. In *Cellular dialogues in the holobiont* (pp. 49-63). CRC Press. doi: 10.1201/9780429277375
- Schmittmann, L., Franzenburg, S., and Pita, L. (2021). Individuality in the immune repertoire and induced response of the sponge *Halichondria panicea*. *Front. Immunol.* 12, 1–13. doi:10.3389/fimmu.2021.689051
- Schmittmann, L. (2021). Establishing the breadcrumb sponge *Halichondria panicea* as an experimental model for sponge symbioses. PhD thesis, Christian Albrechts Universität zu Kiel, Kiel, Germany. <https://oceanrep.geomar.de/id/eprint/57127>
- Schmittmann, L., Rahn, T., Busch, K., Fraune, S., Pita, L., and Hentschel, U. (2022). Stability of a dominant sponge-symbiont in spite of antibiotic-induced microbiome disturbance. *Environ. Microbiol.* 24 (12), 6392–6410. doi:10.1111/1462-2920.16249
- Schmitz, A., Anselme, C., Ravallec, M., Rebuf, C., Simon, J. C., Gatti, J. L., & Poirié, M. (2012). The cellular immune response of the pea aphid to foreign intrusion and symbiotic challenge. *PLoS One* 7(7). doi:10.1371/journal.pone.0042114
- Schneider, M., Zimmermann, A. G., Roberts, R. A., Zhang, L., Karen, V., Rahman, A. H., Conti, B. J., et

- al.. (2013). The innate immune sensor NLRC3 attenuates Toll-like receptor signaling via modification of the signaling adaptor TRAF6 and transcription factor NF- $\kappa$ B. *Nat. Immunol.* 13(9), 823–831. doi:10.1038/ni.2378
- Schröder, H. C., H. Ushijima, A. Krasko, V. Gamulin, N. L. Thakur, B. Diehl-Seifert, I. M. Müller, and W. E. G. Müller. (2003). Emergence and disappearance of an immune molecule, an antimicrobial lectin, in basal metazoa. A tachylectin-related protein in the sponge *Suberites domuncula*. *J. Biol. Chem.* 278(35), 32810–7. doi:10.1074/jbc.M304116200
- Sebé-Pedrós, A., Chomsky, E., Pang, K., Lara-Astiaso, D., Gaiti, F., Mukamel, Z., et al. (2018). Early metazoan cell type diversity and the evolution of multicellular gene regulation. *Nat. Ecol. Evol.* 2 (7), 1176–1188. doi:10.1038/s41559-018-0575-6
- Seneca, F., Davtian, D., Boyer, L., & Czerucka, D. (2020). Gene expression kinetics of *Exaiptasia pallida* innate immune response to *Vibrio parahaemolyticus* infection. *BMC Genom.* 21(768), 1–16. doi:10.1186/s12864-020-07140-6
- Seoane, P. I., & May, R. C. (2020). Vomocytosis: what we know so far. *Cell. Microbiol.* 22(2), 1–6. doi:10.1111/cmi.13145
- Siegl, A., Kamke, J., Hochmuth, T., Piel, J., Richter, M., Liang, C., et al. (2011). Single-cell genomics reveals the lifestyle of Poribacteria, a candidate phylum symbiotically associated with marine sponges. *ISME J.* 5 (1), 61–70. doi:10.1038/ismej.2010.95
- Silver, A. C., Kikuchi, Y., Fadl, A. A., Sha, J., Chopra, A. K., and Graf, J. (2007). Interaction between innate immune cells and a bacterial type III secretion system in mutualistic and pathogenic associations. *Proc. Natl. Acad. Sci. U.S.A.* 104 (22), 9481–9486. doi:10.1073/pnas.0700286104
- Simão, F. A., Waterhouse, R. M., Ioannidis, P., Kriventseva, E. V., & Zdobnov, E. M. (2015). BUSCO: assessing genome assembly and annotation completeness with single-copy orthologs. *Bioinform.* 31(19), 3210–3212. doi:10.1093/bioinformatics/btv351
- Simpson, T. L. (1984). *The cell biology of sponges* (New York: Springer Verlag). Available at: <http://journal.um-surabaya.ac.id/index.php/JKM/article/view/2203>.
- Slaby, B. M., Hackl, T., Horn, H., Bayer, K., & Hentschel, U. (2017). Metagenomic binning of a marine sponge microbiome reveals unity in defense but metabolic specialization. *ISME J.* 11(11), 2465–2478. doi:10.1038/ismej.2017.101
- Smith, L. C., Arizza, V., Barela Hudgell, M. A., Barone, G., Bodnar, A. G., Buckley, K. M., et al. (2018). Echinodermata: the complex immune system in echinoderms. *Adv. Comp. Immunol.* 409-501. doi:10.1007/978-3-319-76768-0\_32
- Smith, L.C., and W.H. Hildemann. (1986). Allogeneic cell interactions during graft rejection in *Callispongia diffusa* (Porifera, Demospongia); a study with monoclonal antibodies. *Proc. R. Soc. Lond. B. Biol. Sci.* 226, 465–477. doi:10.1098/rspb.1986.0004
- Smith-Unna, R., Bournsnell, C., Patro, R., Hibberd, J. M., & Kelly, S. (2016). TransRate: reference-free quality assessment of de novo transcriptome assemblies. *Genome Res.* 26(8), 1134–1144. doi:10.1101/gr.196469.115
- Snyder, G. A., Eliachar, S., Connelly, M. T., Talice, S., Hadad, U., Gershoni-Yahalom, O., et al. (2021). Functional characterization of hexacorallia phagocytic cells. *Front Immunol* 12, 1–13. doi:10.3389/fimmu.2021.662803
- Sokolova, A. M., Pozdnyakov, I. R., Ereskovsky, A. V., & Karpov, S. A. (2019). Kinetid structure in larval and adult stages of the demosponges *Haliclona aquaeductus* (Haplosclerida) and *Halichondria panicea* (Suberitida). *Zoomorphology* 138(2), 171–184. doi: 10.1007/s00435-019-00437-5
- Song, N., & Li, T. (2018). Regulation of NLRP3 inflammasome by phosphorylation. *Front. Immunol.* 9, 1–9. doi:10.3389/fimmu.2018.02305
- Srivastava, M., O. Simakov, J. Chapman, et al. (2010). The *Amphimedon queenslandica* genome and the evolution of animal complexity. *Nature* 466 (7307), 720–726. doi:10.1038/nature09201
- Steindler, L., S. Schuster, M. Ilan, A. Avni, C. Cerrano, and S. Beer. (2007). Differential gene expression in a marine sponge in relation to its symbiotic state. *Mar. Biotechnol.* 9:(5), 543–9. doi:10.1007/s10126-007-9024-2

- Steinmetz, P. R. H. (2019). A non-bilaterian perspective on the development and evolution of animal digestive systems. *Cell Tissue Res.* 377 (3), 321–339. doi:10.1007/s00441-019-03075-x
- Stévenne, C., Micha, M., Plumier, J.-C., & Roberty, S. (2021). Corals and sponges under the light of the holobiont concept: how microbiomes underpin our understanding of marine ecosystems. *Front. Mar. Sci.* 8. doi:10.3389/fmars.2021.698853
- Sun, D., Xu, J., Zhang, W., & Song, C. (2022). Negative regulator NLRC3 : its potential role and regulatory mechanism in immune response and immune-related diseases. *Front. Immunol.* 13, 1–13. doi:10.3389/fimmu.2022.1012459
- Takeda, K. (2005). Evolution and integration of innate immune recognition systems: The Toll-like receptors. *J. Endotoxin Res.* 11(1), 51–55. doi:10.1179/096805105225006687
- Takemura, A. F., Chien, D. M., & Polz, M. F. (2014). Associations and dynamics of Vibrionaceae in the environment, from the genus to the population level. *Front. Microbiol.* 5, 1–26. doi:10.3389/fmicb.2014.00038
- Tame, A., Maruyama, T., & Yoshida, T. (2022). Phagocytosis of exogenous bacteria by gill epithelial cells in the deep-sea symbiotic mussel *Bathymodiolus japonicus*. *R. Soc. Open Sci.* 9(5), 211384. doi:10.1098/rsos.211384
- Tame, A., Maruyama, T., Ikuta, T., Chikaraishi, Y., Ogawa, N. O., Tsuchiya, M., Takishita, K., et al. (2023). mTORC1 regulates phagosome digestion of symbiotic bacteria for intracellular nutritional symbiosis in a deep-sea mussel. *Sci. Adv.* (34), eadg8364. doi:10.1126/sciadv.adg8364
- Tartaro, K., Vanvolkenburg, M., Wilkie, D., Coskran, T. M., Kreeger, J. M., Kawabata, T.T., et al. (2015). Development of a fluorescence-based in vivo phagocytosis assay to measure mononuclear phagocyte system function in the rat. *J. Immunotoxicol.* 12 (3), 239–246. doi:10.3109/1547691X.2014.934976
- Tetreau, G., Pinaud, S., Portet, A., Galinier, R., Gourbal, B., & Duval, D. (2017). Specific pathogen recognition by multiple innate immune sensors in an invertebrate. *Front. Immunol.* 8, 1249. doi:10.3389/fimmu.2017.01249
- Thakur, N. L., S. Perović-Ottstadt, R. Batel, M. Korzhev, B. Diehl-Seifert, I. M. Müller, and W. E. G. Müller. (2005). Innate immune defense of the sponge *Suberites domuncula* against gram-positive bacteria: Induction of lysozyme and AdaPTin. *Mar. Biol.* 146(2), 271–282. doi:10.1007/s00227-004-1438-z
- Thakur, N. L., U. Hentschel, A. Krasko, C. T. Pabel, A. C. Anil, and W. E. G. Müller. (2003). Antibacterial activity of the sponge *Suberites domuncula* and its primmorphs: Potential basis for epibacterial chemical defense. *Aquat. Microb. Ecol.* 31, 77–83. doi:10.3354/ame031077
- Thomas, T., D. Rusch, M. Z. DeMaere, et al. (2010). Functional genomic signatures of sponge bacteria reveal unique and shared features of symbiosis. *ISME J.* 4(12), 1557–67. doi:10.1038/ismej.2010.74
- Thomas, T., Moitinho-Silva, L., Lurgi, M., Björk, J. R., Easson, C., Astudillo-García, C., et al. (2016). Diversity, structure and convergent evolution of the global sponge microbiome. *Nat. Commun.* 7, 1–12. doi:10.1038/ncomms11870
- Thompson, A., Bench, S., Carter, B., & Zehr, J. (2013). Coupling FACS and genomic methods for the characterization of uncultivated symbionts. *Methods in Enzymology* (Elsevier), 45–60. doi:10.1016/b978-0-12-407863-5.00003-4
- Turner, E. C. (2021). Possible poriferan body fossils in early Neoproterozoic microbial reefs. *Nature.* 596(7870), 87–91. doi:10.1038/s41586-021-03773-z
- Turon, X., Galera, J., and Uriz, M. J. (1997). Clearance rates and aquiferous systems in two sponges with contrasting life-history strategies. *J. Exp. Zool.* 278 (1), 22–36. doi:10.1002/(SICI)1097-010X(19970501)278:1<22::AID-JEZ3>3.0.CO;2-8
- Tyanova, S., Temu, T., Sinitcyn, P. et al. (2016). The Perseus computational platform for comprehensive analysis of (prote)omics data. *Nat. Methods* 13(9), 731–740. doi:10.1038/nmeth.3901
- Uchimura, T., Oyama, Y., Deng, M., Guo, H., Wilson, J. E., Rampanelli, E., Cook, K. D., et al. (2018). The innate immune sensor NLRC3 acts as a rheostat that fine-tunes T cell responses in infection and autoimmunity. *Immunity.* 49(6), 1049-1061.e6. doi:10.1016/j.immuni.2018.10.008

- Uribe-Quero, E., & Rosales, C. (2017). Control of phagocytosis by microbial pathogens. *Front. Immunol.* 8, 1–23. doi:10.3389/fimmu.2017.01368
- Uribe-Querol, E., and Rosales, C. (2020). Phagocytosis: our current understanding of a universal biological process. *Front. Immunol.* 11, 1–13. doi:10.3389/fimmu.2020.01066
- van de Water, J. A. J. M., Chaib De Mares, M., Dixon, G. B., Raina, J. B., Willis, B. L., Bourne, D. G., & van Oppen, M. J. H. (2018). Antimicrobial and stress responses to increased temperature and bacterial pathogen challenge in the holobiont of a reef-building coral. *Mol. Ecol.* 27(4), 1065–1080. doi:10.1111/mec.14489
- Vethaak, A. D., Cronie, R. J. A., and van Soest, R. W. M. (1982). Ecology and distribution of two sympatric, closely related sponge species, *Halichondria panicea* (Pallas 1766) and *H. bowerbanki* (Burton 1930) (Porifera, demospongiae), with remarks on their speciation. *Bijdr tot Dierkd.* 52 (2), 82–102. doi:10.1163/26660644-05202002
- Villares, M., Berthelet, J., & Weitzman, J. B. (2020). The clever strategies used by intracellular parasites to hijack host gene expression. *Semin. Immunopathol.* 42(2), 215–226. doi:10.1007/s00281-020-00779-z
- Walle, L. V., & Lamkanfi, M. (2016). Pyroptosis. *Curr.Biol.* 26(13), R568–R572. doi:10.1016/j.cub.2016.02.019
- Webster, N. S., & Thomas, T. (2016). The sponge hologenome. *MBio.* 7(2), 1–14. doi:10.1128/mBio.00135-16
- Wehrl, M. (2006). *Bakterielle Aufnahme, Selektivität und interne Prozessierung bei marinen Schwämmen (Porifera)* (Doctoral dissertation, Universität Würzburg).
- Wehrl, M., Steinert, M., and Hentschel, U. (2007). Bacterial uptake by the marine sponge *Aplysina aerophoba*. *Microb. Ecol.* 53 (2), 355–365. doi:10.1007/s00248-006-9090-4
- Wein, T., Romero Picazo, D., Blow, F., Woehle, C., Jami, E., Reusch, T. B. H., Martin, W. F., & Dagan, T. (2019). Currency, exchange, and inheritance in the evolution of symbiosis. *Trends Microbiol.* 27(10), 836–849. doi:10.1016/j.tim.2019.05.010
- Weiss, Y., Forêt, S., Hayward, D. C., Ainsworth, T., King, R., Ball, E. E., & Miller, D. J. (2013). The acute transcriptional response of the coral *Acropora millepora* to immune challenge: expression of GiMAP/IAN genes links the innate immune responses of corals with those of mammals and plants. *BMC genom.* 14(1), 1-13. doi:10.1186/1471-2164-14-400
- Weissenfels, N. (1976). Bau und Funktion des Süßwasserschwamms *Ephydatia fluviatilis* L. (Porifera) - III. Nahrungsaufnahme, Verdauung und Defäkation. *Zoomorphologie* 85(2), 73–88. doi:10.1007/BF00995405
- Weisz, J. B., Lindquist, N., & Martens, C. S. (2008). Do associated microbial abundances impact marine demosponge pumping rates and tissue densities? *Oecologia* 155(2), 367–376. doi:10.1007/s00442-007-0910-0
- Wiedenmann, J., D’Angelo, C., Mardones, M. L., Moore, S., Benkwitt, C. E., Graham, N. A. J., Hambach, B., Wilson, et al. (2023). Reef-building corals farm and feed on their photosynthetic symbionts. *Nature* 620(7976), 1018–1024. doi:10.1038/s41586-023-06442-5
- Wiens, M., M. Korzhev, A. Krasko, et al. (2005). Innate immune defense of the sponge *Suberites domuncula* against bacteria involves a MyD88-dependent signaling pathway: induction of a perforin-like molecule. *J. Biol. Chem.* 280(30), 27949–27959. doi:10.1074/jbc.M504049200
- Wiens, M., M. Korzhev, S. Perovic-Ottstadt, B. Luthringer, D. Brandt, S. Klein, and W. E. G. Müller. (2007). Toll-like receptors are part of the innate immune defense system of sponges (Demospongiae: Porifera). *Mol. Biol. Evol.* 24(3), 792–804. doi:10.1093/molbev/msl208
- Wilkinson, C. R. (1984). Immunological evidence for the Precambrian origin of bacterial symbioses in marine sponges. *Proc. R. Soc. London - Biol. Sci.* 220(1221), 509–517. doi:10.1098/rspb.1984.0017
- Wilkinson, C. R., Garrone, R., and Vacelet, J. (1984). Marine sponges discriminate between food bacteria and bacterial symbionts: Electron microscope radioautography and in situ evidence. *Proc. R Soc. London - Biol. Sci.* 220(1221), 519–528. doi:10.1098/rspb.1984.0018

- Williams, L. M., & Gilmore, T. D. (2022). An innate ability: how do basal invertebrates manage their chronic exposure to microbes? *PLoS Pathog.* 18(10), 1–8. doi:10.1371/journal.ppat.1010897
- Wolfowicz, I., Baumgarten, S., Voss, P. A., Hambleton, E. A., Voolstra, C. R., Hatta, M., & Guse, A. (2016). *Aiptasia* sp. larvae as a model to reveal mechanisms of symbiont selection in cnidarians. *Sci. Rep.* 6, 1–12. doi:10.1038/srep32366
- Wright, R. M., Kenkel, C. D., Dunn, C. E., Shilling, E. N., Bay, L. K., & Matz, M. V. (2017). Intraspecific differences in molecular stress responses and coral pathobiome contribute to mortality under bacterial challenge in *Acropora millepora*. *Sci. Rep.* 7(1), 1–13. doi:10.1038/s41598-017-02685-1
- Wu, Y. C., Franzenburg, S., Ribes, M., & Pita, L. (2022). Wounding response in Porifera (sponges) activates ancestral signaling cascades involved in animal healing, regeneration, and cancer. *Sci. Rep.* 12(1), 1–13. doi:10.1038/s41598-022-05230-x
- Yahel, G., Eerkes-Medrano, D. I., and Leys, S. P. (2006). Size independent selective filtration of ultraplankton by hexactinellid glass sponges. *Aquat Microb. Ecol.* 45 (2), 181–194. doi:10.3354/ame045181
- Yahel, G., Whitney, F., Reiswig, H. M., Eerkes-Medrano, D. I., and Leys, S. P. (2007). *In situ* feeding and metabolism of glass sponges (Hexactinellida, Porifera) studied in a deep temperate fjord with a remotely operated submersible. *Limnol. Oceanogr.* 52 (1), 428–440. doi:10.4319/lo.2007.52.1.0428
- Yang, J., Liu, Z., & Xiao, T. S. (2017). Post-translational regulation of inflammasomes. *Cell. Mol. Immunol.* 14(1), 65–79. doi:10.1038/cmi.2016.29
- Yang, S., Fujikado, N., Kolodin, D., Benoist, C., & Mathis, D. (2015). Regulatory T cells generated early in life play a distinct role in maintaining self-tolerance. *Science.* 348(6234), 589–594. doi:10.1126/science.aaa7017
- Yuen, B. (2016). Deciphering the genomic tool-kit underlying animal-bacteria interactions. PhD thesis. The University of Queensland. doi:10.14264/uql.2017.39
- Yuen, B., Bayes, J. M., & Degnan, S. M. (2014). The characterization of sponge NLRs provides insight into the origin and evolution of this innate immune gene family in animals. *Mol. Biol. Evol.* 31(1), 106–120. doi:10.1093/molbev/mst174
- Zhang, L., Li, L., & Zhang, G. (2011). A *Crassostrea gigas* Toll-like receptor and comparative analysis of TLR pathway in invertebrates. *Fish Shellfish Immunol.* 30(2), 653-660. doi:10.1016/j.fsi.2010.12.023
- Zhang, Z., Aweya, J. J., Yao, D., Zheng, Z., Tran, N. T., Li, S., & Zhang, Y. (2021). Ubiquitination as an important host-immune response strategy in penaeid shrimp: inferences from other species. *Front. Immunol.* 12, 1–11. doi:10.3389/fimmu.2021.697397

---

# Acknowledgements

---

Many people supported me at different moments and different stages of my four-year Ph.D. journey. I will do my best to thank all of you and just hope that my memory doesn't fail me. First, thank you Ute and Lucia for your supervision and for encouraging me to be independent, trust myself, and to critically think about my questions. I am grateful not only for your scientific but also for your personal support through my ups and downs. I will miss our discussions during the Mediterranean- and Phago-Tuesdays. Lucia, aunque no estuviste físicamente en los últimos años de mi doctorado siempre te esforzaste por brindarme apoyo a distancia. Gracias por estar ahí hasta el final.

I was very fortunate to have a "big Ph.D. sister". Lara, since the first time I contacted you via email you were always kind and open to answer all my doubts. You introduced me to our model sponge and taught me every collection trick. I will remember our office talks, afternoon coffees, yoga sessions, and creative nights.

This work would have not been possible without the help of the "*Halichondria* team". Tyler, Clara, Vasia, and all the snorkelers and helpers who supported me with the sponge collections. I appreciate your strength in going into the "never-warm enough" Baltic Sea with me. I will miss our morning rides to Schilksee and those sunny (sometimes rainy) days in which we swam around the breakwaters to collect sponges without really knowing if we would find good ones and wondering if they were *H. panicea* or *Haliclona* sp.

Moreover, I am grateful for the help I received from all the members of our RUMS team. Andrea, I truly appreciate your technical support with uncountable sponge cell dissociations. Can't tell how many liters of CMFASW you helped me prepare. You were always motivated and willing to teach me for the n-th time your rule of dilutions (I hope I can remember it in the future). Kristina, the "FACS queen", I am thankful that you accepted the challenge of running sponge cells through "Thor" (i.e., the sorter). I will miss playing with our imagination trying to decipher which figures we can see in the cell populations. And of course, I will not forget: "control, control, control...". Sabrina, I really appreciate your technical assistance with the aquaria. Thanks to you our spongy friends always had a home in the climate chamber. I am

also thankful for the many extractions and tests you helped us run for the diseased sponge project. I assure you it was worth it! Leon, you also helped a lot with the climate chamber and even initiated an extreme makeover of it, thanks! I will remember your insightful comments during the seminars and questions regarding sponge filtration. Tanja and Jutta, I learned about bacterial isolates thanks to you. I appreciate your tips on the bacterial cultures and for helping me with the sequencing and identification of the *Vibrio* isolates. Erik, thank you for always being so keen to provide me with advice regarding bacteria isolates and bioinformatics. Bettina, I sincerely appreciate your kindness. You were always open to supporting me with administrative things but also open to talking and listening when I need it.

I want to further thank some of the former members of our group as well as other people that I had the pleasure of meeting and working with. Vasia, you dove into the IMMUBASE project with me and Lucia and helped me with all the experimental work. I am also grateful for your insights regarding transcriptomics and for our focus time sessions that kept us motivated through difficult times. Kathrin, you together with Beate, were the first members of the RUMS team I met. Thank you for sharing with me your microscopy knowledge, for your statistics advice, and for accepting to join the *Ircinia* team. Janis, it was a pleasure being “tu jefa”. I learned so much during your supervision. You put me “on the other side” and this experience allowed me to understand and improve myself. Fabian, you were always willing to selflessly help me with building things for my incubations setup and gave me tips about the aquaria system, thank you a lot for that. Tobias and Katja, I appreciate your participation in my TAC committee. Your fruitful discussions, neutral views, and counseling were very important to me. Ute Jülly, you were another important anchor. Thank you for always listening, providing a clearer perspective of the situation, and for your mental support. I am also happy to have been part of the CRC community and discovered the various layers of the metaorganisms’ research.

Last, but not least, I want to shout out a big thank you to my family and friends who gave me support from the distance. Pa & Ma, sin ustedes simplemente no estaría aquí; ni siquiera sería bióloga. Gracias por apoyarme e incentivar me a seguir mi pasión. Recuerdo cuantas veces nos inculcaron la importancia del estudio y sé todos los grandes esfuerzos que hicieron por brindarnos la mejor educación. Este logro es tanto mío como de ustedes; ¡se los dedico! Herma, gracias por siempre ser mi polo a tierra y brindarme fortaleza en esos momentos en

los que siento que quiero renunciar. Agradezco todas las sesiones de fines de semanas que tuvimos y en las que me enseñaste tus sabios consejos. Mis amores, gracias por su apoyo incondicional; ¡los adoro! Mar, empezamos el doctorado casi a la misma vez, y el haber compartido experiencias a lo largo de este proceso me permitió tener otras perspectivas. Gracias por estar siempre dispuesta a escuchar. Te deseo muchos éxitos en el resto de tu trayecto del Ph.D. Ben, what can I say, there are just not enough words to express my gratitude. It was a hard time, and despite the many challenges you were always there supporting me and being my rational voice during my many crises. I am so thankful for having you as my partner and as a colleague. I learned a lot from our discussions about how to improve the experimental designs and to always think about the story I want to tell. Soon I will be able to also say “Believe me, I’m a Doctor!” ♥





---

## Supplementary Information

---

## Supplements Chapter 2

### **Text S1.** Characterization of microbial consortium treatments by flow cytometry

The concentration of the microbial consortia stocks obtained by enrichment was estimated via flow cytometry and adjusted to reach  $10^{5-6}$  bacteria  $\text{mL}^{-1}$  final concentration in each experimental aquarium. In addition, water samples (2 mL) from each aquarium were collected right before the experiment (time point -1h) and right after (T0) adding the microbial consortium. Samples for flow cytometry were fixed in paraformaldehyde + glutaraldehyde (1% + 0.05% final, respectively) and stored at  $-80^{\circ}\text{C}$  until analysis. Microbial cell concentration was quantified by flow cytometry (FACSCalibur, Becton-Dickinson, 488 nm excitation blue laser) following the method of Gasol and Morán (1999). In short, DNA in microbial cells was stained with Syto13, and detected based on cell-side scatter, forward scatter, and green fluorescence of the stained DNA. Plastic beads were used as reference for plotting. Bacterial cell concentrations were calculated based on number of events and calibrated flow rate.

Although the aquaria were kept overnight in  $1\ \mu\text{m}$ -filtered seawater and an additional  $0.1\ \mu\text{m}$ -filter was applied for 3 h before the experiments, the water in the aquaria was not sterile, some bacterial cells remained (Fig. S1 A and C). We could still detect the addition of the treatment, particularly in the cell population of higher DNA content, in both seawater and *A. aerophoba* symbiont treatments (Fig. S1 B and D, R6 gate). We could detect an increment of one order of magnitude in the bacterial concentrations in the water before and after the addition of microbial consortia, to a final concentration  $\sim 10^6$  cells  $\text{mL}^{-1}$ .

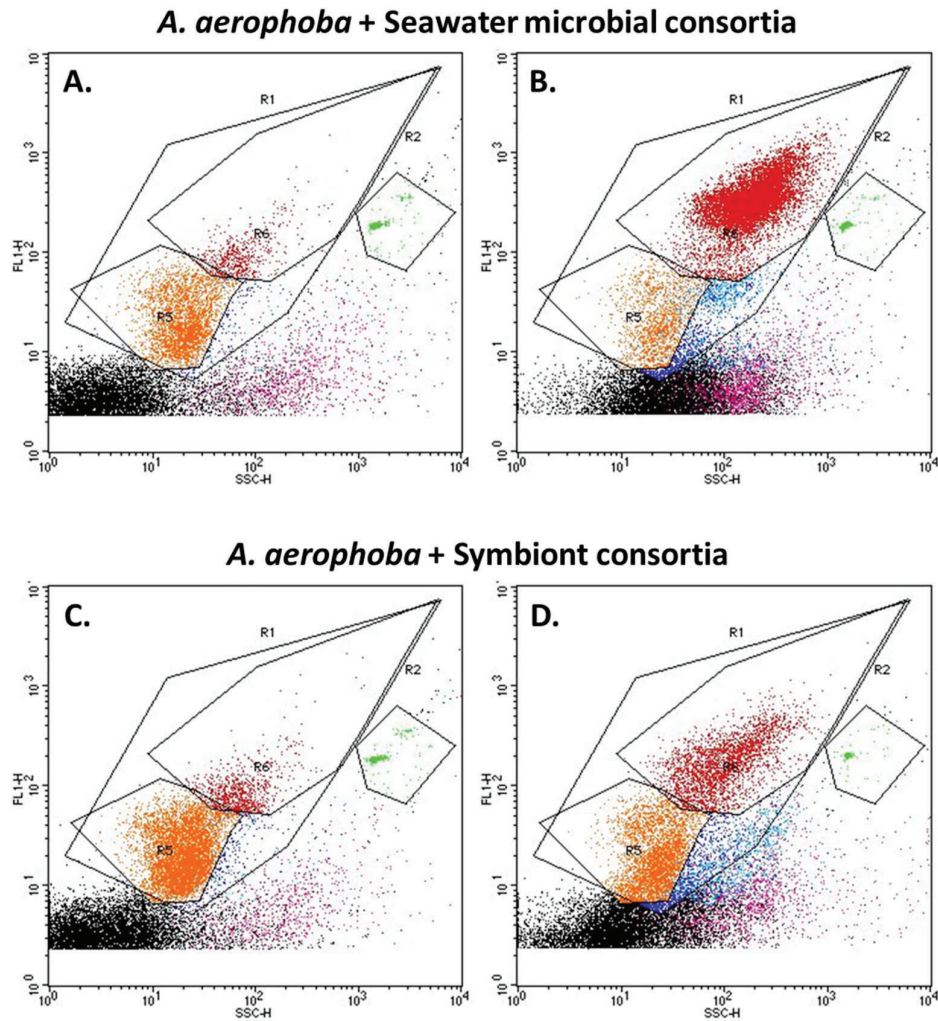


**Fig. S1.** Representative cytograms of seawater consortia (**A-B**) and *A. aerophoba*-symbiont (**C-D**) consortium used for the experiments. The microbial stock concentration was estimated before (T-1) (**A-C**) and after (T0) (**B-D**) adding the bacteria to the incubation tank. R1: all bacteria; R5 and R6: low and high DNA bacteria, respectively; R2: quantification beads. Water samples (2 mL) from all aquaria were collected before the experiment (time point -1h) and every hour during the course of the experiments (time points 0, 1, 2, 3, 4, 5 h), and fixed in paraformaldehyde + glutaraldehyde (1% + 0.05% final, respectively). Microbial cell concentration in the water by was quantified by flow cytometry (FACSCalibur, Becton-Dickinson, 488 nm excitation blue laser) following the method of Gasol and Morán (1999), to assess the sponge filtration activity. The bacterial cells were stained with Syto13, and detected based on cell-side scatter, forward scatter, and green fluorescence of the stained DNA. For comparison with the sponges, control aquaria (i.e., without sponge) were also exposed to the microbial treatments and sampled at the same time points.

**Table S1.** Number of read pairs (million reads). “Raw” refers to the output from sequencing; “Clean” to surviving read pairs after trimming and filtering in trimmomatic-v0.38; and “Eukaryote” to pairs identified as non-prokaryotic and nonmicrobial eukaryote by kaiju-v1.6.2 (Menzel & Krogh, 2015).

Average per library (± standard error)	Raw	Clean	Eukaryote
<i>A. aerophoba</i>	23.8 ± 1.8	22.1 ± 9.2	15.0 ± 6.3
<i>D. avara</i>	19.6 ± 1.2	18.1 ± 10.7	11.7 ± 0.7

**Table S2.** Statistics of the *de novo* transcriptomic assemblies. Transcripts refer to Trinity isoforms, genes refer to Trinity components. Mb: mega bases.

Statistics:	<i>A. aerophoba</i>	<i>D. avara</i>
No. Transcripts – Trinity isoforms	900127	983239
No. Genes – Trinity components	466345	624596
Transcripts with open reading frames, %	60.59	52.88
Average transcript length, nucleotides	535.16	636.86
N50	631	873
Total assembled bases, Mb	481.7	626.2
<b>BUSCO report</b>	<b>C:71.4%</b>	<b>C:78.2%</b>
<b>(metazoan database; 978 genes)</b>	<b>[D:44.1%, F:23.6%]</b>	<b>[D:49.0%, F:17.1%]</b>

**\*Table S3.** Differential Expression analysis for *D. avara* at as identified in edgeR (FDR p-value < 0.005 and  $\log_2|FC| \geq 2$ ) at 1h, 3h and 5h (Excel file)

**\*Table S4.** Annotation of the differentially expressed genes for *D. avara* identified in edgeR (FDR p-value < 0.005 and  $\log_2|FC| \geq 2$ ) at 1h, 3h and 5h (Excel file)

**\*Table S5.** Differential Expression analysis for *A. aerophoba* at as identified in edgeR (FDR p-value < 0.005 and  $\log_2|FC| \geq 2$ ) at 5h (Excel file)

**\*Table S6.** Annotation of differentially expressed genes for *A. aerophoba* identified in edgeR (FDR p-value < 0.005 and  $\log_2|FC| \geq 2$ ) at 5h (Excel file)

**\*Table S7.** Blastp results of *D. avara* differentially expressed NLRs against *Ephydatia muelleri* (e-value <  $1e^{-5}$ ) (Excel file)

\*Tables S3 to S7 are available in Marulanda-Gómez et al. 2023 (submitted to GBE).  
Preprint available in bioRxiv: <https://doi.org/10.1101/2023.11.02.563995>

## Supplements Chapter 4



**Fig. S1.** *H. panicea* nursery. Sponge specimens were collected and at the Kiel fjord (54.329659 N, 10.149104 E; Kiel, Germany) at 1 m water depth in Aug 2023, cleaned from epibionts, trimmed to size, and left to heal and recover from collection on an *in-situ* nursery at the collection site for 10 days.

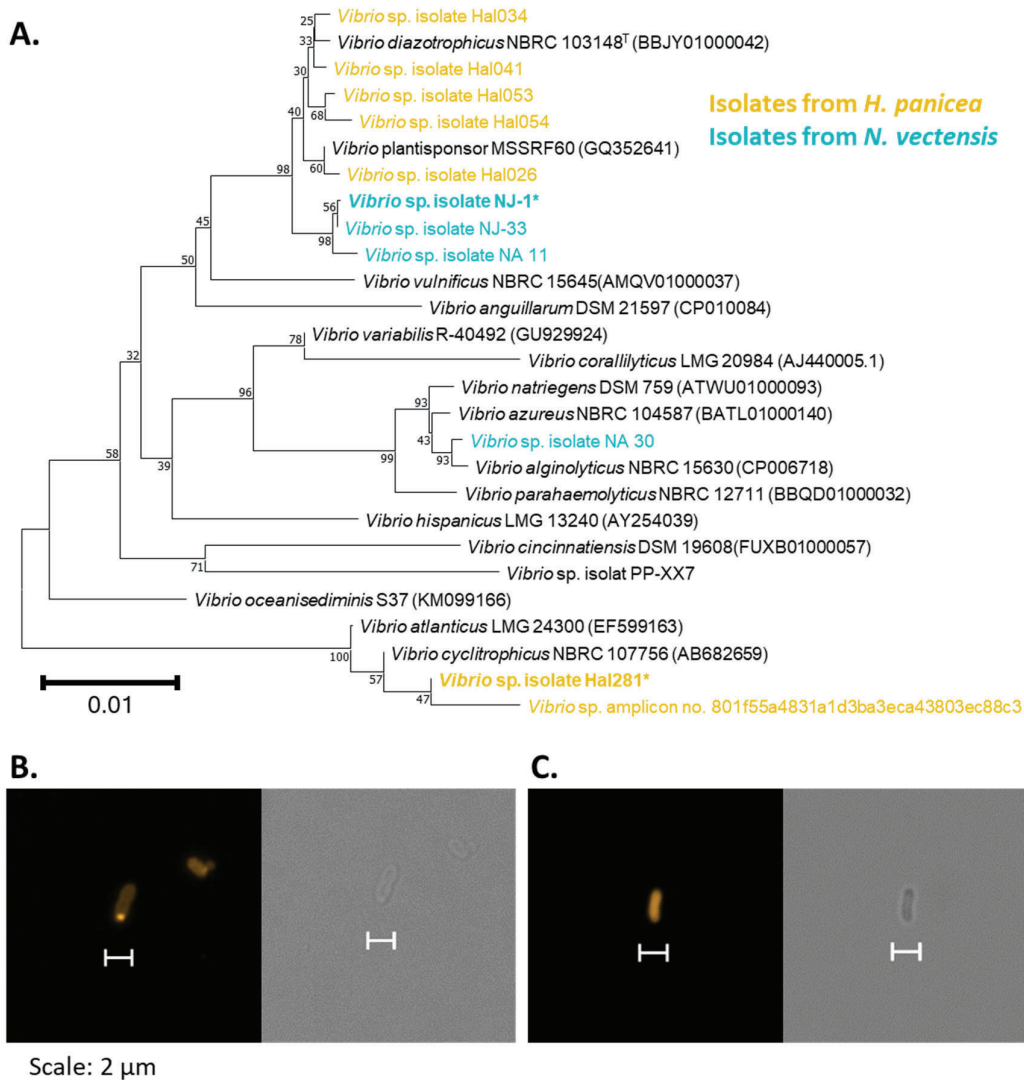


**Fig. S2.** Neighbor-joining phylogenetic tree of *Vibrio* strains isolated from the sponge *Halichondria panicea* (yellow) and the sea anemone *Nematostella vectensis* (blue). Isolates used for the phagocytic assays are depicted in bold and with \*. Environmental isolates were also included (in black) for comparison. The optimal tree is shown. The percentage of replicate trees in which the associated taxa clustered together in the bootstrap test (1000 replicates) are shown next to the branches. The tree is drawn to scale, with branch lengths in the same units as those of the evolutionary distances used to infer the phylogenetic tree. The evolutionary distances were computed using the Tamura-Nei method [3] and are in the units of the number of base substitutions per site. This analysis involved 27 nucleotide sequences based on 16S rRNA gene sequencing. Codon positions included were 1st+2nd+3rd+Noncoding. All ambiguous positions were removed for each sequence pair (pairwise deletion option). There were a total of 1546 positions in the final dataset. Evolutionary analyses were conducted in MEGA11.

**Text S1.** Estimating *H. panicea* bacterial uptake during the phagocytic assays

Water samples were taken through the incubation period (at 0 min, 2 min, 7 min, 14 min, 22 min, 30 min, 45 min, and 60 min), fixed with paraformaldehyde and glutaraldehyde in 1x PBS (final concentration 1% and 0.05%, respectively), and analyze via flow cytometry to assess bacterial uptake (i.e., filtration) by *H. panicea*. Incubations without sponges (seawater only *Vibrio* isolates) served as controls (n = 4). The average initial concentration of the isolate Hal 281 in the seawater at the start of the 30 min and 60 min incubation was on average ( $\pm$  S.D. throughout the text, unless stated otherwise) approx.  $1.2 \times 10^5 \pm 2.2 \times 10^4$  bacteria mL<sup>-1</sup> and  $6.6 \times 10^4 \pm 8.5 \times 10^3$  bacteria mL<sup>-1</sup>, respectively (Fig. S2 A-D, Table S1). In the 30 min incubations, the *Vibrio* concentration at T<sub>0min</sub> and T<sub>2min</sub> was around 1.3 to 1.5 times lower than the concentration estimated for the other time points, suggesting that the isolate Hal 281 needed around 5 to 7 min to be completely mixed in the incubation chamber (Fig. S2 A-B). In the assays that run for 60 min no mixing effect was evident (Fig. S2 C-D). The starting concentration of the isolate NJ 1 was on average  $7.7 \times 10^4 \pm 2.4 \times 10^4$  bacteria mL<sup>-1</sup> in the 30 min incubations and  $4.9 \times 10^4 \pm 1.1 \times 10^4$  in the 60 min incubations (Fig. S2 E-H). No mixing effect was observed in either of the incubation runs. Contrary to Hal281, the concentration of the non-associated sponge isolate NJ1 did not seem to decrease either in the 30 min or the 60 min assays. Uptake rates (filtration) were not possible to estimate for either of the isolates since the flow cytometry analysis from the seawater samples was very variable along the sampled time points and sponge biological replicates.



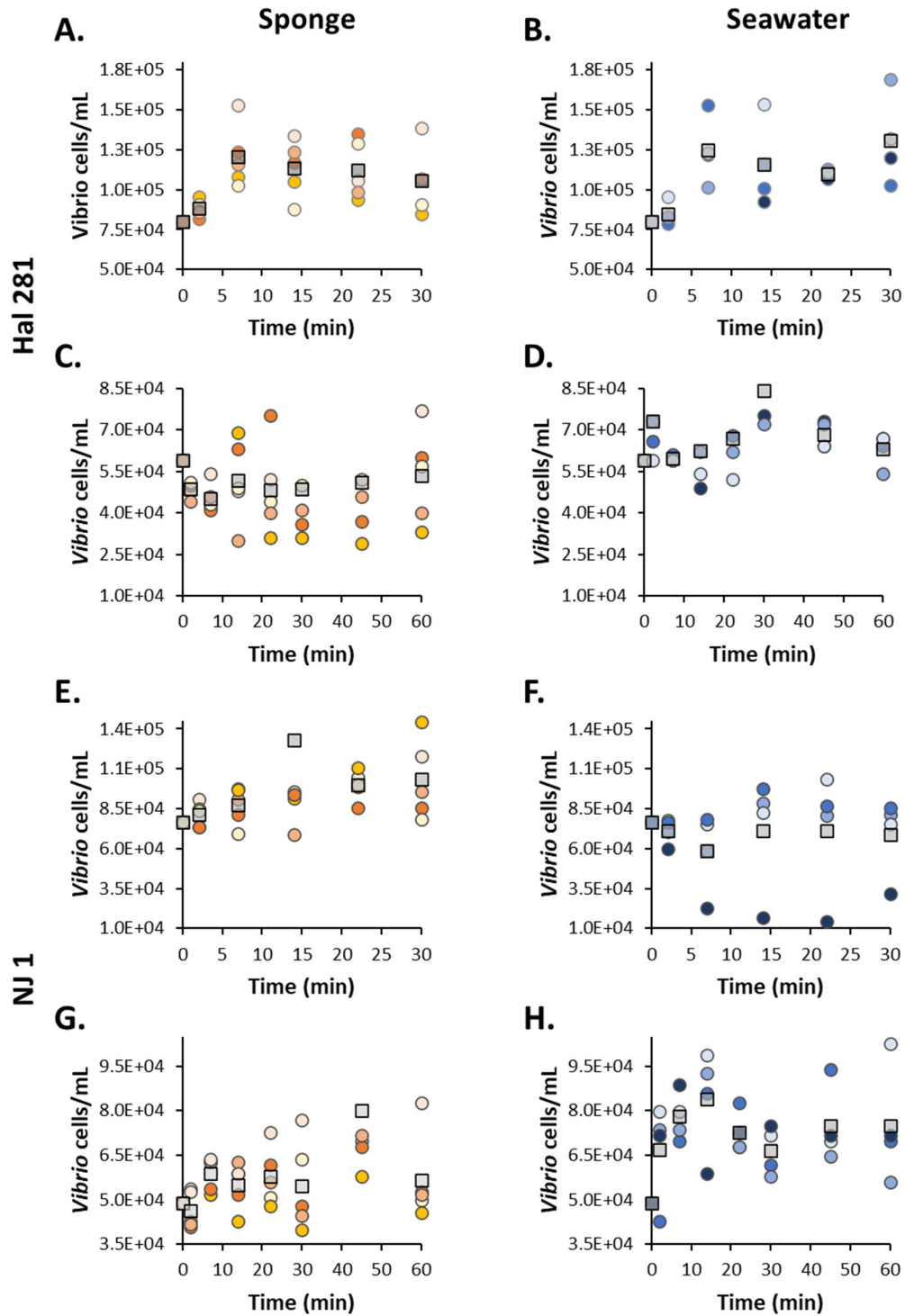


**Fig. S3.** *Vibrio* uptake by *H. panicea* individuals incubated with **A.-D.** a sponge-associated (Hal 281) and **E.-H.** a non-sponge associated (NJ 1) *Vibrio* isolate for 30 min and 60 min based on flow cytometry water sample analyses. Dots of the same color: biological replicates (n = 4-5 per treatment). Squares: averaged data.

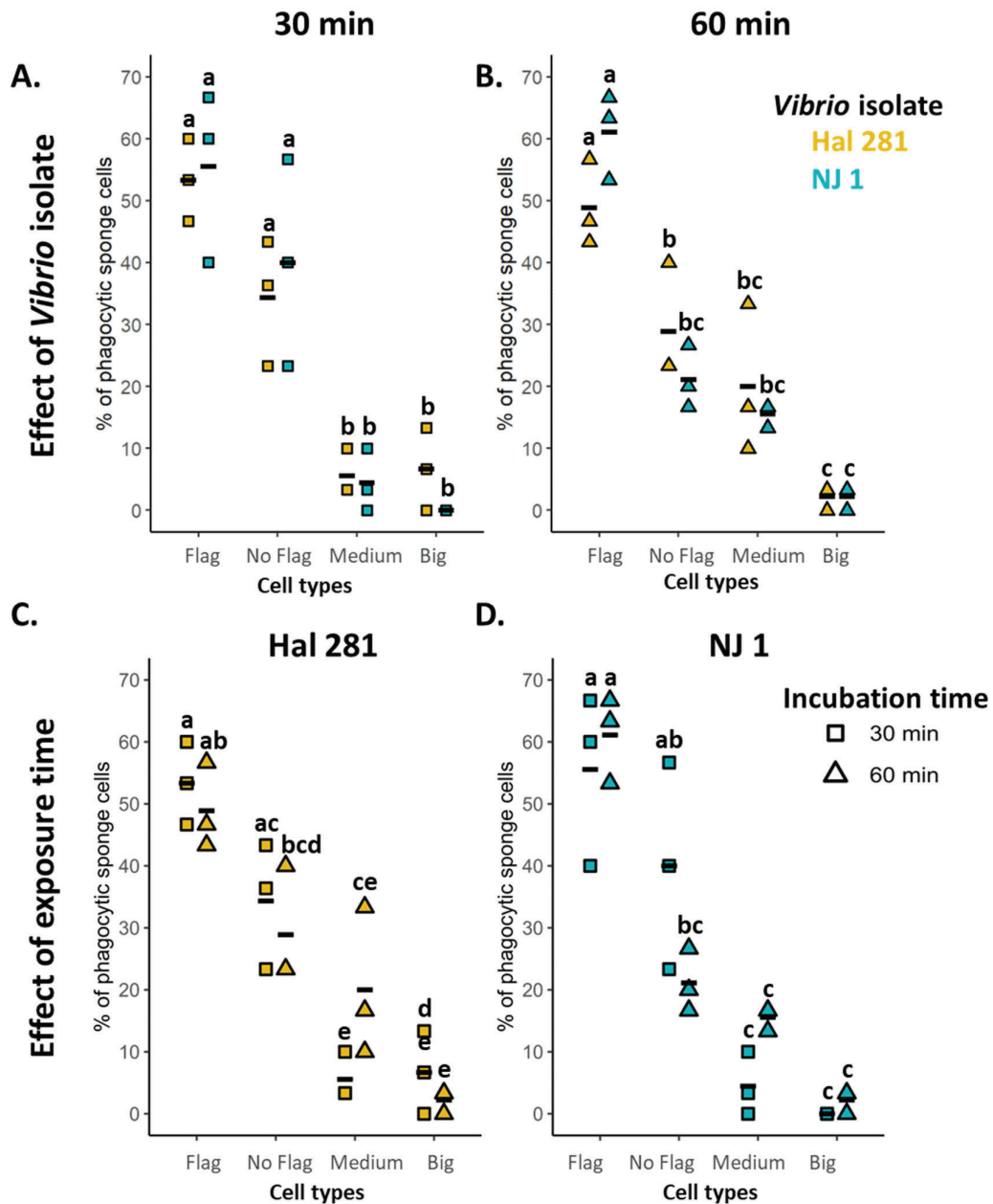


**Fig. S4.** Phagocytic cell types observed in the assays with *H. panicea*. (A) Representative fluorescent microscopy pictures showing different phagocytic cell categories. Scale bars: 5  $\mu$ m. Fl: flagella. (B) – (D) Relative abundance of phagocytic cell types observed after 30 min and 60 min incubations with the *Vibrio* isolates Hal281 and NJ1 based on microscopy cell counts. Bold line: average for the 3 biological replicates. Treatments marked with different letters are significantly different at  $\alpha=0.05$ .

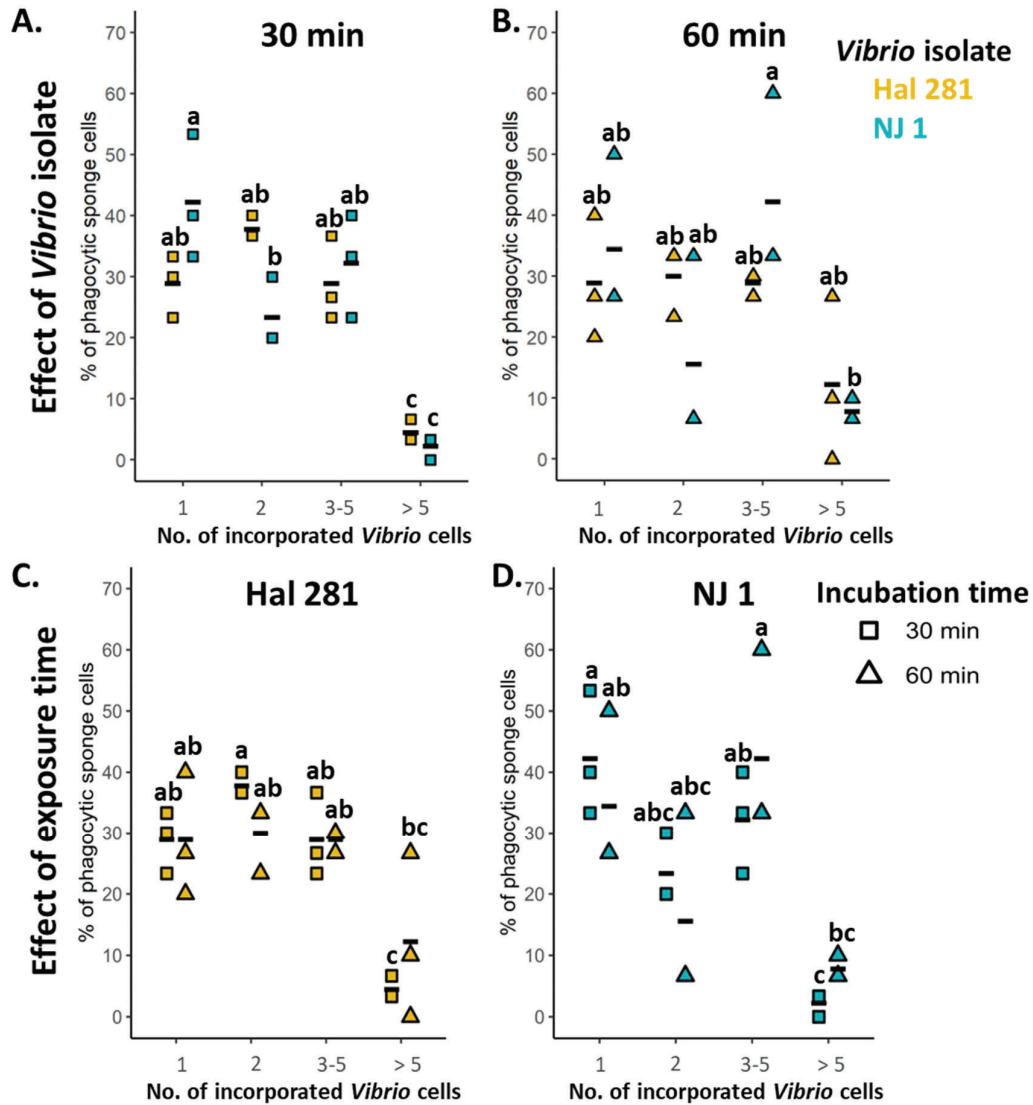
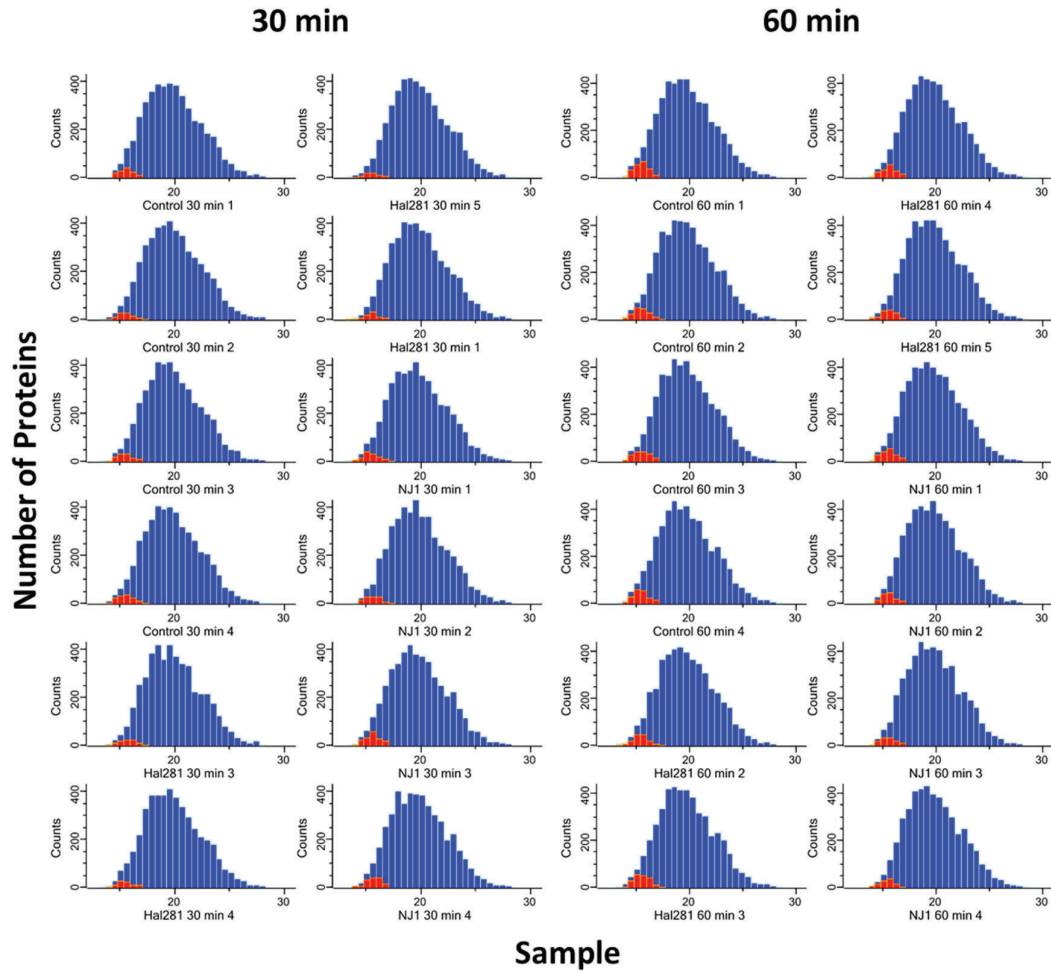


**Fig. S5.** *Vibrio* cells observed per phagocytic cell in the assays with *H. panicea*. (A) Representative fluorescent microscopy pictures of phagocytic cells with different numbers of incorporated *Vibrio* cells. Scale bars: 5  $\mu$ m. Arrowheads: TAMRA-stained *Vibrio*. (B) – (D) Relative abundance of phagocytic cells per *Vibrio* category after 30 min and 60 min incubations with the isolates Hal281 and NJ1 based on microscopy cell counts. Bold line: average for the 3 biological replicates. Treatments marked with different letters are significantly different at  $\alpha=0.05$ .



**Figs S6.** Protein quantification of *H. panicea* individuals incubated with a sponge-associated (Hal 281) and a non-sponge associated (NJ 1) *Vibrio* isolate for 30 min and 60 min. Missing values were imputed from a normal distribution separately for each replicate (Width 0.3, Downshift 1.8).

**Table S1.** Filtration of *Vibrio* by *H. panicea* based on water sample analysis with flow cytometry. Sponges were incubated for 30 min and 60 min with two TAMRA-stained *Vibrio* isolates (Hal 281 extracted from *H. panicea* and NJ 1 extracted from *Nematostella vectensis*). Incubations with seawater (without a sponge) were used as controls. The data presented was corrected based on the averaged starting concentration (T0) of seawater and sponge incubations.

Incubation time	Treatment	Sample type	Sample ID	Sampling time (min)							
				0	2	7	14	22	30	45	60
30 min	Hal281	Seawater	SW5	7.99E+04	7.89E+04	1.53E+05	1.01E+05	1.10E+05	1.03E+05		
			SW6	7.99E+04	8.29E+04	1.22E+05	9.29E+04	1.07E+05	1.20E+05		
			SW7	7.99E+04	8.29E+04	1.02E+05	1.16E+05	1.13E+05	1.69E+05		
			SW8	7.99E+04	9.59E+04	1.23E+05	1.54E+05	1.11E+05	1.32E+05		
			<b>Average</b>		<b>8.51E+04</b>	<b>1.25E+05</b>	<b>1.16E+05</b>	<b>1.10E+05</b>	<b>1.31E+05</b>		
		<b>S.D.</b>		<b>7.41E+03</b>	<b>2.10E+04</b>	<b>2.71E+04</b>	<b>2.50E+03</b>	<b>2.80E+04</b>			
		Sponge	HP9	7.99E+04	9.59E+04	1.08E+05	1.05E+05	9.39E+04	8.49E+04		
			HP10	7.99E+04	8.19E+04	1.24E+05	1.17E+05	1.35E+05	1.06E+05		
			HP11	7.99E+04	9.09E+04	1.03E+05	8.79E+04	1.29E+05	9.09E+04		
	HP12		7.99E+04	8.69E+04	1.53E+05	1.34E+05	1.06E+05	1.39E+05			
	HP13		7.99E+04	8.59E+04	1.16E+05	1.24E+05	9.89E+04	1.07E+05			
			<b>Average</b>	<b>8.83E+04</b>	<b>1.21E+05</b>	<b>1.13E+05</b>	<b>1.12E+05</b>	<b>1.05E+05</b>			
			<b>S.D.</b>	<b>5.32E+03</b>	<b>1.97E+04</b>	<b>1.78E+04</b>	<b>1.83E+04</b>	<b>2.09E+04</b>			
	NJ1	Seawater	SW13	7.67E+04	7.07E+04	5.87E+04	8.87E+04	8.07E+04	8.17E+04		
			SW14	7.67E+04	5.97E+04	2.27E+04	1.67E+04	1.47E+04	3.17E+04		
			SW15	7.67E+04	7.77E+04	7.57E+04	8.27E+04	1.04E+05	7.57E+04		
			SW16	7.67E+04	7.67E+04	7.87E+04	9.77E+04	8.67E+04	8.57E+04		
			<b>Average</b>		<b>7.12E+04</b>	<b>5.89E+04</b>	<b>7.14E+04</b>	<b>7.14E+04</b>	<b>6.87E+04</b>		
<b>S.D.</b>			<b>8.27E+03</b>	<b>2.57E+04</b>	<b>3.70E+04</b>	<b>3.91E+04</b>	<b>2.50E+04</b>				
Sponge		HP19	7.67E+04	9.07E+04	9.77E+04	9.57E+04	1.05E+05	1.18E+05			
		HP20	7.67E+04	7.37E+04	9.07E+04	6.87E+04	9.87E+04	9.57E+04			
		HP21	7.67E+04	8.47E+04	9.67E+04	9.17E+04	1.11E+05	1.40E+05			

60 min			HP22	7.67E+04	7.37E+04	8.17E+04	9.37E+04	8.57E+04	8.57E+04		
			HP23	7.67E+04	8.37E+04	6.97E+04	2.92E+05	9.97E+04	7.87E+04		
			<b>Average</b>		<b>8.13E+04</b>	<b>8.73E+04</b>	<b>1.28E+05</b>	<b>9.99E+04</b>	<b>1.03E+05</b>		
			<b>S.D.</b>		<b>7.44E+03</b>	<b>1.17E+04</b>	<b>9.20E+04</b>	<b>9.26E+03</b>	<b>2.50E+04</b>		
	Hal281	Seawater	SW9	5.91E+04	9.41E+04	5.91E+04	4.91E+04	8.61E+04	7.51E+04	7.31E+04	6.71E+04
			SW10	5.91E+04	7.31E+04	6.01E+04	6.21E+04	6.21E+04	7.21E+04	7.21E+04	5.41E+04
			SW11	5.91E+04	6.61E+04	6.11E+04	8.51E+04	6.81E+04	9.61E+04	6.41E+04	6.41E+04
			SW12	5.91E+04	5.91E+04	5.91E+04	5.41E+04	5.21E+04	9.31E+04	6.41E+04	6.71E+04
			<b>Average</b>		<b>7.31E+04</b>	<b>5.99E+04</b>	<b>6.26E+04</b>	<b>6.71E+04</b>	<b>8.41E+04</b>	<b>6.84E+04</b>	<b>6.31E+04</b>
		<b>S.D.</b>		<b>1.51E+04</b>	<b>9.57E+02</b>	<b>1.59E+04</b>	<b>1.43E+04</b>	<b>1.22E+04</b>	<b>4.92E+03</b>	<b>6.16E+03</b>	
		Sponge	HP9	5.91E+04	5.01E+04	4.21E+04	6.91E+04	3.11E+04	3.11E+04	2.91E+04	3.31E+04
			HP10	5.91E+04	4.81E+04	5.41E+04	4.81E+04	5.21E+04	8.51E+04	5.21E+04	7.71E+04
			HP11	5.91E+04	5.01E+04	4.11E+04	6.31E+04	7.51E+04	3.61E+04	3.71E+04	6.01E+04
			HP12	5.91E+04	5.11E+04	4.31E+04	4.91E+04	4.41E+04	5.01E+04	9.11E+04	5.71E+04
	HP13		5.91E+04	4.41E+04	4.61E+04	3.01E+04	4.01E+04	4.11E+04	4.61E+04	4.01E+04	
	<b>Average</b>		<b>4.87E+04</b>	<b>4.53E+04</b>	<b>5.19E+04</b>	<b>4.85E+04</b>	<b>4.87E+04</b>	<b>5.11E+04</b>	<b>5.35E+04</b>		
	<b>S.D.</b>		<b>2.79E+03</b>	<b>5.26E+03</b>	<b>1.52E+04</b>	<b>1.67E+04</b>	<b>2.15E+04</b>	<b>2.40E+04</b>	<b>1.74E+04</b>		
	NJ1	Seawater	SW17	4.88E+04	4.28E+04	6.98E+04	8.58E+04	8.28E+04	6.18E+04	9.38E+04	6.98E+04
			SW18	4.88E+04	7.98E+04	7.98E+04	9.88E+04	6.78E+04	7.18E+04	6.98E+04	1.03E+05
SW19			4.88E+04	7.38E+04	7.38E+04	9.28E+04	6.78E+04	5.78E+04	6.48E+04	5.58E+04	
SW20			4.88E+04	7.18E+04	8.88E+04	5.88E+04	7.28E+04	7.48E+04	7.18E+04	7.18E+04	
<b>Average</b>				<b>6.70E+04</b>	<b>7.80E+04</b>	<b>8.40E+04</b>	<b>7.28E+04</b>	<b>6.65E+04</b>	<b>7.50E+04</b>	<b>7.50E+04</b>	
<b>S.D.</b>			<b>1.65E+04</b>	<b>8.26E+03</b>	<b>1.77E+04</b>	<b>7.07E+03</b>	<b>8.06E+03</b>	<b>1.28E+04</b>	<b>1.98E+04</b>		
Sponge		HP19	4.88E+04	5.38E+04	6.28E+04	5.88E+04	5.08E+04	6.38E+04	6.98E+04	4.98E+04	
		HP20	4.88E+04	4.28E+04	5.18E+04	4.28E+04	4.78E+04	3.98E+04	5.78E+04	4.58E+04	
		HP21	4.88E+04	4.08E+04	5.38E+04	5.18E+04	6.18E+04	4.78E+04	6.78E+04	5.28E+04	
		HP22	4.88E+04	4.18E+04	6.28E+04	6.28E+04	5.58E+04	4.48E+04	7.18E+04	5.18E+04	
	HP23	4.88E+04	5.28E+04	6.38E+04	5.88E+04	7.28E+04	7.68E+04	1.34E+05	8.28E+04		
<b>Average</b>		<b>4.64E+04</b>	<b>5.90E+04</b>	<b>5.50E+04</b>	<b>5.78E+04</b>	<b>5.46E+04</b>	<b>8.02E+04</b>	<b>5.66E+04</b>			
<b>S.D.</b>		<b>6.35E+03</b>	<b>5.72E+03</b>	<b>7.89E+03</b>	<b>9.92E+03</b>	<b>1.53E+04</b>	<b>3.04E+04</b>	<b>1.49E+04</b>			

**Table S2.** FACS quantification of phagocytic sponge cells of *H. panicea* individuals used during the phagocytic assays. Sponges were incubated for 30 min and 60 min with two TAMRA-stained *Vibrio* isolates (Hal 281 extracted from *H. panicea* and NJ 1 extracted from *Nematostella vectensis*). The sponge (host) cell suspension from each individual was run in the FACS five times (i.e., 5 technical replicates). The average number of events of the replicates is presented. Controls: individuals incubated without *Vibrio* to correct for natural fluorescence in sponge cells. Bulk sponge cells: total DAPI-stained cell fraction; Non-phagocytic cells: cells without incorporated *Vibrio*; Phagocytic cells: cells with incorporated *Vibrio*. Red values: outliers and were not considered in the plots or statistical analysis.

Incubation time	Treatment	Individual	Average bulk sponge cells	Average non-phagocytic cells	Average phagocytic cells	Average % of phagocytic cells	Average % of phagocytic cells corrected
30 min	Control	1	1.38E+05	1.27E+05	1.13E+04	8.18	
		2	1.37E+05	1.28E+05	8.95E+03	6.54	
		3	1.55E+05	1.42E+05	1.23E+04	7.96	
		4	1.48E+05	1.35E+05	1.28E+04	8.65	
		<b>Average</b>	<b>1.44E+05</b>	<b>1.33E+05</b>	<b>1.14E+04</b>	<b>7.83</b>	
	<b>S.D.</b>	<b>8.38E+03</b>	<b>7.14E+03</b>	<b>1.71E+03</b>	<b>0.91</b>		
	Hal281	9	4.71E+04	2.83E+04	1.87E+04	39.83	32.00
		10	5.87E+04	3.89E+04	1.98E+04	33.73	25.90
		11	6.06E+04	3.77E+04	2.29E+04	37.82	29.99
		12	5.78E+04	3.80E+04	1.99E+04	34.37	26.54
		13	6.08E+04	3.77E+04	2.31E+04	37.99	30.16
		<b>Average</b>	<b>5.70E+04</b>	<b>3.61E+04</b>	<b>2.09E+04</b>	<b>36.75</b>	<b>28.92</b>
	<b>S.D.</b>	<b>5.69E+03</b>	<b>4.38E+03</b>	<b>1.99E+03</b>	<b>2.60</b>	<b>2.60</b>	
	NJ1	19	1.24E+05	8.26E+04	4.10E+04	33.19	25.36
		20	1.29E+05	8.60E+04	4.33E+04	33.48	25.65
		21	1.39E+05	1.21E+05	1.78E+04	12.75	4.91
		22	1.41E+05	8.23E+04	5.85E+04	41.56	33.72
		23	1.46E+05	9.36E+04	5.25E+04	35.95	28.12
		<b>Average</b>	<b>1.36E+05</b>	<b>9.32E+04</b>	<b>4.26E+04</b>	<b>31.38</b>	<b>23.55</b>
		<b>S.D.</b>	<b>9.10E+03</b>	<b>1.64E+04</b>	<b>1.56E+04</b>	<b>10.95</b>	<b>10.95</b>

60 min	Control	5	1.51E+05	1.39E+05	1.12E+04	7.44	
		6	1.53E+05	1.43E+05	9.82E+03	6.42	
		7	1.43E+05	1.29E+05	1.39E+04	9.75	
		8	1.17E+05	1.09E+05	7.39E+03	6.34	
		<b>Average</b>	<b>1.41E+05</b>	<b>1.30E+05</b>	<b>1.06E+04</b>	<b>7.49</b>	
		<b>S.D.</b>	<b>1.67E+04</b>	<b>1.52E+04</b>	<b>2.72E+03</b>	<b>1.59</b>	
	Hal281	14	1.50E+05	7.35E+04	7.66E+04	51.04	43.55
		15	1.29E+05	6.76E+04	6.16E+04	47.67	40.18
		16	1.61E+05	8.79E+04	7.29E+04	45.34	37.86
		17	1.54E+05	9.04E+04	6.37E+04	41.34	33.85
		18	1.44E+05	8.15E+04	6.25E+04	43.37	35.88
		<b>Average</b>	<b>1.48E+05</b>	<b>8.02E+04</b>	<b>6.75E+04</b>	<b>45.75</b>	<b>38.26</b>
	NJ1	<b>S.D.</b>	<b>1.20E+04</b>	<b>9.61E+03</b>	<b>6.85E+03</b>	<b>3.77</b>	<b>3.77</b>
		24	130351.6	69963.4	60388.2	46.33	38.84
		25	162501	87562.4	74938.6	46.12	38.64
		26	158317.6	130699.4	27618.2	17.44	9.95
		27	131747.6	82263.2	49484.4	37.56	30.07
		28	144975	94886.6	50088.4	34.54	27.06
	<b>Average</b>	<b>1.46E+05</b>	<b>9.31E+04</b>	<b>5.25E+04</b>	<b>36.40</b>	<b>28.91</b>	
	<b>S.D.</b>	<b>1.48E+04</b>	<b>2.29E+04</b>	<b>1.73E+04</b>	<b>11.81</b>	<b>11.81</b>	



**Table S3.** Fluorescent microscopy counts of sponge phagocytic cells and number of *Vibrio* cells observed *H. panicea* individuals incubated with a sponge-associated (Hal 281) and a non-sponge associated (NJ 1) *Vibrio* isolate for 30 min and 60 min.

Bacteria treatment	Incubation time	Individual	No. of <i>Vibrio</i> cells per phagocytic cell	No. of Phagocytic cell type					% of Phagocytic cell type				
				Flag (3-6 $\mu$ m)	No Flag (3-6 $\mu$ m)	Medium (7 to 10 $\mu$ m)	Big (> 10 $\mu$ m)	Total sponge cells	Flag (3-6 $\mu$ m)	No Flag (3-6 $\mu$ m)	Medium (7 to 10 $\mu$ m)	Big (> 10 $\mu$ m)	Total sponge cells
Hal 281	30 min	9	1 <i>Vibrio</i>	7	3	0	0	10	23.3	10.0	0.0	0.0	33.3
			2 <i>Vibrio</i>	6	6	0	0	12	20.0	20.0	0.0	0.0	40.0
			3-5 <i>Vibrio</i>	3	4	0	0	7	10.0	13.3	0.0	0.0	23.3
			>5 <i>Vibrio</i>	0	0	1	0	1	0.0	0.0	3.3	0.0	3.3
			<b>Total sponge cells</b>	<b>16</b>	<b>13</b>	<b>1</b>	<b>0</b>	<b>30</b>	<b>53.3</b>	<b>43.3</b>	<b>3.3</b>	<b>0.0</b>	<b>100.0</b>
		11	1 <i>Vibrio</i>	4	2	0	1	7	13.3	6.7	0.0	3.3	23.3
			2 <i>Vibrio</i>	6	4	1	0	11	20.0	13.3	3.3	0.0	36.7
			3-5 <i>Vibrio</i>	8	1	2	0	11	26.7	3.3	6.7	0.0	36.7
			>5 <i>Vibrio</i>	0	0	0	1	1	0.0	0.0	0.0	3.3	3.3
			<b>Total sponge cells</b>	<b>18</b>	<b>7</b>	<b>3</b>	<b>2</b>	<b>30</b>	<b>60.0</b>	<b>23.3</b>	<b>10.0</b>	<b>6.7</b>	<b>100.0</b>
		13	1 <i>Vibrio</i>	1	6	0	2	9	3.3	20.0	0.0	6.7	30.0
			2 <i>Vibrio</i>	7	3	1	0	11	23.3	10.0	3.3	0.0	36.7
			3-5 <i>Vibrio</i>	6	2	0	0	8	20.0	6.7	0.0	0.0	26.7
			>5 <i>Vibrio</i>	0	0	0	2	2	0.0	0.0	0.0	6.7	6.7

		<b>Total sponge cells</b>	14	11	1	4	30	46.7	36.7	3.3	13.3	100.0
		<b>Average total sponge cells</b>	16.0	10.3	1.7	2.0		53.3	34.4	5.6	6.7	
60 min	14	1 <i>Vibrio</i>	2	2	4	0	8	6.7	6.7	13.3	0.0	26.7
		2 <i>Vibrio</i>	5	3	2	0	10	16.7	10.0	6.7	0.0	33.3
		3-5 <i>Vibrio</i>	5	2	2	0	9	16.7	6.7	6.7	0.0	30.0
		> 5 <i>Vibrio</i>	1	0	2	0	3	3.3	0.0	6.7	0.0	10.0
		<b>Total sponge cells</b>	13	7	10	0	30	43.3	23.3	33.3	0.0	100.0
	15	1 <i>Vibrio</i>	3	3	0	0	6	10.0	10.0	0.0	0.0	20.0
		2 <i>Vibrio</i>	3	4	0	0	7	10.0	13.3	0.0	0.0	23.3
		3-5 <i>Vibrio</i>	3	4	2	0	9	10.0	13.3	6.7	0.0	30.0
		> 5 <i>Vibrio</i>	5	1	1	1	8	16.7	3.3	3.3	3.3	26.7
		<b>Total sponge cells</b>	14	12	3	1	30	46.7	40.0	10.0	3.3	100.0
	16	1 <i>Vibrio</i>	5	2	4	1	12	16.7	6.7	13.3	3.3	40.0
		2 <i>Vibrio</i>	6	3	1		10	20.0	10.0	3.3	0.0	33.3
		3-5 <i>Vibrio</i>	6	2	0	0	8	20.0	6.7	0.0	0.0	26.7
		> 5 <i>Vibrio</i>	0	0	0	0	0	0.0	0.0	0.0	0.0	0.0
		<b>Total sponge cells</b>	17	7	5	1	30	56.7	23.3	16.7	3.3	100.0

			Average total sponge cells	14.7	8.7	6.0	0.7		48.9	28.9	20.0	2.2		
NJ 1	30 min	19	1 <i>Vibrio</i>	4	11	1	0	16	13.3	36.7	3.3	0.0	53.3	
			2 <i>Vibrio</i>	4	2	0	0	6	13.3	6.7	0.0	0.0	20.0	
			3-5 <i>Vibrio</i>	3	4	0	0	7	10.0	13.3	0.0	0.0	23.3	
			>5 <i>Vibrio</i>	1	0	0	0	1	3.3	0.0	0.0	0.0	3.3	
			<b>Total sponge cells</b>	<b>12</b>	<b>17</b>	<b>1</b>	<b>0</b>	<b>30</b>	<b>40.0</b>	<b>56.7</b>	<b>3.3</b>	<b>0.0</b>	<b>100.0</b>	
		20	1 <i>Vibrio</i>	8	2	0	0	10	26.7	6.7	0.0	0.0	33.3	
			2 <i>Vibrio</i>	4	5	0	0	9	13.3	16.7	0.0	0.0	30.0	
			3-5 <i>Vibrio</i>	5	5	0	0	10	16.7	16.7	0.0	0.0	33.3	
			>5 <i>Vibrio</i>	1	0	0	0	1	3.3	0.0	0.0	0.0	3.3	
			<b>Total sponge cells</b>	<b>18</b>	<b>12</b>	<b>0</b>	<b>0</b>	<b>30</b>	<b>60.0</b>	<b>40.0</b>	<b>0.0</b>	<b>0.0</b>	<b>100.0</b>	
		23	1 <i>Vibrio</i>	8	2	2	0	12	26.7	6.7	6.7	0.0	40.0	
			2 <i>Vibrio</i>	4	2	0	0	6	13.3	6.7	0.0	0.0	20.0	
			3-5 <i>Vibrio</i>	8	3	1	0	12	26.7	10.0	3.3	0.0	40.0	
			>5 <i>Vibrio</i>	0	0	0	0	0	0.0	0.0	0.0	0.0	0.0	
			<b>Total sponge cells</b>	<b>20</b>	<b>7</b>	<b>3</b>	<b>0</b>	<b>30</b>	<b>66.7</b>	<b>23.3</b>	<b>10.0</b>	<b>0.0</b>	<b>100.0</b>	
			<b>Average total sponge cells</b>	<b>16.7</b>	<b>12.0</b>	<b>1.3</b>	<b>0.0</b>		<b>55.6</b>	<b>40.0</b>	<b>4.4</b>	<b>0.0</b>		
				1 <i>Vibrio</i>	5	2	1	0	8	16.7	6.7	3.3	0.0	26.7

60 min	24	2 <i>Vibrio</i>	1	1	0	0	2	3.3	3.3	0.0	0.0	6.7
		3-5 <i>Vibrio</i>	10	5	3	0	18	33.3	16.7	10.0	0.0	60.0
		> 5 <i>Vibrio</i>	0	0	1	1	2	0.0	0.0	3.3	3.3	6.7
		<b>Total sponge cells</b>	<b>16</b>	<b>8</b>	<b>5</b>	<b>1</b>	<b>30</b>	<b>53.3</b>	<b>26.7</b>	<b>16.7</b>	<b>3.3</b>	<b>100.0</b>
	25	1 <i>Vibrio</i>	5	0	2	1	8	16.7	0.0	6.7	3.3	26.7
		2 <i>Vibrio</i>	5	4	1	0	10	16.7	13.3	3.3	0.0	33.3
		3-5 <i>Vibrio</i>	8	1	1	0	10	26.7	3.3	3.3	0.0	33.3
		> 5 <i>Vibrio</i>	1	0	1	0	2	3.3	0.0	3.3	0.0	6.7
		<b>Total sponge cells</b>	<b>19</b>	<b>5</b>	<b>5</b>	<b>1</b>	<b>30</b>	<b>63.3</b>	<b>16.7</b>	<b>16.7</b>	<b>3.3</b>	<b>100.0</b>
	28	1 <i>Vibrio</i>	8	4	3	0	15	26.7	13.3	10.0	0.0	50.0
		2 <i>Vibrio</i>	1	1	0	0	2	3.3	3.3	0.0	0.0	6.7
		3-5 <i>Vibrio</i>	9	1	0	0	10	30.0	3.3	0.0	0.0	33.3
		> 5 <i>Vibrio</i>	2		1	0	3	6.7	0.0	3.3	0.0	10.0
		<b>Total sponge cells</b>	<b>20</b>	<b>6</b>	<b>4</b>	<b>0</b>	<b>30</b>	<b>66.7</b>	<b>20.0</b>	<b>13.3</b>	<b>0.0</b>	<b>100.0</b>
		<b>Average total sponge cells</b>	<b>18.3</b>	<b>6.3</b>	<b>4.7</b>	<b>0.7</b>		<b>61.1</b>	<b>21.1</b>	<b>15.6</b>	<b>2.2</b>	

**Table S4.** PERMANOVA test on the distribution of sponge phagocytic cell types after 30 min and 60 min incubations of *H. panicea* individuals with a sponge-associated (Hal 281) and a non-sponge associated (NJ 1) *Vibrio* isolate.

	Df	Sum of Sqs	R2	F	Pr (> F)
<b>Time</b>	1	0.006481	0.02215	0.2491	0.879
<b>Vibrio Treatment</b>	1	0.075185	0.25696	2.8897	0.030*
<b>Time: Vibrio Treatment</b>	1	0.002778	0.00949	0.1068	0.933
<b>Residual</b>	8	0.208148	0.71139		
<b>Total</b>	11	0.292593	1		

**Table S5.** PERMANOVA test on the distribution of *Vibrio* cells incorporated per sponge phagocytic cell after 30 min and 60 min incubations of *H. panicea* individuals with a sponge-associated (Hal 281) and a non-sponge associated (NJ 1) *Vibrio* isolate.

	Df	Sum of Sqs	R2	F	Pr (> F)
<b>Time</b>	1	0.09478	0.2445	7.9894	0.002**
<b>Vibrio Treatment</b>	1	0.1049	0.27062	8.8427	0.003**
<b>Time: Vibrio Treatment</b>	1	0.09305	0.24005	7.8437	0.003**
<b>Residual</b>	8	0.09491	0.24483		
<b>Total</b>	11	0.38765	1		

**Table S6.** PERMANOVA test on the distribution of *Vibrio* cells incorporated over the different types of sponge phagocytic cells after 30 min and 60 min incubations of *H. panicea* individuals with a sponge-associated (Hal 281) and a non-sponge associated (NJ 1) *Vibrio* isolate.

	Df	Sum of Sqs	R2	F	Pr (> F)
<b>Time</b>	1	0.08991	0.12154	1.5918	0.138
<b>Vibrio Treatment</b>	1	0.14028	0.18964	2.4836	0.025*
<b>Time: Vibrio Treatment</b>	1	0.05769	0.07798	1.0213	0.444
<b>Residual</b>	8	0.45185	0.61084		
<b>Total</b>	11	0.73972	1		

**Table S7.** Annotation of differentially abundant proteins (DAPs) identified after incubating *H. panicea* with a sponge-associated (Hal 281) and a non-sponge-associated (NJ 1) *Vibrio* isolate. Individuals incubated without isolate served as control (n = 4 biological replicates per treatment). DAPs were defined based on an ANOVA, Permutation-based FDR = 0.05. Annotation was performed with Uniprot identifiers of *Amphimedon queenslandica* by BlastP (Uniprot UP000007879\_444682) or to KEGG identifiers by BLASTKOALA using Eukaryotes KEGG gene database.

Cluster	Accession	KO	BLASTKOALA	Blastp	Description Uniprot	Phagocytic-related	Phagocytic Categories
High Ctrl Only	TRINITY_DN8351_c0_g1_i7.p1					No-annotation	
High Ctrl Only	TRINITY_DN2445_c0_g1_i5.p1	K01519	rdgB, ITPA; XTP/dITP diphosphohydrolase [EC:3.6.1.66]	A0A1X7T0D9	Inosine triphosphate pyrophosphatase (ITPase) (Inosine triphosphatase) (EC 3.6.1.9)	No	
High Ctrl Only	TRINITY_DN299_c3_g1_i2.p3	K20526	TAGLN; transgelin	A0A1X7U0W7	Transgelin	No	
High Ctrl Only	TRINITY_DN9283_c1_g1_i9.p1			A0A1X7UN38	Peptidase M28 domain-containing protein	No	
High Ctrl Only	TRINITY_DN5863_c1_g1_i3.p1	K20472	COPZ, RET3; coatomer subunit zeta	A0A1X7VC07	Coatomer subunit zeta	Yes	Membrane traffic
High Ctrl Only	TRINITY_DN2818_c0_g1_i8.p1	K18758	DIS3L2; DIS3-like exonuclease 2 [EC:3.1.13.-]	A0A1X7VCG6	Ribonuclease II/R domain-containing protein	No	
High Ctrl Only	TRINITY_DN13251_c0_g1_i2.p1	K14427	SLC12A4_6, KCC1_3; solute carrier family 12 (potassium/chloride transporter), member 4/6	A0A1X7VDK4	Solute carrier family 12 member 6	No	
High Ctrl Only	TRINITY_DN7336_c0_g1_i7.p3			A0A1X7VQ35	tRNA(His) guanylyltransferase (EC 2.7.7.79) (tRNA-histidine guanylyltransferase)	No	
High Ctrl Only	TRINITY_DN30291_c2_g1_i7.p1	K02150	ATPeV1E, ATP6E; V-type H <sup>+</sup> -transporting ATPase subunit E	A0A1X7VQF5	Uncharacterized protein	Yes	Phagosomal
High Ctrl Only	TRINITY_DN2667_c0_g1_i14.p2			A0A1X7VQM3	116 kDa U5 small nuclear ribonucleoprotein component (U5 snRNP-specific protein, 116 kDa)	No	
High Ctrl Only	TRINITY_DN740_c0_g1_i11.p1	K11997	TRIM2_3; tripartite motif-containing protein 2/3	A0A1X7VR60	Protein rolling stone	No	
High Ctrl Only	TRINITY_DN20166_c0_g3_i5.p2			A0A1X7VS19	urocanate hydratase (EC 4.2.1.49)	No	

					(Imidazolonepropionate hydrolase)		
High Ctrl Only	TRINITY_DN58393_c0_g1_i10.p1			A0A1X7VST2	Actin, cytoplasmic	No	
High Ctrl Only	TRINITY_DN3162_c0_g2_i1.p1	K00789	metK, MAT; S-adenosylmethionine synthetase [EC:2.5.1.6]	A0A1X7VTR8	S-adenosylmethionine synthase (EC 2.5.1.6)	No	
High Ctrl Only	TRINITY_DN2840_c0_g1_i3.p5	K08678	UXS1, uxs; UDP-glucuronate decarboxylase [EC:4.1.1.35]	A0A1X7VUR8	Tubulin/FtsZ GTPase domain-containing protein	No	
High Ctrl Only	TRINITY_DN1353_c0_g1_i3.p1	K17276	LCP1, PLS2; plastin-2	A0A1X7VVY2	Calponin-homology (CH) domain-containing protein	No	
High Hal281 & Ctrl	TRINITY_DN3803_c2_g1_i4.p1					No-annotation	
High Hal281 & Ctrl	TRINITY_DN3803_c0_g1_i3.p1					No-annotation	
High Hal281 & Ctrl	TRINITY_DN926_c7_g1_i11.p1					No-annotation	
High Hal281 & Ctrl	TRINITY_DN20062_c0_g3_i1.p1	K23886	CISD3; CDGSH iron-sulfur domain-containing protein 3			No	
High Hal281 & Ctrl	TRINITY_DN679_c5_g1_i2.p1					No-annotation	
High Hal281 & Ctrl	TRINITY_DN17089_c3_g1_i13.p1					No-annotation	
High Hal281 & Ctrl	TRINITY_DN13061_c0_g1_i1.p1					No-annotation	
High Hal281 & Ctrl	TRINITY_DN867_c0_g1_i4.p1					No-annotation	
High Hal281 & Ctrl	TRINITY_DN14609_c0_g1_i6.p1					No-annotation	
High Hal281 & Ctrl	TRINITY_DN2430_c2_g1_i1.p1			A0A1X7SNZ7	AlG1-type G domain-containing protein	No	
High Hal281 & Ctrl	TRINITY_DN12544_c0_g2_i1.p1	K01623	ALDO; fructose-bisphosphate aldolase, class I [EC:4.1.2.13]	A0A1X7SZF7	Fructose-bisphosphate aldolase (EC 4.1.2.13)	Yes	Lysosomal
High Hal281 & Ctrl	TRINITY_DN95643_c0_g2_i1.p1	K00411	UQCRFS1, RIP1, petA; ubiquinol-cytochrome c reductase iron-sulfur subunit [EC:7.1.1.8]	A0A1X7T0S8	Cytochrome b-c1 complex subunit Rieske, mitochondrial (EC 7.1.1.8)	No	
High Hal281 & Ctrl	TRINITY_DN2016_c0_g1_i3.p1	K03260	EIF4G; translation initiation factor 4G	A0A1X7TEU7	MI domain-containing protein	No	

High Hal281 & Ctrl	TRINITY_DN14023_c0_g3_i1.p1	K02985	RP-S3e, RPS3; small subunit ribosomal protein S3e	A0A1X7THU3	KH type-2 domain-containing protein	No	
High Hal281 & Ctrl	TRINITY_DN114750_c1_g2_i3.p1	K17920	SNX5_6_32; sorting nexin-5/6/32	A0A1X7TMD9	Sorting nexin	Yes	Membrane traffic
High Hal281 & Ctrl	TRINITY_DN6159_c0_g1_i20.p1			A0A1X7TSL3	WW domain-containing protein	No	
High Hal281 & Ctrl	TRINITY_DN10009_c0_g2_i1.p1	K13199	SERBP1; plasminogen activator inhibitor 1 RNA-binding protein	A0A1X7TTK2	Hyaluronan/mRNA-binding protein domain-containing protein	No	
High Hal281 & Ctrl	TRINITY_DN3793_c1_g1_i9.p1			A0A1X7TTU0	DUF4604 domain-containing protein	No	
High Hal281 & Ctrl	TRINITY_DN19096_c0_g1_i1.p1			A0A1X7TY06	Protein MIX23 (Coiled-coil domain-containing protein 58)	No	
High Hal281 & Ctrl	TRINITY_DN10125_c0_g1_i3.p1	K22556	MANF, ARMET; mesencephalic astrocyte-derived neurotrophic factor	A0A1X7TYG8	Mesencephalic astrocyte-derived neurotrophic factor homolog	Yes	Membrane traffic
High Hal281 & Ctrl	TRINITY_DN2771_c0_g1_i4.p1	K01206	FUCA; alpha-L-fucosidase [EC:3.2.1.51]	A0A1X7TZM7	alpha-L-fucosidase (EC 3.2.1.51)	Yes	Lysosomal
High Hal281 & Ctrl	TRINITY_DN14926_c2_g3_i3.p1	K22611	SART3, TIP110; squamous cell carcinoma antigen recognized by T-cells 3	A0A1X7TZW4	RRM domain-containing protein	No	
High Hal281 & Ctrl	TRINITY_DN27077_c0_g1_i4.p1	K06669	SMC3, CSPG6; structural maintenance of chromosome 3 (chondroitin sulfate proteoglycan 6)	A0A1X7U030	Structural maintenance of chromosomes protein	No	
High Hal281 & Ctrl	TRINITY_DN3289_c0_g2_i4.p1			A0A1X7U0Z0	Ig-like domain-containing protein	No	
High Hal281 & Ctrl	TRINITY_DN1226_c0_g3_i1.p1			A0A1X7U3N9	Uncharacterized protein	No	
High Hal281 & Ctrl	TRINITY_DN19303_c0_g2_i1.p1	K08892	FRK, PTK5; fyn-related kinase [EC:2.7.10.2]	A0A1X7U4U3	Tyrosine-protein kinase (EC 2.7.10.2)	No	
High Hal281 & Ctrl	TRINITY_DN9829_c0_g1_i7.p1	K12867	SYF1, XAB2; pre-mRNA-splicing factor SYF1	A0A1X7U5R1	C-terminal of Roc (COR) domain-containing protein	No	
High Hal281 & Ctrl	TRINITY_DN62362_c0_g1_i1.p1	K08738	CYC; cytochrome c	A0A1X7U633	Cytochrome c domain-containing protein	No	
High Hal281 & Ctrl	TRINITY_DN1206_c0_g2_i1.p1	K00103	GULO; L-gulonolactone oxidase [EC:1.1.3.8]	A0A1X7U6Y7	Uncharacterized protein	No	
High Hal281 & Ctrl	TRINITY_DN12127_c0_g3_i3.p1	K11093	SNRP70; U1 small nuclear ribonucleoprotein 70kDa	A0A1X7U7Z5	Uncharacterized protein	No	



High Hal281 & Ctrl	TRINITY_DN4993_c0_g1_i1.p1	K13948	PTGR1, LTB4DH; prostaglandin reductase 1 [EC:1.3.1.74 1.3.1.48]	A0A1X7U9E1	Prostaglandin reductase 1 (EC 1.3.1.48) (EC 1.3.1.74) (15-oxoprostaglandin 13-reductase) (Dithiolethione-inducible gene 1 protein) (Leukotriene B4 12-hydroxydehydrogenase) (NAD(P)H-dependent alkenal/one oxidoreductase)	No	
High Hal281 & Ctrl	TRINITY_DN263_c0_g1_i4.p1	K13948	PTGR1, LTB4DH; prostaglandin reductase 1 [EC:1.3.1.74 1.3.1.48]	A0A1X7U9E1	Prostaglandin reductase 1 (EC 1.3.1.48) (EC 1.3.1.74) (15-oxoprostaglandin 13-reductase) (Dithiolethione-inducible gene 1 protein) (Leukotriene B4 12-hydroxydehydrogenase) (NAD(P)H-dependent alkenal/one oxidoreductase)	No	
High Hal281 & Ctrl	TRINITY_DN33799_c0_g1_i13.p1	K01136	IDS; iduronate 2-sulfatase [EC:3.1.6.13]	A0A1X7UBT9	Sulfatase N-terminal domain-containing protein	Yes	Membrane traffic
High Hal281 & Ctrl	TRINITY_DN20330_c0_g1_i2.p2			A0A1X7UEP5	Trafficking protein particle complex subunit	No	
High Hal281 & Ctrl	TRINITY_DN13864_c1_g1_i21.p2	K11338	RUVBL2, RVB2, INO80J; RuvB-like protein 2 [EC:5.6.2.3]	A0A1X7UGJ6	cysteine--tRNA ligase (EC 6.1.1.16) (Cysteinyl-tRNA synthetase)	No	
High Hal281 & Ctrl	TRINITY_DN5143_c1_g1_i5.p1	K20002	SNAPIN, BLOC1S7; SNARE-associated protein Snapin	A0A1X7UHN4	Biogenesis of lysosome-related organelles complex 1 subunit 7	Yes	Membrane traffic
High Hal281 & Ctrl	TRINITY_DN63123_c0_g2_i1.p1	K00942	gmk, GUK1; guanylate kinase [EC:2.7.4.8]	A0A1X7UIQ5	guanylate kinase (EC 2.7.4.8)	No	
High Hal281 & Ctrl	TRINITY_DN1115_c0_g1_i4.p1	K01115	PLD1_2; phospholipase D1/2 [EC:3.1.4.4]	A0A1X7UIT5	phospholipase D (EC 3.1.4.4)	Yes	Membrane traffic
High Hal281 & Ctrl	TRINITY_DN12364_c4_g1_i1.p1			A0A1X7UM63	UBA domain-containing protein	No	
High Hal281 & Ctrl	TRINITY_DN6631_c0_g2_i2.p1	K02893	RP-L23Ae, RPL23A; large subunit ribosomal protein L23Ae	A0A1X7UMC8	Large ribosomal subunit protein uL23 N-terminal domain-containing protein	No	
High Hal281 & Ctrl	TRINITY_DN14217_c0_g1_i2.p1			A0A1X7UMS0	G-protein coupled receptors family 1 profile domain-containing protein	No	

High Hal281 & Ctrl	TRINITY_DN8122_c0_g1_i5.p1	K25824	ABHD16A; abhydrolase domain-containing protein 16A [EC:3.1.1.23 3.1.-.-]	A0A1X7UN35	AB hydrolase-1 domain-containing protein	No	
High Hal281 & Ctrl	TRINITY_DN3545_c0_g2_i15.p1	K15630	VTC2; GDP-D-glucose phosphorylase [EC:2.7.7.78]	A0A1X7UNE6	GDP-D-glucose phosphorylase 1 (EC 2.7.7.78)	No	
High Hal281 & Ctrl	TRINITY_DN2613_c0_g1_i2.p1	K12599	SKI2, SKIV2L; antiviral helicase SKI2 [EC:3.6.4.13]	A0A1X7UQ17	Helicase SKI2W	No	
High Hal281 & Ctrl	TRINITY_DN30119_c3_g1_i1.p1	K04552	UBE2L3, UBCH7; ubiquitin-conjugating enzyme E2 L3 [EC:2.3.2.23]	A0A1X7UR37	UBC core domain-containing protein	No	
High Hal281 & Ctrl	TRINITY_DN3846_c0_g1_i11.p2	K14411	MSI; RNA-binding protein Musashi	A0A1X7UR52	Cytochrome b5 heme-binding domain-containing protein	No	
High Hal281 & Ctrl	TRINITY_DN5620_c0_g2_i7.p2	K16465	CETN1; centrin-1	A0A1X7USU2	C2 domain-containing protein	No	
High Hal281 & Ctrl	TRINITY_DN42823_c0_g1_i1.p2			A0A1X7UT39	Protein-tyrosine-phosphatase	No	
High Hal281 & Ctrl	TRINITY_DN2297_c0_g1_i10.p1	K11997	TRIM2_3; tripartite motif-containing protein 2/3	A0A1X7UTY4	RING-type E3 ubiquitin transferase (EC 2.3.2.27)	No	
High Hal281 & Ctrl	TRINITY_DN2674_c0_g1_i9.p2			A0A1X7UV34	Molybdopterin synthase catalytic subunit (EC 2.8.1.12) (Molybdenum cofactor synthesis protein 2 large subunit) (Molybdenum cofactor synthesis protein 2B) (MOCS2B)	No	
High Hal281 & Ctrl	TRINITY_DN24605_c0_g1_i4.p2	K17917	SNX1_2; sorting nexin-1/2	A0A1X7UV49	PX domain-containing protein	Yes	Membrane traffic
High Hal281 & Ctrl	TRINITY_DN10958_c0_g2_i3.p2	K02937	RP-L7e, RPL7; large subunit ribosomal protein L7e	A0A1X7UX89	Ribosomal protein L30 ferredoxin-like fold domain-containing protein	No	
High Hal281 & Ctrl	TRINITY_DN1884_c0_g1_i4.p1			A0A1X7UXU9	CUB domain-containing protein	No	
High Hal281 & Ctrl	TRINITY_DN4750_c0_g2_i1.p1	K20371	NUCB; nucleobindin	A0A1X7UY00	EF-hand domain-containing protein	Yes	Membrane traffic
High Hal281 & Ctrl	TRINITY_DN12109_c1_g2_i1.p1	K10141	SESN1_3; sestrin 1/3	A0A1X7UZB9	Sestrin	No	
High Hal281 & Ctrl	TRINITY_DN28151_c0_g2_i11.p2			A0A1X7V001	Prefoldin subunit 3	No	

High Hal281 & Ctrl	TRINITY_DN283_c0_g1_i4.p1	K15261	PARP10_14_15; poly [ADP-ribose] polymerase 10/14/15 [EC:2.4.2.30]	A0A1X7V0F1	Poly [ADP-ribose] polymerase (PARP) (EC 2.4.2.-)	No	
High Hal281 & Ctrl	TRINITY_DN1119_c0_g1_i4.p1	K05762	RDX; radixin	A0A1X7V0M3	Uncharacterized protein	Yes	Cytoskeletal
High Hal281 & Ctrl	TRINITY_DN19838_c0_g1_i6.p1	K24962	CCDC47; PAT complex subunit CCDC47	A0A1X7V0W8	PAT complex subunit CCDC47 (Coiled-coil domain-containing protein 47)	Yes	Membrane traffic
High Hal281 & Ctrl	TRINITY_DN5256_c0_g1_i5.p1	K12828	SF3B1, SAP155; splicing factor 3B subunit 1	A0A1X7V190	Splicing factor 3B subunit 1 domain-containing protein	No	
High Hal281 & Ctrl	TRINITY_DN2376_c0_g3_i1.p3	K02912	RP-L32e, RPL32; large subunit ribosomal protein L32e	A0A1X7V1L2	Leucine-rich repeat protein SHOC-2	No	
High Hal281 & Ctrl	TRINITY_DN11421_c0_g1_i10.p1	K18735	SMG9; protein SMG9	A0A1X7V2I2	Ubiquitin-like domain-containing protein	No	
High Hal281 & Ctrl	TRINITY_DN3416_c0_g1_i4.p1			A0A1X7V3T3	EF-hand domain-containing protein	No	
High Hal281 & Ctrl	TRINITY_DN24793_c0_g2_i1.p1			A0A1X7V3T3	EF-hand domain-containing protein	No	
High Hal281 & Ctrl	TRINITY_DN9871_c0_g1_i5.p1	K15026	EIF2A; translation initiation factor 2A	A0A1X7V3V6	Amidase domain-containing protein	No	
High Hal281 & Ctrl	TRINITY_DN3999_c0_g3_i3.p1			A0A1X7V4F9	ABC transporter domain-containing protein	No	
High Hal281 & Ctrl	TRINITY_DN1665_c0_g1_i5.p2	K11153	RDH12; retinol dehydrogenase 12 [EC:1.1.1.300]	A0A1X7V606	Retinol dehydrogenase 13	No	
High Hal281 & Ctrl	TRINITY_DN6265_c0_g1_i1.p1			A0A1X7V6B1	BIG2 domain-containing protein	No	
High Hal281 & Ctrl	TRINITY_DN7897_c0_g1_i4.p1	K11729	ACAD10; acyl-CoA dehydrogenase family member 10	A0A1X7V919	Acyl-CoA dehydrogenase family member 10	No	
High Hal281 & Ctrl	TRINITY_DN20919_c0_g1_i3.p1	K24086	EIF4H; translation initiation factor 4H	A0A1X7V9Z4	Eukaryotic translation initiation factor 4H	No	
High Hal281 & Ctrl	TRINITY_DN24193_c0_g1_i1.p1			A0A1X7VA11	Splicing factor YJU2	No	
High Hal281 & Ctrl	TRINITY_DN691_c0_g1_i14.p1			A0A1X7VDA5	Pre-mRNA-splicing factor RBM22 (RNA-binding motif protein 22)	No	
High Hal281 & Ctrl	TRINITY_DN12332_c0_g1_i1.p2			A0A1X7VDJ5	tRNA (guanine-N(7))-methyltransferase (EC 2.1.1.33) (tRNA (guanine(46)-N(7))-methyltransferase)	No	

					(tRNA(m7G46)-methyltransferase)		
High Hal281 & Ctrl	TRINITY_DN1366_c1_g1_i7.p1	K04648	DCTN1; dynactin 1	A0A1X7VDP2	Dynein associated protein domain-containing protein	Yes	Cytoskeletal
High Hal281 & Ctrl	TRINITY_DN57904_c0_g2_i2.p1	K03231	EEF1A; elongation factor 1-alpha	A0A1X7VE16	Elongation factor 1-alpha	Yes	Exosomal
High Hal281 & Ctrl	TRINITY_DN19498_c1_g1_i3.p1	K14824	ERB1, BOP1; ribosome biogenesis protein ERB1	A0A1X7VEG3	Uncharacterized protein	No	
High Hal281 & Ctrl	TRINITY_DN3056_c0_g1_i7.p1			A0A1X7VF02	Protein kinase domain-containing protein	No	
High Hal281 & Ctrl	TRINITY_DN1284_c0_g1_i1.p2	K25698	TPPP2; tubulin polymerization-promoting protein family member 2	A0A1X7VF94	RNA transcription, translation and transport factor protein	No	
High Hal281 & Ctrl	TRINITY_DN4917_c0_g1_i3.p3			A0A1X7VHG1	Phenylalanine--tRNA ligase beta subunit (EC 6.1.1.20) (Phenylalanyl-tRNA synthetase beta subunit)	No	
High Hal281 & Ctrl	TRINITY_DN24524_c0_g1_i13.p1	K04373	RPS6KA; ribosomal protein S6 kinase alpha-1/2/3/6 [EC:2.7.11.1]	A0A1X7VHV5	Ribosomal protein S6 kinase (EC 2.7.11.1)	No	
High Hal281 & Ctrl	TRINITY_DN13411_c0_g2_i2.p2			A0A1X7VI08	Beta-catenin-interacting ICAT domain-containing protein	No	
High Hal281 & Ctrl	TRINITY_DN660_c0_g1_i2.p2			A0A1X7VIJ7	PH domain-containing protein	No	
High Hal281 & Ctrl	TRINITY_DN6080_c1_g1_i1.p1	K03259	EIF4E; translation initiation factor 4E	A0A1X7VIM6	EIF-4F 25 kDa subunit	No	
High Hal281 & Ctrl	TRINITY_DN8001_c0_g2_i5.p2	K02872	RP-L13Ae, RPL13A; large subunit ribosomal protein L13Ae	A0A1X7VJE9	J domain-containing protein	No	
High Hal281 & Ctrl	TRINITY_DN21951_c1_g1_i3.p1			A0A1X7VKP2	Uncharacterized protein	No	
High Hal281 & Ctrl	TRINITY_DN90_c3_g1_i2.p1	K11660	MTA; metastasis-associated protein MTA	A0A1X7VL95	BAH domain-containing protein	No	
High Hal281 & Ctrl	TRINITY_DN333_c1_g1_i1.p1			A0A1X7VLI1	AAA+ ATPase domain-containing protein	No	
High Hal281 & Ctrl	TRINITY_DN10641_c0_g1_i11.p3			A0A1X7VM08	Sulfotransferase domain-containing protein	No	

High Hal281 & Ctrl	TRINITY_DN4810_c0_g1_i5.p2	K03139	TFIIF2, GTF2F2, TFG2; transcription initiation factor TFIIF subunit beta [EC:5.6.2.-]	A0A1X7VM74	Uncharacterized protein	No	
High Hal281 & Ctrl	TRINITY_DN7587_c0_g1_i4.p1	K22824	WTAP; pre-mRNA-splicing regulator WTAP	A0A1X7VMA1	Pre-mRNA-splicing regulator WTAP	No	
High Hal281 & Ctrl	TRINITY_DN8663_c0_g2_i1.p1			A0A1X7VMX0	K Homology domain-containing protein	No	
High Hal281 & Ctrl	TRINITY_DN19943_c2_g1_i6.p2			A0A1X7VNC2	Sulfatase N-terminal domain-containing protein	No	
High Hal281 & Ctrl	TRINITY_DN5363_c0_g1_i38.p4	K08512	VAMP8; vesicle-associated membrane protein 8	A0A1X7VNL5	Migration and invasion-inhibitory protein	Yes	Membrane traffic
High Hal281 & Ctrl	TRINITY_DN20317_c0_g1_i5.p1	K11493	RCC1; regulator of chromosome condensation	A0A1X7VNN0	Regulator of chromosome condensation	No	
High Hal281 & Ctrl	TRINITY_DN844_c0_g1_i5.p2			A0A1X7VNP2	Calcineurin-like phosphoesterase domain-containing protein	No	
High Hal281 & Ctrl	TRINITY_DN3194_c2_g1_i2.p1	K22182	TXNRD; thioredoxin reductase (NADPH) [EC:1.8.1.9]	A0A1X7VNZ7	L-tryptophan decarboxylase PsiD-like domain-containing protein	No	
High Hal281 & Ctrl	TRINITY_DN14177_c0_g1_i1.p2	K05609	UCHL3, YUH1; ubiquitin carboxyl-terminal hydrolase L3 [EC:3.4.19.12]	A0A1X7VP25	Magnesium transporter protein 1	No	
High Hal281 & Ctrl	TRINITY_DN46673_c0_g1_i3.p1			A0A1X7VPA2	Protein kinase domain-containing protein	No	
High Hal281 & Ctrl	TRINITY_DN17875_c1_g1_i1.p1			A0A1X7VRJ5	SH2 domain-containing protein	No	
High Hal281 & Ctrl	TRINITY_DN21078_c0_g1_i4.p1	K02955	RP-S14e, RPS14; small subunit ribosomal protein S14e	A0A1X7VRN9	40S ribosomal protein S14	No	
High Hal281 & Ctrl	TRINITY_DN6474_c0_g1_i6.p2			A0A1X7VRZ8	Carboxypeptidase (EC 3.4.16.-)	No	
High Hal281 & Ctrl	TRINITY_DN22032_c0_g2_i1.p1			A0A1X7VRZ8	Carboxypeptidase (EC 3.4.16.-)	No	
High Hal281 & Ctrl	TRINITY_DN55568_c0_g1_i4.p2			A0A1X7VRZ8	Carboxypeptidase (EC 3.4.16.-)	No	
High Hal281 & Ctrl	TRINITY_DN84435_c0_g2_i3.p1	K09548	PFDN1; prefoldin subunit 1	A0A1X7VT33	Prefoldin subunit 1	No	
High Hal281 & Ctrl	TRINITY_DN1513_c0_g4_i2.p2	K05607	AUH; methylglutaconyl-CoA hydratase [EC:4.2.1.18]	A0A1X7VTG8	Enoyl-CoA hydratase	No	

High Hal281 & Ctrl	TRINITY_DN10501_c1_g1_i1.p1			A0A1X7VTJ7	GRIP domain-containing protein	No	
High Hal281 & Ctrl	TRINITY_DN12217_c0_g1_i2.p1	K24660	HMG20A; high mobility group protein 20A	A0A1X7VUJ1	HMG box domain-containing protein	No	
High Hal281 & Ctrl	TRINITY_DN1040_c2_g1_i9.p1			A0A1X7VUT6	Phosphoinositide phospholipase C (EC 3.1.4.11)	No	
High Hal281 & Ctrl	TRINITY_DN6365_c0_g1_i3.p2			A0A1X7VVE6	ABC transporter domain-containing protein	No	
High Hal281 & Ctrl	TRINITY_DN7688_c0_g1_i5.p1			A0A1X7VVH5	DJ-1/Pfpl domain-containing protein	No	
High Hal281 & Ctrl	TRINITY_DN2402_c0_g1_i6.p1			A0A1X7VVV7	Uncharacterized protein	No	
High Hal281 & Ctrl	TRINITY_DN7597_c1_g1_i2.p1	K01869	LARS, leuS; leucyl-tRNA synthetase [EC:6.1.1.4]	A0A1X7VW27	Nucleoporin NDC1	No	
High Hal281 & Ctrl	TRINITY_DN3816_c0_g1_i1.p2	K14012	NSFL1C, UBX1, SHP1; UBX domain-containing protein 1	A0A1X7VW37	Uncharacterized protein	Yes	Membrane traffic
High Hal281 & Ctrl	TRINITY_DN2762_c0_g1_i3.p1			A0A1X7VWN6	HEPN domain-containing protein	No	
High Hal281 & Ctrl	TRINITY_DN315_c0_g1_i7.p1	K01895	ACSS1_2, acs; acetyl-CoA synthetase [EC:6.2.1.1]	A0A1X7VXU5	Delta-like protein	No	
High Hal281 & Ctrl	TRINITY_DN13372_c0_g1_i13.p3	K02951	RP-S12e, RPS12; small subunit ribosomal protein S12e	I1EYW3	40S ribosomal protein S12	No	
High Hal281 & Ctrl	TRINITY_DN22768_c0_g1_i2.p1			I1G9C5	Histone H3	No	
High Hal281 Only	TRINITY_DN564_c0_g1_i17.p1					No-annotation	
High Hal281 Only	TRINITY_DN1173_c0_g1_i3.p1					No-annotation	
High Hal281 Only	TRINITY_DN890_c0_g1_i14.p1					No-annotation	
High Hal281 Only	TRINITY_DN34460_c0_g1_i2.p1					No-annotation	
High Hal281 Only	TRINITY_DN22712_c0_g2_i4.p1					No-annotation	
High Hal281 Only	TRINITY_DN37373_c2_g1_i1.p1					No-annotation	
High Hal281 Only	TRINITY_DN33320_c5_g1_i1.p1					No-annotation	
High Hal281 Only	TRINITY_DN893_c0_g1_i6.p1					No-annotation	

High Hal281 Only	TRINITY_DN39996_c2_g1_i2.p1			A0A1X7TP97	Non-specific serine/threonine protein kinase	No	
High Hal281 Only	TRINITY_DN139476_c0_g1_i1.p1			A0A1X7TXX4	AlG1-type G domain-containing protein	No	
High Hal281 Only	TRINITY_DN509_c0_g1_i4.p1	K12035	TRIM71; tripartite motif-containing protein 71 [EC:2.3.2.27]	A0A1X7U9L5	B-box C-terminal domain-containing protein	No	
High Hal281 Only	TRINITY_DN9690_c0_g1_i4.p1	K17969	FIS1, TTC11, MDV2; mitochondrial fission 1 protein	A0A1X7UDX5	Mitochondrial fission 1 protein	No	
High Hal281 Only	TRINITY_DN3806_c0_g1_i2.p2	K01015	SULT2B; alcohol sulfotransferase [EC:2.8.2.2]	A0A1X7UJA4	Sulfotransferase domain-containing protein	No	
High Hal281 Only	TRINITY_DN216_c0_g2_i1.p1			A0A1X7UW90	Uncharacterized protein	No	
High Hal281 Only	TRINITY_DN7418_c0_g1_i7.p1			A0A1X7UZ7	SH3 domain-containing protein	No	
High Hal281 Only	TRINITY_DN73920_c0_g1_i4.p1	K04077	groEL, HSPD1; chaperonin GroEL [EC:5.6.1.7]	A0A1X7V1A0	Heat shock protein 60	Yes	Exosomal
High Hal281 Only	TRINITY_DN2227_c0_g1_i3.p1	K01870	IARS, ileS; isoleucyl-tRNA synthetase [EC:6.1.1.5]	A0A1X7V5F0	isoleucine--tRNA ligase (EC 6.1.1.5) (Isoleucyl-tRNA synthetase)	No	
High Hal281 Only	TRINITY_DN11946_c0_g2_i7.p1	K04400	CASP10; caspase 10 [EC:3.4.22.63]	A0A1X7VBB3	Caspase-8	No	
High Hal281 Only	TRINITY_DN7047_c0_g1_i1.p1			A0A1X7VCU0	PH domain-containing protein	No	
High Hal281 Only	TRINITY_DN34967_c0_g1_i3.p1	K15559	RTT103; regulator of Ty1 transposition protein 103	A0A1X7VEG0	CID domain-containing protein	No	
High Hal281 Only	TRINITY_DN6238_c0_g1_i4.p1			A0A1X7VH98	Nucleoprotein TPR	No	
High Hal281 Only	TRINITY_DN4500_c0_g1_i3.p2	K09022	ridA, tdcF, RIDA; 2-iminobutanoate/2-iminopropanoate deaminase [EC:3.5.99.10]	A0A1X7VMR6	Ribonucleases P/MRP protein subunit POP1	No	
High Hal281 Only	TRINITY_DN20864_c0_g1_i2.p1			A0A1X7VPY3	FHA domain-containing protein	No	
High Hal281 Only	TRINITY_DN1153_c2_g1_i9.p1	K20406	NPRL3, NPR3; nitrogen permease regulator 3	A0A1X7VQ05	Small ribosomal subunit protein mS26 (28S ribosomal protein S26, mitochondrial)	No	
High Hal281 Only	TRINITY_DN3163_c0_g2_i1.p1			A0A1X7VUQ0	Uncharacterized protein	No	

High Hal281 Only	TRINITY_DN6489_c0_g1_i7.p1	K07195	EXOC7, EXO70; exocyst complex component 7	A0A1X7VV91	Exocyst complex component 7 (Exocyst complex component Exo70)	Yes	Exosomal
High Hal281 Only	TRINITY_DN782_c0_g1_i2.p1			A0A1X7VXI4	START domain-containing protein	No	
High NJ1 & Ctrl	TRINITY_DN3708_c0_g2_i1.p1					No-annotation	
High NJ1 & Ctrl	TRINITY_DN8988_c0_g1_i1.p1	K09702	K09702; uncharacterized protein			No	
High NJ1 & Ctrl	TRINITY_DN35328_c0_g1_i1.p1					No-annotation	
High NJ1 & Ctrl	TRINITY_DN92585_c2_g1_i1.p1			A0A1X7TD70	Amine oxidase domain-containing protein	No	
High NJ1 & Ctrl	TRINITY_DN4049_c0_g1_i8.p1			A0A1X7TRD1	Non-specific serine/threonine protein kinase	No	
High NJ1 & Ctrl	TRINITY_DN6858_c0_g1_i5.p1			A0A1X7TZ57	Protein pelota homolog	No	
High NJ1 & Ctrl	TRINITY_DN3563_c0_g1_i5.p1	K00463	IDO, INDO; indoleamine 2,3-dioxygenase [EC:1.13.11.52]	A0A1X7TZT1	Methyltransferase domain-containing protein	No	
High NJ1 & Ctrl	TRINITY_DN13123_c0_g1_i2.p1	K13352	PEX11B; peroxin-11B	A0A1X7U2E7	Peroxisomal membrane protein 11B	No	
High NJ1 & Ctrl	TRINITY_DN17398_c1_g1_i1.p1	K04615	GABBR; gamma-aminobutyric acid type B receptor	A0A1X7U6B7	G-protein coupled receptors family 3 profile domain-containing protein	No	
High NJ1 & Ctrl	TRINITY_DN145854_c0_g1_i6.p1	K18752	TNPO1, IPO2, KPNB2; transportin-1	A0A1X7U7W8	Importin N-terminal domain-containing protein	No	
High NJ1 & Ctrl	TRINITY_DN15929_c0_g2_i3.p1	K25374	BPI; bactericidal permeability-increasing protein	A0A1X7UE02	Bactericidal permeability-increasing protein	No	
High NJ1 & Ctrl	TRINITY_DN94559_c2_g1_i1.p1	K19788	OLA1; obg-like ATPase 1	A0A1X7UH37	Obg-like ATPase 1	No	
High NJ1 & Ctrl	TRINITY_DN4573_c0_g1_i3.p1			A0A1X7UVX7	Enhancer of mRNA-decapping protein 4 WD40 repeat region domain-containing protein	No	
High NJ1 & Ctrl	TRINITY_DN849_c2_g1_i1.p1			A0A1X7UWI5	SH3 domain-containing protein	No	
High NJ1 & Ctrl	TRINITY_DN895_c0_g1_i2.p1	K00864	glpK, GK; glycerol kinase [EC:2.7.1.30]	A0A1X7V009	Coatomer subunit delta	No	
High NJ1 & Ctrl	TRINITY_DN1958_c0_g1_i10.p1			A0A1X7V085	Ion transport domain-containing protein	No	



High NJ1 & Ctrl	TRINITY_DN6817_c0_g2_i1.p1			A0A1X7V5W1	Alpha-1,4 glucan phosphorylase (EC 2.4.1.1)	No	
High NJ1 & Ctrl	TRINITY_DN6817_c0_g1_i5.p1	K00688	PYG, glgP; glycogen phosphorylase [EC:2.4.1.1]	A0A1X7V5W1	Alpha-1,4 glucan phosphorylase (EC 2.4.1.1)	No	
High NJ1 & Ctrl	TRINITY_DN11779_c0_g1_i10.p1			A0A1X7V712	Phosphoinositide phospholipase C (EC 3.1.4.11)	No	
High NJ1 & Ctrl	TRINITY_DN3868_c0_g2_i4.p1			A0A1X7V883	DRBM domain-containing protein	No	
High NJ1 & Ctrl	TRINITY_DN2192_c0_g1_i16.p1	K18695	GPCPD1; glycerophosphocholine phosphodiesterase GPCPD1 [EC:3.1.4.2]	A0A1X7VD87	FAM194 C-terminal domain-containing protein	No	
High NJ1 & Ctrl	TRINITY_DN12629_c0_g3_i3.p1	K20366	ERGIC2, ERV41; endoplasmic reticulum-Golgi intermediate compartment protein 2	A0A1X7VE51	Endoplasmic reticulum vesicle transporter C-terminal domain-containing protein	Yes	Membrane traffic
High NJ1 & Ctrl	TRINITY_DN4834_c0_g1_i1.p1	K13181	DDX27, DRS1; ATP-dependent RNA helicase DDX27 [EC:3.6.4.13]	A0A1X7VF82	RNA helicase (EC 3.6.4.13)	No	
High NJ1 & Ctrl	TRINITY_DN250_c0_g1_i2.p1			A0A1X7VJ85	Uncharacterized protein	No	
High NJ1 & Ctrl	TRINITY_DN13011_c0_g1_i8.p1			A0A1X7VKI0	DUF255 domain-containing protein	No	
High NJ1 & Ctrl	TRINITY_DN1569_c0_g1_i5.p1	K01438	argE; acetylornithine deacetylase [EC:3.5.1.16]	A0A1X7VKX5	Peptidase M20 dimerisation domain-containing protein	No	
High NJ1 & Ctrl	TRINITY_DN5035_c0_g1_i3.p1	K00111	glpA, glpD; glycerol-3-phosphate dehydrogenase [EC:1.1.5.3]	A0A1X7VLK0	RRM domain-containing protein	No	
High NJ1 & Ctrl	TRINITY_DN1293_c0_g1_i1.p1	K06487	ITGAV, CD51; integrin alpha V	A0A1X7VLW0	Integrin alpha-2 domain-containing protein	Yes	Receptor-like
High NJ1 & Ctrl	TRINITY_DN7953_c0_g1_i4.p1	K19480	ANO5, GDD1, TMEM16E; anoctamin-5	A0A1X7VMK6	Anoctamin	No	
High NJ1 & Ctrl	TRINITY_DN38638_c1_g2_i5.p1	K06528	LAMP1_2, CD107; lysosomal-associated membrane protein 1/2	A0A1X7VPB1	Uncharacterized protein	Yes	Lysosomal
High NJ1 & Ctrl	TRINITY_DN33089_c0_g2_i1.p1	K23460	CHM, CHML; Rab proteins geranylgeranyltransferase component A	A0A1X7VPF8	Rab proteins geranylgeranyltransferase component A	Yes	Membrane traffic

High NJ1 & Ctrl	TRINITY_DN18751_c0_g1_i3.p2	K17497	PMM; phosphomannomutase [EC:5.4.2.8]	A0A1X7VQ42	Phosphomannomutase (EC 5.4.2.8)	No	
High NJ1 & Ctrl	TRINITY_DN2558_c0_g1_i4.p1			A0A1X7VQH3	Caspase family p20 domain-containing protein	No	
High NJ1 & Ctrl	TRINITY_DN11077_c0_g1_i3.p2	K07299	SLC2A1, GLUT1; MFS transporter, SP family, solute carrier family 2 (facilitated glucose transporter), member 1	A0A1X7VQT4	Protein kinase domain-containing protein	No	
High NJ1 & Ctrl	TRINITY_DN60971_c0_g1_i1.p2			A0A1X7VST2	Actin, cytoplasmic	No	
High NJ1 & Ctrl	TRINITY_DN1187_c0_g1_i1.p1			A0A1X7VT99	PPM-type phosphatase domain-containing protein	No	
High NJ1 & Ctrl	TRINITY_DN1948_c1_g1_i13.p1	K15303	AKR7; aflatoxin B1 aldehyde reductase	A0A1X7VTB2	NADP-dependent oxidoreductase domain-containing protein	No	
High NJ1 & Ctrl	TRINITY_DN12115_c0_g2_i1.p1			A0A1X7VTT2	RING-type E3 ubiquitin transferase (EC 2.3.2.27)	No	
High NJ1 & Ctrl	TRINITY_DN15170_c1_g1_i7.p1	K05692	ACTB_G1; actin beta/gamma 1	A0A1X7VTY0	Actin, cytoplasmic	Yes	Cytoskeletal
High NJ1 & Ctrl	TRINITY_DN3328_c0_g1_i2.p1			A0A1X7VUM6	FERM domain-containing protein	No	
High NJ1 & Ctrl	TRINITY_DN16044_c0_g1_i1.p1	K07889	RAB5C; Ras-related protein Rab-5C	A0A1X7VWF4	Uncharacterized protein	Yes	Membrane traffic
High NJ1 & Hal281	TRINITY_DN8308_c0_g2_i1.p1					No-annotation	
High NJ1 & Hal281	TRINITY_DN12383_c2_g2_i2.p1					No-annotation	
High NJ1 & Hal281	TRINITY_DN18949_c0_g1_i4.p1					No-annotation	
High NJ1 & Hal281	TRINITY_DN2808_c0_g2_i7.p1			A0A1X7TKJ8	Death domain-containing protein	No	
High NJ1 & Hal281	TRINITY_DN72691_c1_g1_i5.p1	K10415	DYNC1I, DNCI; dynein cytoplasmic 1 intermediate chain	A0A1X7TSM4	Uncharacterized protein	Yes	Cytoskeletal
High NJ1 & Hal281	TRINITY_DN1099_c0_g2_i10.p1			A0A1X7UJW1	Uncharacterized protein	No	
High NJ1 & Hal281	TRINITY_DN11415_c0_g1_i1.p1	K00134	GAPDH, gapA; glyceraldehyde 3-phosphate dehydrogenase (phosphorylating) [EC:1.2.1.12]	A0A1X7UQP4	Glyceraldehyde-3-phosphate dehydrogenase (EC 1.2.1.12)	No	

High NJ1 & Hal281	TRINITY_DN4622_c0_g1_i8.p1	K20180	VPS16; vacuolar protein sorting-associated protein 16	A0A1X7V6T3	Vacuolar protein sorting-associated protein 16 homolog	Yes	Membrane traffic
High NJ1 & Hal281	TRINITY_DN19_c0_g1_i8.p1			A0A1X7VB32	RING-type E3 ubiquitin transferase (EC 2.3.2.27)	No	
High NJ1 & Hal281	TRINITY_DN2567_c0_g1_i7.p1	K01011	TST, MPST, sseA; thiosulfate/3-mercaptopyruvate sulfurtransferase [EC:2.8.1.1 2.8.1.2]	A0A1X7VIT8	Glutamine synthetase (EC 6.3.1.2)	No	
High NJ1 & Hal281	TRINITY_DN3189_c0_g1_i1.p1			A0A1X7VKE7	Ashwin	No	
High NJ1 & Hal281	TRINITY_DN2255_c0_g1_i6.p1	K04958	ITPR1; inositol 1,4,5-triphosphate receptor type 1	A0A1X7VSW4	Inositol 1,4,5-trisphosphate receptor	Yes	Receptor-like
High NJ1 & Hal281	TRINITY_DN7688_c0_g1_i6.p3			A0A1X7VVH5	DJ-1/Pfpl domain-containing protein	No	
High NJ1 Only	TRINITY_DN93186_c1_g1_i1.p1					No-annotation	
High NJ1 Only	TRINITY_DN8869_c0_g1_i1.p1					No-annotation	
High NJ1 Only	TRINITY_DN9634_c0_g3_i1.p1					No-annotation	
High NJ1 Only	TRINITY_DN96913_c0_g1_i1.p1					No-annotation	
High NJ1 Only	TRINITY_DN371_c0_g1_i2.p1					No-annotation	
High NJ1 Only	TRINITY_DN67_c0_g1_i5.p1					No-annotation	
High NJ1 Only	TRINITY_DN14253_c2_g1_i3.p1					No-annotation	
High NJ1 Only	TRINITY_DN1973_c0_g2_i3.p1					No-annotation	
High NJ1 Only	TRINITY_DN613_c0_g1_i1.p1			A0A1X7SNM8	AIG1-type G domain-containing protein	No	
High NJ1 Only	TRINITY_DN173_c0_g1_i5.p1			A0A1X7TK10	AIG1-type G domain-containing protein	No	
High NJ1 Only	TRINITY_DN3176_c1_g1_i1.p1			A0A1X7TK65	Non-specific protein-tyrosine kinase	No	
High NJ1 Only	TRINITY_DN1691_c0_g2_i8.p2			A0A1X7TS74	WW-binding domain-containing protein	No	
High NJ1 Only	TRINITY_DN35543_c0_g1_i4.p1	K12833	SF3B14; pre-mRNA branch site protein p14	A0A1X7U351	RRM domain-containing protein	No	
High NJ1 Only	TRINITY_DN12190_c2_g2_i1.p1			A0A1X7U7C8	Uncharacterized protein	No	

High NJ1 Only	TRINITY_DN97_c0_g1_i4.p1			A0A1X7U7W2	AIG1-type G domain-containing protein	No	
High NJ1 Only	TRINITY_DN32524_c0_g1_i1.p1			A0A1X7UD33	Death domain-containing protein	No	
High NJ1 Only	TRINITY_DN42391_c0_g2_i6.p1	K15436	TRPO3, MTR10; transportin-3	A0A1X7UEC9	Exportin-1/Importin-beta-like domain-containing protein	No	
High NJ1 Only	TRINITY_DN209113_c0_g1_i1.p1	K04628	CGT, UGT8; ceramide galactosyltransferase [EC:2.4.1.47]	A0A1X7UGC0	UDP-glucuronosyltransferase	No	
High NJ1 Only	TRINITY_DN34420_c0_g4_i2.p1			A0A1X7UHE0	Septin-type G domain-containing protein	No	
High NJ1 Only	TRINITY_DN10790_c0_g1_i7.p1	K01867	WARS, trpS; tryptophanyl-tRNA synthetase [EC:6.1.1.2]	A0A1X7UL45	tryptophan--tRNA ligase (EC 6.1.1.2) (Tryptophanyl-tRNA synthetase)	No	
High NJ1 Only	TRINITY_DN10790_c0_g1_i8.p1	K01867	WARS, trpS; tryptophanyl-tRNA synthetase [EC:6.1.1.2]	A0A1X7UL45	tryptophan--tRNA ligase (EC 6.1.1.2) (Tryptophanyl-tRNA synthetase)	No	
High NJ1 Only	TRINITY_DN12277_c0_g1_i2.p2	K14319	RANGAP1; Ran GTPase-activating protein 1	A0A1X7UM55	SRA1/Sec31 domain-containing protein	No	
High NJ1 Only	TRINITY_DN7876_c0_g1_i17.p2			A0A1X7UMC1	C2H2-type domain-containing protein	No	
High NJ1 Only	TRINITY_DN14176_c0_g1_i1.p1	K20293	COG6, COD2; conserved oligomeric Golgi complex subunit 6	A0A1X7UMG8	Conserved oligomeric Golgi complex subunit 6 (COG complex subunit 6) (Component of oligomeric Golgi complex 6)	Yes	Membrane traffic
High NJ1 Only	TRINITY_DN2929_c0_g1_i1.p1	K03936	NDUFS3; NADH dehydrogenase (ubiquinone) Fe-S protein 3 [EC:7.1.1.2]	A0A1X7UMH4	NADH dehydrogenase [ubiquinone] iron-sulfur protein 3, mitochondrial	No	
High NJ1 Only	TRINITY_DN8712_c0_g2_i2.p1	K00413	CYC1, CYT1, petC; ubiquinol-cytochrome c reductase cytochrome c1 subunit	A0A1X7UMH9	Cytochrome c domain-containing protein	No	
High NJ1 Only	TRINITY_DN8863_c0_g2_i1.p1	K00799	GST, gst; glutathione S-transferase [EC:2.5.1.18]	A0A1X7UNK7	Glutathione transferase	No	
High NJ1 Only	TRINITY_DN21587_c0_g2_i3.p1	K10362	MYO18; myosin XVIII	A0A1X7UQG0	Myosin motor domain-containing protein	No	
High NJ1 Only	TRINITY_DN21776_c0_g2_i1.p1	K02264	COX5A; cytochrome c oxidase subunit 5a	A0A1X7USS8	Cytochrome c oxidase subunit 5A, mitochondrial (Cytochrome c oxidase polypeptide Va)	No	
High NJ1 Only	TRINITY_DN4122_c1_g1_i1.p1	K03283	HSPA1_6_8; heat shock 70kDa protein 1/6/8	A0A1X7USZ6	Heat shock protein 70	Yes	Exosomal

High NJ1 Only	TRINITY_DN109820_c0_g1_i3.p2	K00072	SPR; sepiapterin reductase [EC:1.1.1.153]	A0A1X7UUS2	Tubulin/FtsZ GTPase domain-containing protein	No	
High NJ1 Only	TRINITY_DN1451_c1_g1_i8.p1	K15779	PGM2; phosphoglucomutase / phosphopentomutase [EC:5.4.2.2 5.4.2.7]	A0A1X7UVZ2	Glucanase	No	
High NJ1 Only	TRINITY_DN11540_c0_g1_i2.p1	K12366	ELMO1, CED12; engulfment and cell motility protein 1	A0A1X7UWA1	ELMO domain-containing protein	Yes	Cytoskeletal
High NJ1 Only	TRINITY_DN6221_c0_g1_i7.p1	K00940	ndk, NME; nucleoside-diphosphate kinase [EC:2.7.4.6]	A0A1X7UX19	G-protein coupled receptors family 1 profile domain-containing protein	No	
High NJ1 Only	TRINITY_DN2739_c1_g1_i6.p1			A0A1X7V013	Uncharacterized protein	No	
High NJ1 Only	TRINITY_DN9126_c0_g2_i1.p2	K21437	ANKRD13; ankyrin repeat domain-containing protein 13	A0A1X7V059	RNA 3'-terminal-phosphate cyclase (ATP) (EC 6.5.1.4)	Yes	Receptor-like
High NJ1 Only	TRINITY_DN18411_c0_g1_i10.p1			A0A1X7V1N0	Thioredoxin domain-containing protein	No	
High NJ1 Only	TRINITY_DN23565_c1_g1_i5.p1	K06269	PPP1C; serine/threonine-protein phosphatase PP1 catalytic subunit [EC:3.1.3.16]	A0A1X7V2W0	Serine/threonine-protein phosphatase (EC 3.1.3.16)	Yes	Cytoskeletal
High NJ1 Only	TRINITY_DN3558_c1_g1_i11.p1			A0A1X7V4G4	SAM domain-containing protein	No	
High NJ1 Only	TRINITY_DN14868_c0_g1_i3.p1	K06083	WASF3; WAS protein family, member 3	A0A1X7V7F6	Wiskott-Aldrich syndrome protein family member (WASP family protein member)	Yes	Cytoskeletal
High NJ1 Only	TRINITY_DN10555_c0_g1_i5.p1	K23781	ADAP, CENTA; Arf-GAP with dual PH domain-containing protein	A0A1X7V8C9	Uncharacterized protein	No	
High NJ1 Only	TRINITY_DN17479_c0_g2_i5.p1	K17509	PDPR; pyruvate dehydrogenase phosphatase regulatory subunit	A0A1X7VB39	Aminomethyltransferase (EC 2.1.2.10) (Glycine cleavage system T protein)	No	
High NJ1 Only	TRINITY_DN2457_c0_g1_i4.p1	K20032	ZDHHC13_17, HIP14; palmitoyltransferase ZDHHC13/17 [EC:2.3.1.225]	A0A1X7VBF2	Dol-P-Glc:Glc(2)Man(9)GlcNAc(2)-PP-Dol alpha-1,2-glucosyltransferase (EC 2.4.1.256)	No	
High NJ1 Only	TRINITY_DN8728_c0_g1_i1.p1			A0A1X7VC64	SH3 domain-containing protein	No	

High NJ1 Only	TRINITY_DN11221_c0_g1_i15.p2	K01262	pepP; Xaa-Pro aminopeptidase [EC:3.4.11.9]	A0A1X7VCQ7	Cyclic AMP-dependent transcription factor ATF-2	No	
High NJ1 Only	TRINITY_DN3085_c0_g1_i1.p1			A0A1X7VD02	CAP-Gly domain-containing protein	No	
High NJ1 Only	TRINITY_DN66162_c0_g3_i2.p1			A0A1X7VD75	Jacalin-type lectin domain-containing protein	No	
High NJ1 Only	TRINITY_DN1919_c0_g1_i1.p1			A0A1X7VDC1	Nose resistant-to-fluoxetine protein N-terminal domain-containing protein	No	
High NJ1 Only	TRINITY_DN1118_c1_g1_i3.p1			A0A1X7VDQ2	UDENN domain-containing protein	No	
High NJ1 Only	TRINITY_DN26170_c5_g1_i1.p1	K01137	GNS; N-acetylglucosamine-6-sulfatase [EC:3.1.6.14]	A0A1X7VDU3	Sulfatase N-terminal domain-containing protein	Yes	Lysosomal
High NJ1 Only	TRINITY_DN72124_c1_g1_i2.p1	K01134	ARSA; arylsulfatase A [EC:3.1.6.8]	A0A1X7VJT9	Sulfatase N-terminal domain-containing protein	Yes	Lysosomal
High NJ1 Only	TRINITY_DN16025_c1_g1_i3.p1	K08956	AFG3; AFG3 family protein [EC:3.4.24.-]	A0A1X7VKN7	AAA+ ATPase domain-containing protein	No	
High NJ1 Only	TRINITY_DN8604_c0_g1_i2.p1			A0A1X7VLI1	AAA+ ATPase domain-containing protein	No	
High NJ1 Only	TRINITY_DN1598_c0_g1_i12.p1			A0A1X7VLX4	F5/8 type C domain-containing protein	No	
High NJ1 Only	TRINITY_DN11142_c0_g1_i4.p1	K17302	COPB2, SEC27; coatomer subunit beta'	A0A1X7VLZ7	Uncharacterized protein	Yes	Membrane traffic
High NJ1 Only	TRINITY_DN12221_c1_g1_i5.p2	K07048	PTER, php; phosphotriesterase-related protein	A0A1X7VMK4	Phosphotriesterase-related protein (Parathion hydrolase-related protein)	No	
High NJ1 Only	TRINITY_DN9634_c0_g2_i2.p1			A0A1X7VMQ6	Uncharacterized protein	No	
High NJ1 Only	TRINITY_DN11500_c0_g1_i6.p2	K12175	GPS1, COPS1, CSN1; COP9 signalosome complex subunit 1	A0A1X7VMS4	PCI domain-containing protein	No	
High NJ1 Only	TRINITY_DN17853_c0_g2_i21.p2	K08515	VAMP7; vesicle-associated membrane protein 7	A0A1X7VMU6	Longin domain-containing protein	Yes	Membrane traffic
High NJ1 Only	TRINITY_DN76_c0_g1_i1.p1	K07375	TUBB; tubulin beta	A0A1X7VND0	Ribosomal RNA small subunit methyltransferase NEP1	Yes	Cytoskeletal
High NJ1 Only	TRINITY_DN11860_c0_g2_i1.p1	K18584	ACTR3, ARP3; actin-related protein 3	A0A1X7VP88	Actin-related protein 3	Yes	Cytoskeletal
High NJ1 Only	TRINITY_DN68791_c0_g2_i3.p1			A0A1X7VQ83	J domain-containing protein	No	

High NJ1 Only	TRINITY_DN9571_c0_g1_i3.p1	K00799	GST, gst; glutathione S-transferase [EC:2.5.1.18]	A0A1X7VQ95	VWFA domain-containing protein	No	
High NJ1 Only	TRINITY_DN19560_c2_g1_i10.p1	K10251	HSD17B12, KAR, IFA38; 17beta-estradiol 17-dehydrogenase / very-long-chain 3-oxoacyl-CoA reductase [EC:1.1.1.62 1.1.1.330]	A0A1X7VQC6	Uncharacterized protein	No	
High NJ1 Only	TRINITY_DN18479_c0_g2_i5.p1			A0A1X7VR16	E3 SUMO-protein ligase RanBP2	No	
High NJ1 Only	TRINITY_DN47142_c0_g2_i5.p1	K07374	TUBA; tubulin alpha	A0A1X7VTR9	Tubulin alpha chain	Yes	Cytoskeletal
High NJ1 Only	TRINITY_DN2009_c0_g1_i1.p1			A0A1X7VTV7	Rhodanese domain-containing protein	No	
High NJ1 Only	TRINITY_DN11865_c0_g1_i2.p1	K12400	AP4E1; AP-4 complex subunit epsilon-1	A0A1X7VTW8	Uncharacterized protein	Yes	Membrane traffic
High NJ1 Only	TRINITY_DN1560_c0_g1_i10.p1			A0A1X7VUC9	ABC transmembrane type-1 domain-containing protein	No	
High NJ1 Only	TRINITY_DN7071_c0_g2_i7.p1	K14006	SEC23; protein transport protein SEC23	A0A1X7VW61	Protein transport protein SEC23	Yes	Membrane traffic
High NJ1 Only	TRINITY_DN7141_c0_g1_i1.p1			A0A1X7VW71	Uncharacterized protein	No	

---

## Eidesstattliche Erklärung

---

Hiermit erkläre ich, Angela Maria Marulanda Gómez (geboren am 24.03.1992 in Cali, Kolumbien), dass ich die vorliegende Dissertation bis auf die Beratung durch meine BetreuerIn in Inhalt und Form selbstständig angefertigt habe. Ich versichere, dass ich diese Arbeit unter Einhaltung der Regeln guter wissenschaftlicher Praxis der Deutschen Forschungsgemeinschaft verfasst habe. Alle benutzten Quellen und Hilfsmittel habe ich vollständig angegeben und die Zusammenarbeit mit anderen WissenschaftlerInnen habe ich kenntlich gemacht. Weder diese noch eine ähnliche Arbeit wurden an einer anderen Abteilung oder Hochschule im Rahmen eines Prüfungsverfahrens vorgelegt, veröffentlicht oder zur Veröffentlichung eingereicht. Mir wurde kein akademischer Grad entzogen und dies ist mein erstes und einziges Promotionsverfahren.

---

## Declaration Statement

---

I, Angela Maria Marulanda Gómez (born 24.03.1992 in Cali, Colombia), hereby declare that I have prepared this dissertation independently in terms of content and form, with the exception of advice from my supervisor. I confirm that I have written this thesis in compliance with the rules of good scientific practice of the German Research Foundation. I have cited all sources and aids used in full and have indicated any collaboration with other scientists. Neither this nor any similar work has been submitted to another department or university as part of an examination procedure, published or submitted for publication. I have not been deprived of any academic degree and this is my first and only doctoral procedure.



---

Angela M. Marulanda G. Kiel, 14.12.2023



